

**Vidya Vikas Mandal's
Sitaram Govind Patil Arts,
Science and Commerce College,
Sakri Tal. Sakri Dist. Dhule 424 304**



**NAAC
ACCREDITED**

**विद्या विकास मंडळाचे,
सिताराम गोविंद पाटील कला,
विज्ञान आणि वाणिज्य महाविद्यालय,
साक्री ता. साक्री जि. धुळे ४२४ ३०४**

Affiliated to Kavayitri Bahinabai Chaudhari North Maharashtra University, Jalgaon

Website : www.sgpcsakri.com

Email : vidyavikas2006@rediffmail.com

Ph : 02568-242323

3.3.2.1 Research Paper Published in UGC Care Listed Journals

**CONSUMER BEHAVIOR REGARDING PURCHASING DECISION OF FOUR WHEELER
IN DHULE DISTRICT**

Prof. A. P. SONAWANE, Research student, Associate Professor in Commerce, VVMS S. G. Patil Arts, Science and Commerce College, Sakri, Tal. Sakri Dist. Dhule (Maharashtra)

Prof.Dr. Yogesh V. Torawane, Research Guide Pratap College, Amalner, Dist. Jalgaon

Abstract -

The study of consumer behavior is the study of how individual make decisions to spend their available resources (money, time, and effort) on consumption-related items. It includes the study of what they buy, why they buy it, how they buy it, when they buy it, where they buy it, and how often they buy it. Consumer behavior is the process whereby, individuals decide whether, what, when, where, how, and from whom to purchase goods and services. The automobile industry today is the most lucrative industry. Due to the increase in disposable income in both rural and urban sector and easy finance being provided by all the financial institutes, the passenger car sales have been significantly increased. In this research paper an attempt has been made to get answer the some of questions regarding brand preferences, brand loyalty, impact of price and quality on the market of four wheeler, consumer preferences regarding selection of dealer and mode of payment and impact of promotional strategies, after sale services, mileage, resale value on the purchase decision of durable goods like four- wheeler.

The term consumer behaviour is defined as the behaviour that consumer display in searching for, purchasing, using, evaluating and disposing of product, services and ideas that they expect will satisfy their needs.

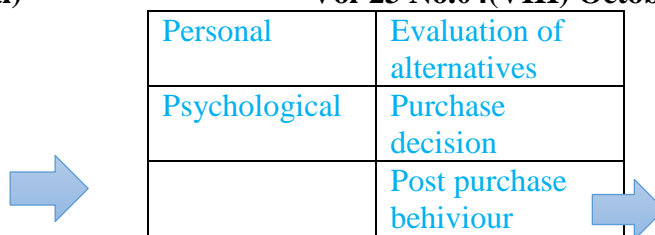
Key Words:- Consumer Behaviour; Brand Preferences; Brand Loyalty; Promotional strategies; After Sales Services; Resale Value.

Introduction-

The aim of marketing is to meet and satisfy target customers' needs and wants. The field of consumer behavior studies how individuals, groups, and organizations select, buy, use and dispose of goods, services, ideas, or experiences to satisfy their needs and desires. Understanding consumer behavior and "knowing customers "is never simple. Customers may say one thing but do another. They may not be in touch with their deeper motivations. They may respond to influences that change their minds at the last minute. Therefore marketing managers of four-wheeler showroom companies trying to understand their consumers how and why they purchase their brand of four wheeler. Consumer is a king in the kingdom of market. To understand his behaviour is very necessary for the marketing man. Consumer is the focus of all the marketing activities. Knowledge of his activities and behaviour is one of the most important aspects of the marketing. The consumers buy the goods to satisfy a number of needs and drives. Human wants are unlimited and varying time to time; from place to place and man to man. The study of consumer behaviour holds great interest for us as consumers, as students and scientists, and as marketers. The starting point for understanding buyer behavior is the stimulus-response model shown as under-

Model of Buyer Behaviour-

Buyers characteristics	Buyers decision process
Cultural	Problem recognition
Social	Information search



Source: Marketing Management, Eleventh Edition By Philip Kotler, Page no.184

Marketing and environmental stimuli enter the buyer’s consciousness. The buyer’s characteristics and decision processes lead to certain purchase decisions. The marketer’s task is to understand what

Marketing stimuli	Other stimuli
Product	Economic
Price	Technological
Place	Political
Promotion	Cultural

happens in the buyer’s consciousness between the arrival of outside stimuli and the purchase decisions. A customer’s buying behavior is influenced by cultural, social, personal and psychological factors. Cultural factors exert the broadest and deepest influence. Consumer Behaviour is a rapidly growing discipline of study. The study of consumer behaviour developed as a separate marketing discipline due to various reasons such as shorter product life cycles, increased interest in consumer protection, growth in marketing services, growth of international marketing, development of computer and information technology

Buyers decisions
Product choice
Brand choice
Dealer choice
Purchase timing
Purchase amount

and increasing competition, etc. Consumer research process involves six major steps (1) defining research objectives (2) collecting and evaluating secondary data (3) primary research design (4) collecting primary data (5) analysing data and (6) report preparation.

Consumer behaviour never remains the same or constant in every situation it changes time to time. There are various factors which affect consumer behaviour. As these factors change, consumer behaviour also changes. Following are the factors which affect consumer behaviour: (1) age (2) sex (3) marital status (4) income (5) family background (6) education (7) occupation (8) family size (9) geographic factors (10) psychological factors. In this grim battle for snatching maximum share of market, only those producers are destined to emerge victorious who will be able to read the pulse of the buyers? And this is here, where buyer behaviour has a very important role to play.

REVIEW OF LITERATURE—

It is necessary to review of literature on the past research Studies. Though voluminous literature is available in these areas, only a few important related studies are reviewed here. Review of literature helps to understand the various dimensions of the present study. Knowledge on consumer behaviour is very essential for the people in the field of marketing to make crucial decisions. Even a very minor aspect cannot be ignored as it may cause very serious repercussions.

The topic taken for research is Consumer Behavior towards Four Wheelers, information obtained from the previous studies about brand awareness in car market, brand preference and factors influencing the brand choice, brand loyalty, impact of advertisement, and buying habits is discussed in the following paragraphs-

Schmitt, Bernd H. and Laurette, Dube-Rioux (1988), using the context of Advertising, packing and consumer choice, three experiments were concluded to test the predictions of gender Schema theory that gender-schematic (sex-typed) individuals and gender-aschematic (non-sex-typed) individuals differ in the way they process and evaluate information related to gender. Results Indicate strong sex effects, but the predicated sex-type effects were not obtained.

S. Subadra et al. (2007), postulates the changing perceptions and behavior of the consumers with special reference to the car owners. Through this research paper the authors discussed how India is witnessing a change in consumerism. Market has now become predominantly consumer-driven. The focus has now been shifted from product based marketing to the need based marketing. Consumer is given many options to choose. This paper discussed the consumer perceptions and behavior of the car owners which was supposed to give a feedback on how marketing strategies work. This study throws light on various features that the manufacturers should concentrate on to attract the prospective buyers. The authors trace the factor-analysis which influencing purchase.

Yeung, W. M. and Robert, S. (2009), when consumers get verbal information about a products attributes, the influence of the affect they are experiencing on their product evaluations depends on their belief that the product should be judged on the basis of hedonic versus utilitarian criteria. When consumers see the product before they receive attributes information, however, the products appearance can stimulate them to form an affect-based initial impression that they later use as a basis for judgments independent of the criteria they would otherwise apply. Consequently, the mood that consumers happen to be in has different effects on their judgments than it would otherwise.

RESEARCH METHODOLOGY:

1. METHODOLOGY OF DATA COLLECTION:

The present study has been conducted with the help of primary and secondary data to understand the consumer behaviour towards Four Wheeler.

PRIMARY DATA -The primary data for the study has been collected with the help of interviews, personal observation, pilot survey and questionnaire.

SECONDARY DATA -

The secondary data has been collected from the following sources:

1. Books and journals.
2. Research reports.
3. Dealers.
4. Magazines, articles from newspapers.
5. Websites.

2. SAMPLE SIZE AND SAMPLE DESIGN:

Dhule District acts as the universe and every consumer who has four wheeler of any company in the district under study as on Dec. 31, 2014 is the population for the study. Keeping in view the time factors for the completion of the present study only a sample of 100 consumers has been selected. The sample constitutes proportionately all major brands of four-wheeler sold by different companies in the Dhule District under study. Further, designing a sample, due care has been taken to cover all demographic variables like age, sex, income, education, background of consumers, etc. in order to make the sample more representative.

3. SAMPLING METHOD:

Random sampling method (lottery method) has been used. Fifty percent samples have been taken from rural area and fifty percent samples taken from urban area.

OBJECTIVES OF THE STUDY:

The objectives of the present study are:

1. To study the brand preference & brand loyalty of consumer.
2. To examine the impact of price and quality on the market of four wheeler.
3. To study the consumer preference regarding the selection of dealer and mode of payment.
4. To highlights the impact of promotional activities, after sale services, mileage and resale value on the purchase decision of durable goods like four-wheeler.

DATA ANALYSIS AND INTERPRETATION:

TABLE-1.1 BACKGROUND OF CONSUMER AND BRAND OF FOUR WHEELER

Background	Brand of four wheeler					
	MARUTI SUZUKI	MAHINDRA AND MAHINDRA	TATA MOTORS	HYUNDAI MOTORS	TOYOTA MOTORS	TOTAL
RURAL	22 (44)	12(24)	9(18)	4(8)	3(6)	50 (100)
URBAN	23 (46)	7 (14)	7 (14)	8 (16)	5 (10)	50 (100)
TOTAL	45 (45)	19 (19)	14 (14)	11 (11)	10 (10)	100 (100)

Note: Figure in parenthesis depicts the percentage.

Source: Data collected through questionnaire.

The table 1.1 shows that the consumer who belongs to rural area, majority of them have purchased four wheeler of Maruti Suzuki, Mahindra & Mahindra and Tata Motors, whereas consumers who belong to urban area majority of them have purchased four wheeler of Maruti, Hyundai, Mahindra and Mahindra and Tata motors. So it can be concluded that the demand of four wheeler of Maruti, Mahindra and Tata Motors is higher in rural area than that of urban area. The demand of Toyota Motors is higher in the urban area than the rural area.

TABLE-1.2 INCOME OF CONSUMER AND BRAND OF FOUR WHEELER

INCOME	BRAND OF FOUR-WHEELER					
	MARUTI SUZUKI	MAHINDRA & MAHINDRA	TATA MOTORS	HYUNDAI MOTORS	TOYOTA MOTOR	TOTAL
Up to 20000	4 (66.67)	-	2 (33.33)	-	-	6 (100)
20001-30000	21 (52.5)	5 (12.5)	4 (10)	8 (20)	2 (5)	40 (100)
30001-40000	15 (39.47)	12 (31.58)	7 (18.42)	2 (5.26)	2 (5.27)	38 (100)
40001-50000	4 (28.57)	3 (21.43)	3 (21.43)	3 (21.43)	1 (7.14)	14 (100)
More than 50000	-	1 (50)	1 (50)	-	-	2 (100)
	44 (44)	21 (21)	17 (17)	13 (13)	5 (5)	100

Note: Figure in parenthesis depicts the percentage.

Source: Primary Data collected through questionnaire.

The table1.2 reveals that the consumers whose income level is less, they have purchased four wheeler of Maruti Suzuki company, Tata Motors and the consumers whose income level is higher, they have purchased four wheeler of Tata Motors, Hyundai Motors and Mahindra and Mahindra brands.

TABLE-1.3 BRAND OF FOUR WHEELER AND COMMITMENT OF PURCHASE

BRAND	COMMITMENT TO PURCHASE			
	Take What Showroom co. Offers	Ask for next preference	Same brand from other showroom co.	Total
Maruti suzuki	2 (4.44)	3 (6.67)	40 (88.89)	45 (100)
Mahindra and Mahindra	3 (15)	1 (5)	16 (80)	20 (100)
Tata motors	2 (11.76)	1 (5.88)	14 (82.36)	17 (100)
Hundai motors	2 (16.67)	3 (25)	7 (58.33)	12 (100)
Toyoto motors	-	2 (33.33)	4 (66.67)	6 (100)
	9 (9)	10 (10)	81 (81)	100 (100)

Note: Figure in parenthesis depicts the percentage.

Source: Primary Data collected through questionnaire.

The table 1.3 reveals that commitment to purchase Maruti Suzuki, Tata Motors and Mahindra & Mahindra is very strong. Commitment to purchase Hyundai and Toyota brand is quite unsatisfactory.

TABLE-1.4 BRAND OF FOUR WHEELER AND SATISFACTION WITH THE QUALITY

BRAND	SATISFACTION WITH THE QUALITY			
	HIGH SATISFIED	MODERATELY SATISFIED	LOW SATISFIED	TOTAL
MARUTI SUZUKI	25 (55.56)	19 (42.22)	1 (2.22)	45 (100.0)
MAHINDRA & MAHINDRA	15 (75.0)	5 (25.0)	-	20 (100.0)
TATA MOTORS	9 (60)	6 (40)	-	15 (100.0)
HYUNDAI MOTORS	6 (60)	3 (30.)	1 (10.0)	10 (100.0)
TOYOTA MOTORS	7 (70.0)	2 (20)	1 (10)	10 (100.0)
Total	62 (62)	35 (35)	3 (3)	100 (100)

Note: Figure in parenthesis depicts the percentage.

Source: Primary Data collected through questionnaire.

It is apparent from table 1.4 that majority of the consumers are highly satisfied with the brand they have purchased. But the consumers of Toyota Motors, Mahindra and Mahindra other brand are higher in percentage who strongly opine that they are highly satisfied with the quality of their brand, whereas consumer of Maruti Suzuki, Tata Motors and Hyundai Motors, have not supported the statement strongly that they are highly satisfied with the quality of their four wheeler.

TABLE-1.5 CLASSIFICATION OF CONSUMERS RESPONSES ON THE BASIS OF THEIR OPINION REGARDING PRICE AFFECT THE PURCHASE DECISION OF CONSUMER REGARDING FOUR WHEELER.

NATURE OF RESPONSES	SCALING	PRICE AFFECT THE PURCHASE DECISION OF CONSUMER REGARDING FOUR WHEELER	
		FREQUENCY	Percentage
HIGH IMPACT	4	62	62
MODERATE IMPACT	3	33	33
LOW IMPACT	2	3	3
NO IMPACT	1	2	2
TOTAL	----	1,00	100

Source: Primary Data.

It is evident from the table 1.5 that 62% consumers have opined that price highly affects the purchase decision of consumers regarding four wheeler and only 2% consumers opined that it does not affect the purchase decision of consumers of four wheeler. This shows that majority of the respondents have agreed that price affects the purchase decision of four wheeler.

TABLE-1.6 CLASSIFICATION OF CONSUMERS RESPONSES ON THE BASIS OF THEIR OPINION REGARDING QUALITY AFFECT THE MARKET OF FOUR WHEELER.

NATURE OF RESPONSES	SCALING	AFFECT OF QUALITY ON THE MARKET OF FOUR WHEELER	
		FREQUENCY	PERCENTAGE

HIGH IMPACT	4	65	65
MODERATE IMPACT	3	34	34
LOW IMPACT	2	1	1
NO IMPACT	1	0	0
TOTAL	----	1,00	100

Source: Primary Data.

The table 1.6 reveals that 65% consumers have opined that quality highly affects the purchase decision of consumers in the market of four wheeler, no consumer has opined that it does not affect the market of four wheeler.

TABLE-1.7 BACKGROUND OF CONSUMER AND SELECTION OF DEALER

BACKGROUND	SELECTION OF DEALER		TOTAL
	AUTHORISED DEALER	ANY OTHER DEALER	
RURAL	47 (94)	3 (6)	50 (100)
URBAN	43 (86)	7 (14)	50 (100)
TOTAL	90 (90)	10 (10)	100 (100)

Source: Primary Data.

It is obvious from table 1.7 that 94% rural and 86% urban consumers have opined that they would like to buy four wheeler from authorized dealer only. Only 6 % rural and 14 % urban consumers have replied that they would like to purchase the four wheeler from any other dealer only.

TABLE-1.8 BACKGROUND OF CONSUMER AND SELECTION OF MODE OF PAYMENT

BACKGROUND	SELECTION OF MODE OF PAYMENT		TOTAL
	CASH PAYMENT	INSTALLMENT PAYMENT	
RURAL	13 (26)	37 (74)	50 (100)
URBAN	9 (18)	41 (82)	50 (100)
TOTAL	22 (22)	78 (78)	100 (100)

Source: Primary Data.

It has been observed from table 1.8 that irrespective of their background majority of consumers i.e. 74 % of rural and 82% of urban have opined that they like installment method of payment for purchasing four wheeler. Only 26% rural and 18% of urban consumers would like to purchase four wheeler by cash payment.

TABLE- 1.9 INCOME OF CONSUMER AND SELECTION OF MODE OF PAYMENT

INCOME (MONTHLY)	SELECTION OF MODE OF PAYMENT		TOTAL
	CASH PAYMENT	INSTALLMENT PAYMENT	
Up to 20000	2 (33.33)	4 (66.67)	6 (100)
20001-30000	11 (27.5)	29 (72.5)	40 (100)
30001-40000	8 (21.05)	30 (78.95)	38 (100)
40001-50000	2 (14.29)	12 (85.71)	14 (100)
More than 50000	1 (50)	1 (50)	2 (100)

Total	24 (24)	76 (76)	100
-------	---------	---------	-----

Source: Primary Data.

It is depicted from the table 1.9 that majority of consumers whether they belong to lower income group or higher income group like installment method of payment. The consumers whose income level is low are less in percentage who have opined that they prefer installment method, whereas the consumers whose income level is higher they are higher in percentage who have opined that they prefer installment method of payment. Only those consumers whose income is more than Rs.50000 have preferred fifty-fifty percent cash and installment method of payment.

TABLE-1.10 BRAND OF FOUR WHEELER AND RATING OF PROMOTIONAL ACTIVITIES

BRAND	RATING OF PROMOTIONAL ACTIVITIES				TOTAL
	EXCELLENT	VERY GOOD	GOOD	POOR	
MARUTI SUZUKI	13 (28.89)	24 (53.33)	8 (17.78)	-	45 (100.0)
MAHINDRA & MAHINDRA	4 (20)	7 (35)	6 (30)	3 (15)	20 (100.0)
TATA MOTORS	6 (40)	4 (26.67)	3 (20)	2 (13.33)	15 (100.0)
HYUNDAI MOTORS	6 (60.0)	4 (40.0)	-	-	10 (100.0)
TOYOTA MOTORS	3 (30)	2 (20)	4 (40)	1 (10)	10 (100.0)
TOTAL	32 (32)	41 (41)	21 (21)	6 (6)	100 (100.0)

Source: Primary Data.

It is evident from the table 1.10 that promotional activities of Hyundai, Maruti and Tata Motors are very good, promotional activities of Mahindra & Mahindra and Toyota Motors are average. So, it is suggested to Mahindra & Mahindra and Toyota Motors brand of four wheeler companies to improve the level of their promotional activities.

TABLE-1.11 BRAND OF FOUR WHEELER AND RATING OF AFTER SALE SERVICES

BRAND	RATING OF AFTER SALE SERVICES					TOTAL
	EXCELLENT	VERY GOOD	GOOD	POOR	VERY POOR	
MARUTI SUZUKI	15 (33.33)	24 (53.33)	5 (11.11)	1 (2.23)		45 (100)
MAHINDRA & MAHINDRA	-	2 (10)	6 (30)	10 (50)	2 (10)	20 (100)
TATA MOTORS	-	-	2 (13.33)	11 (73.33)	2 (13.34)	15 (100)
HYUNDAI MOTORS	-	-	4 (40)	5 (50)	1 (10)	10 (100)
TOYOTA MOTORS	-	-	2 (20)	6 (60)	2 (20)	10 (100)
TOTAL	15 (15)	26 (26)	19 (19)	33 (33)	7 (7)	100 (100)

Source: Primary Data.

It is obvious from the table 1.11 that consumers are highly satisfied with after sale services of Maruti Suzuki. Majority of consumers unsatisfied with after sale services of Mahindra and Mahindra, Tata Motors, Toyota Motors and Hyundai Motors companies.

TABLE-1.12 BRAND OF FOUR WHEELER AND RATING OF MILEAGE

BRAND	RATING OF MILEAGE					TOTAL
	EXCELLENT	VERY GOOD	GOOD	POOR	VERY POOR	
MARUTI SUZUKI	11 (24.44)	23 (51.11)	11 (24.45)	-	-	45 (100)
MAHINDRA & MAHINDRA	-	6 (30)	10 (50)	4 (20)	-	20 (100)
TATA MOTORS	-	2 (13.33)	11 (73.33)	2 (13.34)	-	15 (100)
HYUNDAI MOTORS	7 (70)	3 (30)	-	-	-	10 (100)
TOYOTA MOTORS	3 (30)	4 (40)	3 (30)	-	-	10 (100)
TOTAL	21 (21)	38 (38)	35 (35)	6 (6)	-	100 (100)

Source: Primary Data.

The table 1.12 depicts that consumers are highly satisfied with the mileage of Maruti Suzuki and Hyundai Motors, moderately satisfied with the mileage of Toyota Motors and less satisfied with the mileage of Mahindra & Mahindra and Tata Motors brand of four wheeler

TABLE-1.13 BRAND OF FOUR WHEELER AND RATING OF RESALE VALUE

BRAND	RATING OF RESALE VALUE					TOTAL
	EXCELLENT	VERY GOOD	GOOD	POOR	VERY POOR	
MARUTI SUZUKI	11 (24.44)	26 (57.78)	8 (17.78)	-	-	45 (100)
MAHINDRA & MAHINDRA	-	3 (15)	7 (35)	9 (45)	1 (5)	20 (100)
TATA MOTORS	-	4 (26.67)	5 (33.33)	6 (40)	-	15 (100)
HYUNDAI MOTORS	-	-	3 (30)	6 (60)	1 (10)	10 (100)
TOYOTA MOTORS	-	-	2 (20)	5 (50)	3 (30)	10 (100)
TOTAL	11 (11)	33 (33)	25 (25)	26 (26)	5 (5)	100 (100)

Source: Primary Data.

It observed from the table 1.13 that consumers have rated the resale value of Maruti Suzuki as very good, resale value of Tata Motors as average and resale value of Mahindra, Hyundai and Toyota Motors brand as poor.

TABLE-1.14 CLASSIFICATION OF CONSUMERS RESPONSES ON THE BASIS OF THEIR OPINION REGARDING AFTER SALE SERVICES AFFECT THE PURCHASE DECISION

NATURE OF RESPONSES	SCALING	AFFECT OF AFTER SALE SERVICES ON PURCHASE DECISION	
		NO	OF PERCENTAGE

		RESPONSES	
STRONGLY AGREE	3	70	70
MODERATELY AGREE	2	26	26
DISAGREE	1	4	4
TOTAL	---	1,00	100

Source: Primary Data.

It has been observed from the table 1.14 that there is significant difference in the opinion of consumers over the affect of after sale services on the purchase decision of consumer.

TABLE-1.15 CLASSIFICATION OF CONSUMERS RESPONSES ON THE BASIS OF THEIR OPINION REGARDING SATISFACTION AFFECTS THE PURCHASE DECISION

NATURE OF RESPONSES	SCALING	SATISFACTION WITH THE AFTER SALE SERVICES	
		NO OF RESPONSES	PERCENTAGE
STRONGLY AGREE	3	54	54
MODERATELY AGREE	2	36	36
DISAGREE	1	10	10
TOTAL	---	100	100

Source: Primary Data.

It is observed from the table 1.15 that majority of the respondents have opined that their satisfaction with after sales services affects the purchase decision.

TABLE-1.16 CLASSIFICATION OF CONSUMER RESPONSES ON THE BASIS OF THEIR OPINION REGARDING MILEAGE AFFECT THE PURCHASE DECISION OF CONSUMER

NATURE OF RESPONSES	SCALING	AFFECT OF MILEAGE ON THE PURCHASE DECISION	
YES	3	83	83
NO	2	12	12
CAN NOT SAY	1	5	5
TOTAL	---	1,00	100

Source: Primary Data.

It is evident from the Table 1.16 that majority of consumers opined that mileage affects the purchase decision of consumer.

TABLE 1.17 CLASSIFICATION OF CONSUMER RESPONSES ON THE BASIS OF THEIR OPINION REGARDING PROMOTIONAL ACTIVITIES AFFECT THE PURCHASE DECISION.

NATURE OF RESPONSES	SCALING	AFFECT OF PROMOTIONAL ACTIVITIES ON THE PURCHASE DECISION	
		FREQUENCY	PERCENTAGE
HIGH IMPACT	4	63	63
MODERATE IMPACT	3	37	37
LOW IMPACT	2	0	0
NO IMPACT	1	0	0
TOTAL	-	1,00	100

Source: Primary Data.

It is revealed from the table 1.17 that promotional activities highly as well as moderately affect the purchase decision. No consumer opined that promotional activities do not affect the purchase decision.

CONCLUSION:

It is observed from the study that the demand of the four wheeler of Maruti Suzuki, Mahindra and Mahindra and Tata Motors is higher in rural area than that of urban area. On other hand, in urban area the demand of Maruti Suzuki, Hyundai, Mahindra and Mahindra and Toyota motors brand is higher. It is evident from the research that commitment to purchase Tata Motors, Maruti Suzuki and Mahindra & Mahindra is very strong. Commitment to purchase Hyundai and Toyota brand is quite unsatisfactory.

It is observed that 62% consumers have opined that price highly affects the purchase decision of four wheeler and only 2% consumers opined that it does not affect the purchase decision of four wheeler. This shows that majority of the respondents do agree that price affects the purchase decision of four wheeler. It is evident from the research that 65% consumers have opined that quality highly affects the market of four wheeler; no consumer has opined that it does not affect the market of four wheeler. The study revealed that majority of consumers opined that they would like to buy four wheeler from authorized dealer only. It has been observed that irrespective of their background majority of consumers have opined that they like installment method of payment for purchasing four wheeler. It is depicted from the study that majority of consumers whether they belong to lower income group or higher income group like installment method of payment. Only 50% consumers whose monthly income is more than Rs.50000/ like purchasing four wheeler by cash payment.

It has been observed from the research that there is significant difference in the opinion of consumers over the affect of after sale services on the purchase decision of consumer. The research revealed that majority of the respondents have opined that resale value affects the purchase decision. It is evident from the research that majority of consumers opinioned that mileage affect the purchase decision of consumer. It is revealed from research that promotional activities moderately affect the purchase decision. No consumer opined that promotional activities do not affect the purchase decision.

SUGGESTIONS:

(A) For the Consumers:

- 1) It is suggested for the consumers that if they are going to purchase four wheeler, then they should purchase any of the four wheeler from the following list, which is arranged in order of their performance (a) Maruti Suzuki, (b) Mahindra & Mahindra, (c) Tata Motors, (d) Hyundai Motors, (e) Toyota Motors.
- 2) It is suggested to the buyers that such product should be purchased after getting adequate information from published and unpublished sources.
- 3 It is also suggested to the buyers to take the opinion of their family members, relatives, friends and neighbors before the purchase of four wheeler.
- 4 The price, quality, brand of product, warranty period, mileage, resale value and after sale services should be taken into consideration before the purchase of four wheeler.
- 5 It is advised to the buyers to purchase four wheeler from authorized showroom dealer only.
- 6 It is suggested to the consumers that the price of the product must be taken into consideration but the quality should also not to be ignored.

(B) For show companies Dealer:

1. It is advised to Hyundai Motors and Toyota Motors brands to improve the quality, improve the after sale services, enlarge warranty period and spend huge amount on advertisement so that the demand of their four wheelers could be increased.
2. It is suggested to all the four wheeler manufacturing companies to appoint more authorized dealer and service stations in rural areas.
3. It is advised to Hyundai Motors and Toyota Motors brand of four wheeler companies to improve the features of their four wheelers.
4. It is advised to Mahindra & Mahindra and Toyota Motors brand of four wheeler companies to improve the level of their promotional activities.

5. All four wheeler companies should take necessary steps towards providing better after sale services.
6. It is suggested to Mahindra & Mahindra, Hyundai Motors and Tata motors brand of four wheeler to take necessary actions to increase the resale value of their four wheelers.
7. It is advised to Maruti Suzuki, Tata Motors and Hyundai Motors to extend the warranty period of their four wheelers.
8. It is suggested to the manufacturers to introduce low price four wheeler in the rural areas.
9. Finding revealed that quality and durability of Mahindra, Hyundai and Tata motors brand of four wheeler is not up to the mark as compared to other popular brands. Thus these brands need to improve the quality and durability.
10. Customers should be informed about the quality, price, mileage, resale value, after sale services and warranty period of the four wheeler by comparing these with other brand of four wheelers. It may be helpful in attracting more customers.

REFERENCES:

- 1) **Marketing Management, Eleventh Edition, By Philip Kotler. Page no.182 to 184.**
Published by Pearson Education (Singapore) Pte. Ltd, Indian Branch, 482 F.I.E. Patparganj, Delhi 110092,India.
- 2) Consumer Behaviour in Four Wheeler Industry –A Case Study of Himachal Pradesh. By Rakesh Kumar, Assistant Professor in Commerce, Shaheed Bhagat Singh College, University of Delhi- India
- 3) Schmitt Bernd H., and Laurette, Dube-Rioux. (1988). Sex Typing and Consumer Behaviour. A Test of Gender Schema Theory.
- 4) Yeung, W.M., And Robert S. Affect, Appraisal and Consumer Judgment. (2009).
- 5) www.marutisuzuki.com
- 6) www.hyundai.com
- 7) www.tatamotors.com
- 8) www.toyota.com
- 9) www.mahindra.com
- 10) www.carwale.com
- 11) www.gaadi.com
- 12) www.google.com

Resent Trends and Issues in Social Science & Science towards Sustainable Development

*Dr. Chandrakant S. Kadhare

Asst. Prof. in Political Science

(S. G. Patil Arts, Sci. and Com. College, Sakri Dist. Dhule)

Abstract

The need for twenty-first century to achieve sustainable development has become urgent and compelling. Although draped in natural resources in abundance, continues to trail the rest of the world in many areas such as education, healthcare, decent employment, infrastructural amenities, food security, considerable per capita income, technological progress and access to technological tools per capita, security and others. This research paper attempt to dissect the rubric of sustainable development in twenty-first century and the role of the social science & science. Using the theoretical paradigms of Modernisation and Human Development theories, the research paper the need for societies to embrace the secrets of development as employed by developed countries and to priorities human development in place of statistics-laden & science economic growth and development. This research paper identify the role that the social science academy can should play for the sustainable development particularly regarding the realization of the 2030 Sustainable Development Agenda with its 17 goals.

Keywords: Social Sciences, Social Science Academy, Sustainable Development, Sustainable Development Goals

Introduction:

The imperative for sustainable development in twenty-first century world continues to perturb international governments, leaders, development institutions, civil society groups, and a cortege of stakeholders including academia, particularly those belonging to the social science family and science disciplines. When such human development indices (HDIs) as education, healthcare (covering the gamut of child, maternal and adult healthcare), decent employment, which affords decent income to workers, infrastructural amenities, food security, considerable per capita income, technological progress and access to technological tools per capita and security are consider.

For instance, out of the 47 least developed countries (LDCs), designated by the Committee for Development Policy (CDP), a group of independent experts working for and reporting to the United Nations Economic and Social Council (ECOSOC), 33 (about 70%) of these countries are found in Africa, 8 are in Asia but none in Europe and America (United Nations Conference on Trade and Development [UNCTAD], 2018). The African countries that made this list include Angola, Benin, Burkina Faso, Burundi, the Central African Republic, Chad, the Comoros, the Democratic Republic of the Congo, Djibouti, Eritrea, Ethiopia, the Gambia, Guinea, Guinea-Bissau, Lesotho, Liberia, Madagascar, Malawi, Mali, Mauritania, Mozambique, Niger, Rwanda, Sao Tome and Principe, Senegal, Sierra Leone, Somalia, South Sudan, Sudan, Togo, Uganda, the United Republic of Tanzania and Zambia. These countries show negative indicia of either failed, failing or struggling states. In fact, they are specifically characterised by agrarian economies, dominance of the informal sector, chronic current account deficits and they remain highly dependent on external resources to finance a significant portion of their investments and part of their consumption (UNCTAD, 2018).

Social Science:

The social sciences are academic disciplines or fields of learning that focus on understanding the society and the relationships of human beings within it. They often rely on or deploy empirical approaches in the methodological process of data gathering, analysis and interpretation of modern academic practice, often employ eclectic or multiple methodologies (for instance, by combining the quantitative and qualitative techniques) in the investigation of a particular phenomenon notes that the social sciences are branches of science that deal with human behaviour in its social and cultural aspects. Thus, unlike the physical or natural sciences that deal with inanimate or animate things, the social sciences focus on social phenomena as they affect human beings or are affected by human beings. Therefore, the laboratory of social sciences is the society, peopled by human beings with their unique behaviours, perspectives, opinions, feelings, subjectivities, preferences, natural inclinations, world views, experiences and so on. For instance, two individuals exposed to

the same situation, the same time, the same place, and having similar opportunities, may not respond the same way. This unpredictability is what defines and underlines theories within the social sciences.

Emerging Approaches in the Social Sciences:

Considering the changing environmental conditions as well as the dynamic process of rapid transformation which societies are undergoing in the present situation, sustainability stresses the need to focus on the dynamic character of the process of societal change in which the natural environment is involved as a central dimension. Hence, sustainability should not refer to the conservation of specific structures or to static qualities of societies or the natural environment, but, rather, should refer to stabilized and preserved patterns within socioecological transformations. Both approaches are providing important insights into the societal implications of sustainability. This is especially true with respect to the conceptualization of the society/nature relationship as it has been worked out within Ecological Economics. However, the limitations of both approaches are obvious as they take social activities and processes into account only as far as they are part of the economy. A remarkable attempt to move beyond economic concerns by introducing issues of social justice and political participation in the debate on sustainability has been formulated by Ignacy

Sachs (Sachs 1996). Drawing on a "whole sustainability" approach, Sachs distinguishes between environmental and social sustainability in terms of "outer" and "inner" limits of society. While environmental sustainability is concerned with the biophysical limits of social activities, social sustainability is related to the internal organization of individual societies as well as of the world community as a whole.

Sustainable Development

The doctrine of 'sustainable development' derives from a discipline in economics that has been evolving for almost two centuries. The debate about whether Earth's limited natural resources will continue to provide life support for humanity's burgeoning population began with the work of the English political economist Thomas Malthus in the early 1800's. In *An Essay on the Principle of Population*.

According to Šlaus and Jacobs (2011), sustainable development impinges on a wide array of economic, social, political, ecological, and technological issues, including energy, water, mineral resources, climate, urban congestion, population, pollution, industrialisation, technological development, public policy, health, education, and employment. The goal of sustainable development is that development should not only be reproducible but should also be sustainable. The definition of sustainable development, to which many scholars have subscribed and derived their various interpretations, is that mooted by the United Nations World Commission on Environment and Development (WCED) as enshrined in the Brundtland Report. This definition states that sustainable development is that development which meets the needs of the present generation without compromising the ability of future generations to meet their own needs (Brundtland Report, 1989).

The Rio Declaration on Environment and Development further illuminates the subject of sustainable development by identifying 27 principles of sustainability (The Rio Declaration, 1992) some of them as presented below:

- Human beings are at the centre of concerns for sustainable development. They are entitled to a healthy and productive life in harmony with nature
- States shall cooperate in a spirit of global partnership to conserve, protect and restore the health and integrity of the Earth's ecosystem with developed countries taking the lead because of the pressures their societies place on the global environment and of the technologies and financial resources they command.
- States should reduce and eliminate unsustainable patterns of production and consumption and promote appropriate demographic policies in order to achieve sustainable development and a higher quality of life for all people
- Environmental issues are best handled with the participation of all concerned citizens, at the relevant levels. At the national level, each individual shall have appropriate access to information concerning the environment that is held by public authorities, including information on hazardous materials and activities in their communities, and the opportunity to participate in decision-making processes. States shall facilitate and encourage public awareness and participation by making information widely available. Effective access to judicial and administrative proceedings, including redress and remedy, shall be provided.

Conclusion:

World's countries are resource-endowed but have continued to struggle and straggle behind nations those hitherto are their contemporaries in the past. The social sciences are important fields of knowledge whose researchers, academics, thinkers and scholars can help in rescuing world from underdevelopment and placing it on the path of sustainable development. By utilising what it has in abundance such as research ability or propensity, building industry-academy partnership, framing policies, providing qualitative social science education, the social sciences in world would be able to turn the continent around from its downward course of underdevelopment and carve a new trajectory that the continent and its people can walk on to sustainable development. Particularly, the role of the social sciences cannot be underestimated in the realisation of the 2030 Sustainable Development Agenda and its 17 goals.

References:

1. Brundtland Commission (1987). Report of the World Commission on Environment and Development. New York and Geneva: United Nations
2. Edewor, P. A. Imhonopi, D. & Amusan, T. (2014). Sociocultural and demographic dynamics in sustainable entrepreneurial development in Nigeria. *Developing Country Studies*, 4(4), 58- 64.
3. World teachers' day: Another round of empty promises? *The Punch*. Retrieved from <https://punchng.com/world-teachers-day-another-round-of-empty-promises/>
4. Riti, J. S., & Kamah, M. (2015). Entrepreneurship, employment and sustainable development in Nigeria. *International Journal of Academic Research in Economics and Management Sciences*, 4(1), 179-199
5. Sustainable Development Goals Fund. (n.d.). Millennium Development Goals. Retrieved from <http://www.sdgfund.org/mdgs-sdgs>
6. United Nations Development Programme [UNDP]. (2019). Millennium Development Goals. Retrieved from http://www.undp.org/content/undp/en/home/sdgoverview/mdg_goals.html
7. Gowdy, John M. (1996). „Sustainability as a Concept of Social Sciences: Economic Concepts of Sustainability”
8. Guha, Ramachandra (1996). “Traditions of Social-Ecological Research in Modern India”
9. Wang, Rusong (1996). “Man and Nature Be in One: Human EcoloUnderstanding of Sustainable Development in China”.
10. United Nations Educational, Scientific and Cultural Organisation. [UNESCO]. (2017). Education for sustainable development goals: Learning objectives.

**IDENTITY CRISIS IN THE POETRY OF DALIT WRITER S. JOSEPH****DR. DHANANJAY P. PATIL**

Asst. Professor

Vidya Vikas Mandal's S. G. Patil Arts,
Science and Commerce College,
Sakri, Dhule**ABSTRACT:**

The Present study is an attempt to find identity crisis in the poetry of Dalit writer S Joseph. Dalit literature has for a long time been literary and social tool in the present day from the rise in everyday violence against Dalits and other marginalized communities. The caste issue is transformed into a problem of the social and economic marginalization of one section of society and the caste problem is seen as a problem only for the lower caste who suffers from it. It resists the tendency to treat Dalit poetry as social documentary, and instead unravels an aesthetic that builds on the realist mode but moves beyond it. Dalit poets are voices raised on behalf of thousands of exploited Dalits. The paper represents Identity crisis in the poetry of Dalit literature of S. Joseph. The poet proposes the realist mode of pain, suffering, depression, suppression in everyday life of Dalit. Their lives reflected in poetry seems to be searching for identity.

Keywords: Marginalized, Identity Crisis, Discrimination, Dalit Poetry, Agony.

Introduction

With the emergence of Dalit literature, the lives and histories of the marginalized have gained representation. Since Dalit literature is written in several languages, translation into English is the only way its collective vision and ideals can be made available for the world to read. In Communist Kerala, S Joseph emerged as the forerunner of the Malayalam Dalit literary tradition. He was able to challenge Brahminical poetic traditions while offering verses that soothed the wounds of the lower caste people. The Naxalite movement was critical for public life in Kerala during 1970s. Though Joseph witnessed and attracted to it, he only watched from a distance. He has been writing poetry since he was sixteen, but he has not been directly involved with the Dalit movement either by action or through his poetry.

As we trace the history of Malayalam poetry, it's evident that it had undergone colossal changes in its style, language, poetic techniques with the changes in the contemporary social and political scenario. Contemporary Malayalam poetry stood far apart from the affluent



poetic tradition of Malayalam poetry which began with 'Manipravaalam' and has witnessed eminent works of great poets in the literary field. Writers in Dalit literature like S. Joseph captures Dalit community life in Urban and Rural setting. In their arguments and narratives, the caste acquires a new meaning. Narrating the firsthand experience of agony and alienation, Joseph emerged as a pioneer of contemporary Malayalam Dalit poetry, which gives an authentic and genuine voice for Dalit community.

'Underlying all Poetry is prose. But Poetry that is simply prose is anti-Poetic... Traditional poetry achieved its form and meter by forgetting certain experiences and people. That is the mode in which poetry became poetic and prose acquired its genius. Now poetry is discovering those forgotten people. The prose of their experiences is pushing its way into poetry.' Says S. Joseph, one of the leading contemporary poets in his 2004 article titled Poetry in search of a prose. He feels poetry is poetry it should not be gripped by a movement. But knowingly or unknowingly his writings are leaning towards a generalized subaltern outlook.

He says, 'I have taught and lived among tribal children, fisher people, blacksmith. My poetry is about them. Today when I look back, I can see that my poetry is about all these people who are "outside" the mainstream. It is a world that is not found even in Naxalite poetry.'

Dalits have hitherto been burdened with imposed identities as untouchables, depressed classes, harijans or scheduled castes. Though the modern society promises equality and freedom to all the dark ages of religious difference are not left behind. What he encounters is not a traditional taboo, but a modern stigma. In the poems *Identity card* and *Group Photo*, what we encounter is modern means of discrimination in a modern institution. Kerala state is renowned for its educational achievement. But in the very same state, how the class of a person turns out to be a cause of discrimination is well expressed by S. Joseph in *Identity Card*.

*"A girl came to class with a smiling face,
shares a bench and food,
enjoy the thrill of touch,"*

But at the moment she noticed the salary amount he receives in his identity card it marked the end of their relationship. The card and stipend mark his caste and class, and costs him his love. Anti-reservationist considered those who had made use of reservations and stipend as inefficient.

While most of the poets express the precarious life of the untouchables by narrating how an upper class humiliates the lower caste, *Group photo* shows the invitation of an upper caste girl to stand beside her in the college group photo. Due to the ongoing caste discrimination and humiliation that he had gone through he was reluctant to accept the invitation this foreground caste and colour consciousness of a subaltern person. Even if he can change her stalker that took his place in photo with the current photo techniques the complex that drags him back and believes it's as his fate.

*"How does a poor, low caste fellow,
Dark to boot, live in Kerala?"*



The question he raised is highly commendable and the narrator's words

"I will disappear once in a while..."

echoes the cursed life of a community whose appearance and disappearance get unnoticed in the social life. The inner complex generated in the mind of subaltern is the result of the continuous oppression faced by his community so far. His poems discuss both class and caste discrimination, here though the boy and girl equally educated and main equality in class wise their caste identity drew him back. Poet satirizes the attitude of upper-class caste through the invitation of girl; the high class is regarded as kind to all but they never knew the mental agony of the subalterns.

A letter to Malayalam Poetry' is significant in two levels - one is it focuses on the transition in the Malayalam poetry with the advent of poets like him and the other is it highlight the living condition of poor people through the voice of a rag picker in the poem. Rag picker invites poetry to his thatched hut, where she can enjoy freedom as a bird, burn in sun, bath in the brook, have gruel and sprouts by sitting on a mat in veranda. Poetry used to live and well looked after in big bungalows, speeding in cars, speaking only in meter and rhyme. Though it sounds as an invitation to poetry, poet attempts to explore the life of poor people and says poetry should reverberate the voice of this voiceless class.

This idea is further explained in the poem *Different Poems* where the ploughman, the reaper the forest dweller the toddy tapers the mason the beggar, the boatman, the grave digger all of them who belongs to the lower class if the society says about their labor through their own poetry. Poet narrates his experience when he goes to work with a builder in the poem titled as *Mason* which again proves poets urge to documents the life of poor.

He has no pretensions to being an environmentalist but the ardent beauty of nature and the environmental degradations portrayed in his poems express the chaotic situation of nature as well as the subalterns. Landscape of his Poetry is startlingly new it moves into hitherto unknown places where the subaltern people belong abundantly. Hill side, river banks, rocky-mountains, bamboo plants, screw pine leaves, sugarcane fields etc. in his poems like *one's Own, running Ant, Dhvani, The Fishmonger, The song, water, fading away in the shade of umbrella* etc. are vivid examples to prove this argument. Poet thus emphasized how the marginalized live in close union with nature than the other sections of society. The narrator in the poem *One's own*, lives in a hillside where he used to wash bath and went fishing in the rivulet. He went further with the rivulet doing the same tasks until it merges with a large river. He announces, "I am only a poet of rivulets a small poet My own rivulets call out."

Rivulet stand as a metaphor for the marginalized people and the poets' hesitation to go with river exemplify the lower- class peoples fear to come for front due to the humiliations they had suffered so far. Solidarity of marginalized is visible in the poems of S. Joseph raising the issues encountered by nature and its resources, subalterns as well as woman.

Modern developments and innovations are meant for the well-being of the people but it reaches only within the privileged classes relegating the poor people to even more marginalized position. Emphasizing the pathetic condition of a fishmonger, who died of



epilepsy while washing vessel in a tiny stream poet emphasized this perspective. His dead body floats and disappeared in the water without being noticed by anyone "There is no sign of fishmonger now" The Plasters wall of a motor workshop parallel to M.C. road indicates the modern progress hinders the view of dead body in the stream to an onlooker opposite to the wall. Everything that we have across can be re written as something new and worthy but the life city dwellers and plight of villagers is written and read as such. Poet acclaims this in Running Ant and feels sad that even in literary works their fate can't be rewritten. The predicament of a Fishmonger in the fishmonger signifies the life and death of an ordinary man is irrelevant.

This clearly indicates how the world of privileged and non-privileged class gets divided in the ongoing innovations. Narrating the life of basket makers and their world in Basket poet further discusses the plight of marginalized 'Ottal is a rare plant which is used to make baskets, hemispherical in shape. Conjoining two baskets results a sphere, shape of the earth the planet we live poet compares 'Ottal plant' with the marginalized both are at the verge of extinction. Basket making represents the creation of their own world by ma marginalized class who strives hard to meet their livelihood amidst of the discrimination and humiliations.

In Prison the poet speaks of two prisons, the real one the convicts are held behind the iron bars and the outer one where the bars are made by religion caste and colour culprits in the real prison seem to be the victims of the class chaos of the outside prison. Narrator says about the prison without have any experience with the real prison but engages with the prison outside every day.

Black on black is the most beautiful combination declares the poet in Black.

*"On a black face
Eyebrows eyelashes and
Lips have a special charm."*

The strays of eyeliner on a drenched black woman the black shirt worn by a black man, black colour of hair and skin etc. through the images of this poem the poet shakers the concept of other black has its significance on if there is the contrasting white. When black colour of hair considered as a sign but the black skin of a man is low while the animals entice. Basically, colour of human race is black. Due to the emergence of colonial power, politically, economically and socially the white dominates the black. Even in the post-colonial and postmodern age, the same practice continues thus the black remains as a trade mark of subaltern. Though once the black was regarded the symbol strength, now it is the reason to push away the people mainstream due to black. With the status of skin white, the black got crushed and side lined without allow to enjoy any privileges that the modern society guarantees to all. Black and white remains as rightful combination except in the case of human, where black is always hidden under white,

"Black you can say, lies hidden beneath white."

When the poet sees the picture of an extinct fish on the college wall, he thinks of his own race is getting extinct slowly from the society. When these images and descriptions of the animals facing extinction helps to prepare a list and take measures to protect them, where a group of



people facing the same threat that got unnoticed as it's a racial extinction, said the poet in *On the college Wall* in Just a few narrator wonders why only a few people anxious about the pathetic life of poor or marginalized or the environmental hazards. This implicates that he too among those few people, those who are poor who worries about their community. Their problems and hazard reverberate among themselves unheard to the world outside. When the people ran for the developments, they ignore the pain of poor which get noted in *Eases and Difficulties*. When the Engineers think of the railway doubling poets concern is for the man standing on a sand hill which gets depleted in the construction. Most of the facilities that we are enjoying today are the results of the difficulties suffered by poor.

He creates a powerful impact on the Dalit theme with *My Sister's Bible* this bible has everything- a ration book, loan application form, card from money lender notices of feast, photograph of brothers, child a hundred rupee note an SSLC book except the old Testament and the New. According to a subaltern his day-to-day life and joys meets with these things not the preface and contents of a real bible. What helps them to fill their belly and mind is the real God for them.

The poet uses a lot of other similes and metaphors from the Daily life of people to expressing the plight of the outcaste rather than grand images used in the traditional poetry. The image of a 'captive elephant' in *Elephant* "No place to go? The question used to ask his mother when he was a child marks in the poem *Dhwani*, poets who recalls the time when they had no well and had to collect water from the wells of the affluent drawing it with an arecanut- palm-spathe pail tied to rope in water the image of a young girl who faded away in the shade of an Umbrella in *Fading away in the shade of an Umbrella* are proclaim him as a poet of marginalized and bring forth the paradigm shift in the contemporary Malayalam poetry.

Conclusion:

S. Joseph tries to recover and represent all those nameless and faceless figures, their memories sorrowful experiences through his poetry. His poems meditate on the cruelties of caste while simultaneously speaking of identity crisis with which a Dalit person deals with such cruelties. The question of identity and equality is dominant theme in writings of Dalit writer, S. Joseph. Compared to upper-caste progressive writers, Dalit writer S. Joseph realistically portray their lives, environment and situations. The ultimate purpose of Dalit literature is to ensure the uprooting of caste oppression; it rejects Varna order of Hindu belief. Dalits are nameless and faceless people in dominant Indian culture

REFERENCES:

1. Dr. B. R. Ambedkar. Castes in India: Their Mechanism Genesis and Development, Paper presented at an Anthropology Seminar taught by A. A. Goldenweizer, Columbia University, 9th May 1961.
2. Joseph S. My sister's Bible. New Delhi: Authors. 2016. Print
3. Satyanarayana, K, Susie Tharu. Ed. No Alphabet in sight. New Delhi: Penguin. 2011. Print
4. Poetry. Wikipedia: The Free Encyclopedia, 17 oct 2016
5. Joseph, S. Representing Marginalized in Poetry. Personal Interview. 20 Oct. 2016.

Depiction of Empowered Women Characters in the Novel of Ashok Banker

Dr. Dnyaneshwar S. Chavan

*Assistant Professor, Department of English,
Vidya Vikas Mandal's S.G.Patil
Arts, Science and Commerce College,
Sakri, Dist- Dhule*

Ashok Banker is a renowned post-colonial Indian English writer. Who writes on cross-cultural themes. The *Ramayana Series* written by Ashok Banker which consists the eight-volume series based on the story of the *Ramayana* in English. Ashok Banker has depicted the story with his creativity in the modern sense. He has depicted women characters as empowered personalities. *Sons of Sita* is the last novel in this series. This novel depicts the story of Sita. In the present paper, the female characters in the novel, *Sons of Sita*, is discussed in light of the women empowerment.

Women can be empowered by eliminating violence against them in society. It can be achieved by giving equal status to women in all respects. In this modern world, women are marching towards empowerment. It is not achieved yet but steps are successfully taken in this direction. Sita is considered as the ideal of Indian womanhood. Hence her perspective, her actions, her thinking has influenced the psyche of Indian women. Sita is one of the major characters presented by Ashok Banker in this novel. Her life in the ashram of Sage Valmiki is depicted minutely. She was abandoned by her husband Rama. In a modern sense, it is said that women should be empowered with the weapon of education. But in ancient time, education was imparted in Ashramas. In those days, archery was of prime importance.

Sita and her attendant Nakhudi are portrayed as skilful archers. When a group of people has attacked Valmiki ashram and has started their massacre, Sita and Nakhudi, both fight with the group in order to protect the ashramites. Such kind of the wrong deed that takes the lives of peaceful people is itself a vice. These soldiers destroy the very foundation of devotion. Ashramas are meant to study. In such a situation, the only empowered heart can take the challenge and Sita has proven her capacity. As a woman character, she is not depicted as a delicate woman rather she is presented as a woman who can not only challenge the situation but also

face it positively for a social purpose. To save and protect people is considered to be the duty of each and every real Kshatriya. Sita plays the role of Kshatriya. She has shown through her capacity that she is empowered. Empowered personalities only protect weak people.

Sita is not only fearless on the battlefield but also in the debate. Asking a question on injustices is the reflection of empowered consciousness. Sita possesses it perfectly. That is why she can ask a question to King Rama.

she asks Rama,

Do this and prove to them that to doubt an honest woman is itself a stain on her reputation. To point a finger is itself a sully of honour. To gossip and speak to someone without their being found guilty of any wrongdoing is itself a crime...the world. (Banker, *Sons of Sita* 341) She has emphasised the equality of man and woman in the name of the dharma. In the name of dharma, she does not want to accept the concept of equality. Sita expresses her clear view that after all, she is also a woman before being the queen. She wants justice for her womanhood which stays away from her husband, her soulmate for ten years. In spite of her facing the test, she is punished.

Regarding her love towards Rama, Sita always enshrines Rama in her heart. She always asks his companionship but now she is banished by her love. She is truly dejected by their departure and now she silently but firmly opposes Rama's notion of dharma. Because of his fulfilling dharma, many have sacrificed their whole life. Sita has suffered more. B. V. Ramana rightly observes, "When there is an intense love there is no fear, no other attachment that one which binds that pain is an inseparable and all-absorbing bond"(26).

When Rama says, "Yes. But you serve dharma too. In your own way. Surely you see that?"(Banker, *Sons of Sita* 3) But Sita presents her views of love, "I don't want to serve dharma. I don't want dharma. I just want you"(Banker, *Sons of Sita* 3). That means she puts Rama first and foremost rather than any dharma. Rama for her is more than dharma. It shows her peerless devotion and sense of love towards Rama. Her attitude is not only emotional but also thoughtful. It must be taken into account what Swami Vivekananda says about Sita. He says, "You may exhaust the literature of the world that is past, and future, before finding another Sita. Sita is unique; that character was depicted once and for all. There may have been several Ramas, perhaps, but never more than one Sita! ...Sita" (530).

Sita's behaviour and character always inspire the Indian womanhood. Sita is always considered as the ideal wife. Her ideal hood lies in her pure love for Rama. The unshakable love of Sita towards Rama is an ideal one because, at the end of the novel, when Rama comes to visit Valmiki in order to ask for forgiveness from Maharishi Valmiki for the misdeed by Rama's soldiers. Sita herself is very angry with the incident that has recently taken place. So she cannot just tolerate such as inhuman act. Her love is not limited only to Rama but she loves humanity. Her heart also cries for them who are innocent but killed. It is found only in a human being who is stable within. For getting stability within one has to be empowered not only superficially. It must be inwardly. Sita explores her inner determination. So she is presented herself as the empowered personality. Ashok Banker rightly presented her character so that modern age women should be inspired by Sita's character.

Conclusion :

Ashok Banker has depicted Sita as a strong-hearted character. In spite of all odd situation, she stands firm. She faces all circumstances with her strong determination. Empowerment lies in the attitude also. Man or woman can be empowered within. Her example gives impetus humanity how to live with a stable mindset in spite of any kind of circumstances one has to face. Sita has that capacity hence she is presented as a great symbol of empowerment in this novel.

Work Cited :

- Banker, Ashok. *Sons of Sita*. New Delhi: Wisdom Tree, 2012. Print.
Ramana, B.V. "Bhakti Yoga of Sarojini Naidu- Analysis of Selective Poems." *Academic Research* 7.2 (2013). Print.

Knoevenagel Condensation of Substituted Aldehydes and Active Methylene Compounds Using Ferrite Magnetic Nanoparticles

[†]PRAVINSING S. GIRASE, ^{††}DEEPAK V. NAGARALE, ^{†††}BHIKAN J. KHAIRNAR
AND ^{††}BHATA R. CHAUDHARI*[†]

[†]Department of Chemistry, JET's Z. B. Patil College, Dhule

*^{††}SSVPS's Arts, Commerce and Science College, Shindkheda.

^{†††}Department of Chemistry, VVM's S. G. Patil Arts, Science and Commerce College, Sakri.

^{†††}Department of Chemistry, SSVPS's L. K. Dr. P.R, Ghogrey Science College, Dhule.

Corresponding Authors Email: psgirase65@gmail.com, brc155@gmail.com

Abstract:

Conducting the reactions, using heterogeneous catalysts should compensate some of drawbacks observed in previously reported reactions. In this kind of reaction, the catalyst can be separated by filtration. Magnetite nanoparticles (Fe_3O_4) have attracted much attention in the past decade, due to their unique features including low preparation cost, high thermal as well as mechanical stability and adaptability for large-scale production. Magnetite nanoparticles (Fe_3O_4) can be easily separated from reaction mixture by using an external magnet. We have demonstrated a very simple and highly efficient method for the Knoevenagel reaction of aromatic aldehydes with various active methylene containing compounds to give Knoevenagel products in good to excellent yields at refluxed temperature. In the above research we suggest that the present method of environmentally benign Fe_3O_4 displace all other methods that use various homogeneous catalysts and that are performed at high temperature.

Keywords: Magnetite Nanoparticles, Knoevenagel Condensation, Active Methylene Compounds, Heterogeneous Catalysts

INTRODUCTION:

Today organic synthesis based on magnetic nanomaterial's are found a major role in

many fields including industrial procedure, biotechnology, biomedicine, environmental remediation and especially catalysis[1-2]. Most of these reactions are generally carried out in organic solvents, with a few aqueous phase organocatalytic processes as recent exceptions[3]. Although water is an environmentally benign solvent[4]. The use of environmentally benign solvents like water[5] and absent of organic solvent reactions represent very effective green chemistry[6] methods from economical as well as synthetic point of view[7]. They not only reduce the load of organic solvent but also improve the speed of many organic reactions. Therefore efforts have been made to carry out the Knoevenagel condensation in aq. medium [8]. It was found that the Knoevenagel condensation reaction of aromatic aldehydes with malononitrile or ethyl cyanoacetate take place in aq. medium[9]. The separation and recycling of the catalyst is highly favorable because catalysts are very expensive.

Surface reform via functional group immobilization provides unique prospect to engineer the interfacial properties of solid substrates while holding their mechanical strength and basic geometry. Surface engineering can be attained either by physically adsorbing or chemically creating functional groups onto a suitable matrix. Chemical bonding of functional groups offers a unique advantage since the implanted molecule detachment is prevented due to strong covalent bonding of the molecule to the substrate. Immobilization of molecules on organic/inorganic support has been extensively studied [10] with much attention given to establishment of new covalent bond on the desired surface [11]. There are wide reports [12-13] on immobilization of modifiers like chelate forming organic reagents, polymers, natural compounds, metal salts some microorganisms on solid mediums like ion-exchange resins, cellulose, fibers, sand, clay, zeolites, polymers, metal oxides, activated carbon and highly dispersed silica. Such researches of immobilization of groups or compounds depend on substitution reaction between the surface of the supporting material and the modifiers. An active adsorbent should have good adsorption capacity, chemical stability under experimental

condition and especially high selectivity [14]. Among the different adsorbents, silica gel particularly restrained with various organic compounds with metal chelating ability has received great attention [15-20]. Immobilization of organic functional groups on a siliceous surface has been effectively employed to produce ranges of modified silica. In this process, organic reagent or manufactured organic molecule having the preferred organic functional group is directly attached to the support or to the original chain bonded to the support via sequence of reactions to increase the main chain, where other basic centers can be added to ensure the improvement of a specific adsorption [21].

Conducting the reactions by using heterogeneous catalysts had reduced some of drawbacks observed in previously reported reactions. In this type of reactions, the catalyst can be recovered by filtration and it can be reuse for the next cycle. However, it is worthy to mention in spite of several advantages experienced practically in using of heterogeneous catalysts, due to the nanosized particles used, few limitations to the sustainability are observed [20]. To get around these problems, the use of a heterogeneous catalyst which can be separated practically other than filtration is desirable. Magnetite nanoparticles (Fe_3O_4) have attracted much attention in the past decade due to their unique features including low preparation cost, high thermal and mechanical stability and adaptability for large scale production. In addition, their paramagnetic nature allows their facile and effective separation from the reaction mixture, without using standard filtration, required in separation of heterogeneous catalysts. Magnetite nanoparticles (Fe_3O_4) can be easily separated from reaction mixture by using Just an external magnet [21]. Thus, in recent years, nano- Fe_3O_4 [22] has attracted a great attention as heterogeneous catalyst [23] due to its simple handling, easy recovery by an external magnet [24, 25]. Magnetic nanoparticles (MNPs) have emerged as viable alternatives to conventional materials as robust, readily available, oxidative stability, biological compatibility and high catalytic activities in various organic transformations [26-31]. The nano particles enhance the exposed surface area of the active constituent of the

catalyst [32, 33], thereby increasing the contact between reactants and catalyst dramatically [34–38] these nano-catalysts bridge the gap between homogeneous and heterogeneous catalysis [39], thus preserving the desirable attributes of both systems [40, 41].

We have carried out reaction of various substituted benzaldehyde with acyclic active methylene compounds (malononitrile, ethyl cyanoacetate, ethyl acetoacetate) and cyclic active methylene compounds (barbituric acid and thiobarbituric acid) in presence of ferrite heterogeneous catalyst as shown in **scheme 1**.

Experimental

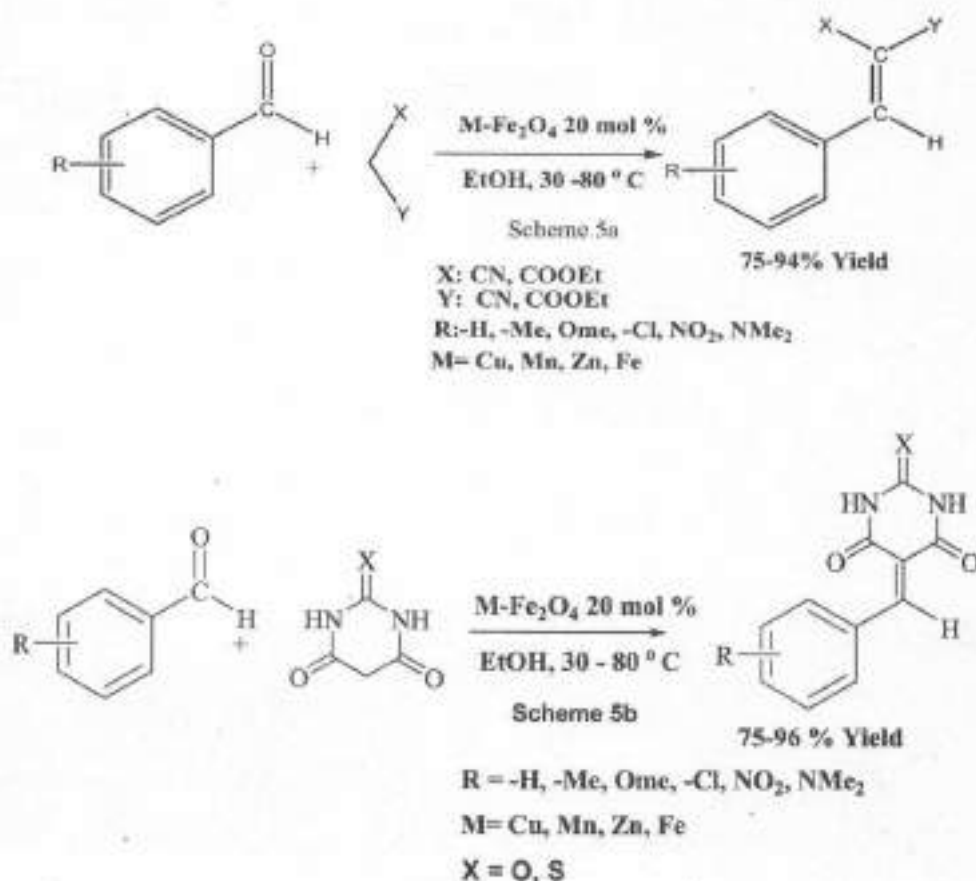
Material and Methods:

Preparation of magnetic Fe_3O_4 nanoparticles (MNPs):

The mixture of $\text{FeCl}_3 \cdot 6\text{H}_2\text{O}$ (5.838 g, 0.022 mol) and $\text{FeCl}_2 \cdot 4\text{H}_2\text{O}$ (2.147 g, 0.011 mol) were dissolved in 100 mL of deionized water in a round bottom flask (250 mL) at room temperature under stirring. Thereafter, 10 mL of aq. NH_3 solution (32%) was then added into mixture within 40 min with vigorous mechanical stirring. Finally the black precipitate solid was collected by magnetic decantation, washed with distilled water until solution becomes neutral, and then washed with ethanol two times. After the performed of procedure the magnetic nano materials have been characterized using an Infrared spectroscopy and the structure of magnetic catalysts was determined by X-ray diffraction (XRD) study. The crystal size of catalyst was checked by scanning electron microscope (SEM).

General procedure:

We have carried out reaction of various substituted benzaldehyde with acyclic active methylene compounds (malononitrile, ethyl cyanoacetate, ethyl acetoacetate) and cyclic active methylene compounds (barbituric acid and thiobarbituric acid) in presence of ferrite heterogeneous catalyst as shown in **scheme 5**.



Scheme-1 M-Ferrite catalyst Knoevenagel condensation (a&b).

Results and Discussion

We have made an effort to develop a catalytic system that would address the limitations of the earlier reported Knoevenagel reactions. During the preliminary studies benzaldehyde (1a) and malononitrile (2a) used as a model system. A sequence of experiment were conducted to optimize a variety of reaction parameters, such as the type of catalyst, catalyst quantity, solvent, temperature and time (Table 1). Initially we developed the paramount magnetically separable catalysts, MFe_2O_4 ($M=Fe^{2+}$, Zn^{2+} , Mn^{2+} and Ni^{2+}), have been synthesized by thermal decomposition and were consequently screened for the model system of reaction as shown in **scheme 5**. Among the catalysts examined, Fe_3O_4 was found to be the best, providing excellent yields of the desired product 3a (Table 1, entries 1-5). We further studied catalysts concentration ranging from 5 to 20mol% rises the yield of product 3a up to 94%, a further increase of catalyst concentration to 25mol% did not improve the yield

of 3a (Table 1 entries 1,2,6). As the solvent have an impact on the overall process, the effect of various solvents (Table 1 entries 2,7-11,13) were examined; the best results was obtained with ethanol which afforded 3a in 94% yield (Table 1 entry 2). We also studied the effect of the temperature and found that the 3a obtained good yield at room temperature for complete consumption of aldehyde. (Table 1 entry 2,12). After optimizing the reaction conditions, we explore the substrate scope of the ferrite catalyzed Knoevenagel condensation of substituted aldehydes with acyclic active methylene compounds (malononitrile, ethyl cyanoacetate, ethyl acetoacetate) and cyclic active methylene compounds (barbituric acid and thiobarbituric acid) for the synthesis of styrene derivatives containing different functional groups. We observed that electron donating as well as electron withdrawing substituents provide remarkable yield of products. Satisfyingly this protocol endured a range of common functional groups such as alkyl, ether, halogen and nitro groups irrespective of the positions. The results of these reactions are summarized in Table 2.

In order to make our catalytic system more economical, we focused on the reusability of Fe_3O_4 catalysts in this condensation reaction. As shown in Table 3, the catalysts shown surprising activity in all three recycles. The completion of the reaction was monitored by TLC. Followed by touching the external magnet to wall of the round bottom flask and the reaction mixture was decant in the small beaker, washed the catalyst with ethanol (3×5ml) and dried it for 1hr at 120°C in oven, then the catalyst was used directly in the next cycle. The catalyst was recycled three times and gives constant yields.

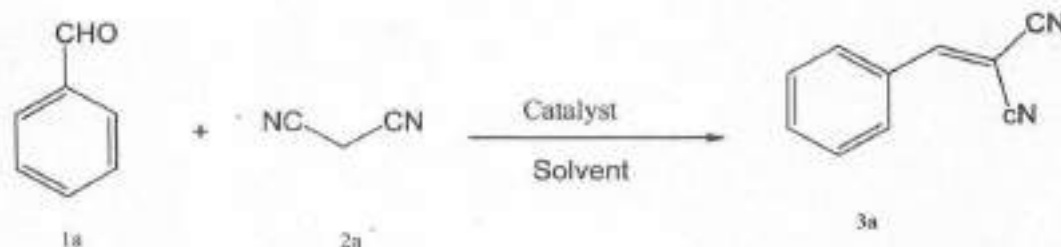
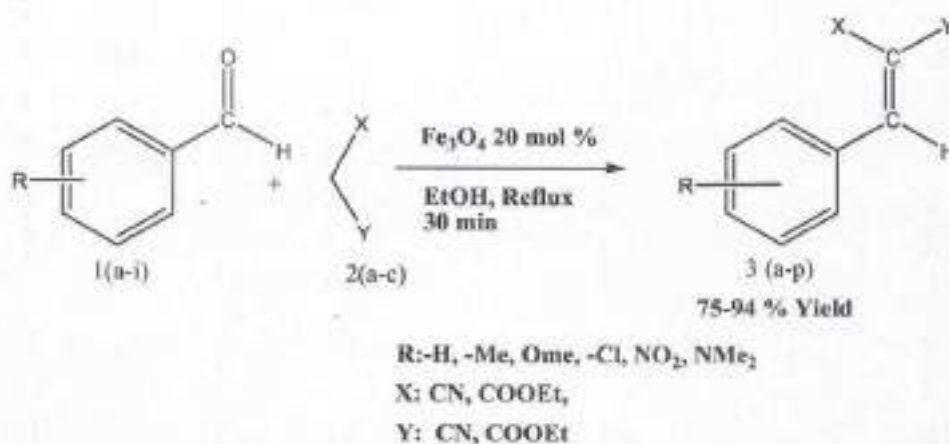


Table 01: The reaction parameters study

Entry	Catalyst	Catalyst (mol%)	Solvent	Temp (°C)	Time (min)	Yield (%)
1	--	--	EtOH	Reflux	120	19
2	Fe ₃ O ₄	20	EtOH	Reflux	30	94
3	ZnFe ₂ O ₄	20	EtOH	Reflux	30	85
4	MnFe ₂ O ₄	20	EtOH	Reflux	30	88
5	NiFe ₂ O ₄	20	EtOH	Reflux	30	86
6	Fe ₃ O ₄	25	EtOH	Reflux	30	94
7	Fe ₃ O ₄	20	ACN	Reflux	30	87
8	Fe ₃ O ₄	20	H ₂ O	Reflux	30	46
9	Fe ₃ O ₄	20	MeOH	Reflux	30	64
10	Fe ₃ O ₄	20	CHCl ₃	Reflux	30	26
11	Fe ₃ O ₄	20	PEG-400	80	30	43
12	Fe ₃ O ₄	20	EtOH	60	30	81
13 ^c	Fe ₃ O ₄	20	--	80	30	59

*Reaction conditions:

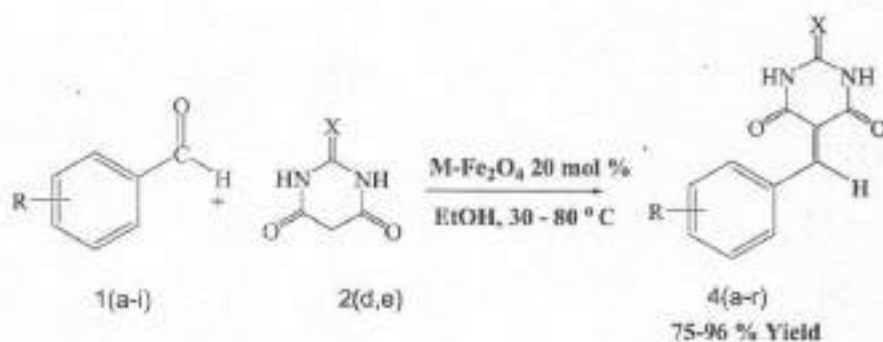
Benzaldehyde (1mmol), Malononitrile (1 mmol), Solvent (3 mL), ^bIsolated yield, ^cNeat reaction**Table 2: Substrate study catalyzed by Fe₃O₄**

Entry	Aldehyde (-R)	X	Y	Product	Yield (%)	M.P. (°C)
1.	-H	CN	CN	3a	94	82-84
2.	-H	CN	COOEt	3b	91	47-49
3.	-H	COOEt	COOEt	3c	90	Oil
4.	4-Cl	CN	CN	3d	89	162-164

5.	4-Cl	COOEt	COOEt	3e	90	84-86
6.	2-Cl	CN	CN	3f	82	96-98
7.	2-Cl	CN	COOEt	3g	86	Oil
8.	4-NMe ₂	CN	CN	3h	84	186-188
9.	4-NMe ₂	CN	COOEt	3i	86	124-126
10.	4-NO ₂	CN	CN	3j	94	158-169
11.	4-NO ₂	CN	COOEt	3k	93	168-170
12.	3-NO ₂	CN	CN	3l	90	104-106
13.	2-NO ₂	CN	CN	3m	90	140-142
14.	3-OMe	COOEt	COOEt	3n	80	240-242
15.	3,4-di OMe	CN	CN	3o	86	142-144
16.	3,4-di OMe	CN	COOEt	3p	82	156-158

^aReaction conditions:

Aldehyde (1 mmol), acyclic active methylene compound (1 mmol), Ethanol(3 mL), ^bIsolated yield,



R = -H, -Me, Ome, -Cl, NO₂, NMe₂

X = O, S

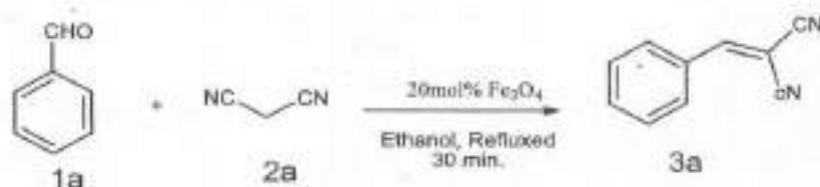
Entry	Aldehyd e (-R)	Active methylene	Product	Yield (%)	M.P. (°C)
1	-H	Barbituric acid	4a	96	270-272
2	2-Cl	Barbituric acid	4b	90	220-222
3	4-Cl	Barbituric acid	4c	93	232-234
4	4-NMe ₂	Barbituric acid	4d	88	276-278
5	4-NO ₂	Barbituric acid	4e	96	>290
6	3-NO ₂	Barbituric acid	4f	92	256-258
7	2-NO ₂	Barbituric acid	4g	92	258-260

8	3-OMe	Barbituric acid	4h	93	268-270
9	3,4-di-O Me	Barbituric acid	4i	90	
10	-H	Thiobarbituric acid	4j	96	271-272
11	2-Cl	Thiobarbituric acid	4k	90	234-236
12	4-Cl	Thiobarbituric acid	4l	94	288-290
13	4-NMe ₂	Thiobarbituric acid	4m	90	254-256
14	4-NO ₂	Thiobarbituric acid	4n	96	240-242
15	3-NO ₂	Thiobarbituric acid	4o	92	246-248
16	2-NO ₂	Thiobarbituric acid	4p	93	240-242
17	3-OMe	Thiobarbituric acid	4q	90	236-238
18	3,4-di-O Me	Thiobarbituric acid	4r	89	

^aReaction conditions: Aldehyde (1 mmol), cyclic active methylene compound (1 mmol), Ethanol(3 mL),

^bIsolated yield,

Table 3: Recycling of Catalyst



Entry	Run No.	Yield (%)
1	1 st	94
2	2 nd	88
3	3 rd	76

After the performed of synthesis procedure of the magnetic nano materials have been characterized using an Infrared spectroscopy and the structure of magnetic catalysts was determined by X-ray diffraction (XRD) study. The crystal size of catalyst was checked by scanning electron microscope (SEM).

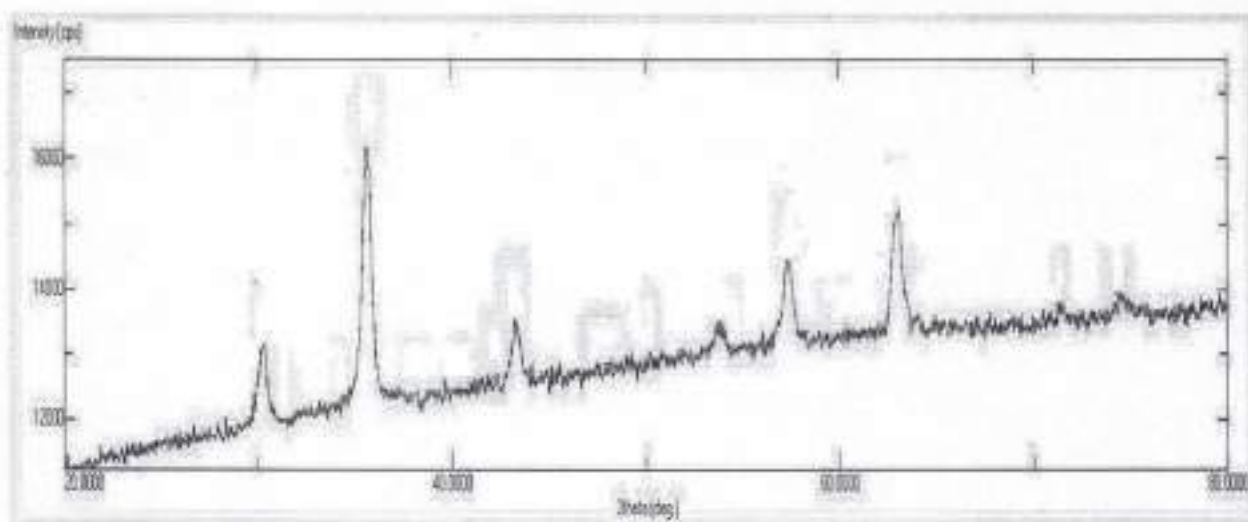


Figure 1: X-ray diffraction (XRD) study of ferrite catalyst

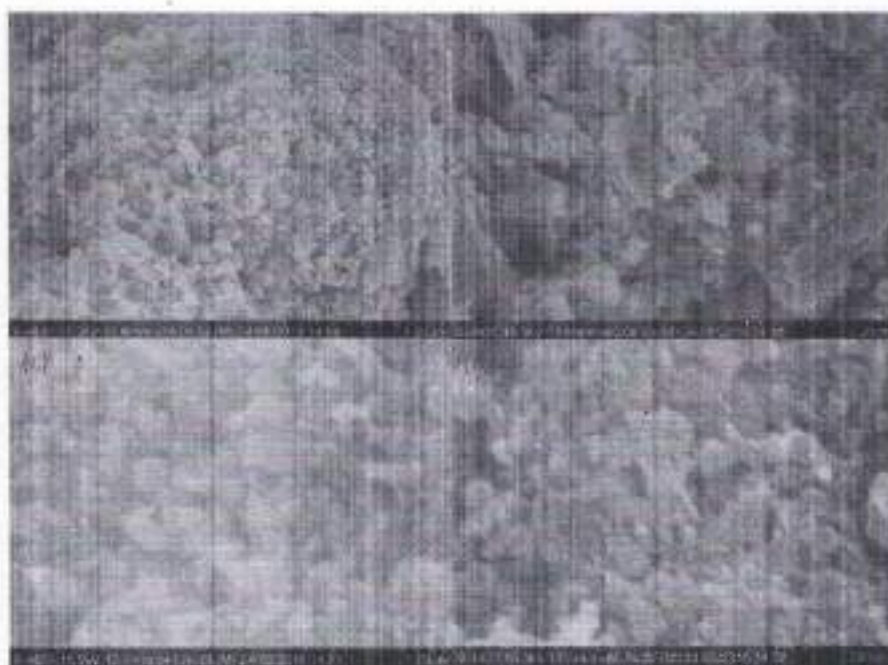


Figure 2: Scanning Electron Microscope (SEM) images of ferrite catalyst

Synthesis of styrene compounds:

A mixture of benzaldehyde (1 mmol), malononitrile (1 mmol), Fe_3O_4 (20 mol%) in ethanol (3 mL) was heated at reflux for 30 min. Progress of the reaction was monitored by TLC. The catalyst was recovered by simple magnetically decantation of reaction mixture by pouring in to ice water and the product was filter and purified by aq. ethanol. The recovered catalyst was washed with ethanol and dried in oven. The catalyst is

ready for next cycle of reaction.

Spectral data of some selected compounds:

1) 2-(2-Chlorobenzylidene)malononitrile (3d)

M.P.: 94-96°C. ¹H NMR (DMSO-d₆) δ: 8.295(s, 1H), 8.205(d, 1H, J = 8.0Hz), 7.576(d, 2H, J=3.6Hz), 7.495 – 7.435(m, 1H); C¹³: 156.05, 136.35, 135.04, 130.72, 129.51, 129.07, 127.80, 113.22, 111.91, 85.81. IR (cm⁻¹): 3055, 2927, 2222, 1907, 1587, 756, 619;

2) 2-(4-chlorobenzylidene) malononitrile (3f).

M.P 162-164°C ;¹H NMR (DMSO-d₆) δ: 7.880(d, 2H, J=8.4Hz), 7.760(s, 1H), 7.545(d, 2H, J=8.4Hz); C¹³: 158.30, 141.18, 131.86, 130.09, 129.28, 113.45, 112.35, 83.37. IR: 3030, 2227, 1955, 1558, 779, 617

3) 2-(2-nitrobenzylidene)malononitrile (3m).

M.P 140-142°C ;¹H NMR (DMSO-d₆) δ: 8.474(s, 1H), 8.393 - 8.369(m, 1H), 7.931-7.891(m, 1H), 7.855-7.816(m, 2H), C¹³: 158.83, 146.80, 134.98, 133.44, 130.49, 126.72, 125.88, 112.24, 110.98, 88.55. IR: 3047, 2239, 1975, 1591, 1523, 1440

4) 2-(3,4-dimethoxybenzylidene)malononitrile (3o).

M.P.: 142-144°C ;¹H NMR (DMSO-d₆) δ: 7.683 (t, 2H, J = 2.0 & 12.0Hz), 7.399(q, 1H, J= 2.4 & 6.0 Hz), 7.283(s, 1H), 4.003(s 3H), 3.953(s, 3H); C¹³: 159.15, 154.28, 149.56, 128.22, 124.29, 114.42, 113.59, 111.10, 11, 0.78, 78.45, 56.34, 56.09. IR: 2933, 2833, 2218, 1909, 1467, 1251, 1147

5)(Z)-ethyl 2-cyano-3-(3,4-dimethoxybenzylidene)acrylate (3p).

M.P. 156-158°C ;¹H NMR (DMSO-d₆) δ: 8.162 (s, 1H), 7.808(s, 1H), 7.482 (d, 1H, J = 7.6 Hz), 6.955(d, 1H, J = 7.6 Hz), 4.377 (q, 2H, J = 7.2 Hz), 3.900(s, 6H), 3.400(t, 3H, J= 7.2 Hz); C¹³: 163.11, 154.70, 153.68, 149.28, 127.89, 124.61, 116.36, 111.65, 110.95, 99.38, 62.46, 56.15, 56.05, 14.21. FT-IR: 3003, 2845, 2222, 1928, 1710, 1512, 1159, 1097

Characterization of cyclic active methylene compounds:

1) 5-benzylidenepyrimidine-2,4,6(1H,3H,5H)-trione(4a).

M.P. 270-272°C ; ¹H NMR (DMSO-d₆) δ: 11.735(bs,2H), 7.913(t,1H, J =6.8 &1.6 Hz), 7.615 (t,1H, J= 6.8 & 7.6Hz),7.180(t,1H, J= 7.6 Hz), 7.075(t,1H, J= 7.2 Hz), 7.015(d,2H, J = 8.0 Hz), 5.946(s,1H); C¹³: 193.74, 173.30, 163.50, 142.89, 136.64, 135.07, 133.89, 129.96, 129.63, 128.61, 128.17, 126.99, 125.44, 96.35, 31.06.FT-IR: 3512, 3313,3074, 2845, 1880, 1701, 1581,1438

2) 5-(3-methoxybenzylidene)pyrimidine-2,4,6(1H,3H,5H)-trione(4h)

M.P. 268-270°C ; ¹H NMR (DMSO-d₆) δ: 11.407(s, 1H), 11.256(s, 1H), 8.259(s, 1H), 7.845(t, 1H, J = 2.0Hz); 7.611(q, 1H, J = 7.2,0.8Hz &.0.4Hz;), 7.395(t, 1H, J = 8.0 Hz), 7.142 – 7.117(m, 1H,) 3.797(s,3H);. C¹³: 163.87, 162.09, 159.08, 154.98, 150.64, 134.31, 129.59, 126.55, 119.74, 118.91, 118.07,55.68. IR:3518, 3458, 3007, 2828, 1938, 1660, 1570, 1444, 1163

3)5-(2-chlorobenzylidene)-dihydro-2-thioxopyrimidine-4,6(1H,5H)-dione (4k)

M.P.: 234-236°C ;¹H NMR (DMSO-d₆) δ: 11.491(s, 1H), 11.272(s, 1H), 8.292,(s, 1H), 7.747 (t, 1H, J= 6.8 & 0.8 Hz;), 7.556, (q,1H, J= 1.2Hz & 6.8Hz;), 7.497 – 7.456, (m, 1H), 7.392 - 7.352, (m,1H);C¹³: 163.12, 161.38, 150.69, 150.17, 133.64, 132.74, 132.44, 132.40, 129.35, 126.80, 122.26.FT-IR: 3633, 3388, 3076, 1718, 1583, 1215, 1049,725, 642

4)5-(3-methoxybenzylidene)-dihydro-2-thioxopyrimidine-4,6(1H,5H)-dione (4q) M.P.: 236-238°C ;

¹H NMR (DMSO-d₆) δ: 12.477(s,1 H), 12. 357(s,1H), 8.271(s, 1H), 7.892(s, 1H), 7.676 -7.657(d,1H, J= 7.6Hz),7.430 7.390(m,1H, J = 8.0Hz), 7.172-7.147, (m,1H), 3.803 (s, 3H);C¹³: 179.02, 162.18, 159.94, 159.12, 155.88, 134.29, 129.68, 126.92, 119.80, 119.45, 118.31, 55.72.IR: 3485, 3070, 2904, 1944, 1701,1651, 1548,1228, 1151, 1047

5)(3,4-dimethoxybenzylidene)-dihydro-2-thioxopyrimidine-4,6(1H,5H)-dione (4r) M.P

°C, ¹H NMR (DMSO-d₆) δ: 12.403- 12.300(d, 2H), 8.438(d, 1H, J= 1.6Hz), 8.275(s,1H), 7.969 (t, 1H, J= 1.2 & 7.2 Hz), 7.157(q, 1H, J = 8.0 & 9.2 Hz), 3.830(s,6H); C¹³: 191.86,

178.65, 162.76, 160.60, 156.97, 154.70, 154.66, 149.63, 148.35, 132.84, 130.09, 126.60, 125.91, 117.43, 115.79, 111.74, 111.69, 109.87, 56.42, 56.35, 55.98, 55.93. IR: 3577, 3363, 3138, 2926, 1923, 1712, 1685, 1535, 1201, 1018

Conclusion:

We have demonstrated a very simple and highly efficient method for the Knoevenagel reaction of aromatic aldehydes with various active methylene containing compounds to give Knoevenagel products in good to excellent yields at refluxed temperature. In the above research we suggest that the present method of environmentally benign Fe_3O_4 displace all other methods that use various homogeneous catalysts and that are performed at high temperature.

Acknowledgment:

The authors are thankful to the Management, Principal & Head (Dept. of Chemistry), JET's Z. B. Patil College, Dhule for providing the lab facilities and constant encouragement. One of the author Dr. B. R. Chaudhari is thankful to the University Grant Commission, Western Zone Poona (M.S.) for providing the financial support through minor research project. Sanction File no.47-258/12(WRO) dated 25.02.2013.

References:

1. Kurt Rorig, *J. Am. Chem. Soc.*, 1951, 73, 3, 1290-1292.
2. Radoslaw Mrowczynski, ab Alexandrina and Jurgen Liebscher *RSC Adv.*, 2014, 4, 5927
3. a) A. P. Brogan, T. J. Dickerson and K. D. Janda, *Angew. Chem., Int. Ed.*, 2006, 45, 8100; (b) Y. Hayashi, S. Samanta, H. Goto and H. Ishikawa, *Angew. Chem., Int. Ed.*, 2008, 47, 6634; (c) J. Huang, X. Zhang and D. W. Armstrong, *Angew. Chem., Int. Ed.*, 2007, 46, 9073.
4. C. J. Li and L. Chen, *Chem. Soc. Rev.*, 2006, 5, 68.
5. Lindstrom, U. M. *Chem. Rev.* 2002, 102, 2751-2772

6. Bigi, F.; Conforti, M.L.; Maggi, R.; Piccinno, A.; Sartori, G. *Green Chem.* 2001,3, 101–104;
7. Cao, Y.-Q.; Dai, Z.; Zhang, R.; Chen, B.-H. *Synth. Commun.* 2004, 34, 2965– 2971.
8. Jin, T.-S.; Zhang, J.-S.; Wang, A.-Q.; Li, T.-S. *Synth. Commun.* 2004, 34, 2611–2616.
9. Wang, S.H.; Ren, Z.J.; Cao, W.G.; Tong, W.Q. *Synth. Commun.* 2001,31 (5), 29.
10. Perez-Quintanilla, D.; Sanchez, A.; delHierro, I.; FaJardo, M.; Sierra, I. *J. Colloid. Interface Sci.*, 2007, 313, 551. 228) Goubert-Renaudin, S.; Gaslain, F.; Marichal, C.; Lebeau, B.; Schneider, R.; Walcarius, A. *New J. Chem.*, 2009, 33, 528.
11. Muresanu, M.; Reiss, A.; Parvulescu, V.; Stefanescu, I.; David, E. *RevistaChim.*, 2007, 58, 502.
12. Bagshaw, S. A.; Prouzet, E.; Pinnavaia, T. *J. Science*, 1995, 269, 1242.
13. Prouzet, E.; Pinnavaia, T. *J. Angew. Chem. Int. Edit.*, 1997, 36, 516.
14. Zaporohets, O. A.; Gover, O. M.; Sukhan, V. V. *Russ. Chem. Rev.*, 1997, 66, 636.
15. Tong, A.; Akama, Y.; Tanaka, S. *Analyst*, 1990, 115, 947.
16. KocJan, R. *Microchim. Acta*, 1999, 131, 153.
17. Kim, J. S.; Yi, J. *Sep. Sci. Technol.*, 1999, 34, 2957. 134) Prado, A. G. S.; Airoidi, C. *Anal. Chem. Acta*, 2001, 432, 201.
18. Lee, B. I.; Paik, U. *J. Mater. Sci.*, 1992, 27, 5692.
19. Trans, P.; Denoyel, R. *Langmuir*, 1996, 12, 2781.
20. Van der Voort, P.; Vansant, E. F. *Polish J. Chem.*, 1997, 71, 550.
21. Pyell, U.; Stork, G. *Fresenius, J. Anal. Chem.*, 1992, 342, 342
22. Ali Maleki, SepideAzadegan, *InorgOrganometPolym*, 10.1007/s10904-017-0514-z
23. Udayabhaskar, R.; Sreekanth, P.; Karthikeyan, B. *Optical and Nonlinear Optical Limiting Properties of AgNi Alloy Nanostructures. Plasmonics* 2016, 1–6.

24. Zhang, Y.; Chu, W.; Foroushani, A. D.; Wang, H.; Li, D.; Liu, J.; Barrow, C. J.; Wang, X.; Yang, W. New Gold Nanostructures for Sensor Applications: A Review. *Materials* 2014, 7, 5169–5201
25. Suresh, S.; Arivuoli, D. Nanomaterials for Nanolinear Optical (NLO) Applications: A Review. *Rev. Adv. Mater. Sci.* 2012, 30, 243–253.
26. Crudden, C. M.; Sateesh, M.; Lewis, R. Mercaptopropyl-Modified Mesoporous Silica: A Remarkable Support for the Preparation of a Reusable, Heterogeneous Palladium Catalyst for Coupling Reactions. *J. Am. Chem. Soc.* 2005, 127, 10045–10050.
27. Raveendran, P.; Fu, J.; Wallen, S. L. A simple and "green" method for the synthesis of Au, Ag, and Au-Ag alloy nanoparticles. *Green Chem.* 2006, 8, 34–38
28. Salis, A.; Fanti, M.; Medda, L.; Nairi, V.; Cugia, F.; Piludu, M.; Sogos, V.; Monduzzi, M. Mesoporous Silica Nanoparticles Functionalized with Hyaluronic Acid and Chitosan Biopolymers. Effect of Functionalization on Cell Internalization. *ACS Biomater. Sci. Eng.* 2016, 2, 741–751.
29. He, F.; Zhao, D. Preparation and Characterization of a New Class of Starch-Stabilized Bimetallic Nanoparticles for Degradation of Chlorinated Hydrocarbons in Water. *Environ. Sci. Technol.* 2005, 39, 3314–3320.
30. Polshettiwar, V.; Len, C.; Fihri, A. Silica-supported palladium: Sustainable catalysts for cross-coupling reactions. *Coord. Chem. Rev.* 2009, 253, 2599–2626.
31. Salame, C.; Aillerie, M.; Papageorgas, P.; Karnib, M.; Kabbani, A.; Holail, H.; Olama, Z. Technologies and Materials for Renewable Energy, Environment and Sustainability (TMREES14–EUMISD) Heavy Metals Removal Using Activated Carbon, Silica and Silica Activated Carbon Composite. *Energy Procedia* 2014, 50, 113–120.
32. Ketchie, W. C.; Murayama, M.; Davis, R. J. Selective oxidation of glycerol over carbon-supported AuPd catalysts. *J. Catal.* 2007, 250, 264–273.

33. Tsoncheva, T.; Genova, I.; Paneva, D.; Dimitrov, M.; Tsyntsarski, B.; Velinov, N.; Ivanova, R.; Issa, G.; Kovacheva, D.; Budinova, T.; Mitov, I.; Petrov, N. Cobalt- and iron-based nanoparticles hosted in SBA-15 mesoporous silica and activated carbon from biomass: Effect of modification procedure. *Solid State Sci.* 2015, 48, 286–293.
34. Lengke, M. F.; Fleet, M. E.; Southam, G. Synthesis of palladium nanoparticles by reaction of filamentous cyanobacterial biomass with a palladium(II) chloride complex. *Langmuir* 2007, 23, 8982–7.
35. Iranpoor, N.; Firouzabadi, H.; Riazi, A.; Shakerpoor, A. Phosphorylated PEG (PPEG) as a new support for generation of nano-Pd(0): application to the Heck–Mizoroki and Suzuki–Miyaura coupling reactions. *Appl. Organomet. Chem.* 2013, 27, 451–458.
36. Lim, Y.; Kim, S. K.; Lee, S.-C.; Choi, J.; Nahm, K. S.; Yoo, S. J.; Kim, P. One-step synthesis of carbon-supported Pd@Pt/C core-shell nanoparticles as oxygen reduction electrocatalysts and their enhanced activity and stability. *Nanoscale* 2014, 6, 4038–4042.
37. Clapham, B.; Reger, T. S.; Janda, K. D. Polymer-supported catalysis in synthetic organic chemistry. *Tetrahedron* 2001, 57, 4637–4662.
38. Zhu, G.; Graver, R.; Emdadi, L.; Liu, B.; Choi, K. Y.; Liu, D. Synthesis of zeolite@metal-organic framework core-shell particles as bifunctional catalysts. *RSC Adv.* 2014, 4, 30673–30676.
39. Yasukawa, T.; Miyamura, H.; Kobayashi, S. Cellulose-supported chiral rhodium nanoparticles as sustainable heterogeneous catalysts for asymmetric carbon-carbon bond-forming reactions. *Chem. Sci.* 2015, 6, 6224–6229.
40. Stephen, Z. R.; Kievit, F. M.; Zhang, M. Magnetite nanoparticles for medical MR imaging. *Mater. Today* 2011, 14, 330–338.
41. Baeza, A.; Guillena, G.; Ramon, D. J. Magnetite and Metal-Impregnated Magnetite Catalysts in Organic Synthesis: A Very Old Concept with New Promising Perspectives. *ChemCatChem* 2016, 8, 49–67.

42. Anu/ K. Rathi, RadekZboril, Ra/ender S. Varma, and Manoj B. Gawande,
10.1021/bk-2016-1238.ch002
43. A.T. Taher, H.H. Georgey, H.I. El-Sabbagh, Novel 1,3,4-heterodiazole analogues:
Synthesis and in-vitro antitumor activity, *Eur. J. Med. Chem.* 47 (2012) 445–451.
44. N. Swathi, T. Kumar, K. Haribabu, C. Subrahmanyam, Synthesis and biological evaluation
of substituted thiazolamines, imidazo[2,1-b]thiazol-6(5H)-ones,
thiazolo[3,2-a]pyrimidin-5-ones and thiazolythioureas, *Indian J. Heterocycl. Chem.* 21
(2012) 263–268.
45. A. Andreani, A. Leoni, A. Locatelli, R. Morigi, M. Rambaldi, M. Recanatina, V.
Garaliene, Potential antitumor agents. Part 291: Synthesis and potential coanthracyclinic
activity of imidazo[2,1-b]thiazoleguanylhydrazones, *Bioorg. Med. Chem.* 8 (2000)
2359–2366.
46. A. Locatelli, S. Cosconati, M. Micucci, A. Leoni, L. Marinelli, A. Bedini, P. Ioan, S.M.
Spampinato, E. Novellino, A. Chiarini, R. Budriesi, Ligand based approach to L-type
calcium channel by imidazo[2,1-b]thiazole-1,4-dihydropyridines: from heart activity to
brain affinity, *J. Med. Chem.* 56 (2013) 3866–3877

**Vidya Vikas Mandals
Sitaram Govind Patil Arts,
Science and Commerce College,
Sakri Tal. Sakri Dist. Dhule 424 304**



**NAAC
ACCREDITED**

**विद्या विकास मंडळाचे,
सिताराम गोविंद पाटील कला,
विज्ञान आणि वाणिज्य महाविद्यालय,
साक्री ता. साक्री जि. धुळे ४२४ ३०४**

Affiliated to Kavayitri Bahinabai Chaudhari North Maharashtra University, Jalgaon

Website : www.sgpcsakri.com

Email : vidyavikas2006@rediffmail.com

Ph : 02568-242323

3.3.2.1 Research Paper Published in UGC Care Listed Journals

A Geography Analysis of Sex Ratio: A Case Study of Nandurbar District (M.S.)

Dr. M. M. Saindane
Associate Professor
Head, Department of Geography
S. G. Patil Arts, Commerce & Science College
Sakri dist. Dhule
saindanemanohar@yahoo.in

Abstract

Sex ratio is an important factor for determining the death rate of an any population. It is an important component of population which is demographically significant and reflect socio-economy and cultural pattern of society. Not only the demographer and the sociologist but also the policy makers, planners, researchers and the society in general are also interested to know the sex ratio and the variation in it. As per the past in census 2011 also the district has recorded a better sex ratio of 978. In the present paper an attempt has been made to throw the light on sex ratio of the study region. For this purpose sex ratio of last four decades is considered. As per 2011 census sex ratio for the district was 978.

Keyword : Sex ratio, male, female, population, higher, lower.

STUDY REGION

Nandurbar is one of the tribal district of Maharashtra. The study area situated at north-western tip of Maharashtra state. The ancient name of the region was Rasika. The extent of study area 21°50' to 22°17' N latitude and 73° 31' to 74° 50' longitude. The geographical area of this district is 5034.23 Sq.km. The entire district forms the part of Tapi valley border by Satpura on north, boundary of Gujarat state on the waste district of Dhule on south M.P. and Dhule on the east. It is a part of Deccan plateau. As per 2011 census Nandurbar district population was 1648295. The study region contributes 1.63 % of total geographical area of Maharashtra state as per 2011 census. Physiographical the study region falls under the Tapi - Purna valley there is considerable

variation in relief and drainage characteristic within the study region. The district can be divided into three major groups of landforms

1. The northern Satpura ranges
2. The central Tapi river valley
3. The south offshoots of Sahyadri hills.

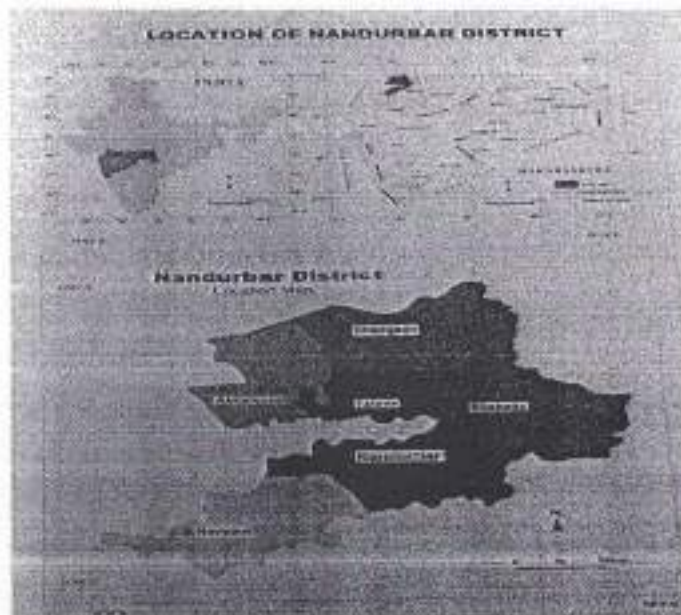
OBJECTIVE

The main objective of the present study is to study sex ratio of this region.

DATABASE AND METHODOLOGY

The present work is based on secondary data. The secondary data is obtained from the district census handbook of Dhule and Nandurbar district of 1981 to 2011.

For the present study data regarding is obtained from secondary data. - source i.e.Dhule and Nandurbar district census and socio-economic abstract, research, journal, reference books and articles are presented in the form of tables and figures.



SEX RATIO

Sex ratio is important factor for determining the death of rate on any population. Women generally have lower death rate than men at age at most countries. If the females constitute more than half of the population, the total death rate is considerable affected.

Sex ratio is defined as the number of females per 1000 males, is an important social indicator to measure the extent to prevailing equality between males and females in a society at given point of time. The sex ratio indicates the relative proportion of males and females in population of sex ratio composition of population is one of the most basic aspects of all demographic characteristic. The sex ratio influences the births, deaths, marriage and economic opportunities characteristic are influenced by sex ratio. The tehsilwise sex ratio is calculated and given in the table no. 1 and fig. no.

Table no. 1
NANDURBAR DISTRICT TAHASIL WISE SEX-RATIO

Sr. No.	Name of Tehsil	Decades			
		1981	1991	2001	2011
1	Akkalkuva	1001	983	959	926
2	Akarani	1001	992	1008	999
3	Taloda	985	991	985	1004
4	Shahada	971	956	967	984
5	Nandurbar	966	966	967	983
6	Navapur	998	992	994	1017
	District	982	975	977	978

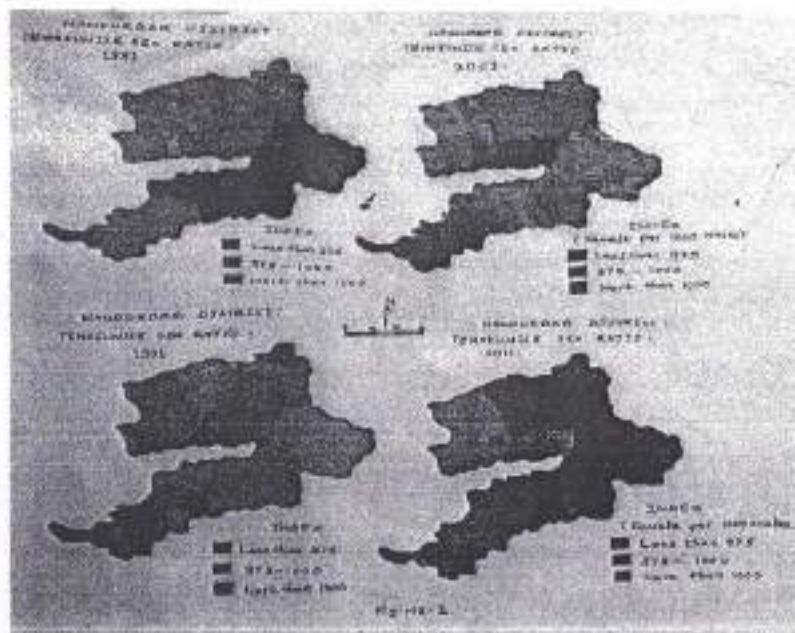
(Source - Census 1981, 1991, 2001 and 2011)

In the study region there is variation in the sex ratio from 1981. In every census the sex ratio of the study region is in between 975 to 982. In Akkalkuva tehsil the sex ratio is forever lower than the district total sex ratio.

According to the census of 1981, the average sex ratio is 982 female per thousand male. The tehsilwise sex ratio varied from 966 to 1001. This reveals that the sex ratio is unevenly distributed all over the region. One remarkable thing that the sex ratio is higher and equal in this region.

According to the census 2011, the average sex ratio is 978. The tehsilwise sex ratio varied from 926 to 1017 per thousand male. This reveals that the sex ratio is very unevenly distributed all over the region. Tehsilwise sex ratio is Akkalkuwa-926, Akrani-999, Taloda-1004, Shahada-984, Nandurbar-983 and Navapur-1017. In the tehsil Navapur (1017) is a highest sex ratio in this study region and the lowest sex ratio in Akkalkuwatehsil (926) respectively.

Overall the statistic information between from 1981 to 2011 all four decades Navapurtehsil has highest sex ratio (1017) and Akkalkuwa tehsil is lowest sex ratio in this study region.(926)



CONCLUSION

According to the above research, according to the census of 1981, the sex ratio of Nandurbar District was 982, but the census of 1991 the sex ratio came to 975, which is mean the sex ratio decrease by 7point in the decades. According to the 2001 and 2011 census the sex ratio of Nandurbar District is slowly increasing. In fact, according to the 2001 census, Akrani taluka has the highest sex ratio of 1008 while Nandurbar and Shahada Taluka have the same sex ratio of 967 and the lowest.

According to the census Navapur taluka has the highest sex ratio in 2011 and all talukas and district have the highest sex ratio in four decades, but akkalkuwa taluka has the lowest sex ratio in all four decades. Lack of education, malnutrition of children, consequence of social and economic situation and low literacy rate also reflected in the gender into decreased.

The ultimate effect of above mentioned reasons is shown in the improvement of sex ratio of Nandurbar district. In fact, the female rate is observed lower because the female psyche is not occupied by modern day progress in term of education.

REFERENCES

1. Ahmed D.A. (2010) "Population Geography" Omega publication, New Delhi.
2. Census of India 1981, 1991, part A&B District census handbook Dhule -1991.
3. Census of India 2001 & 2011 Maharashtra, District census handbook Series -28 part 12 A
4. Ghosh B.N. Fundamentals of population geography, Sterling Publisher private limited New Delhi Pp.133
5. Patil S. B. Chittan R.S.- Geographical Analysis of sex ratio in Dhule District

Forest Management and Water Management “: A Case Study in Baripada, taluka Sakri Dist. Dhule

Paper Submission: 05/03/2021, Date of Acceptance: 21/03/2021, Date of Publication: 22/03/2021

Abstract

The concept of resource management is very important in today's world. Resources are extremely important in human life. Because of the daily wood chopping, urbanization, shifting cultivation, carelessness and lack of planning etc. Resources are being depleted due to various reasons; this includes forest resources or water resources.

In the present research paper, Baripada is tribal pada in sakri taluka. Under the guidance of shri. Chaitram Pawar, a study has been done on the excellent management of forest and water resources in the environment by creating awareness among the local people.

Keywords: Concept Management, Water Management, Forest Management, Deforestation, Desertification, Urbanization.

Introduction

Humans have been dependent on the environment since ancient time so humans had a very close relationship with the environment. Trying to unravel the mystery of nature, there was a belief that we can change the environment beyond any limit that was the human understanding. This includes deforestation, Desertification, Urbanization etc. In the name of development excessive of water, Soil erosion about information due to incomplete information of environmental studies. Therefore the study of environment has become more necessary and necessary than ever before, so the study of forest management and water management has become necessary.

Study Area

Baripada a remote forest in Sakri taluka of Dhule district. Baripada is located on the border of Dhule, Nashik and Dang districts.

Objective of the Study

1. To discover and study forest management techniques.
2. To know and study how water management is done.

Hypothesis

To find out what forest management techniques are used under the guidance of Shri. Chaitram Pawar and with the help of local people.

Research Methodology

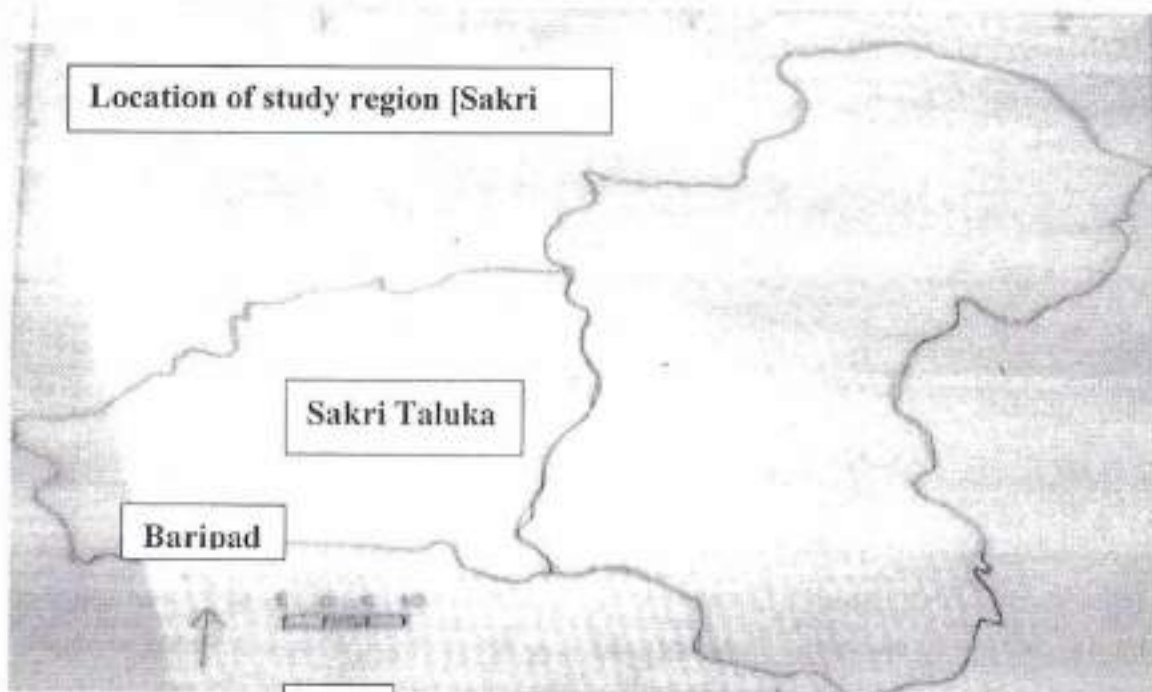
The primary and secondary information is considered in the present research paper.

A deserted village before 1992, in the desert malran, There is not a drop of water in the well, there is no address for green tree up to the hillside, there is no crop in agriculture, and crops do not have water we had to depend on the neighboring village for drinking water. In the village illiteracy addiction family strife, Uncleanliness, Distance between people and terrible poverty. Such in the condition of this village.



M. M. Saindane

Head,
Associate Professor,
Dept. of Geography,
S.G.Patil Arts, Com. and Sci.
College,
Sakri, India



Today, however the people in the village have changed. Shri. Chaitram Pawar was the first post graduate in the village. There is a job opportunity and this job is not accepted. Because they had a mindset to work differently. This person belongs to an illiterate person in the village forest and water management with the help of intellect and hard work. Baripada is a prime example. Baripada has 94 houses, 713 population. This project was built on 1100 acres of land.

Analysis of Forest Management

Forest is an integral part of tribal life. Since 1990, the village of Baripada has undertaken the forest conservation through public participation. The axe ban and grazing ban were given priority for this a local forest Ranger was formed. Women were also given priority in this committee. The rules were made. It was a bold decision to implement it from his own home.

They follow the rules:

1. Cutting down a green tree in the forest will be penalized.
2. Bullock carts are strictly prohibited in the forest.
3. It is forbidden to cut wood for the forest.
4. If caught stealing a reward will be given.
5. For firewood, once a year a dried tree is cut down and wood is brought to the head.

A fine of Rs 1051 especially if you found cutting down tree. A fine of Rs 751 will be levied for taking a bullock cart through the forest. A fine of Rs 551 is found for breaking and entering. A variety of such fine were imposed. The result was that the trees in the forest were protected and the chirping of 42 kinds of birds began to be heard. The 50 year old fuel problem of the village has been solved. Deforestation led to a significant increase in supplementary production. For example wax, honey, forest medicine plants etc.

Analysis of Water Management

The people of this village dug 20 feet long

have been constructed by the villagers. Dug flat variables in a row. As the result the water level of the wells in the village increased. Soil erosion is stopped and soil fertility increase. In 1984 the government of Maharashtra has constructed 1 seep pond but today there are big seep lake and 13 small seep ponds for a total of 16 seep lakes. With the participation of the people some cement concrete and some stone dams were constructed.

Effective water management has been achieved through this public participation. As result the water level of the wells in the village increased. Today the village supplies water to five villages. Horticulture area increased from 10 acres to 120 acres.

Conclusion

The 450 hectares of deforested forest was restoring. The 50 years old fuel problems of the villages has been solved. The ground water level of the wells increased and the villages became self sufficient in drinking water. The village got its own identity. The concept of education and health took root. A sense of co-operation was created in the village and any festivals are celebrated collectively.

References

1. Ahirao and Alizad; *Environmental Science*, Nirali Publishing, House Pune.
2. Dhake, Ingale and Patil; *Paryavaran Shtra*, Prashant Publication Jalgoan.
3. Chaudhari S. R.; *Paryavarn Abbhayas*, Himalaya Publishing House, Mumbai.
4. Swindra Sing (1997) : "Environmental Geography" Prayag Pustak Bhavan, Allahabad.
5. Internet/Web
6. *Socio-Economic Abstract of Dhule District*.

**A Study of Migration of Families from Affected Villages in Nandurbar District
Due to Sardar Sarovar Project**

By

Dr. M. M. Saindane

Head and Associate Professor

Department of Geography

S.G.Patil Arts, Com. and Sci. College, Sakri

Saindanemanohar@yahoo.in

Abstract:

Many small, medium, large and multinational project in India are built for irrigation, hydropower and flood control. The dam brought land under irrigation but many villages were submerged due to this reservoir as a result, the villages lost their homes, social ties and their own hands. So, it was time for a forced migration. In the present research paper, a total 33 villages in Akkalkuwa and Akrani taluka of Nandurbar district have been affected due to this project and their migration has been studied.

Study area:

Nine village Akkalkuwa taluka of Nandurbar district and 24 affected villages in Akrani taluka have been studied.

Objective:

To study the migration of families from villages affected by sardar sarovar project.

Hypothesis:

To study the migration families of Akkalkuwa and Akrani talukas of Nandurbar district due to sardar sarovar project.

Database and Research methodology:

Primary and secondary information has been used for the present study. Support has been obtained through direct interviews with the Narmada development department, Nandurbar and direct rehabilitation of people from the villages.

Sardar sarovar project is done according to Narmada water dispute. Due to construction of sardar sarovar project 9 villages of Akkalkuwa and 24 villages of Akrani taluka total 33 villages of Nandurbar district of Maharashtra state are being affected families are 4227 out of which 1488 are land owners 714 are landless and 1925 are major son and daughters.

Due to this project Akkalkuwa taluka Manibeli, Dhankedi , Chimalkhadi, Sinduri, Danel, Gaman, Mndawa, so in Akrani tehasil paula Pimaplekhop, Shelgada, Junavane, Khardi, Mal, Bilgaon,Sauarya, Bhusha, Sadari, Warwali Udadya, Bhadal, Surung Roshanmal BK Chinchkhedi ,etc.

Table No :1

Current status of family migration in affected villages in Nandurbar district.

1.Akkalkuwa Tehsil

Sr. No	Location code	Affected villages	PAE's	No of Rehabilittee			No of remaining PAF's to be rehabilitation
				Guj	Mah	Total	
1	01	Manibeli	225	203	00	203	52
2	02	Dhankhedi	112	78	07	85	27
3	03	Chimalkhadi	220	70	55	125	95
4	04	Sinduri	249	110	62	172	77
5	05	Bamani	270	01	136	137	133
6	07	Mukhadi	204	03	122	125	79
7	06	Danel	437	09	212	221	216
8	08	Gaman	130	47	38	85	45
9	28	Mandawa	29	00	14	14	15

2. Akrani Tehsil

Sr. No	Location code	Affected villages	PAE's	No of Rehabilitated			No of remaining PAF's to be rehabilitation
				Guj	Mah	Total	
1	01	Paula	128	21	94	115	13
2	03	Pimaphhop	125	11	102	113	12
3	02	Shelgada	44	00	29	29	15
4	04	Atti	83	00	60	60	23
5	05	Keli	44	00	36	36	08
6	06	Thuwani	51	00	38	38	13
7	07	Bharad	221	45	161	206	15
8	08	Shikka	195	70	95	165	30
9	12	Domkhedi	188	00	175	175	13
10	09	Nimgavhan	156	00	154	154	02
11	85	Shelda	104	25	76	101	03
12	86	Junavane	113	00	98	98	15
13	87	Khardi	02	00	02	02	00
14	88	Mal	00	00	00	00	00
15	90	Bilgoan	28	00	14	14	14

16	144	Sawarya	62	00	50	50	12
17	140	Bhusha	307	34	268	302	05
18	134	Sadri	102	00	89	89	13
19	133	Warwali	72	00	65	65	07
20	135	Udadya	51	05	32	37	14
21	136	Bhadal	129	25	14	39	90
22	10	Surung	61	00	44	44	17
23	21	Roshanmal{BK}	41	00	40	40	01
24	13	Chinchkhedi	14	00	09	09	05

Source: Note on Sardar Sarovar Project, Nandurbar

In this table shows that the total number of affected families is 4227 out of 2391 {56.6%} in Maharashtra and 757 families {17.9%} migrate in state of Gujarat 1079 families {24.5} are yet to be relocated.



Conclusion:

The following finding appear in this research paper.

1. The project has affected a total of 33 villages including 9 in Akkalkuwa taluka and 24 in Akrani taluka in Nandurbar district and total includes 4227 families.
2. Out of 1906 affected families in Akkalkuwa taluka 646 families have migrated to Maharashtra and 521 affected families have migrate to Gujarat due to this project. This shows 33.9% migration in Maharashtra and 27.3% Gujarat. There are still 38.8 migration to be made.
3. Due to this project out of 2321 affected families in Akrani taluka 1745 {75.2%} affected families have migrated to Maharashtra and 236 affected families {10.16%} to Gujarat state. There are 340 affected families to be relocated.

4. Considering the total migration 56.6 families have migrated in Maharashtra and 25.5 in Gujarat. There are still 25.5 affected families to be migrated. The actual project is in the state of Gujarat and a large amount of migration has reached the state of Maharashtra.
5. It is safe to say that the above migration in voluntary and compulsory, as can be seen the interview of the people there.

Reference:

1. Socio-Economic abstract and Nandurbar distract 2005-2006.
2. Note of Sardar Sarovar project Irrigation Narmada Department Nandurbar.
3. Census of India 2001
4. Bhaise S.D. and Chaudhari S. R. Punarvasit Khedyatil Aarthik Badalacha Taulanik Abhyas
5. Web\ Internet

Impact of Slope on Distribution of Rural Settlement of Nandurbar District By

Dr. M. M. Saindane

Head and Associate Professor

Department of Geography

S.G.Patil Arts, Com. and Sci. College, Sakri

Saindanemanohar@yahoo.in

ABSTRACT

An attempt has been made in this paper to study slope and settlement distribution of Nandurbar district. The study area is concern the ranges of Satpura and Sahyadri Hills. The present relationship is chiefly based on topographic Map and support by the field observation of the study area. Slope is main constraint against the development of settlements. The distribution of settlements is mainly governed by slope. To understand the distributional pattern of settlements and their relationship with slope have been calculated. For the analysis of slope and topography of the study area, contour pattern, spot height, Bench Mark, trigonometric height, provide a significant tool. The toposheet of the study area 1:50,000 scales with contour interval of 20 Meter has been considered.

INTRODUCTION:

Physical, cultural and economic factors affect the location, types, size, spacing and place names of settlement. Therefore, it is necessary to study how these factors influence on settlement of particular district. Physical factors are much more important particularly include Physiography, Soil, Climate and Drainage. These factors are more important than economic and cultural factors.

The study region is a part of northwestern Maharashtra. It contributes 1.63% total geographical area of the state. The district of Nandurbar comes into existence on July 1st 1998 by dividing the erstwhile district of Dhule. The study area forms distinct geographical units as it is occupied by Satpura ranges in the north and Sahyadri hills in the south. The extent of study area 21^{00'} to 22^{00'} N. Latitudes and 73^{00'} 31' to 74^{00'} 32' E longitudes. The total area of the district 5034.23 sq. kms. The entire district from the Tapi valley bordered by Satpura on the north, boundary of Gujarat state on the west, district of Dhule on south, Madhya Pradesh and Dhule on the east. There are total 947 villages include 12 uninhabited villages in the study area.

OBJECTIVES:

The main object of the present study is to access relationship between slope and settlements distribution of Nandurbar district.

HYPOTHESIS:

Slope is influenced on settlements distribution of Nandurbar district. These factors can be also determined from the settlements distribution of study area.

PHYSIOGRAPHY:

The study region is physiographically Tapi river basin divides the study region into Northern and Southern sectors. The northern sectors form a part of Satpura Mountain and hilly regions, displaying a highly rugged and dissected topography with steep scrapes and gorges. The maximum elevation is 1329 meters above M.S.L. 2 km. southeast of Astamba and minimum elevation is 124 meter above M.S.L. near Taloda. The study region of south part exhibits and undulatory topography. Physiographically, the whole district may be broadly divided into the following regions.

- 1) The Northern Mountainous region.
- 2) The Central Plain region.
- 3) The Southern Hilly region.

The drainage is clearly indicative of riverine tracts a steep and gently slope region, north and south flowing river run-off is speedily, In this study area, major two rivers that constituted the drainage system of the region namely Tapi and Narmada.

DATABASE AND METHODOLOGY:

The present work is carried out by using following methodology.

- 1-Literature: - The available literature on the above topic of research from various research paper and books.
- 2-Field Work: - Number of sites are visited to the study area.
- 3-Laboratory Work: - The toposheet is obtained from survey of India. These toposheet uses for slope and topography of the area under investigation, contour pattern, spot height, benchmark and trigonometric height is a significant tools. The slope and settlement distribution Map has been prepared.

ANALYSIS OF SLOPE:

The purpose of this paper is to relationship between slope and settlement distribution. A slope may be formed by a covering of weathered rock resting on bed rock. Another type of slope consists of bed rock, forming the basal slope, covered by a weathered rock, often including a surface layer of soil. (P.C.Panda, 1990)

The slope loss or gain in altitude per unit horizontal distance in a direction of any segmental elements of the earth surface with the datum, express in degree is a

function of multiple processes. The slope also refers to the levelness of the region. Therefore, it influences on the distribution of settlements.

Average slope of an area is the most important controlling factor for settlements. For the present study, average slope is calculated with using following formula.

$$\text{Slope} = \frac{VI}{HE} = \tan O$$

With using, the above Wentworth (1930) formula slope of the study area has been calculated by using grid of 2sq.km. Then the isopleths map of the slope has been prepared. The superimposed map of the average slope on settlements of the Nandurbar district shows relation between slope and distribution of settlements.

Table No.1

S N	Slope (0 ⁰)	Name of the Tehsil						No of Rural Settleme nts	% of Rural Settlement s
		Akkalk uwa	Akr ani	Talo da	Shaha da	Nandur bar	Navap ur		
1	0 ⁰ -2.5 ⁰	114	55	81	183	152	147	732	77.30
2	2.5 ⁰ - 5.0 ⁰	41	73	06	-----	01	09	130	13.73
3	5.0 ⁰ - 7.5 ⁰	17	26	03	-----	-----	01	47	04.96
4	7.5 ⁰ - 10 ⁰	17	08	02	-----	-----	05	32	03.38
5	10.0 ⁰ - 12.5 ⁰	01	01	01	-----	-----	-----	03	00.32
6	12.5 ⁰ - 15.0 ⁰	01	----- --	----- -	-----	-----	-----	01	00.10
7	Above 15.0 ⁰	02	----- --	----- -	-----	-----	-----	02	00.21
	Total No. of Settlements	193	163	93	183	153	162	947	100.00

Source: Compiled by the researcher.

The slope map of Nandurbar district (Fig. No.01) and (Table No.1) shows that the area of Nandurbar district may be grouped into seven classes at uniform interval of 2.5⁰ except the lowest and highest groups.

The lowest slope group i.e. below 2.5⁰ covers 732 settlements and it contribute for the 77.30 percent of the total settlements. In Shahada tehsil cover 183 settlements is highest of this groups. This region is mainly includes the fertile land area along the banks of Tapi and Gomai. This area of slope coincides with very low.

The gentle slope of group (2.5⁰- 5.0⁰) mainly includes these area having slope up to 5⁰. This group includes 130 settlements and it contributes for the 13.73 percent of the

Publishing URL : <http://www.researchreviewonline.com/issues/volume-7-issue-94-february-2021/RRJ072919>

total settlement. In this group, the Akrani tehsil is highest settlements than other tehsils. This area is occupied by the foothills of Satpura Mountain in northern part of district. The level slope of the banks of the Narmada, Tapi, Gomai, Udai and Nesu rivers. This region is preferred by people for settlements.

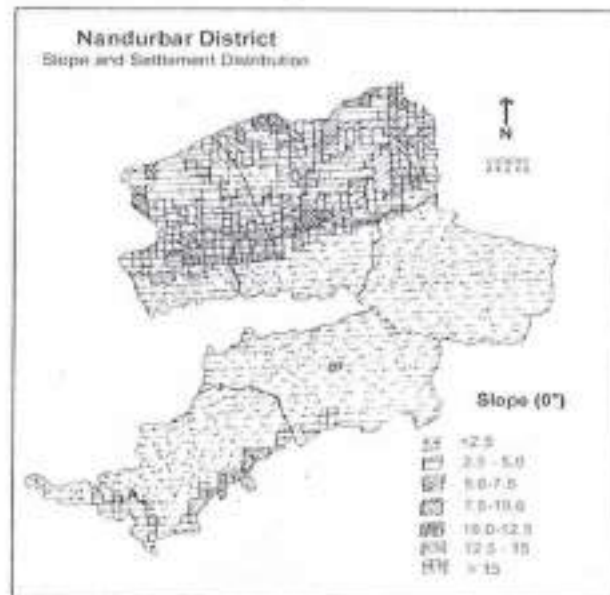
The moderate slope (5° - 10°) accounts for low number of settlements. It includes only 79 settlements, which contribute to the 8.34 percent of the total rural settlements.

The moderately steep (10° - 15° and above 15°) slope is a very low number of settlements. It includes only 06 settlements, which contribute to the 0.63 percent of the total settlements.

CONCLUSION:

It may be concluded that the comparative study of the relationship between slope and settlements distribution reveals a Negative correlation between slope and number of settlements. It is observed that the gentle and moderate slope support a large number of settlements, whereas the steep slopes does not favour for the growth of settlements.

Fig. No.1



REFERENCES: -

1. PANDA P.C. (1990) Geographical and rural settlements in India.
2. Patil S.B. (2009) "Geomorphology And Settlements in Dhule" (M.S.) Unpublished Ph.D. thesis, N.M. University, Jalgaon. 2009.
3. Singh Kailasnath (1980) "Quantitative analysis of landforms and settlement distribution in southern upland of eastern UP." Vimal Prakashan, Varanasi.

Kan River Water Pollution and its Impact on the Environment

By

Dr. M. M. Saindane

Head and Associate Professor

Department of Geography

S. G. Patil Arts, Com. and Sci. College, Sakri

Saindanemanohar@yahoo.in

Abstract:

The environment and human beings are closely related. The environment affects human health, animals and plants. But in a polluted environment are affected with various diseases. About 80% diseases are spread due to polluted water. Human being are responsible for the adverse effects of polluted water on plants and animals.

In the present research paper, the study of water pollution and its effect on environment of Kan River in Sakri taluka is done.

Study Area:

A 3Km stretch of Kan river from Krishi Bazar Samiti in west of Sakri town to K. T. Weir dam in the east has been taken for study.

Objective:

1. To study the water pollution caused by various human activities.
2. To study the environmental impact of Kan river water pollution.

Hypothesis:

To explore and study the water pollution of the Kan river due to human activities and its impact on the environment.

The geographical location of sakri taluka 27^o17' to 20^o49'N and 73^o55' to 74^o15' longitude and the altitude is 600m above sea level Sakri taluka is bounded on the west by Navpur and the south by Gujarat, on the north by Nashik district and on the east by Dhule and Shinkheda talukas.

The taluka covers an area of 2398sq.km and is bounded on the west by the sahyadri range. The Kan river originates at Hanumant pada near rainpada in sakri taluka. The river flows so it is called as purvahini river. It is tributary of Panjar river. There is a confluence of panzara and Kan rivers near Dattarti villages.

Analysis of Water pollution:

Changes in the physical and chemical properties of water that make it harmful to drinking water for washing and other uses if the water is polluted. Chemically, water is

never pure. It contain various airborne plant residues bacteria etc, so the colour and properties of water change.

The main source of water pollution is sewage discharge from village sewage factories through agricultural activities and waste products etc.

This causes a large amount of water pollution in the daily process. It mainly consists of excrement food particles, paper, cloth rags, Soap and various detergent power etc. The use of various soaps and detergent powers used through face to face interviews with woman washing clothes in their river basin. Appears to have caused a great deal of water pollution. Also washing clothes and washing utensils in the river basin. Religious ritual {Ganpati visarjan, Gauri, Bhulabai and Laxshami visarjan}.

In the cementary ashes, village sewage vitabhatti on the river bank, insecticides used by farmers and chemicals, medical solid waste, Improper disposal of dead animal, Improper disposal of polyethylene waste salon waste and wound decomposition on the water etc. The Kan river appears to have been heavily polluted.

Impact on environment:

Water pollution has a huge impact on the environment. It features aquatic animal and algae. The effect of the vitabhatti on the river bank is from the food chain and the air is warmed by the release of toxic fumes so there are very few birds. Due to the high level of phosphate in the river, blue moss grows in the water and on the surface of water. Algae cover the plant and increase the oxygen rate in the water. Therefore, aquatic plants are destroyed due to not getting enough sunlight for under water photosynthesis. The release of toxic substances from factories into river water poses a threat to plant and animals.

Conclusion:

Domestic and sewage chemical substances from agriculture vegetables that have escaped the market, Garbage animals remains, polyethylene bags. In the cemetery ash risk of increased streak blue water content etc.

Reference:

1. Savindra Sing {1997}: "Environment Geography", prayag pustak Bhavan, Alahabad
2. Ahirrao and Alizad: Environmental Science, Nirali Publishing House, Pune
3. Dhake, Ingale, Patil : Paryavaenshatra, Prashant Publication, Jalgoan.
4. S. R. Chaudhari: Paryavarn Abhyas, " Himalaya Publishing House, Muumbai.
5. Internet|Web

14. Impact of Geographical Factors on Place Names of Navapur Taluka, Dist Nandurbar

Dr. M. M. Saindane

Head and Associate Professor, Department of Geography
S.G.Patil Arts, Com. and Sci. College, Sakri.

Abstract

An attempt has been made in this paper to study the place name in Navapur taluka district Nandurbar. The study region part of khandesh and northern Maharashtra. The entire taluka surrounded by north in Gujarat and south in Sakri taluka. It is overlooked by hills on one side. The taluka covers an area of 976.68 sq km. Rangavali river passes by Navapur. With the help of the data available from Census hand book. The village of Navapur taluka are classified according to their place names. Various physical and cultural factors influencing on place name of villages. There are total 162 villages in the Navapur taluka. These villages are classified according to their place names in the present paper.

Introduction

Physical, cultural and economics factors affect the location, types, shape, size, spacing and place name of settlement. Therefore it is necessary to study how these factors influence on settlement of particular taluka. Physical factors are much more important. Physical factors particularly includes physiography, soil, climate, drainage and building materials. These factors are more important than economic and cultural factors. We can say that cultural factors and economic factors determined by physical factors.

Objectives

The main objective of present study is to access impact of geographical factor on place names in Navapur taluka of Nandurbar Distract.

Hypothesis

Settlements are influenced by physical, cultural and economic factors. The influence of these factors can be determined from the name of settlement.

Study Area

The study area is located 60 km tower the west on the distract headquarters of Nandurbar. The extent of study area 22°18'N to 73°30' E longitudes. It is surrounded by songdh taluka towards west, sagbara taluka toward North, Dang taluka toward south and sakri taluka at east. It is near to Gujarat border. The taluka cover an area of 976.68sq km. There are total villages 162 in navapur taluka. Rangavli river passes by Navapur taluka. Total population of this taluka is 239507.

Data Base and Research Methodology

The present work is carried out by using following methodology district census handbook and topographical map.

- A. Literature Survey: The available literature on the above topic of research is scanned from various research paper and book.
- B. Field Work: Number of sites is visited to the study the impact of physical and cultural factors on location and place names in the study area.
- C. Laboratory Work: Laboratory work includes classification of place name of the study area according to physical and cultural factors. Detail classification of the place names has been done and representing physiography, drainage, soil is prepared. The classification of place names according to the physical and cultural factor is shown with the help of pie diagram.

Analysis of Place Names

The two main and sub types of factors affecting all place names. In a large number of instance the place names are connected with natural feature like flora and fauna, mountain, river and soil. The study of the place names show that many suffix and prefixes are related to character of topography, hydrology and geology. Cultural factors such as caste, personality, ethnic groups, deity, size and cultural history.

Table No: 1

Impact of Geographical factors on place names of Navapur Taluka District Nandurbar

Name of Tahasil	No of Settlements	Physical Factors				Cultural Factors				Other	Total
		Geology	Topography	Hydrology	Flora & Fauna	Caste and Culture	Personality deity, Community	Size, land, space	Culture history, Settlement process		
Navapur		5	6	17	52	5	4	11	35	27	162
	%	3.08	3.72	10.49	32.10	3.09	2.42	6.79	21.60	16.66	100%

Source: Compiled by the researcher

A. Place names associated with physical with physical factors

Brunches (1920) "The place names as fossils of human geography" There are many place names which are named after physical factors sing (1998). A scrutiny of the place name reveal that the place name after geological factors such as sand sonkhadake, Kholgar, Khaidiki etc. The geological and topographical factors together with having 11 (6.80%) settlement which is named after these factors. The place names related with flora and fauna are named after Amalan, Nandavan, Thuwa. The total number of village such as 52 (32.10%). The impact of hydrology on place e.g. Nagziri, Borzar etc. The total number of such villages are 17 (10.49%). The total number of village having their names after physical factor are 80 (49.39). The contribute to the 49.39% of the total village in the taluka.

B. Place names associated with cultural factors:

Some place names occur after the cultural factors such as caste, ethnic group, personality deity, community, size of settlement, cultural landscape, cultural history, and cultural settlement process.

The place names which related with personality deity, Community are 4 (2.47%) e.g. Gokalnar Bijadevi, Timmauli etc. They contribute 11 (6.79%) name occurs after the size of settlement such as Dapur, vavadi, etc some place names are found after the cultural history area such as Raipur, Vijapur, and Pratapur etc. They are 35 in number and contribute 21.60%. The place name which are named after caste, ethnic group such as Bilbar, Sonare etc. are 5 number and they contribute 3.09%.



Conclusion

It is observed that the cultural factors are influencing in more than 33.95% the settlement of Navapur taluka. Among the cultural factors caste and personality is least influencing factors. The personality deity and community is showing their influence on more than 2.47% of the settlement. The impact of physical factors on the place names reveals that 52 (32.1%) settlement place names of related with flora and fauna. We find that most of cultural feature are related with size of settlement and cultural history area having 46 villages (28.39%).

About 16.66% of the total place names could not be put under any of the categories identified above. As such they were group under the other or miscellaneous.

References

1. Brunches J. (1920) Human Geography, London P-579.
2. Chaudhari S. R. (1985) Khandesh- A studies in rural settlement geography unpublished thesis university of Pune.
3. Dhule district census handbook, 1991 and 2001
4. Patil Y. V. and Patil S. B. (2006) Geographical study of place name in Dhule dist. Paper presented in 1st International NAGI 5th to 7th oct 2006 held at Osmania university, Hydrabad
5. Shinde Vasant (1998) early settlement in central tapi Basin, New Delhi
6. Sing R. Y. (1998) Geography of settlement, Rawat publication 3-Na-20 Jawahar Nagar, Jaipur Pp 73 to 80

**Vidya Vikas Mandal's
Sitaram Govind Patil Arts,
Science and Commerce College,
Sakri Tal. Sakri Dist. Dhule 424 304**



**NAAC
ACCREDITED**

**विद्या विकास मंडळाचे,
सिताराम गोविंद पाटील कला,
विज्ञान आणि वाणिज्य महाविद्यालय,
साक्री ता. साक्री जि. धुळे ४२४ ३०४**

Affiliated to Kavayitri Bahinabai Chaudhari North Maharashtra University, Jalgaon

Website : www.sgpcsakri.com

Email : vidyavikas2006@rediffmail.com

Ph : 02568-242323

3.3.2.1 Research Paper Published in UGC Care Listed Journals

Cite this: *Mater. Adv.* 2021,
2, 6306

The detection of Al³⁺ and Cu²⁺ ions using isonicotinohydrazide-based chemosensors and their application to live-cell imaging†

In-ho Song,[‡] Pratik Torawane,[‡] Jung-Seop Lee,[‡] Shrikant Dashrath Warkad,[‡]
Amulrao Borase,[‡] Suban K. Sahoo,[‡] Satish Balasaheb Nimse^{‡*} and
Anil Kuwar^{‡*†}

A new Schiff base receptor (**3**) was synthesized by an equimolar reaction between isonicotinic hydrazide and 2,4-dihydroxybenzaldehyde in ethanol. Receptor **3** demonstrated excellent selectivity and sensitivity towards Cu²⁺ ions and Al³⁺ ions by UV-vis absorption spectroscopy and fluorescence spectroscopy, respectively. Receptor **3** showed a detectable color change from colorless to yellow with a red-shift ($\Delta\lambda \approx 70$ nm) in the absorption spectra in the presence of Cu²⁺. In the emission study of **3**, Al³⁺ showed significant fluorescent enhancement ($\lambda_{em} = 473$ nm) over a wide range of tested metal ions. The quantum yield of receptor **3** ($\phi = 0.0021$) increases ~ 230 folds in the presence of Al³⁺ ions to form receptor **3**-Al³⁺ complex ($\phi = 0.484$). Receptor **3** showed high selectivity for Al³⁺ with a K_a of 4.8×10^4 M⁻¹ and LOD of 3.0 nM. In comparison, K_a for Cu²⁺ was 1.3×10^4 M⁻¹ and LOD of 1.9 μ M. Receptor **3** is an excellent chemosensor for detecting Al³⁺ ions as indicated by its nanomolar range LOD. The quick response, easy-synthesis, and high sensitivity make receptor **3** an ideal sensor for detecting Al³⁺ ions in a semi-aqueous medium and living cells.

Received 29th June 2021,
Accepted 15th August 2021

DOI: 10.1039/d1ma00564b

rsc.li/materials-advances

1. Introduction

Development of highly specific and sensitive chemosensors has attracted significant interest in detecting bioactive metal ions and toxic metal ions due to their importance in chemical, biological, medical, material, and environmental sciences.^{1–4} Development of colorimetric and fluorescence-based detection methods that target precise recognition of bioactive metals such as copper (Cu²⁺) and aluminum (Al³⁺) is a topic of high interest among researchers.^{5–11}

Cu²⁺ is the third most abundant heavy metal after Fe³⁺ and Zn²⁺ in the human body. Several biological processes require Cu²⁺ in optimum amounts.^{12–23} Enzymes such as tyrosinase, lysyl oxidase, cytochrome c oxidase, and superoxide dismutase

require Cu²⁺ for redox reactions.^{16,17} Even though Cu²⁺ is potentially toxic, it is an essential element.¹⁸ The deficiency of Cu²⁺ leads to Menkes disease.^{19,20} Whereas, the accumulation of Cu²⁺ is correlated to the Wilson disease,^{21,22} Amyotrophic Lateral Sclerosis,^{23,24} and Alzheimer's disease.^{25,26} The crucial physiological relevance of Cu²⁺ and its associated biomedical insinuations has resulted in substantial attention for the scheming of highly selective and sensitive copper chemosensors.²⁷

Al³⁺ is one of the most abundant biosphere elements at approximately 8% of the total mineral components. The neurotoxicity of Al³⁺ has been known to humans for over one hundred years.^{28,29} Al³⁺ can cause many health issues, including Alzheimer's disease³⁰ and osteomalacia,³¹ and increased risk of breast cancer.³² The World Health Organization (WHO) recommends 3–10 mg of Al³⁺ as an average daily intake. At the same time, the weekly tolerable dietary intake is about 7 mg kg⁻¹ body weight. Thus, recognizing Al³⁺ in life and environmentally significant samples is critical to address.^{33,34} The detection of Al³⁺ has been challenging compared to other metal ions because of poor spectroscopic characteristics, meager coordination ability, and easy hydration.^{35–37} The development of highly sensitive and selective chemosensor for Al³⁺ detection is in great demand. Therefore, it is of substantial importance to build receptors for the selective detection of Al³⁺.

According to recent literature, noncyclic receptors containing multiple coordination sites have considerably improved in

[‡]Institute of Applied Chemistry and Department of Chemistry, Hallym University, Chuncheon 200702, Republic of Korea. E-mail: satish_nimse@hallym.ac.kr

[‡]School of Chemical Sciences, KBC-North Maharashtra University, Jalgaon 425001, India. E-mail: kuwaras@gmail.com

[‡]BioMetric Technology, Inc., 3-3 Bio Venture Plaza 56, Chuncheon 24212, Korea

[‡]Department of Applied Chemistry, SV National Institute of Technology, Surat 395007, India

† Electronic supplementary information (ESI) available: Tables S1–S3 and Fig. S1–S9 are available. CCDC 2031947. For ESI and crystallographic data in CIF or other electronic format see DOI: 10.1039/d1ma00564b

‡ These authors contributed equally. Hence, both should be considered as first authors.



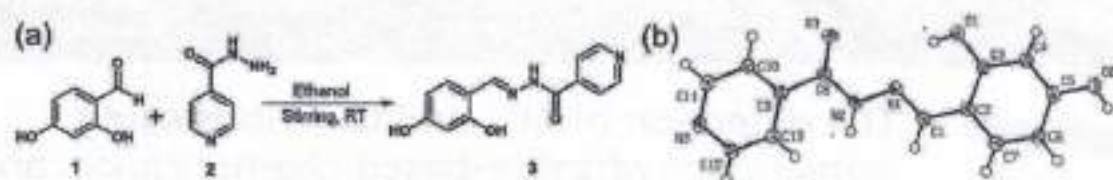


Fig. 1 (a) Scheme for the synthesis of receptor 3. (b) Single X-ray crystal structure of receptor 3 (50% probability ellipsoids).

the chemosensor design because of their ability to recognize different ionic and neutral molecules.^{28–40} Such noncyclic receptors are well known to show interesting coordination properties due to heteroatoms in chelating sites. With this in mind, a Schiff base (receptor 3, Fig. 1a) was prepared from isonicotinohydrazide and 2,4-dihydroxybenzaldehyde and evaluated as the target receptor for the metal ions. It was hypothesized that N atoms of the $-\text{CH}=\text{N}-$ bond and the O atom of *ortho*-OH in receptor 3 could coordinate with the metal ion to form a stable complex. Herein, we report receptor 3 as a selective chemosensor for Cu^{2+} as it showed the distinctive red shift in the absorption maxima but without any fluorescence signal for the complex. Receptor 3 was found to be an excellent fluorescence sensor for Al^{3+} , as evident from the chelation-enhanced fluorescence (CHEF) effect. The application of receptor 3 in fluorescence imaging was evaluated by confocal fluorescence microscopy in A549 cells, proving receptor 3 as a convenient tool for tracking Al^{3+} *in vivo*.

2. Material and methods

2.1 Materials and instrumentation

All reagents were purchased from Sigma-Aldrich and were used as received unless stated otherwise. The reaction was carried out under an inert atmosphere (Argon gas) and monitoring the reaction using thin-layer chromatography (TLC) to confirm the formation of the product. The developed plates were visualized under UV light (254 nm). The synthesized compound was characterized by ^1H and ^{13}C NMR on a Jeol FT-NMR spectrometer (400 MHz; JEOL, Japan) in $\text{DMSO}-d_6$. The chemical shifts (δ ppm) and the coupling constants (J Hz) are reported. UV-visible spectra were recorded on a Shimadzu UV-24500 (Shimadzu, Japan) in the range of 200–600 nm at room temperature using a quartz cuvette of 1 cm optical path length. Fluorescence emission spectra were measured on an Agilent Cary Eclipse fluorescence spectrophotometer (Agilent Technologies, USA). FT-IR spectra were recorded on a Nicolet iS5 FT-IR (ThermoScientific) spectrometer in the range of 400–4000 cm^{-1} using KBr pellets. The JMS-700 MStation Mass Spectrometer (JEOL, Japan) was used for recording the high-resolution mass spectra of receptor 3. The mass spectra of 3-Al^{3+} complex were obtained by matrix-assisted laser desorption/ionization (time-of-flight), MALDI-TOF mass spectrometry on a Bruker Autoflex speed TOF/TOF spectrometer (Bruker Daltonics, Bremen, Germany). X-ray analysis was performed using a Bruker AXS D8 Quest CMOS diffractometer (Bruker, USA). The microplate reader was Spectramax Plus 384 (Molecular Devices, USA),

and the fluorescent microscope Zeiss-ScopeA1 (Germany) was used in this study.

2.2 Synthesis of receptor 3

Isonicotinohydrazide (0.198 g, 1.0 mmol) and 2,4-dihydroxybenzaldehyde (0.200 g, 1.0 mmol) were reacted in ethanol (25 mL) at room temperature until the completion of the reaction (5 h). The yellow color solid obtained was filtered and dried. Then, the obtained yellow colored crude product was recrystallization from ethanol (yield = 90%). ^1H NMR (400 MHz, $\text{DMSO}-d_6$): δ 6.36 (d, 2H, Ar-H), 7.36 (s, 1H, Ar-H), 7.82 (d, 2H, Ar-H), 8.54 (s, 1H, CH=N), 8.77 (d, 2H, Ar-H), 10.08 (s, 1H, Ar-OH), 11.29 (s, 1H, NH), 12.14 (s, 1H, Ar-OH); ^{13}C NMR (100 MHz, $\text{DMSO}-d_6$): δ 102.61, 107.84, 110.40, 121.43, 131.20, 140.07, 150.29, 159.49, 161; mass expt. m/z = 258.0870 [$\text{C}_{13}\text{H}_{11}\text{N}_2\text{O}_5$ [M + H] $^+$], calc. m/z = 257.245.

2.3 UV-vis and fluorescence spectral measurements

All stock and working solutions were prepared using double distilled water and spectroscopic grade DMSO. A stock solution of receptor 3 (1×10^{-3} M) was prepared in DMSO, and the corresponding working solutions (10×10^{-6} M) were prepared simply by diluting with DMSO. Similarly, stock solutions of cations (1×10^{-2} M) were prepared in double-distilled water, and the corresponding working solutions (1×10^{-3} M) were prepared by diluting with water. The UV-visible absorption and emission spectra of the receptor 3 (10×10^{-6} M) dissolved in DMSO were recorded by adding the aqueous solution of various metal ions (Na^+ , K^+ , Ag^+ , Cs^+ , Sr^{2+} , Ca^{2+} , Co^{2+} , Cu^{2+} , Pd^{2+} , Mn^{2+} , Mg^{2+} , Ba^{2+} , Ni^{2+} , Zn^{2+} , Cd^{2+} , Pb^{2+} , Al^{3+} , Cr^{3+} , Fe^{3+} , Fe^{2+}) to examine the selectivity at room temperatures (298 K). For the sensitivity study, UV-visible absorption and emission titration experiments were performed through a stepwise addition of four equivalents of metals (1×10^{-3} M) to a solution of receptor 3 (10×10^{-6} M) in DMSO. The absorbance intensity and emission intensity were recorded in the range of 200–600 nm and 360–600 nm, respectively, alongside a reagent blank. Receptor 3 showed selectivity for detecting Cu^{2+} in the absorption titrations and detecting Al^{3+} in the fluorescence titrations. The binding stoichiometry of receptor 3 with Cu^{2+} ion (UV-visible absorption spectroscopy) and Al^{3+} ion (fluorescence spectroscopy) were investigated by Job's plot method. A receptor 3 was titrated with successive addition of Cu^{2+} or Al^{3+} ($1 \mu\text{L}$, 1.0×10^{-3} M) in water to a receptor 3 (1.0 mL) solution in DMSO. The collected data were processed using the Benesi-Hildebrand equation⁴¹ to determine the association constant (K_a) of analyte Cu^{2+} and Al^{3+} ion with receptor 3. The absorbance changes at 413 nm were used alongside a reagent blank for the



detection of Cu^{2+} ions. The fluorescence intensity was recorded at $\lambda_{\text{ex}}/\lambda_{\text{em}} = 343/473$ nm alongside a reagent blank with the excitation and emission slits set to 5.0 nm. The limit of detection (LOD) was estimated by applying the IUPAC recommended equation, $\text{LOD} = 3\sigma/\text{slope}$.⁴² Where σ is the standard deviation of ($n = 10$) blank samples and the slope is the slope for calibration curves.

2.4 Crystal growth for single X-ray crystallography

The single crystals of receptor 3 were obtained by slow diffusion of ethanol in DMSO. However, several attempts to obtain the single crystals of receptor 3 and Al^{3+} complex (3-Al^{3+}); receptor 3 and Cu^{2+} complex (3-Cu^{2+}) were unsuccessful. A suitable single crystal was carefully mounted for X-ray crystallography with the help of a trace of Fomblin oil on a Mitegen micromesh mount. Then it was transferred to the goniometer head with a fixed chi angle, a molybdenum K_{α} wavelength fine focus sealed X-ray tube ($\lambda = 0.71073$), a single crystal curved graphite incident beam monochromator, a Photon100 CMOS area detector, and an Oxford Cryosystems low-temperature device. X-ray diffraction data were collected at 150 K using ω and ϕ scans to a maximum resolution of $\theta = 33.221^{\circ}$. Data reduction, scaling, and absorption corrections were performed using SAINT (Bruker, V8.38A). The final completeness is 89.00% out of 33.221° in θ . Multi-scan absorption correction was performed using SADABS 2016/2.⁴³ The absorption coefficient μ of this material was 0.107 mm^{-1} at this wavelength ($\lambda = 0.71073 \text{ \AA}$). The space group was determined based on systematic absences using XPREP⁴⁴ as $Pna2_1$. The structure was solved using direct methods with ShelXS-97 and refined by full-matrix least-squares on F^2 using ShelXL-2018/3 and the graphical interface ShelXLE (Rev937).⁴⁵ All non-hydrogen atoms were refined anisotropically. Hydrogen atom positions were calculated geometrically and improved using a riding model. Mercury, PyMol, and POVray were utilized for molecular measurements and molecular visualization.⁴⁶

2.5 Effect of pH on the detection of Al^{3+} and reversibility of receptor 3

The effect of pH (pH = 2–12) on receptor 3 was examined by fluorescence spectroscopy both in the absence and presence of Al^{3+} ions. The pH was adjusted by adding perchloric acid and tetrabutylammonium hydroxide in the HEPES buffered system. Reversibility is a critical aspect of the fluorescent recognition process. Hence, we examined the reversibility of receptor 3 in the presence of ethylenediaminetetraacetic acid disodium salt (EDTANa_2). For the reversibility study, EDTANa_2 (4 equiv.) was added to the solution containing receptor 3- Al^{3+} complex obtained by adding Al^{3+} at a 1 : 4 mole ratio. The reversibility was recorded by alternate additions of Al^{3+} (4 equiv.) and EDTANa_2 (4 equiv.).

2.6 Determination of quantum yield of receptor 3 and receptor 3- Al^{3+} complex

Quantum yields (ϕ) of receptor 3 and its complexes with Al^{3+} were measured using the following formula.

$$\phi_{\text{sample}} = \left\{ \frac{(\text{OD}_{\text{standard}} \times A_{\text{sample}} \times \eta_{\text{sample}}^2)}{(\text{OD}_{\text{sample}} \times A_{\text{standard}} \times \eta_{\text{standard}}^2)} \right\} \times \phi_{\text{standard}}$$

where A is the area under the emission spectral curve, OD is the compound's optical density at the excitation wavelength, and η is the refractive index of the solvent. The quantum yield of receptor 3 and its complexes with Al^{3+} was determined using β -carbolone ($\phi = 0.570$) as the standard.⁴⁷

2.7 Cell culture studies

The cytotoxicity assay (MTT (3-(4,5-dimethylthiazol-2-yl)-2,5-diphenyltetrazolium bromide) assay) and cell imaging study of receptor 3, Al^{3+} , and Al^{3+} combined with receptor 3 was conducted using A549 cells (colorectal carcinoma cell line). The A549 cells were procured from the Korea cell line bank, Seoul, South Korea. Dulbecco Modified Eagle Medium (DMEM), fetal bovine serum (FBS), trypsin, 3-(4,5-dimethyl thiazol-2-yl)-2,5-diphenyl tetrazolium bromide was procured from Thermo Fisher Scientific, USA. DMSO was procured from Biosesang, Korea. Cell culture plates and glass coverslips were procured from SPL Life Sciences, Korea. A549 cells were grown in an incubator at 37°C and 5% CO_2 using DMEM media containing 2 mM glutamine and 10% FBS. Cells were trypsinized for seeding at 70–90% of cell confluency.

2.8 Cytotoxicity assay and cell imaging

About 2000 A549 cells per well were seeded in 96-well plates. After 24 h, the media containing receptor 3, Al^{3+} ion, and receptor 3 with Al^{3+} (1, 10, 25, and 50 μM) were added to the wells and incubated for another 24 h. Control wells were treated with equivalent volumes of dimethyl sulfoxide (DMSO). 200 μL of fresh media containing MTT solution and incubated for four hours at 37°C . The absorbance was recorded at 570 nm to evaluate the cell viability. Each experiment was executed three times. The data analysis was performed using the Origin software.

For cell imaging, A549 cells were seeded separately on poly-L-lysine coated 14 mm coverslips in 6 well plates and allowed to grow for 24 h. For cell imaging control experiments, 10 μM of Al^{3+} ion and 10 μM of receptor 3 were incubated separately for 30 min at 37°C and 5% CO_2 in the dark. For cell imaging of receptor 3 and Al^{3+} complex, 10 μM of Al^{3+} ion was incubated separately for 30 min. The media was then replaced with 10 μM of receptor 3 and incubated for an additional 30 min. The cells were washed with PBS buffer (pH = 7.4), followed by fixing with 2% paraformaldehyde for 30 min after removing the media. Coverslip was mounted on a glass slide, and imaging was performed under a fluorescence microscope (Zeiss-ScopeA1, Germany). Images were taken through a green channel.

3. Results and discussion

3.1 Synthesis of receptor 3

The Schiff base (\mathcal{E})- N' -(2,4-dihydroxybenzylidene)isonicotinohydrazide (receptor 3) was synthesized with a slight modification of the reported⁴⁸ method through a direct reaction between isonicotinohydrazide and 2,4-dihydroxybenzaldehyde (Fig. 1a) in ethanol with stirring and refluxing for 5 h. The molecular structure of



receptor **3** was characterized using various spectral techniques (FT-IR, ^1H NMR, ^{13}C NMR, and Mass), data (ESI† Fig. S1–S3) and finally confirmed by single-crystal X-ray crystallography (Fig. 1b). The crystallographic data, selected bond parameters, and hydrogen-bond parameters are presented in Tables S1, S2 and S3, respectively. The CIF file for receptor **3** was placed in the Cambridge Structure Database (CCDC 2051947†). The orange-colored crystal ($0.55 \times 0.42 \times 0.05 \text{ mm}^3$) of receptor **3** demonstrated an orthorhombic system having a $Pna2_1$ space group within the unit cell. The ORTEP diagram with numbering and packing diagram is shown in Fig. 1b. The receptor **3** in its free form displays the molecular association via intramolecular hydrogen bonding between the phenolic hydroxyl to imine nitrogen. Receptor **3** shows an intramolecular hydrogen bond (O(1)–H...N(1)) with a distance of 1.92 (3) Å and a bond angle of 150 (2) Å, which is in the expected range of such hydrogen bonds. Receptor **3** undergoes a solvent-assisted keto tautomerization suitable for the intramolecular charge transfer (ICT) process.⁴⁹ The fluorescence intensity enhancement of receptor **3** in the presence of Al^{3+} is attributed to the ICT process.

3.2 Determination of selectivity of receptor **3** as a chemosensor for metal ions

The selectivity of receptor **3** for cation detection was investigated using the UV-visible absorption and fluorescence spectroscopy. The UV-vis absorption spectra of receptor **3** ($10 \times 10^{-6} \text{ M}$, in DMSO) were recorded in the absence and presence of 4 equivalents of various metal ions, such as Na^+ , K^+ , Ag^+ , Cs^+ , Sr^{2+} , Ca^{2+} , Co^{2+} , Cu^{2+} , Pd^{2+} , Mn^{2+} , Mg^{2+} , Ba^{2+} , Ni^{2+} , Zn^{2+} , Cd^{2+} , Pb^{2+} , Al^{3+} , Cr^{3+} , Fe^{3+} , Fe^{2+} ($1 \times 10^{-3} \text{ M}$, in H_2O).

Receptor **3** showed an absorption band at 343 nm, most likely due to the π to π^* transition (Fig. 2a). Upon addition of Cu^{2+} ions, the absorption band at 343 nm was red-shifted to 413 nm ($\Delta\lambda \approx 70 \text{ nm}$), indicating that receptor **3** has a higher binding affinity towards Cu^{2+} ions than other surveyed metal ions. Receptor **3** showed two additional shoulder peaks at 428 nm and 475 nm to the major peak at 413 nm. In the presence of other metal ions, receptor **3** showed either no change or moderate decrease in the absorption intensity

relative to the receptor. These results indicated the intramolecular charge transfer (ICT) character of the synthesized receptor **3** by recognizing Cu^{2+} ions through imine-N, amide carbonyl, and hydroxyl groups.⁵⁰ The push-pull character of the ICT state due to multiple coordination resulted in a red-shift ($\Delta\lambda \approx 70 \text{ nm}$). These results indicated that receptor **3** shows selectivity for Cu^{2+} ions.

The fluorescence emission spectra of receptor **3** ($10 \times 10^{-6} \text{ M}$, in DMSO) were recorded in the absence and presence of 4 equivalents of various metal ions, such as Na^+ , K^+ , Ag^+ , Cs^+ , Sr^{2+} , Ca^{2+} , Co^{2+} , Cu^{2+} , Pd^{2+} , Mn^{2+} , Mg^{2+} , Ba^{2+} , Ni^{2+} , Zn^{2+} , Cd^{2+} , Pb^{2+} , Al^{3+} , Cr^{3+} , Fe^{3+} , Fe^{2+} ($1 \times 10^{-3} \text{ M}$, in H_2O). Receptor **3** showed weak fluorescence emission at 473 nm upon excitation at 343 nm. Fascinatingly, fluorescence was remarkably enhanced (~ 430 -folds) in the presence of Al^{3+} ions (Fig. 2b). Interestingly, there was no change in the emission performance of receptor **3** in the presence of other cations, including Cu^{2+} . The increase in fluorescence emission intensity was due to the azomethine group of receptor **3**. Receptor **3** is reducibly fluorescent due to the C=N double bond's isomerization at the excited state and the excited-state proton transfer (ESPT). The ESPT involves the phenolic proton of the substituted dihydroxyl moieties of salicylaldehyde in receptor **3**. Upon stable chelation with Al^{3+} , the C=N isomerization is inhibited. The coordination of receptor **3** with the Al^{3+} prohibits the ESPT process, as indicated by the fluorescence enhancement.^{51–53}

3.3 Binding mechanism and association constant

Job's plot was used to determine the binding stoichiometry of receptor **3** with Cu^{2+} ions (UV-visible absorption spectroscopy) and Al^{3+} ions (fluorescence spectroscopy). The molar ratio of metal ions was changed from 0.1 to 1.0 by keeping the total concentration of receptor **3** and Cu^{2+} ions at $10 \times 10^{-5} \text{ M}$. The absorption maxima ($\lambda = 413 \text{ nm}$) was observed when the molar ratio of the receptor **3** to Cu^{2+} was 0.33, indicating the formation of a 2:1 **3**- Cu^{2+} complex (Fig. S4a, ESI†). Similarly, the change in fluorescence intensity ($\lambda_{\text{ex}} = 343 \text{ nm}$, $\lambda_{\text{em}} = 473 \text{ nm}$) was used to determine the binding stoichiometry of receptor **3**

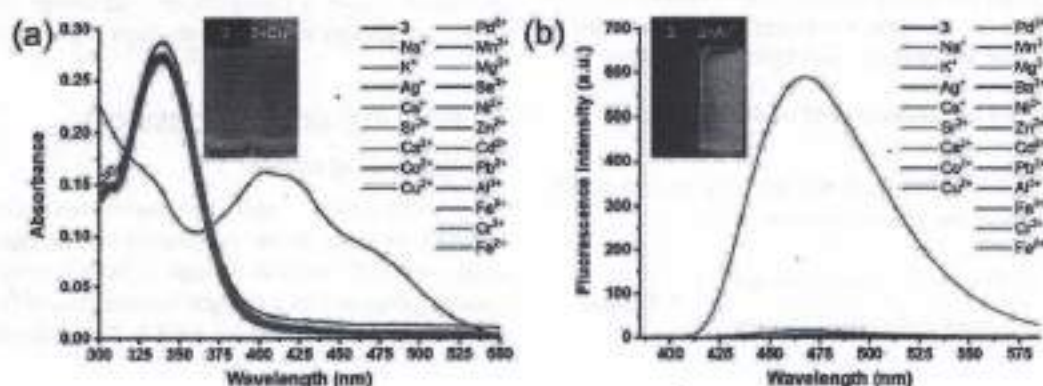


Fig. 2 (a) Changes in UV-vis absorption spectra and (b) fluorescence intensity ($\lambda_{\text{ex}} = 343 \text{ nm}$, $\lambda_{\text{em}} = 473 \text{ nm}$) of receptor **3** ($10 \times 10^{-6} \text{ M}$) upon the addition of 4 equivalents of different metal ions ($1 \times 10^{-3} \text{ M}$, in H_2O). Inset shows the color change of the solutions from colorless to pale green and fluorescence 'turn-on' effect.



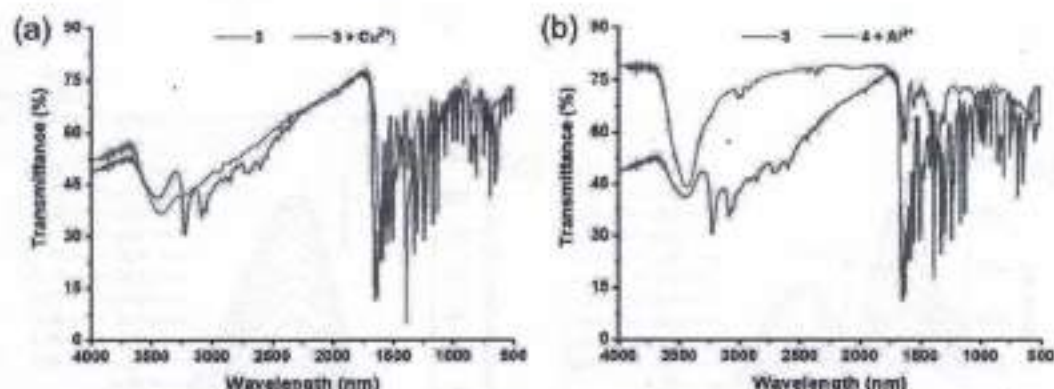


Fig. 3 FT-IR spectra of (a) 3-Cu^{2+} complex and (b) 3-Al^{3+} complex recorded using the reflectance technique ($4000\text{--}400\text{ cm}^{-1}$).

with Al^{3+} . The molar ratio of Al^{3+} was changed from 0.1 to 1.0 by keeping the total concentration of receptor **3**, and Al^{3+} ions at $10 \times 10^{-6}\text{ M}$. The emission maxima ($\lambda = 473\text{ nm}$) was observed when the molar ratio of the receptor **3** to Al^{3+} was 0.33, indicating the formation of a 2:1 3-Al^{3+} complex (Fig. S4b, ESI†). The complexes 3-Cu^{2+} and 3-Al^{3+} were obtained by refluxing four equivalents of Cu^{2+} and Al^{3+} with receptor **3** in an ethanoic solution. To ascertain the formation of receptor 3-Cu^{2+} complex and 3-Al^{3+} complex, we compared FT-IR spectra for receptor **3** with that of respective complexes, as shown in Fig. 3.

The FT-IR spectrum of receptor **3** (Fig. 3a) demonstrated signals at 3436.05 , 3224.39 (amide), 3086.99 (intramolecular bonded O-H), and 1647.39 (imine) cm^{-1} . For the receptor 3-Cu^{2+} complex, the FT-IR spectrum demonstrated a broad signal at 3422.06 (amide), no frequency for intramolecular bonded O-H, and 1621.84 (imine) cm^{-1} . These results indicate that receptor **3** forms a stable complex with Cu^{2+} . Similarly, the FT-IR spectrum of receptor 3-Al^{3+} complex demonstrated a broad signal at 3430.74 (amide), no frequency for intramolecular bonded O-H, and 1623.77 (imine) cm^{-1} . The FT-IR spectrum shifts in the 3-Cu^{2+} and 3-Al^{3+} complexes compared to the receptor **3**, confirming the involvement of imine and amide groups in the complexation process.

As shown in Fig. 4, the $^1\text{H NMR}$ titration experiment was conducted using the mixture of 0.5% $\text{D}_2\text{O-d}_2$ in DMSO-d_6 . The $^1\text{H NMR}$ of receptor **3** demonstrated sharp peaks at δ_{H} 12.12 (amide N-H), δ_{H} 11.25, and δ_{H} 10.01 (phenolic -OH). The signals for one N-H proton and two -OH protons gradually disappeared upon increasing the amount of Al^{3+} ions (0–1 equiv.). However, there was no significant change in the peak corresponding to imine C-H (δ_{H} 8.52). These results indicate that the amide group, imine group, and phenolic moiety of receptor **3** take part in the complexation with Al^{3+} ions. Further, the MALDI-TOF mass spectrum of receptor 3-Al^{3+} complex showed a signal at an m/z value of 544.129 and 561.133 (Fig. S5, ESI†). These results rationalize the formation of the 2:1 complexation pattern for the 3-Al^{3+} complex. The paramagnetic property of Cu^{2+} results in the peak broadening in proton NMR spectra. Thus, the binding process of receptor **3** with Cu^{2+} could not be monitored by NMR studies.²⁴

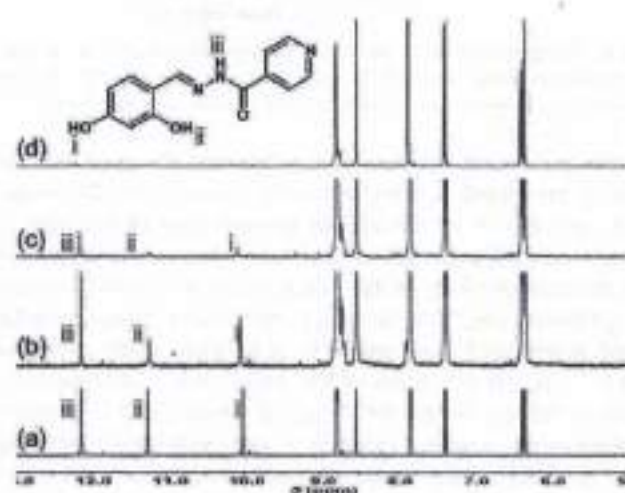


Fig. 4 $^1\text{H NMR}$ spectral changes of receptor **3** in the mixture of 0.5% $\text{D}_2\text{O-d}_2$ in DMSO-d_6 . (a) $3 + \text{Al}^{3+}$ (0 equiv.). (b) $3 + \text{Al}^{3+}$ (0.25 equiv.). (c) $3 + \text{Al}^{3+}$ (0.5 equiv.). (d) $3 + \text{Al}^{3+}$ (1 equiv.).

The association constants (K_a) of Cu^{2+} (UV-visible absorption spectroscopy) and Al^{3+} (fluorescence spectroscopy) complexes with receptor **3** were determined by Benesi-Hildebrand equations (eqn (S1) and (S2), ESI†). As shown in Fig. 5a, the receptor **3** (1.0 mL , $10 \times 10^{-6}\text{ M}$) in DMSO was titrated with successive addition of Cu^{2+} ($0\text{--}20\text{ }\mu\text{L}$ in H_2O , $c = 10 \times 10^{-4}\text{ M}$) to measure the association constant (K_a). The absorbance values at absorption maxima ($\lambda = 413\text{ nm}$) were processed using the Benesi-Hildebrand equation (eqn (S1), ESI†) to obtain the binding curve (Fig. S6a, ESI†). The K_a value for the complexation of Cu^{2+} with receptor **3** was $1.3 \times 10^4\text{ M}^{-1}$.

As shown in Fig. 5b, receptor **3** (1.0 mL , $10 \times 10^{-6}\text{ M}$) in DMSO was titrated with successive addition of Al^{3+} ($0\text{--}20\text{ }\mu\text{L}$ in H_2O , $c = 10 \times 10^{-4}\text{ M}$). The changes in fluorescence intensity ($\lambda_{\text{ex}} = 343\text{ nm}$, $\lambda_{\text{em}} = 473\text{ nm}$) were used to determine the K_a value by plotting the binding curve (Fig. S6b, ESI†) according to the Benesi-Hildebrand equation (eqn (S2), ESI†). The K_a value for the complexation of Al^{3+} with receptor **3** was $4.8 \times 10^4\text{ M}^{-1}$. The binding affinity of Al^{3+} for receptor **3** is 4-fold higher than that of Cu^{2+} ions.



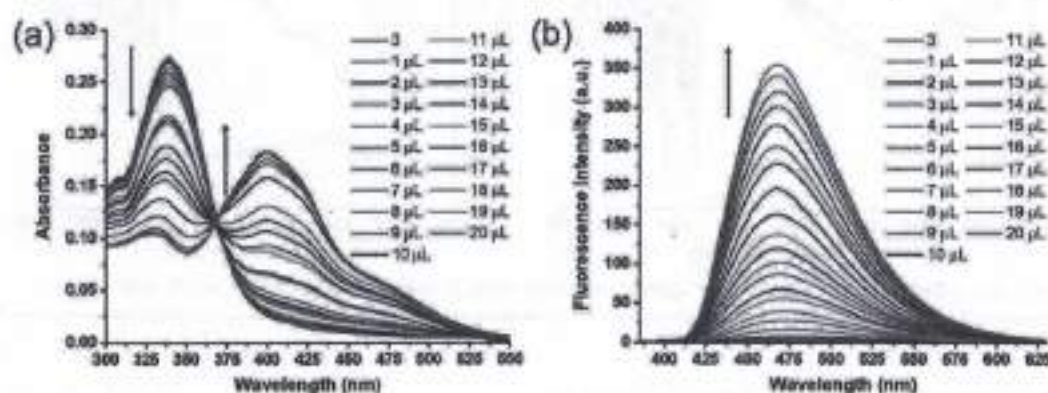


Fig. 5 Changes in (a) UV-vis absorption spectra and (b) fluorescence spectra ($\lambda_{\text{exc}} = 343 \text{ nm}$, $\lambda_{\text{em}} = 473 \text{ nm}$) of receptor **3** (in 1 mL DMSO, $10 \times 10^{-6} \text{ M}$) up on successive addition of Cu^{2+} (0 to 20 μL in H_2O , $c = 10 \times 10^{-4} \text{ M}$), and Al^{3+} (0 to 20 μL in H_2O , $c = 10 \times 10^{-4} \text{ M}$), respectively.

Computational studies were conducted by applying the density functional theory (DFT) using Gaussian 09. The molecular geometries of the singlet ground state of receptor **3**, 3- Cu^{2+} complex, and 3- Al^{3+} complex were optimized using hybrid B3LYP functions with a 6-31G++(d,p) (C, H, N, O) and LANL2DZ (Cu, Al) basis sets.⁵⁵ The HOMO, LUMO results, information for bond length, and bond angles were obtained using Avogadro 1.2.0.⁵⁶ The 3D structures of the 3- Cu^{2+} and 3- Al^{3+} complexes were calculated by the DFT method using the 2:1 binding stoichiometry between receptor **3** and respective ions. The DFT computed structure of receptor **3** and its complexes are presented in Fig. S7 (ESI[†]). The LUMO-HOMO bandgap (ΔE (eV) = $E_{\text{LUMO}} - E_{\text{HOMO}}$) for receptor **3** was found to be 0.293.

In contrast, the LUMO-HOMO bandgap for 3- Cu^{2+} and 3- Al^{3+} complexes were 0.279 and 0.078, respectively. These results provided the basis for ascertaining the ICT between receptor **3** and Cu^{2+} and Al^{3+} ions. Comparing the electron densities of the HOMO and LUMO of receptor **3** with the 3- Cu^{2+} complex supported the charge transfer occurring between the receptor and metal ions that further lowered the bandgap. The lowering of the bandgap upon complexation supported the red-shift of the absorbance of receptor **3** upon the addition of Cu^{2+} . On the contrary, the significant decrease in the LUMO-HOMO bandgap ($\Delta E = 0.078$) indicated the formation of a relatively stable 3- Al^{3+} complex as compared to the 3- Cu^{2+} complex. The increase in fluorescence enhancement was complemented by a sharp decrease in energy HOMO-LUMO bandgap of the receptor **3**.

3.4 Receptor **3** as a chemosensor for Cu^{2+} and Al^{3+} ions

The detection of the target analyte in the presence of possibly competing analytes is a crucial aspect for any compound to be an excellent chemosensor. Therefore, we evaluated the specificity of receptor **3** for Cu^{2+} in a competition experiment by recording the absorption ($\lambda = 413 \text{ nm}$) receptor **3** in the presence of Cu^{2+} (1 equiv.) ion mixed with other cations (4 equiv.). The results of the competition experiments are presented in Fig. S8a (ESI[†]). Similarly, we determined the efficiency of receptor **3** for detecting Al^{3+} ions in a competition experiment by recording the fluorescence intensity

($\lambda_{\text{exc}} = 343 \text{ nm}$, $\lambda_{\text{em}} = 473 \text{ nm}$). As shown in Fig. S8b (ESI[†]), the fluorescence intensity for receptor **3** was measured in the presence of Al^{3+} (1 equiv.) ion mixed with other cations (4 equiv.). The coefficient of variation in the change of absorbance and fluorescence intensity for Cu^{2+} detection and Al^{3+} detection, were below $\pm 10\%$, respectively. These results indicate that receptor **3** is a highly valuable chemosensor for detecting Cu^{2+} by UV-vis absorption spectroscopy. Moreover, receptor **3** demonstrated its excellence in detecting Al^{3+} ions with high specificity by fluorescence spectroscopy. Therefore, the high selectivity and specificity of receptor **3** for Cu^{2+} and Al^{3+} ions make it an excellent chemosensor for analytical applications. The absorbance ($\lambda = 413 \text{ nm}$) and fluorescence intensity ($\lambda_{\text{exc}} = 343 \text{ nm}$, $\lambda_{\text{em}} = 473 \text{ nm}$) were plotted at various concentrations of Cu^{2+} ions and Al^{3+} ions, respectively, to obtain the calibration plots (Fig. S9, ESI[†]). The LOD for detecting Cu^{2+} ions by UV-vis absorption spectroscopy was 1.86 μM . Whereas, the LOD for the detection of Al^{3+} ions by Fluorescence spectroscopy was 3.08 nM. The approximately 600-fold lower sensitivity of receptor **3** for Al^{3+} ions compared to Cu^{2+} ions was attributed to the ~ 4 -fold higher binding constant for 3- Al^{3+} complex. It is important to notice that receptor **3** demonstrated relatively lower detection limits for Cu^{2+} and Al^{3+} than some of the reported methods presented in Tables S4 and S5 (ESI[†]).

3.5 Effect of pH on the detection of Al^{3+} and reversibility of receptor **3**

The effect of pH on receptor **3** for detecting Al^{3+} ions was tested in the pH range of 2.0–12.0, as shown in Fig. 6a. The emission intensity ($\lambda_{\text{em}} = 473 \text{ nm}$) of receptor **3** did not change significantly with the pH change. However, equimolar Al^{3+} ions changed the fluorescence intensity of receptor **3**- Al^{3+} complex considerably with the pH change. The receptor **3**- Al^{3+} complex's emission intensity was significantly high at pH 2.0–8.0 than pH 9.0–12.0. These results indicate that interactions of Al^{3+} ions with receptor **3** are pH dependant. The decrease in emission intensity at higher pH values (9.0–12.0) specifies that the Al^{3+} ions are freed from the complex, possibly due to more robust interactions with increased -OH levels. Nonetheless, receptor **3**



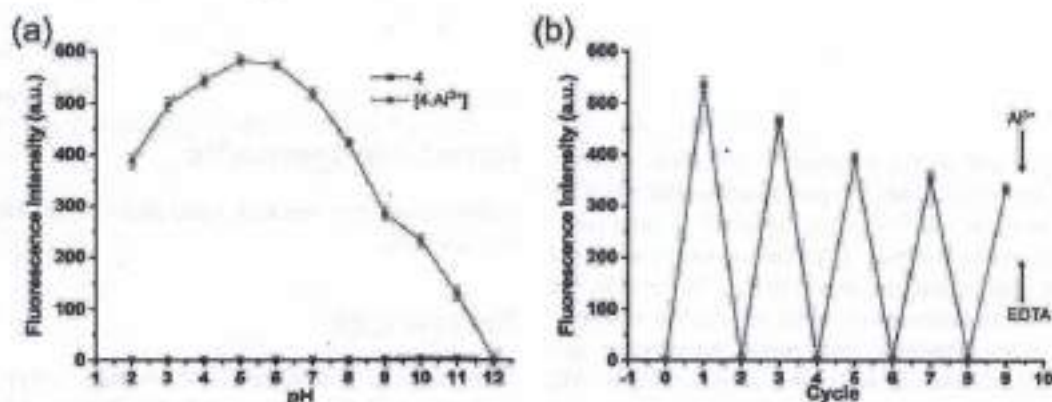


Fig. 6 (a) Changes in the fluorescence intensity of receptor **3** and receptor $3 \cdot \text{Al}^{3+}$ complex in a binary mixture of DMSO : HEPES buffer (at various pH values) (9 : 1; v/v). (b) fluorescence intensities ($\lambda_{\text{exc}} = 343 \text{ nm}$, $\lambda_{\text{em}} = 473 \text{ nm}$) of $3 \cdot \text{Al}^{3+}$ complex (1 : 1) in the presence of EDTA for many cycles in DMSO.

demonstrated significant fluorescence intensity at pH 5.0–8.0 in the presence of Al^{3+} ions, indicating its applicability for the detection of intracellular Al^{3+} ions.

It is of a great advantage if a sensor can be reversible and reusable for sensing cations with high selectivity. A literature survey revealed that most of the reported Al^{3+} ion sensors are based on chemodosimetry that is typically irreversible.⁵⁷ Reversibility test experiments were conducted by alternate additions of Al^{3+} ion and EDTA (Fig. 6b) to the solution of receptor **3**. As shown in Fig. 6b, the emission spectra of receptor **3** in the presence of Al^{3+} (4 equiv.) showed high emission intensity, which was quenched by EDTA (Na_2 , 6 equiv.) on the solution. However, further addition of Al^{3+} (4 equiv.) demonstrated fluorescence signal, but this time slightly lower than the previous cycle. Adding Al^{3+} ions (4 equiv.) causes emission enhancement, which can be quenched by adding another portion of EDTA (Na_2 , 6 equiv.). The reversibility of receptor **3** was repetitive, with a slight loss in fluorescence efficiency due to Al^{3+} /EDTA additions. The observed decrease in fluorescence intensity for each cycle results from an excess of EDTA (Na_2 , 6 equiv.) compared to Al^{3+} (4 equiv.). This experiment suggests that receptor **3** can act as a likely environmental receptor for Al^{3+} detection.

3.6 Quantum yield of receptor **3** and receptor $3 \cdot \text{Al}^{3+}$ complex

Quantum yields of receptor **3** and $3 \cdot \text{Al}^{3+}$ complex were determined using norharmine as a standard. The quantum yield of receptor **3** ($\Phi = 0.0021$) increases ~ 230 folds in the presence of Al^{3+} ions to form receptor $3 \cdot \text{Al}^{3+}$ complex ($\Phi = 0.484$).

3.7 Application of receptor **3** in cell imaging application for detection of intracellular Al^{3+} ions

The complexation-induced fluorescence “turn on” or “turn off” effect is crucial for bio-imaging applications of small molecular probes designed to detect the cationic analyte. Receptor **3** did not show any change in fluorescence intensity upon binding with Cu^{2+} ions. However, the fluorescence signal of receptor **3** was increased by a few hundred folds in the presence of Al^{3+} ions. Therefore, receptor **3** was used to detect Al^{3+} ions in the living A549 cell lines to explore their biological applications. The MTT assay allowed us to estimate the cytotoxicity of receptor **3**, Al^{3+} , and receptor $3 \cdot \text{Al}^{3+}$ complex after exposure of cells to concentrations of 1, 10, 25, and 50 μM for 24 h with DMSO as a control. As depicted in Fig. 7a, the results are shown as the percent cell growth for each group compared to the control. There was no significant cell death even after 24 h of

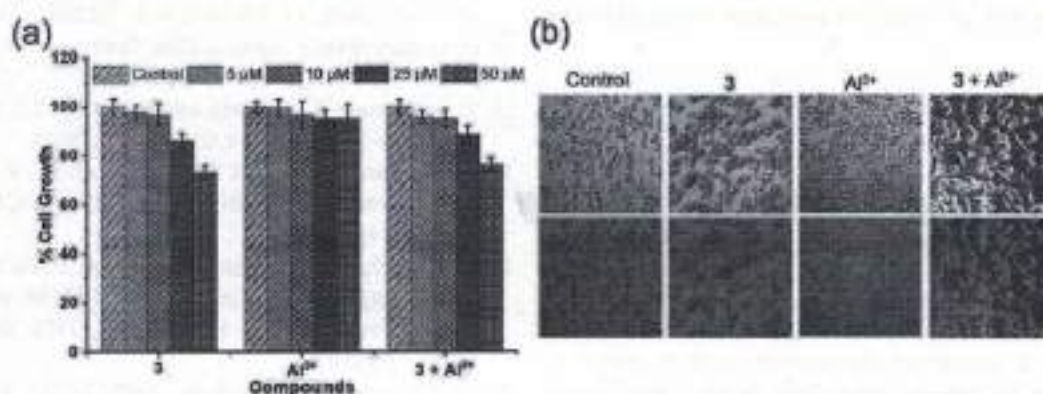


Fig. 7 (a) Cytotoxicity's of receptor **3**, Al^{3+} , and receptor $3 + \text{Al}^{3+}$ on the A549 cells after 24 h, (b) bright-field images (top row) and green channel (bottom row), control, receptor **3**, Al^{3+} , and receptor $3 + \text{Al}^{3+}$.



Paper

treatment at 1–25 μM of the receptor 3, Al^{3+} ions, and the receptor 3- Al^{3+} complex. However, upon treatment at 50 μM of receptor 3 and receptor 3- Al^{3+} complex, about a 20% decrease in cell growth was observed. Hence, 10 μM of receptor 3 was used for cell imaging applications. As shown in Fig. 7b, the cells did not show significant fluorescence upon incubation with Al^{3+} ions (10 μM) alone. However, very weak fluorescence was observed upon incubation of cells with receptor 3 (10 μM). Interestingly, the fluorescence intensity was increased upon incubation of cells with receptor 3 (10 μM) in the presence of Al^{3+} ions (10 μM). These results indicated that receptor 3 has a high potential in biological applications to detect Al^{3+} in an *in vitro* assay.

4. Conclusions

In conclusion, we have developed a new optical receptor 3 based on Schiff base chemistry that demonstrated excellent selectivity and sensitivity towards Cu^{2+} ions in UV-vis absorption spectroscopy. Whereas the developed receptor 3 showed excellent selectivity and sensitivity for the detection of Al^{3+} ion by using fluorescence spectroscopy. In either case, the receptor did not show any interference from other tested metal ions. The 2:1 binding stoichiometry of receptor 3 and Al^{3+} ions was confirmed by FT-IR, NMR, and mass spectroscopy. The reversibility of receptor 3 for Al^{3+} ions in the presence of EDTA ensures its ability as an excellent probe for detecting Al^{3+} in various samples, including living cells. Receptor 3 showed high selectivity for Al^{3+} with a K_a of $4.8 \times 10^4 \text{ M}^{-1}$ and LOD of 3.0 nM. In comparison, the K_a for Cu^{2+} was $1.3 \times 10^4 \text{ M}^{-1}$ and LOD of 1.9 μM . Receptor 3 is an excellent chemosensor for detecting Al^{3+} ions indicated by its nanomolar range LOD. The quick response, easy synthesis, and high sensitivity make receptor 3 an ideal sensor for detecting Cu^{2+} and Al^{3+} ions. Further, the synthesized receptor showed a highly sensitive and highly specific fluorescent 'turn-on' effect ($\lambda_{\text{em}} = 473 \text{ nm}$) for the 2:1 binding with Al^{3+} ions in a semi-aqueous medium and living cells.

Author contributions

I. S. and P. T. contributed equally. Hence, both should be considered as the first authors. S. B. N. and A. K. designed the study; I. S., P. T., J. L., A. B., and S. D. W. performed the experiments; S. B. N., S. K. S., and A. K. analyzed and interpreted the data. S. K. S. completed the theoretical calculation. S. B. N. and A. K. supervised the research. S. B. N. and A. K. wrote the paper. All authors analyzed the data and commented on the paper.

Conflicts of interest

The authors declare no competing interests.

Acknowledgements

Hallym University Research Fund (HRF-202012-009) supported this research.

References

- H. S. Jung, P. S. Kwon, J. W. Kwon, J. I. Kim, C. S. Hong, J. W. Kim, S. Yan, J. Y. Lee, J. H. Lee, T. Joo and J. S. Kim, *J. Am. Chem. Soc.*, 2009, **131**(5), 2008–2012, DOI: 10.1021/ja908611d.
- Z. Q. Guo, W. Q. Chen and X. M. Duan, *Org. Lett.*, 2010, **12**(10), 2202–2205, DOI: 10.1021/ol100381g.
- M. Royzen, A. Durandin, V. G. Young, N. E. Geacintov and J. W. Canary, *J. Am. Chem. Soc.*, 2006, **128**, 3854–3855, DOI: 10.1021/ja056631g.
- C. Gou, S.-H. Qin, H.-Q. Wu, Y. Wang, J. Luo and X.-Y. Liu, *Inorg. Chem. Commun.*, 2011, **14**(10), 1622–1625, DOI: 10.1016/j.inoche.2011.06.024.
- J. Ting, F. Mei, Z. Mengyao, Q. Jianwen, Z. Hu and G. Yong, *Spectrochim. Acta, Part A*, 2020, **227**, 117530, DOI: 10.1016/j.saa.2019.117530.
- J. J. Xiong, P. C. Huang, C. Y. Zhang and F. Y. Wu, *Sens. Actuators, B*, 2016, **226**, 30–36, DOI: 10.1016/j.snb.2015.11.113.
- G. Zhang, H. Zhang, J. Zhang, W. Ding, J. Xu and Y. Wen, *Sens. Actuators, B*, 2017, **253**, 224–230, DOI: 10.1016/j.snb.2017.06.144.
- K. P. Carter, A. M. Young and A. E. Palmer, *Chem. Rev.*, 2014, **114**, 4564–4601, DOI: 10.1021/cr400546e.
- N. Dey and S. Bhattacharya, *Dalton Trans.*, 2018, **47**, 2352–2359, DOI: 10.1039/C7DT03401F.
- H. Rao, W. Liu, K. He, S. Zhao, Z. Lu, S. Zhang, M. Sun, P. Zou, X. Wang, Q. Zhao, Y. Wang and T. Liu, *ACS Sustainable Chem. Eng.*, 2020, **8**, 8857–8867, DOI: 10.1021/acssuschemeng.0c03354.
- S. L. Gu, Y. Y. Huang, F. Hu, Y. L. Jin, G. X. Zhang, L. S. Yan, D. Q. Zhang and R. Zhao, *Anal. Chem.*, 2015, **87**, 1470–1474, DOI: 10.1021/ac504153c.
- M. Kumar, N. Kumar, V. Bhalla, P. R. Sharma and T. Kaur, *Org. Lett.*, 2013, **14**, 406–409, DOI: 10.1021/ol3034059.
- D. G. Barceloux, *J. Toxicol., Clin. Toxicol.*, 1999, **37**, 217–230, DOI: 10.1081/CLT-100102421.
- T. G. Thomas, K. Sreenath and K. R. Gopidas, *Analyst*, 2012, **137**, 5358–5362, DOI: 10.1039/C2AN35904A.
- A. K. Manna, K. Rout, S. Chowdhury and G. K. Patra, *Photochem. Photobiol. Sci.*, 2019, **18**(6), 1512–1525, DOI: 10.1039/c9pp00114j.
- S. N. Gacheru, P. C. Trackman, M. A. Shah, C. Y. O'Gara, P. Spaccapoli, F. T. Greenaway and H. M. Kagan, *J. Biol. Chem.*, 1990, **265**(31), 19022–19027, DOI: 10.1016/S0021-9258(17)30618-X.
- H. Beinert, *Eur. J. Biochem.*, 1997, **245**(3), 521–532, DOI: 10.1111/j.1432-1033.1997.t01-1-00521.x.
- J. F. Mercer, *Trends Mol. Med.*, 2001, **7**(2), 64–69, DOI: 10.1016/s1471-4914(01)01920-7.
- H. Tapiero, D. M. Townsend and K. D. Tew, *Biomed. Pharmacother.*, 2003, **57**(9), 386–398, DOI: 10.1016/s0753-3322(03)00012-x.



- 20 O. Bandmann, K. H. Weiss and S. G. Kaler, *Lancet Neurol.*, 2015, **14**(1), 103–113, DOI: 10.1016/S1474-4422(14)70190-5.
- 21 R. Hait-Darshan, T. Babushkin and Z. Malik, *J. Environ. Pathol. Toxicol. Oncol.*, 2009, **28**(3), 209–221, DOI: 10.1615/jenvironpatholtoxiconcol.v28.i3.20.
- 22 E. Koutsouraki, D. Michmizos, O. Patsi, J. Tzartos, M. Spilioti, M. Arnaoutoglou and M. Tsolaki, *Viral J.*, 2020, **17**(1), 35, DOI: 10.1186/s12985-020-01309-x.
- 23 E. Tokuda and Y. Furukawa, *Int. J. Mol. Sci.*, 2016, **17**(5), 636, DOI: 10.3390/ijms17050636.
- 24 K. A. Trumbull and J. S. Beckman, *Antioxid. Redox Signaling*, 2009, **11**(7), 1627–1639, DOI: 10.1089/ars.2009.2574.
- 25 R. Squitti, D. Lupoi, P. Pasqualetti, G. Dal Forno, F. Vernieri, P. Chiowenda, L. Rossi, M. Cortesi, E. Cassetta and P. M. Rossini, *Neurology*, 2002, **59**(8), 1153–1161, DOI: 10.1212/wnl.59.8.1153.
- 26 P. G. Georgopoulos, A. Roy, M. J. Yonone-Lioy, R. E. Opiekun and P. J. Lioy, *J. Toxicol. Environ. Health, Part B*, 2001, **4**(4), 341–394, DOI: 10.1080/109374001753146207.
- 27 U. A. Fegade, S. K. Sahoo, A. Singh, N. Singh, S. B. Attarde and A. S. Kuwar, *Anal. Chim. Acta*, 2015, **872**, 63–69, DOI: 10.1016/j.aca.2015.02.051.
- 28 A. K. Manna, S. Chowdhury and G. K. Patra, *New J. Chem.*, 2020, **44**, 10819, DOI: 10.1039/D0NJ01954B.
- 29 M. L. D. R. Crapper, W. J. Lukiw and T. P. Kruck, *Environ. Geochem. Health*, 1990, **12**, 103–114, DOI: 10.1007/BF01734059.
- 30 C. N. Martyn, D. J. Barker, C. Osmond, E. C. Harris, J. A. Edwardson and R. F. Lacey, *Lancet*, 1989, **333**, 61–62.
- 31 G. C. Woodson, *Bone*, 1998, **22**, 695–698, DOI: 10.1016/S8756-3282(98)00060-x.
- 32 P. D. Darbre, *J. Inorg. Biochem.*, 2005, **99**, 1913–1919, DOI: 10.1016/j.jinorgbio.2005.06.001.
- 33 S. Kim, J. Y. Noh, K. Y. Kim, J. H. Kim, H. K. Kang, S. W. Nam, S. H. Kim, S. Park, C. Kim and J. Kim, *Inorg. Chem.*, 2012, **51**(6), 3597–3602, DOI: 10.1021/ic2024583.
- 34 C. Gao, P. Zang, W. Liu and Y. Tang, *J. Fluoresc.*, 2016, **26**, 2015, DOI: 10.1007/s10895-016-1895-z.
- 35 X. Sun, Y. W. Wang and Y. Peng, *Org. Lett.*, 2012, **14**, 3420–3423, DOI: 10.1021/ol301390g.
- 36 K. K. Upadhyay and A. Kumar, *Org. Biomol. Chem.*, 2010, **8**, 4892–4897, DOI: 10.1039/C0OB00171F.
- 37 K. Soroka, R. Vithanage, D. A. Phillips, B. Walker and P. K. Dasgupta, *Anal. Chem.*, 1987, **59**, 629–636, DOI: 10.1021/ac00131a019.
- 38 P. Torawane, K. Keshav, M. K. Kumawat, R. Srivastava, T. Anand, S. Sahoo, A. Borse and A. Kuwar, *Photochem. Photobiol. Sci.*, 2017, **16**, 1464–1470, DOI: 10.1039/C7PP00182G.
- 39 U. A. Fegade, S. K. Sahoo, A. Singh, N. Singh, S. B. Attarde and A. S. Kuwar, *Anal. Chim. Acta*, 2015, **872**, 63–69, DOI: 10.1016/j.aca.2015.02.051.
- 40 A. Kuwar, R. Patil, A. Singh, R. Bendre and N. Singh, *ChemPhysChem*, 2014, **15**, 3933–3937, DOI: 10.1002/ephc.201402534.
- 41 H. A. Benesi and J. H. Hildebrand, *J. Am. Chem. Soc.*, 1949, **71**(8), 2703–2707, DOI: 10.1021/ja01176a030.
- 42 G. L. Long and J. D. Winefordner, *Anal. Chem.*, 1983, **55**, 712A–724A, DOI: 10.1021/ac00258a724.
- 43 L. Krause, R. Herbst-Irmer, G. M. Sheldrick and D. Stalke, *J. Appl. Crystallogr.*, 2015, **48**, 3–10, DOI: 10.1107/S1600576714022985.
- 44 G. M. Sheldrick, *Acta Crystallogr., Sect. A: Found. Crystallogr.*, 2008, **64**, 112–122, DOI: 10.1107/S2053229614024218.
- 45 G. M. Sheldrick, *Acta Crystallogr., Sect. C: Struct. Chem.*, 2015, **71**, 3–8, DOI: 10.1107/S2053229614024218.
- 46 C. F. Macrae, P. R. Edgington, P. McCabe, E. Pidcock, G. P. Shields, R. Taylor, M. Towler and J. van de Streek, *J. Appl. Crystallogr.*, 2006, **39**, 453–457, DOI: 10.1107/S002188980600731X.
- 47 A. Pardo, D. Reyman, J. M. L. Poyato and F. Medina, *J. Lumin.*, 1992, **51**, 269–274, DOI: 10.1016/0022-2313(92)90077-M.
- 48 K. Tayade, S. K. Sahoo, B. Bondhopadhyay, V. K. Bhardwaj, N. Singh, A. Basu, R. Bendre and A. Kuwar, *Biosens. Bioelectron.*, 2014, **61**, 429–433, DOI: 10.1016/j.bios.2014.05.053.
- 49 S. Patil, U. Fegade, S. K. Sahoo, A. Singh, J. Marek, N. Singh, R. Bendre and A. Kuwar, *ChemPhysChem*, 2014, **15**, 2230–2235, DOI: 10.1002/ephc.201402076.
- 50 R. Patil, A. Moirangthem, R. Butcher, N. Singh, A. Basu, K. Tayade, U. Fegade, D. Hundiwal and A. Kuwar, *Dalton Trans.*, 2014, **43**, 2895–2899, DOI: 10.1039/c3dt52770k.
- 51 D. S. Huerta-José, J. G. Hernández-Hernández, C. A. Huerta-Aguilar and P. Thangarasua, *Sens. Actuators, B*, 2019, **293**, 357–365, DOI: 10.1016/j.snb.2019.04.011; C. A. Huerta-Aguilar, T. Pandiyan, N. Singh and N. Jayanthi, *Spectrochim. Acta, Part A*, 2015, **146**, 142–150, DOI: 10.1016/j.saa.2015.03.082; C. A. Huerta-Aguilar, B. Ramírez-Guzmán, P. Thangarasu, J. Narayanan and N. Singh, *Photochem. Photobiol. Sci.*, 2019, **18**, 1761–1772, DOI: 10.1039/C9PP00060G.
- 52 C. A. Huerta-Aguilar, T. Pandiyan, P. Raj, N. Singh and R. Zanella, *Sens. Actuators, B*, 2016, **223**, 59–67, DOI: 10.1016/j.snb.2015.09.064; C. A. Huerta-Aguilar, P. Raj, P. Thangarasu and N. Singh, *RSC Adv.*, 2016, **6**, 37944–37952, DOI: 10.1039/C6RA01231K; C. A. Huerta-Aguilar, T. Pandiyan, N. Singh and N. Jayanthi, *Spectrochim. Acta, Part A*, 2015, **146**, 142–150, DOI: 10.1016/j.saa.2015.03.082; J. A. O. Granados, P. Thangarasu, N. Singh and J. M. Vázquez-Ramos, *Food Chem.*, 2019, **278**, 523–532, DOI: 10.1016/j.foodchem.2018.11.086.
- 53 A. K. Manna, S. Chowdhury and G. K. Patra, *New J. Chem.*, 2020, **44**, 10819–10832, DOI: 10.1039/D0NJ01954B; A. K. Manna, K. Rout, S. Chowdhury and G. K. Patra, *Photochem. Photobiol. Sci.*, 2019, **18**, 1512–1525, DOI: 10.1039/C9PP00114J.
- 54 P. Kaur, D. Sareen and K. Singh, *Talanta*, 2011, **83**(5), 1695–1700, DOI: 10.1016/j.talanta.2010.11.072.
- 55 H. J. Xu, Z. D. Liu, L. Q. Sheng, M. M. Chen, D. Q. Huang, H. Zhang, C. F. Song and S. S. Chen, *New J. Chem.*, 2013, **37**, 274–277, DOI: 10.1039/C2NJ40767A.
- 56 J. S. Lee, S. D. Warkad, P. B. Shinde, A. Kuwar and S. B. Nimse, *Arabian J. Chem.*, 2020, **13**(12), 8697–8707, DOI: 10.1016/j.arabj.2020.09.061.
- 57 S. Liu, L. Zhang, W. Zan, X. Yao, Y. Yang and X. Liu, *Sens. Actuators, B*, 2014, **192**, 386–392, DOI: 10.1016/j.snb.2013.10.134.





INVESTIGATIVE REPORT ON SICKLE CELL ANEMIA FROM SAKRI TEHSIL

L. B. Pawar and P. P. Rathod

S.G. Patil Arts, Science & Commerce College, Sakri Dist. Dhule 424304

Email: lahupawar2322@gmail.com

ABSTRACT:

Sickle cell Disease (SCD) is a group of genetic disease commonly seen in United States and three countries of the world. The term disease is applied to this condition because the inherited abnormality causes a pathological condition in which red blood cells becomes sickle shaped. In Maharashtra, the sickle gene is widespread in all the eastern districts, also known as the Sakri region, in the Satpura ranges in the west and in some parts of Khandesh. The prevalence of sickle cell carriers in different tribes varies from 0 to 35 percent. The tribal groups with a high prevalence of HbS (20-35 %) include the *Bhils*, *Madias*, *Pawaras*, *Paridhans* and *Otkars*. In present study from Sakri tehsil of Dhule district there are 39.6% in male and 60.3% in female sickle cell anemic patients found and its ratio was 94.8% in ST category and 14.6% in other categories found

INTRODUCTION:

Sickle cell disorder is a group of diseases caused by a point mutation at sixth position in beta globin chain, valise substituting glutamic acid due to which in deoxygenated state, shape of erythrocytes change to sickle shape and also the fragility of cell member acne increase. In India, it is more common in central and southern parts of the country it is the second most common hemoglobin apathy. Next to thalassaemia in India in 1952, Lehman and catbush reported the presence of the disease in India among the tribal of Nigeria hills for the 1st time. This was largely because most of the subsequent reports spread a misconception that the sickle gene in India was confined to the tribal population are some scheduled caste only.

The sickle gene is widespread among many tribal population groups in India with prevalence of heterozygotes varying from 1-40 per cent. Co-inheritance of the sickle gene with β -thalassaemia, HbD Punjab and glucose-6-

phosphate dehydrogenase (G6PD) deficiency has also been reported. Most of the screening programmes in India now use high performance liquid chromatography (HPLC) analysis although the solubility test is also sensitive and cheap. Sickle cell disease (SCD) among tribal populations is generally milder than among non-tribal groups with fewer episodes of painful crises, infections, acute chest syndrome and need for hospitalization. (Roshan B. et al., 2015)

Sickle cell disease (SCD) is a very devastating condition caused by an autosomal recessive inherited haemoglobinopathy. This disease affects millions of peoples globally which results in serious complications due to vasoocclusive phenomenon and haemolysis. This genetic abnormality is due to substitution of amino acid valine for the glutamic acid at the sixth position of beta chain of haemoglobin. This disease was described about one hundred year ago. The haemoglobin S (hbS) produced as result of this defect is

poorly soluble and polymerized when deoxygenated. Symptoms of sickle cell disease are due to chronic anaemia, pain full crises, acute chest syndrome, stroke and susceptibility to bacterial infection. In recent years measures like prenatal screening, better medical care, parent education, immunization and penicillin prophylaxis have successfully reduced morbidity and mortality and have increased tremendously life expectancy of affected individuals. (KAUR M et al. 2013).

Sickle cell disease is a major genetic disorder amongst Scheduled Caste (SC), Scheduled Tribe (ST), and Other Backward Communities (OBC) population groups of Maharashtra. We modified diagnosis technique and developed simple laboratory technology to identify carrier (Hb SS) and sufferer (Hb AS) suitable for field work. In order to find out prevalence for sickle cell disorder we screened major communities from the state and found high prevalence amongst SC, ST and OBC. The overall prevalence amongst SC, ST and OBC is 10%. Severe joint pains and milder type of jaundice are peculiar symptoms amongst sicklers from the state of Maharashtra. (S. L. Kate and D. P. Lingojwar 2002).

Chances are that you might not have heard much about Sickle Cell Disease ("SCD") lately. That doesn't mean that it has gone away. It certainly hasn't. SCD is still negatively impacting the lives of millions of people worldwide. There are as many as 150,000 babies born with the disease each year in Nigeria, alone. Gary A. Gibson 2011

MATERIAL AND METHODS:

Study area- Study was conducted in rural area of Sakri tehsil from Jan. 2018 to Dec. 2018. The villages from Sakri tehsil were selected by proportional randomization.

The population was screened by holding camps in each village at evening time as village people are available in the evening time only after 6.00 pm. The population was screened by dithionite tube test CDTT or solidity test.

Dithionite tube turbidity test -

1. Few drops of blood were collected by pricking ring finger and added to glass tube containing sodium citrate in normal saline solution.
2. After mixing, it was centrifuged for 2 to 3 min. at 3000 rpm.
3. 1ml of phosphate buffer reagent was taken in a glass tube.
4. A small quantity of sodium dithionite was added to it and was mixed well to dissolve.
5. A small drop washed red cell of blood is added and was mixed well to produce light pinkish colour.

RESULT, DISCUSSION AND CONCLUSION:

In present study, solubility (DTT) test was used as a screening test as it is a rapid method and easy to be carried out in the field setting, used by ICMR network on sickle cell disorder coordinated by Institute of Immunohematology. The prevalence of disorder was more in age group of 10-20 yrs.

As per data of Govt. rural hospital, Sakri electrophoresis test report shows,

Total test – 116 patients 1 Normal patient –
15 - 12.9% 2 Sickle cell trait – 94 -
81% 3 Sickle cell disease – 7 - 6%

Sex wise percentage 1 Female patient – 39.6% 2 Male patient – 60.3%

Caste wise patient 1 ST category – 84.8%
2. OBC category - 14.6%

Age wise percentage the percentage of disease was more in 10-20 yrs. And minimum in age group 31-50

The sex wise prevalence was 39.6% in male and 60.3 % in female. The maximum prevalence was found in ST category people i.e. 94.8% and in OBC category people was 14.6% respectively. The electrophoresis pattern revealed that 81.0% were sickle cell traits and 6.0% were sickle cell anemic as well as 12.9% is normal.

REFERENCE :

- Gary A. Gibson., Sickle Cell Disease: Still Here and Still Causing Pain., Martin Center., 2011, 1-19
- Kaur M, Dangl Cbs & Singh M., An Overview On Sickle Cell Disease Profile., *Asian J Pharm Clin Res*, Vol 6, Suppl 1., 2013, 25-37
- Roshan B. Colah, Malay B. Mukherjee, Snehal Martin & Kanjaksha Ghosh., Sickle cell disease in tribal populations in India., *Indian J Med Res* 141., 2015, 509-515
- S. L. Kate and D. P. Lingojwar., Epidemiology of Sickle Cell Disorder in the State of Maharashtra., *Int J Hum Genet*, 2(3), 2002, 161-167

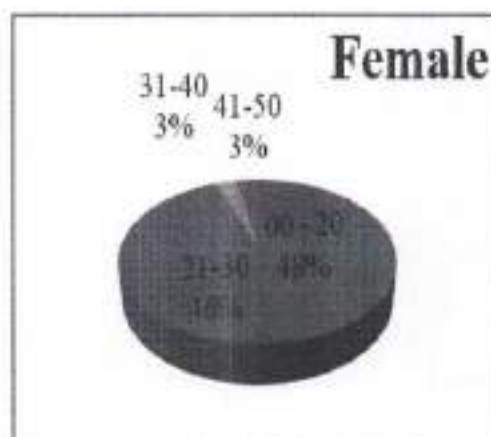
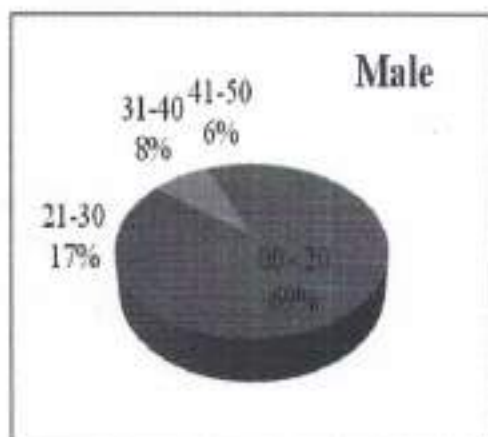
Sr. No.	Age	Gender			
		Male	%	Female	%
1	10-20	33	28.4	33	28.4
2	21-30	8	6.8	31	26.7
3	31-40	4	3.4	2	1.7
4	41-50	3	2.5	2	1.7



Normal Red Blood Cell



Sickle Cell



Vidya Vikas Mandals
Sitaram Govind Patil Arts,
Science and Commerce College,
Sakri Tal. Sakri Dist. Dhule 424 304



NAAC
ACCREDITED

विद्या विकास मंडळाचे,
सिताराम गोविंद पाटील कला,
विज्ञान आणि वाणिज्य महाविद्यालय,
साक्री ता. साक्री जि. धुळे ४२४ ३०४

Affiliated to Kavayitri Bahinabai Chaudhari North Maharashtra University, Jalgaon

Website : www.sgpcsakri.com

Email : vidyavikas2006@rediffmail.com

Ph : 02568-242323

3.3.2.1 Research Paper Published in UGC Care Listed Journals

जागतिकीकरण आणि मराठी कविता

डॉ. प्रकाश श्रीराम साळुंके

मराठी विभाग प्रमुख

सी. गो. पाटोल महाविद्यालय साकी.

जि. पुणे

Abstract:-

जागतिकीकरण आणि मराठी कविता या शोधनिबंधात जागतिकीकरण या संकल्पनेविषयी माहिती, नवदोत्तर कालखंडात उदयाला आलेल्या जागतिकीकरण खाजगीकरण आणि उदारीकरण ह्या त्रीसुत्रीचा समाजजीवनावर पडलेल्या प्रभावाबरोबरच मानवी संस्कृतीच्या बदलत्या स्वरूपाचे विन्न रेखाटलेले असून बदलते खेडे व महानगरीय जीवन-जाणीव,माहिती आणि तंत्रज्ञानाचा प्रचंड वापर, बहुराष्ट्रीय कंपन्यांचे वाढत जाणारे वर्चस्व, कृषीसंस्कृतीचा ऱ्हास,मानवी मूल्यांचे अवमूल्यन,धंगळवादी वृत्ती अशा सर्व बाबींचा मराठी कवितेवर कसा प्रभाव पडला ? तो मराठी कवितेतून कसा साकार झाला या संबंधी विचार मांडलेला आहे.हे करतांना मराठी कवींच्या कवितेतील जागतिकीकरणाच्या बाबतीतल्या काही महत्त्वाच्या निवडक ओवी, त्यांचे विश्लेषण,समारोप,निष्कर्ष आणि सदभसूची देण्यात आलेली आहे.

विज्ञप्ति (Key Words) :- जागतिकीकरण संकल्पना, नवदोत्तर कालखंड, बदलते भावविश्व,महानगरीय जीवन,सायबर जग.

प्रस्तावना :-

विसाव्या शतकाच्या अखेरच्या कालखंडातील एक महत्त्वपूर्ण घडामोड म्हणून जागतिकीकरणाचा उल्लेख केला जातो. जागतिकीकरण, खाजगीकरण आणि उदारीकरण याविषयीची चर्चा १९९१ पासून होऊ लागली. जागतिकीकरण, खाजगीकरण प्रभाव जगातील सर्वच राष्ट्रांवर पडलेला आहे. आपल्या भारत देशातही तत्कालीन पंतप्रधान पी. व्ही. नरसिंहराव व अर्थमंत्री डॉ. मनमोहनसिंग यांच्या पुढाकाराने भारताने नवे आर्थिक धोरण स्वीकारले. त्यात जागतिकीकरण, खाजगीकरण व उदारीकरण ह्या त्रिसूत्रीचा स्वीकार करण्यात आला. जागतिकीकरण आज काळाची गरज बनली आहे. प्रवास साधनांच्या क्षेत्रातील क्रांती व माहिती तंत्रज्ञानाचा विस्फोट यामुळे संपूर्ण जग एकत्र येणे अटळ बनले आहे.

जागतिकीकरणामुळे भांडवली अर्थव्यवस्था आणि आधुनिक जीवनमानाची नवी परिमाणे निर्माण झालीत. संपूर्ण जग हा एक मुक्त बाजारपेठ बनली. विज्ञान तंत्रज्ञानाच्या प्रभावामुळे नवनवे शोध आणि त्यांचा मानवी जीवनावरील प्रभाव वाढला. नवी विचार प्रणाली, बदलती मूल्यव्यवस्था आणि विकासाचे नवे सिद्धांत यांचा मानवी जीवनावरील प्रभाव वाढला. नवीन विचारप्रणाली, बदलते मूल्यव्यवस्था आणि विकासाचे नवे सिद्धांत यांचा मानवी जीवनावर प्रभाव पडू लागला. जागतिकीकरणात पैसा हा जगण्याचा मूलाधार बनला. पैसा मिळवण्यासाठी वाटेल त्या मार्गांचा मानस अवलंब करू लागली. त्यातून जगण्याची झेळी बदलली. सुखवाद व चंगळवादाने माणसाला घेरले. जागतिकीकरण हे खाजगीकरणाचा प्राधान्य देणारे असल्याने भांडवलदारांसाठी ही एक पर्वणी ठरली असून सर्वसामान्यांसाठी मात्र श्वाप ठरला आहे. जागतिकीकरण आज फक्त आर्थिक क्षेत्रापुरतेच मर्यादित न राहता सामाजिक, राजकीय, सांस्कृतिक व साहित्यिक क्षेत्र ही त्याने काबीज केले आणि ग्लोबल सांस्कृतिक्या नावाखाली संस्कृतीचे विकृतीकरण सुरू

झाले. पाश्चात्य वेपभूषेने आज संपूर्ण युवावर्गाला आपल्या कवेत घेतले आहे. संगीत व कला क्षेत्रासाठी संपूर्ण विश्व हे व्यासपीठ बनले आहे. या सर्व बाबींचा प्रभाव मराठी कवितेवरही पडलेला असल्यामुळे मराठीतील अनेक सर्जनशील व संवेदशील साहित्यिकांच्या लेखणीतून जागतिकीकरणाचा मानवी जीवनावर पडलेला प्रभाव आपल्या साहित्यात दिसून येतो. त्याला 'कविता' हा साहित्य प्रकारही अपवाद नाही.

जागतिकीकरणाचा मराठी कवितेवर झालेला परिणाम :-

नव्वोत्तर कालखंडातील मराठी कवितेला जागतिकीकरणाचा संदर्भ आहे. माणसाच्या भाव-भावना-संवेदना, विचार, जीवनविषयक जाणीवा, नवी दृष्टी, नाते संबंध आदि बाबींकडे पाहण्याचा दृष्टीकोन बदलला आणि हेच बदलते भावविश्व कवी सुनील अवचार, अरुण काळे, उत्तम कांबळे, महेंद्र भवरे, इंदुजीत भालेराव, हेमंत दिवटे, मंगेश काळे, संतोष पवार, भुजंग मैत्राम, अशोक कोतवाल, अशोक इंगळे, श्रीकांत देशमुख, पी. विठ्ठल, प्रजा लोखंडे, कविता महाजन, प्रज्ञा गोळे आदि कवी कवयित्रींच कवितांमधून प्रकर्षाने प्रकटलेले आहे.

माहिती आणि तंत्रज्ञानामुळे जग जवळ आले मात्र माणूस माणसापासून दूर जातो आहे. मानवी भाव-भावना-संवेदना बोधट झाल्या असून मानवी संस्कृतीचेही बाजारीकरण होत आहे. नव्या साम्राज्यशाही धोरणांच्या मायावी षडपंक्तात महानगरे कशी सामील झाली आहेत हे बदलते भावविश्व कवी सुनील अवचारांनी आपल्या कवितेतून अचूक टिपले आहे.-

"या ग्लोबल वर्तमानात भावना झाली आहे जाहिरात

आणि मेंदूचे झाले आहे कॉम्प्युटर,

तंत्रज्ञान झाले आहे युज अँड थ्रो

संस्कृती झाली आहे रखेल..."

महानगरीय जाणीवा बदलल्यामुळे जागतिकीकरणात मानवी भाव-भावनेला किंमत राहिलेली नाही. मानवी मॅदू कॉम्प्युटर प्रमाणे वागतांना दिसतो. मात्र त्यामुळे माणसाचे तंत्रज्ञान आज युज अँड थ्रो वाटू लागले आहे. या तंत्रज्ञानामुळे मानवी संस्कृतीची जागा विकृतीने घेतली आहे. जणू ही संस्कृती बहुराष्ट्रीय कंपन्याची रखेल झाल्याचे कवीला वाटते.

कवी अरुण काळे यांच्या 'नंतर आलेले लोक' या कवितासंग्रहामधून जागतिकीकरणाचे प्रतिबिंब नेमकेपणाने प्रतिबिंबित झालेले आहे. आपल्या कवितेत नव्या प्रतिमासृष्टीचा वापर करून 'खाउजा' संस्कृतीचे महाभयंकर संकट त्यांनी अधोरोलेखित केले आहे.-

"जे बळी तुरुंगाच्या स्फोटाचे

तेच बळी माहितीच्या स्फोटाचे

हे बदललेले फॉर्म जातीय द्वेषाचे

हे विषाणू बहुजन हिताचा प्रोयाम नष्ट करणारे

हे जागतिकीकरण" (नंतर आलेले लोक पृ.१२)

कवी अरुण काळे यांनी आपल्या कवितेत वरीलप्रमाणे संगणक क्रांती, तंत्रज्ञान युगाची परिभाषा योजून वर्तमानात माणूस संगणकाचा उपयोग मोठ्या प्रमाणावर करू लागला. मात्र याच संगणकीय

कार्यप्रणालीत प्रोग्राम नष्ट करणारा 'विषाणू' असल्याचे सांगून तो 'विषाणू' समान्य माणसाच्या हिताआड येणारा असल्याचेही म्हटले आहे.

कवी अशोक कोतवाल यांच्या कवितेने जागतिकीकरण लोकशाही आणि संस्कृती यांच्या बदलत्या स्वरूपाचे चित्र रेखाटले आहे. मधल्या सुटीत झाळेतून पळून जाणाऱ्या मुलांचे मन चित्रित करताना कवी म्हणतात.-

"त्यांच्या लेखी झाळा होऊ शकत नाही! विरंगुळा

सायबर कॅफेतील

डर्यू डर्यू डर्यू डॉट कॉम व्हावी एक वेबसाईट झाळा"

(कृपीय कसे बोलत नाही पृ.२४)

वर्तमान स्थितीत झाळेत शिकणाऱ्या मुलांचा कल झाळेपेवजी सायबर कॅफेकडे वळलेला आहे. कारण झाळेतील शिक्षणाच्या मनोरंजनापेक्षा सायबर कॅफेतील मनोरंजनात्मक शिक्षण मुलांना सहज अवगत होत असते म्हणून मुलांचा झाळेत जाण्याकडे ओढा निर्माण करण्यासाठी झाळाच एक वेबसाईट व्हावी अशी अपेक्षा कवी करतो.

कवी पी.विठ्ठल आपल्या कवितेतून महानगरीय जीवनाने एका विपरीत बळपावर मानवी जीवन आणून ठेवल्याचे तसेच संस्कृतीला निव्वळ मनोरंजनाच्या पातळीवर आणून ठेवल्याचे आणि हरबत घाललेल्या मानवी संवेदनाचे भाव व्यक्त करतात. पावलांचे ठसे,झाडाची सावली,रवताला फुटणारे कोवळे कोब अशा मातीशी मानवाचे असलेले अतूट नाते सांभाळणाऱ्या गोष्टी नाहीशा झालेल्या आहेत असे

कवीला वाटते.मातीची संवादी मानवी जीवनाचा आवाज ऐकू येत नाही म्हणून कवी व्यथित होतो आणि म्हणतो.-

"डोक्यावरून सळसळत धावतो फ्लायओव्हर

आणि गाडीच्या कर्पाकर्कश

आवाजानं हृदयाचा सेन्सेक्स पार कोसळतो."

अशा प्रकारे कवीची अवस्था झाली आहे.महानगरीय भौतिक संपन्नतेतही अस्वस्थ असणारे हे कविमन महानगरीय जगण्याच्या सांस्कृतिक अंगोपांगाच्या नटव्या तऱ्हा पाहून अधिकच वेचून झालेले आहे.-

"लेखक-बिखक,वही-पेन-पुस्तक

हवेयत कुषाला ?

हाउसफुल्ल मल्टीप्लेक्स, मॉल्स आणि

चायनीज डीव्हर उडतोच पेशावा पतंग"

महानगरीय जीवनाचे संस्कृतीला निव्वळ मनोरंजनाच्या पातळीवर आणून ठेवल्यामुळे लेखक-बिखक, वही-पेन-पुस्तक हवेयत कुषाला? असा उद्दिग्ग प्रश्न कवी येथे उपस्थित करतो.

जागतिकीकरणाच्या प्रक्रियेमुळे घडून आलेला प्रचंड सामाजिक बदल आणि महानगरीय जीवन जाणिवेची घुसमट कवी महेंद्र भबरे आपल्या कवितेतून व्यक्त करतात.माहिती आणि तंत्रज्ञानाच्या प्रचंड

वापरामुळे महानगरीय जीवनात प्रचंड उलथापालथ घडून आलेली आहे. महानगरातला माणूस व्यक्ती केंद्रित बनला त्यामुळे त्याची नजर फायबर ग्लासाकडून सायबर जगाकडे वळलेली दिसते. इथे माणसाकडे ग्राहक म्हणून बघितले जाते त्यामुळे मानवी मूल्यांचे अवमूल्यन घडत असल्यामुळे या युगाला ते 'पत्थरदिल युग' संबोधतात -

"फायबर ग्लास्कडून सायबर न्याहळणारी नजर

नपुंसक जगावर घालते दगड

पर्थरदिल युगाच्या आधुनिक वळणावर

थवकते जाग्यावर"

महानगरीय वास्तवामुळे मानवी जीवनात होणाऱ्या बदलांचा आणि त्यातील वेगवेगळ्या अवस्थांचा वेध कवी महेंद्र भावरे आपल्या कवितेतून घेतात.

कवी हेमंत दिवटेच्या कवितेतही महानगरीय जाणिवेचाच आविष्कार आहे. शहरी माणसाच्या नदीत माणुसकी सापडणे कठीण झाले आहे . पंगळवादी संस्कृती उदयास आली असून माणसाने आपल्या जीवन जाणीवा बदललेल्या आहेत. पप्रत्येक्ष वस्तूपेक्षा वस्तूच्या जाहिरातींवरच माणसाचा जास्त विश्वास आहे. म्हणूनच आपल्या कवितेत त्यांनी जागतिकीकरणातील जाहिरातींच्या भाषेचा अज्ञानाभिन्नतेसाठी धांयला वापर केला आहे 'मेगामॉल झॉपिंग' वा कवितेतून त्याचा प्रत्यय घेतो

"तर या मेगा झॉपिंग मॉलमध्ये झॉप करतांना

अतिमायको विचार येत राहतात

जस की मी आहे पहिल्या रँकमधला

व्हीसपर नॅपकीन पॅक

नेक्स्ट रँकमधला हमीचा पॅक बनून मी

कूठल्याही बाळाचं मलमूत्र साचवून ठेवतोय"

(धांबलाच येत नाही पृ.७)

याच कावितेत कवीने सातला व्हीसपर नॅपकीन,हमीचा पॅक असे संबोधले असून आपण असाचवर्गीयांच्या उपभोगाची वस्तु असल्याची खंत व्यक्त केली आहे.

कवी उत्तम कांबळे यांनी जागतिकीकरणामुळे आर्थिक,समाजिक,सांस्कृतिक स्तरावर घडून येत असलेल्या दुष्परिणामापेक्षा कृषीसंस्कृतीवरझालेले दुष्परिणाम किती दूरगामी स्वरूपाचे आहेत ते त्यांच्या पुढील ओव्यांमधून जाणवते -

"शेताच्या काळजावरील

असंख्य भेगावर अश्रू गाळत

वाधावरून फिरणारी माझी कविता

जागतिकीकरणाच्या लाटेत

हातातून निसटणारी सबसिडी

गद्य पकडण्याचा प्रयत्न करित होती."

(जागतिकीकरणात माझी कविता पृ.८८)

सदर ओळीमधून कवी उत्तम कावळे यांनी जागतिकीकरणामुळे कृषीसंस्कृतीवर किती दूरगामी परिणाम झाले आहेत त्याचे वास्तव चित्रण केले आहे.

कवी अशोक इंगळे आपल्या कवितेतून जागतिकीकरणामुळे बदललेले नागरी वास्तव चितारतात.जागतिकीकरणामुळे ग्रामजीवनातही कसे परिवर्तन घडून येत आहे. आज खेडे बदलले आहे मात्र हे बदल मानवी नात्यांची घडी विस्कटून टाकणारे आहेत. ग्रामीण भागातही पैसे कमवण्याची जणू धर्यतच लागलेली आहे. कोणत्याका मानाने असेना पैसा आला पाहिजे असा ग्रामसमज निर्माण झालेला आहे.'गावाच्या इन्स्टट प्रगतीसाठी' या कवितेत त्यांनी जागतिकीकरणामुळे ग्रामजीवनात कसे परिवर्तन झालेले आहे ते अतिशय मार्मिक शब्दात मांडलेले आहे.-

"आताशा गावाला जडलाय रोग

जमीन एन.ए.करून घेण्याचा

घोंट पाडून विकण्याचा

पोल्ट्रीफॉर्म, धावा टाकण्याचा इन्स्टट प्रगतीचा

महासत्तेच्या स्पर्धेत धावण्यासाठी गावाने पकडलाय वेग कालीपितीचा

म्हणून गावाच्या उत्पनाचा आलेख झळकतो.

डिजिटल पोस्टर्सच्या होलिंगवर...."

(गावाच्या इन्स्ट प्रगतीसाठी काव्यसंग्रह 2013 पृ.६७)

अशा प्रकारे ग्रामजीवनातही स्वतःच्या काव्या आईला (शेतीला)विकून त्या जागेवर ग्राॅट पाडणे,हॉटेल टाकणे,पोल्ट्रीफॉर्म टाकणे आदि वेगवेगळ्या गोष्टीतून पैसा कमवण्याची चढाओढ चालल्याचे दिसून येते. मात्र गावाची ही प्रगती दिखाऊ असल्याचे कवी म्हणतात. कवी कालीपिलीच्या वेगाशी गावाच्या प्रगतीच्या वेगाची तुलना करतात. मात्र कालीपिली ही केव्हाही कुठेही बंद पडू शकते तसा गावाच्या विकासाचा वेगही केव्हाही मंदाऊ शकतो याचे सूचनाही कवी करतात.नुसत्याच पोष्टरवर फोटो झळकल्याने आपले कर्तृत्व सिद्ध होत नसल्याचेही ते सांगतात म्हणजे जागतिकीकरणामुळे ग्रामजीवनातही अशा प्रकारे बदल घडत असल्याचे उपहासात्मक मत कवी व्यक्त करतात.

समारोप :-

अशा प्रकारे नव्वदोत्तर कालखंडात उदयास आलेल्या जागतिकीकरण, खाजरीकरण आणि उदारीकरण या त्रिमूर्तीचा समाजजीवनावरोबरच मानवी संस्कृतीच्या बदलत्या स्वरूपाचे विच मराठी कवितेत रेखाटलेले असून गाव-शहरांचे बदलते स्वरूप, तेथील जीवन-जाणीव,माहिती तंत्रज्ञानाचा प्रचंड वाढता वापर,बहुराष्ट्रीय कंपन्यांचे वाढत जाणारे वर्चस्व,कृषीसंस्कृतीचा ऱ्हास, मानवी मूल्यांचे अवमूल्यन,तेथील एकाकीपणा,बोधट संवेदना, स्वार्थीवृत्ती,यात्रिकता,मूल्यशून्यता,धंगळवादी वृत्ती,संस्कृतीचे बाजारीकरण,विकृतीकरण आणि सामाजिक बदलांचा वेध मराठी कवींनी आपल्या कवितांमधून समर्थपणे घेतला आहे.

निष्कर्ष :-

१) नव्वदोत्तर मराठी कविता ही जागतिकीकरणाच्या परिणामांचा वेध घेणारी कविता आहे.

- २) जागतिकीकरणामुळे मराठी कवितेचे आश्रयविद्य बदलले.
- ३) मानवी म्म मुल्यांची घसरण व मापसा-मापसातील दुरावा यांचे देधक चित्रण मराठी कवितेत चित्रित झालेले आहे.
- ४) विदेशी संस्कृती व सायबरचे जग यामुळे मानवी नवी पिढी उदस्त होण्याच्या मार्गावर असल्याचा इशारा मराठी कविता देत आहे.
- ५) जागतिकीकरणामुळे कृषीसंस्कृती, सामाजिक व सांस्कृतिक नितीमूल्य यांचे अस्तित्व धोक्यात येत असल्याची जाणीव मराठी कवितेने अधोरेखित केली आहे.

संदर्भ :-

- १) अवचार सुनील- 'होबल वर्तमानाच्या कविता' दत्ता प्रकाशन अमरावती.पृ.१
- २) Awachar Sunil- 'Poetry Against Human Injustice' पृ. १ ते ८
- ३) गोविलकर लीला- 'अनिवार्य मराठी' के.सागर पब्लिकेशन्स पुणे. पृ.७३,७४
- ४) जाधव मा.मा.(संपा दक) 'अक्षरगाथा' ऑक्टोबर २०११ मधील. डॉ.अशोक इंगळे यांचा लेख पृ.४३ ते ५२
- ५) पाटील व्ही.बी. 'मानवी हक्क' के.सागर पब्लिकेशन्स पुणे पृ. ३१५,३३८

- ६) सुरवाडे मोहन 'ग्रामीण साहित्य प्रकार स्वरूप आणि विकित्सा' सुगम प्रकाशन अमरावती पृ. १८१ ते १८३
- ७) मराठी अभ्यास मंडळ कबचौ उमवि जळगाव (संपादन) 'काव्यांकुर'- प्रशांत पत्रिकेखन्स जळगाव. पृ.३३,३६
- ८) वले वसुदेव (संपादक) 'जागतिकीकरणाचा मराठी भाषा व साहित्यावरील प्रभाव' मधील डॉ. अशोक इंगळे यांचा लेख पृ.२७४ ते २८१

जस की मी आहे पहिल्या रँकमधला
व्हीसपर नॅपकीन पॅक
नेक्स्ट रँकमधला हग्गीचा पॅक वनून मी
कूठल्याही बाळाचं मलमूत्र साचवून ठेवतोय"
(धाबताच येत नाही पृ.७)

याच कावितेत कवीने खतला व्हीसपर नॅपकीन, हग्गीचा पॅक असे संबोधले असून आपण
असाचवर्गीयांच्या उपभोगाची वस्तु असल्याची खंत व्यक्त केली आहे.

कवी उच्चम कांबळे यांनी जागतिकीकरणामुळे आर्थिक, समाजिक, सांस्कृतिक स्तरावर घडून येत
असलेल्या दुष्परिणामापेक्षा कृषीसंस्कृतीवर झालेले दुष्परिणाम किती दूरगामी स्वरूपाचे आहेत ते त्यांच्या
पुढील ओव्यांमधून जाणवते -

"शेताच्या काळजावरील
असंख्य भेगांवर अश्रू गाळत
बांधांवरून फिरणारी माझी कविता
जागतिकीकरणाच्या लाटेत
हातातून निसटणारी सबसिडी

गव्ह पकडण्याचा प्रयत्न करित होती."

२६. संत साहित्यातील संत कवयित्री: विशेष संदर्भ संत कान्होपात्रा

प्रा. डॉ. प्रकाश श्रीराम साळुंके

सी. गो. पाटील महाविद्यालय, सात्री - जि. धुळे.

प्रस्तावना

महाराष्ट्र भूमी ही संतांची पावन भूमी आहे. येथे वैराग्याची परंपरा मांदलेली आहे. मध्यदुर्गान महाराष्ट्राच्या सांस्कृतिक आणि वाङ्मयीन परंपरेत संतांचे कार्य आणि महत्त्व अनन्यसाधारण आहे. सामाजिक अस्मितेचे व सांस्कृतिक ऐक्याचे संतच खरे शिल्पकार होत. तेराव्या शतकामध्ये संत ज्ञानेश्वर महाराजंनी भागवत धर्माचा म्हणजेच वारकरी संप्रदायाचा पाया रचला आणि महाराष्ट्रात धार्मिक व सामाजिक प्रबोधनाची मुहूर्तमेढ रोवली. संत नामदेवांनी आपल्या भावोपकटने, श्रद्धावळने आणि समर्पणशील वृत्तीने भागवत धर्माच्या पताकाखाली सर्व जाती-धर्मांच्या लोकांना एकत्रित आणले जातीभेदापलीकडे जाऊन समतावादी विचाराने एकत्रित आलेल्या वारकऱ्यांमध्ये भक्तीमधून स्नेहभाव रूजवला. आणि पंढरीच्या पांडुरंगाच्या प्रांगणात, चंद्रभागेच्या वाळवंटात अठरापगड जातीच्या वारकऱ्यांची मांदियाळी जमवून, वर्णाभिमान विसरून अध्यात्मिक लोकशाहीची प्रतिष्ठापना केली. रूढीग्रस्त अज्ञ जनांना आत्मोन्नतीचा मार्ग दाखविला. संत ज्ञानेश्वरांनी त्यांना खऱ्या खऱ्या धर्माचा अर्थ सांगितला. संपूर्ण समाज भक्तीच्या एका सूत्रात बांधला. भक्तीच्या क्षेत्रात कोणी श्रेष्ठ नाही, कोणी कनिष्ठ नाही, लहान-बोर, स्त्री-पुरुष, उच्च-निच्य सर्वांनाच भक्तीचा अधिकार असून भक्तीच्या बळवर इथे पापी माणसाचाही उद्धार होत असल्याचे सांगितले. देव भावाचा भूकेला असतो. त्याला जाती कुळाशी काही देखेणे नसते ही विचारसरणी मांडून अध्यात्मिक लोकशाहीचे, समतेचे बंधत्वाने मर्म सांगितले हे सर्व संत ग्रामसंस्थेतील अलुतेदार-बलुतेदार होते. फार काही शिकलेले नव्हते. त्यांनी जमेल तसे आपले भाव देवापुढे निरूपण केले. प्रपंचात आलेले भलेबुरे अनुभव, व्यक्तिगत सुखदुःखे, समाजात होणारी उपेक्षा मुक्तीची अस, समतेचा ध्वास याचेच प्रतिबिंब त्यांच्या निवेदनात उमटलेले आहे. त्यांची भावा साधी-सोपी-सरळ, रसाळ, अनलंकृत आणि हृदयाचा ठाव घेणारी आहे. उच्च जातीच्या संतांना जातीचा अभिमान नाही आणि हीन जातीच्या संतांनी जातीबद्दल कमीपणाही अनुभवला नाही. या भक्तीमार्गात सर्व स्तरातील आणि व्यवसायातील स्त्री-पुरुष एकत्र आलेत. संत ज्ञानेश्वरांपासून ते संत चोखामेळ्यापर्यंत अठरा पगड जातीच्या या संत पुरुषांसोबत संत मुक्ताबाई, जनाबाई, सोयराबाई, निर्मळ, पागू, कान्होपात्रा यासारख्या स्त्रीसंतांचाही समावेश आहे. या सर्व संतांनी भक्तीभागामध्ये आपापले योगदान दिलेले आहे. संत कान्होपात्रेचे जीवन भाग या सर्व संत कवी-कवयित्रीपेक्षा मला वेगळे जाणवल्यामुळे 'सदर निबंधातून त्यांचे स्मरण करण्याचा प्रयत्न केलेला आहे.

संत कान्होपात्रा यांचा जीवन परिचय

पंढरपूरपासून २४ को.मी. अंतरावर असलेल्या मंगळवेढा या गावी कान्होपात्रेचा जन्म रामा नामक गणिकेच्या पोटी इ.स. १४६८ मध्ये झाल्याचे मानले जाते. अवध्या तीस वर्षांचे आयुष्य तीला लाभले. गणिकेच्या पोटी जन्मल्याने तिला पित्याचे छत्र लाभले नाही. नाचगाण्याची कला कुळतच असलेली कान्होपात्रा तारुण्यात अधिकच सुंदर दिसू लागली होती

तीच्या रूपाची व नृत्यगायन कलेची कीर्ती चोहीकडे पसरली होती. आपल्या मुलीने आपल्यासारखेच गणिक व्हावे असे शामला वाटत होते. तिच्या जीवाने आपलं श्रीमंती उपभोगू असा शामलाचा मनोदय होता आणि तो मनोदय शामाने कान्होपात्रेस बोलून दाखवला मात्र तीला मान्य नव्हते. तीला आईप्रमाणे देहविक्रय करावया नव्हता. कारण ती लहानपणापासूनच ती श्रीकृष्णाची भक्त होती. 'कै मी उद्धार पावेन । कै कृपा करील नारायण ।' अशी भक्तीची आर्तता तिच्या वृत्तीत होती. तीला अध्यात्मात रुजावचे होते. मात्र तीला आपण गणिकेच्या कुळात म्हणजे हीन कुळात जन्मल्यामुळे परमेश्वर आपली भक्ती मान्य करील काय? परमेश्वर आपणास प्राप्त होईल काय? आपला उद्धार करील काय? असे अनेक प्रश्न तीला सतावत होते तरीही ती कृष्णभक्तीत आपले जीवन व्यतित करते.

कृष्णभक्तीत तल्लीन असल्यामुळे तीला पंढरीच्या वारकऱ्यांची झुजे ऐकण्याचा छंद लागला. त्यांच्याबरोबर तीही पंढरपूरस गेली. पांडुरंगाचे सावळे सगुण रूप पाहून तीला त्याचा लोभ बडला. ती पांडुरंगाचे गुणगाण गाऊ लागली.

कान्होपात्रेच्या सौंदर्याची कीर्ती बिदरच्या राजाच्या कानावर जाते. राजा तीला आणण्यासाठी सैनिक पाठवतो. ते सैनिक तिच्यापुढे बादराहाच्या तारुण्याचे व वैभवाचे वर्णन करतात आणि आम्ही-तुला राजाकडे घेऊन जाण्यासाठी आलो असल्याचे सांगतात मात्र तीला ते काहीही नको होते. तीला आपले चरित्र व शील जपायचे होते. पांडुरंगाच आपल्याला यातून मार्ग दाखवेल असा विश्वास तीला असल्यामुळे ती मनोमनी विठ्ठलाच्या धावा करते स्वतःच्या आईपेक्षाही तीला पंढरीची विटाई, कृष्णाई, कान्हाई पिच्छासाठी वाटल असल्यामुळे ती त्या सैनिकांना सांगते की 'बिदरला येण्यापूर्वी मला पांडुरंगाचे दर्शन घ्यायचे आहे. तुम्ही इथे बसा मी मंदिरात जाऊन येते. पांडुरंगाचा निरोप घेऊन येते.' आणि ती मंदिरात जाते दुवासन्मुख बसून ती पांडुरंगाला विनवनी करते त्याला त्याच्या जिदाची आठवण करून देते अखेर तिची निस्सिम भक्ती पाहून पांडुरंग त्याच्या जिदास जागतो आणि कान्होपात्रेचे संरक्षण करण्यासाठी तिचे प्राण स्वरूपात विलीन करून घेतो. तिची आत्मज्योत देवाच्या ज्योतीत एकरूप होते व तीचा अचेतन देह देवाच्या पायाशी पडतो.

अशा प्रकारे पंढरपूरच्या विठ्ठल मंदिरात आपले जीवन व्यतित करणारी, विठ्ठलाची अनन्यभावे भक्ती करणारी, यातीहीन अशा गणिका कुळात जन्मलेली कान्होपात्रा आपल्या भक्तीच्या बळावर संत पदास पोहचली.

संत कान्होपात्रेची अभंग रचना

संत कान्होपात्रेचे २३ अभंग उपलब्ध असून ती विठ्ठल दर्शनाचा आनंद, विठ्ठल जिदाची आठवण, यातिहीनतेची भावना, विठ्ठलाची आर्त वाचना अशा अभंगरचनेबरोबरच उपदेशपर अभंगाची रचनाही तीने केल्याचे दिसून येते.

विठ्ठल दर्शनाचा आनंद

पंढरपूरच्या विटाईच्या दर्शनासाठी येणाऱ्या वारकऱ्यांसोबत कान्होपात्राही विठ्ठल दर्शनास येते. मात्र माझ्यासारख्या यातिहीन भक्ताचा पांडुरंग स्वीकार करील काय? अशी प्रश्नवजा शंका तीच्या मनात येते मात्र विठ्ठलाने दर्शन घेताना तीची शंका दूर होते व विठ्ठल दर्शनाने मनस्वी आनंदाची प्राप्ती येते -

“जन्मांतरीचे सुकृत आजी फळासी आले ।

म्हणोनी देखिले विठ्ठल चरण ॥”

जन्मोजन्मी केलेल्या सत्कृत्यांचे फळ आज मिळाले. विद्वत् चरणाचे दर्शन घेण्याची आस आज पूर्ण झाली असल्याचे ती आपल्या अभंगातील सदर ओव्यांतून सांगते.

विद्वत् ब्रिदाची आठवण :- संत कान्होपात्रा आपल्या पुढील अभंगातून विद्वत्तास त्याच्या ब्रिदाची आठवण करून देते-

“पतित पावन म्हणविसी आधी ।
तरी कां उपाधी भक्तामगे ॥१॥
तुझे म्हणवितां दुजे अंगसंग ।
उणेपणा सांग कोणाकडे ॥२॥
सिंहाचे भातुकें जंबुकें पै नेलां ।
धोरोबिया माथां लाज वाटे ॥३॥
म्हणे कान्होपात्रा देह समर्पणें ।
करावा जतन ब्रीदासाठी ॥४॥

वरील अभंगातून कान्होपात्रा विद्वत्तास त्याच्या ब्रिदाची आठवण करून देतांना म्हणजे हे विद्वत्ता, तुझ्या भक्तांनी तुला 'पतितपावन' ही उपाधी दिलेली आहे. तू स्वतःलाही पतितपावन म्हणवतोस, भक्तांना आपले मानतोस मग मलाच का मदत करत नाहीस ? मग उणेपणा तुझ्याचकडे येणार. सिंहाचे खाद्य जर जंबुक घेऊन नेला तर तो सिंहाचा अपमान नाही का? तसेच मला बिदरच्या बादशहाने नेले तर तो तुझा अपमान होणार नाही का? म्हणून तू तुझे ब्रीद खरे करून दाखव. भक्तांचे रक्षा करून तुझे ब्रीद जतन कर.

यातीहीनतेची भावना :- संत कान्होपात्रा गणिकाकुळत म्हणजे हीन कुळत जन्मल्यामुळे आपली भक्ती पांडुरंग स्वीकारील काय? अशी चिंता तीला लागून राहते आणि म्हणूनच यातीहीनतेची भावना ती पुढी अभंगातून व्यक्त करते -

“दीन पतित अन्यायी । शरण आले विठाबाई ॥१॥
मी तो आहे यातीहीन । नकळे काही आचरण ॥२॥
मज अधिकार नाही । भेटी देईं विठाबाई ॥३॥
ठाव देईं चरणापाशी । तुझी कान्होपात्रा दासी ॥४॥

सदर अभंगातून कान्होपात्रा विद्वत्तास म्हणते की, यातीहीन असल्याने भक्ती मार्गावर कसे आचरण करावे हे मला कसे कळेल ? मला तो अधिकार नाही. विठाबाई तू मला भेट व माझी भक्ती स्वीकार. माझी करूना येऊ दे. मी तुझी दासी तुला शरण आलेली आहे अशी यातीहीनतेची भावना सदर अभंगातून कान्होपात्रा व्यक्त करते.

विद्वत्ताची आर्त याचना :- स्वतःच्या जन्मदायीकडूनच गणिकेचा वंशपरंपरागत व्यवसाय करण्याचा आग्रह कान्होपात्रेला होतो. मात्र तीला हे नको असते म्हणून ती विद्वत्ताकडून पुढील अभंगातून याचना करतांना दिसते -

“जीवींचे जीवलगे माझे कृष्णई कान्हाई ।
सांवळे डोळसे करूणा येऊंदे कांही ॥१॥

आता अपवाद याती संबंध लौकीक पाही ।
 सांवळे डोळसे करुणा येऊंदे काही ॥२॥
 दीनोद्वार ऐसे वेद शाखें गर्वती पाही ।
 सांवळे डोळसे करुणा येऊंदे काही ॥३॥
 शरण कान्होपात्रा तुजला वेळोवेळां पाही ।
 सांवळे डोळसे करुणा येऊंदे काही ॥५॥

संत कान्होपात्रा विदूमाळलीत कृष्णाचे रूप पाहते व विनंती करते की, तू माझ्या बीवाची जीवलग आहे. तुला माझी कीव देऊ दे. मी हीन कुहातील असल्यामुळे भक्तीचा आधिकार नसलेली आहे. परमेश्वराला प्राप्त करून घेण्याचा अधिकार नसतानाही मी तुझी आज्ञावणी करते आहे.

वेद-शास्त्र पुराणात दीनोद्वाराला महत्व दिले असल्याचे लक्षात घेऊन तू माझी भक्ती स्वीकारली. माझा उद्धार करावा. मी तुला सदैव शरण आहे. आर्त वाचना सदर अभंगगतून कान्होपात्रा विद्वलाला करते.

उपदेशपरता :- विद्वलाला विनवणी करणाऱ्या, शरण जाणाऱ्या संत कान्होपात्रेने विषय वासनेच्या आहारी माणसाने जावू नये असा उपदेशही केलेला आहे. त्याचा प्रत्यय तींच्या पुढील अभंगगतून वेणे ----

"विणयाचे संगती । नाश पावले विक्षिती ॥१॥
 भगें पडलीं इंद्राला । भस्मासूर भस्म झाला ॥२॥
 चंद्रा लागला कतंक । गुरुपलीसी रतला देख ॥३॥
 रवण मुकला प्राणासी । कान्होपात्रा म्हणे दासी ॥४॥

सदर अभंगगतून संत कान्होपात्रा उपदेश करते की, ज्या दुराचान्यांची विषय-वासनेचा नाद घेतला त्या सर्वांचा नाश झाला. इंद्र, चंद्र रावण यांनी परस्त्रीची किटंबना केली. वासनेच्या आहारी गेले त्यामुळे ते नष्ट झाले म्हणून माणसाने विषय-वासनेच्या आहारी जावू नये.

वरील प्रकारे संत कान्होपात्रेच्या अभंगगतून वेगवेगळे विषय हाताळल्याचे जाणवते.

संत कान्होपात्रेच्या अभंगांची वैशिष्ट्ये

१. संत कान्होपात्रेचे अभंग भक्तीने भरलेले, भक्तीरसात न्हालेले, अर्बनी असे आहेत.
२. संत कान्होपात्रेच्या अभंगात प्रेमभाव, करुणा, श्रद्धा, दास्यभाव, साफल्यभाव व्यक्त होतो.
३. विद्वलाची आर्तता हा कान्होपात्रेच्या वाणीचा स्थायीभाव आहे.
४. संत कान्होपात्रेची अभंगरचना रसाळ, प्रासारिक असून भावार्पितेने ती ओतप्रोत आहेत.
५. संत कान्होपात्रेच्या अभंगातील रसाद्रिता व भावपरिपोष तिच्या त्यागमय जीवनाशी एकरूप होऊन प्रकट झाले आहेत.

समारोप

महाराष्ट्राच्या सांस्कृतिक आणि वाङ्मयीन परंपरेत संतांचे कार्य अनमोल आहे. सामाजिक अस्मितेचे ते खरे शिलपकार असल्यामुळे त्यांनी खऱ्या अर्थाने समाज जडण-घडणीचा आलेख मांडला. सामाजिक विषमता दूर करण्यासाठी सर्व जाती-धर्मातील लोकांना एकत्र आणून पंढरीच्या पांडुरंगाच्या प्रांगणांत आध्यात्मिक लोकशाहीची प्रतिष्ठापण केली. रुढीप्रस्त अज्ञानांना आत्मोन्नतीचा मार्ग दाखविला. अभंग, कीर्तन, भारूड, प्रवचन आदि माध्यमातून लोकांना प्रबोधन व उपदेश केला. स्त्रीवांना आणि सुद्वितीशुद्धांना परमार्थाची दारे खुली करून दिली. या सकार्यांत ज्ञानेश्वरी पुरुष संतांसोबतच स्त्री संतांनी देखील भरीव कामगिरी केलीली आहे. त्या स्त्रीसंतांमध्ये यातीहीन अशा गणिका कुळत जन्मलेल्या संत कान्होपात्रेचे स्थान अवळ आहे.

निष्कर्ष

१. संतांची स्त्री-शुद्धांना आत्मोन्नतीचा मार्ग दाखवून त्यांचे नैतिक बळ वाढवले.
२. सामाजिक जडणघडणीसाठी संतांनी अध्यात्मिक लोकशाहीचा मार्ग अवलंबला.
३. समाजातील वर्णभेद, उच्चनिचत्व, विषमता, कर्मकांड, अंधश्रद्धा, अज्ञान या गोष्टींवर संतांनी आपल्या अभंगवाणीने कोरडे ओढले.
४. संत कान्होपात्रेचे अभंग भक्तीने भरलेले असून तिची अभंगवाणी अर्जवी, करुणापर श्रद्धाळू, दय्यभाव, साफल्यभावपर आहे.
५. कान्होपात्रेचे अभंग तिच्या मनातील दुःखदभाव व उत्कट व्यथा यांचे दर्शन घडवणारे आहेत.
६. यातीहीन अशा गणिका कुळत जन्मलेली असतानाही आपल्या आर्तवाणीमुळे आणि निस्सिम भक्तीच्या बळावर कान्होपात्रा संत पदापर्यंत पोहचली आहे.

संदर्भ

१. बडवे सतिष - 'साहित्याची सामाजिकता' - शब्दालय प्रकाशन श्रीरामपूर पृ. १३ ते १७.
२. बागुल फुला - 'बहुजनातील संत कवी कवयित्री' - अथर्व पब्लिकेशन्स जळगांव पृ. ४९ते५३.
३. घाटोळे रा.ना. - 'मराठी वाङ्मयाचा इतिहास १८४० पासून आजपर्यंत' श्री मंगेश प्रकाशन नागपूर पृ.३३.
४. पाटील शिरीष (संपादक) 'संतांची अभंगवाणी मध्ययुगीन निवडक संत' प्रशांत पब्लिकेशन्स जळगांव पृ. ८,९,४९ ते ५१.

Digital Literacy and Women Empowerment

©Reserved

ISBN : 978-81-951217-4-8

Publisher & Printer : Yogeshwar L. Jalgaonkar
Dnyanpeeth International Publisher

- Aurangabad** : Banjara Colony, Near Datta Mandir,
Bahadarsingpura, Aurangabad
Dist. Aurangabad - 431001
Contact : 9823724705
- Nandurbar** : Manik Chowk, Opp. Hutatma Shirishkumar
Smarak, Nandurbar Dist. Nandurbar - 425412
Contact : (02564) 220155, 9175510724
- Email** : dnyanpeeth.publisher@gmail.com
- First Edition** : 31 December 2021
- Type Setting** : Rudra Creations, Nandurbar
- Price** : 300/-

Disclaimer : The Authors are solely responsible for the contents of the papers compiled in this volume. The Editors or Publishers do not take responsibility for the same in any manner. Errors if any are purely unintentional and readers are requested to communicate such error to the Editors or Publishers to avoid discrepancies in future.

All rights reserved. No part of this publication may be reproduced, stored in a retrieval system or transmitted, in any form or by any means, electronic, mechanical, photocopying (xerox copy), recording or otherwise, without the prior permission.

INDEX

- **A Study on the Implementation of Digital Initiative for Women Empowerment**09
- Mrs. Dakshayini E.
- **Digital Dissimilarity: Looking Gender-wise into the Mirror**.....13
- Dr. Shailesh Jagdish Bahadure
- **Digital Literacy For Women Empowerment**.....19
- Dr. Alpana Vaidya
- **E-Governance and Women**.....22
- Dr. Sudhir Kumar Srivastava
- Mr. Pankaj Laxman Sonawane
- **Digital India and Women Empowerment**.....27
- Vijay Bhaidas Bachchhao
- **Empowering Rural Women through Digital Literacy, Global Market & Local Self Government**.....31
- Dr. Pradip G. Sonawane
- **Dalit Women in Digital World : Review of Article 15 Cinema**.....38
- Dr. Sidhartha B. Sawant
- **Empowering Woman in India with Digital Drive: A Case Study**.....43
- Dr. Gajanan P. Patil
- **Depiction of Empowered Women Characters in the Novel of Ashok Banker**.....49
- Dr. Dnyaneshwar S. Chavan
- **Role of Women as an Environmentalist in Ruskin Bond's Short Stories**.....52
- Dr. Nilesh Bhatেশwar Malichakar

- **A Study of Different Scheme of Women Entrepreneur Development for Women Empowerment.....55**
- Mr. Sachin Karbhari Jadhav
- **Empowerment of women through Digital Literacy.....62**
- Anju Ashok Pakhale
- **Education : Guiding Light to Women Empowerment.....69**
- Mr. AjabraoRavji Ingle
- **The Role of Women in Economic Development.....73**
- Dr. Jyoti Sahadev Wakode
- **लिंगभावात्मक जमातवाद आणि राष्ट्रीय एकात्मतेचा प्रश्न.....76**
- डॉ. पी. यु. नेरपगार
- प्रा. भुषण अहिरराव
- **डिजीटल भारत आणि महिला सशक्तिकरण.....83**
- प्रा.डॉ. मोहन दे. वानखेडे
- **डिजिटल इंडिया आणि महिला सबलीकरण.....89**
- प्रा. डॉ. महेंद्र पाटील
- **डिजिटल साक्षरता उपक्रम आणि महिला सक्षमीकरण.....95**
- प्रा.डॉ. वसुमतो पी. पाटील
- **महिलांची सुरक्षितता व डिजीटल तंत्रज्ञानाची वास्तविकता.....98**
- प्रा.डॉ. अरुणा व्ही. नेरे
- **Women Literacy in Digital World.....102**
- डॉ.संतोष शिवकुमार खत्री
- **डिजीटल साक्षरतेत स्त्रियांचे प्रमाण व आरोग्य सेवांचा अभ्यास.....106**
- प्रा.वासुदेव गोविंदा मेश्राम

- आदिवासींच्या शैक्षणिक विकासात शासकीय योजनांचे यशापयश.....111
- बाळासाहेब नलावडे
- महिला सबलीकरणात डिजीटल तंत्रज्ञानाची भुमिका व कार्य.....117
- प्रा. डॉ. एस. आर. गोवर्धने
- संगणकीकृत भारत व महिला सबलीकरण.....121
- श्री. अमृत नामदेव पाटील
- डिजीटल बँकिंग व महिला सक्षमीकरण.....126
- राठोड लक्ष्मण महारू
- डिजीटल इंडिया : ग्रामीण भागातील समस्या व उपाय.....129
- प्रा. डी. एल. पावरा
- साक्री तालुक्यातील अहिराणी बोलीच्या ओव्यांतून
प्रकट झालेले स्त्री जीवनाचे चित्रण.....132
- डॉ. प्रकाश श्रीराम साळुंके
- महिला सक्षमीकरण : ऐतिहासिक-राजकीय सिंहावलोकन.....136
- प्रा. शरद बाबुराव सोनवणे
- स्त्री सबलीकरण व डिजिटल इंडिया.....141
- डॉ. कांतीलाल दाजभाऊ सोनवणे
- डिजीटल इंडिया सुनहरे भारत का भविष्य.....146
- प्रा. आबासाहेब माणिकराव देशमुख

साक्री तालुक्यातील अहिराणी बोलीच्या ओव्यांतून प्रकट झालेले स्त्री जीवनाचे चित्रण

डॉ. प्रकाश श्रीराम साळुंके

मराठी विभाग प्रमुख,

सी.गो.पाटील कला, विज्ञान व वाणिज्य

महाविद्यालय, साक्री ता. साक्री, जि. धुळे

प्रास्ताविक :

साक्री तालुक्यात बोलल्या जाणाऱ्या अहिराणी बोलीत गायल्या जाणाऱ्या ओवीगीतांचे समृद्ध दालन आहे. त्या ओव्यांतून लोकजीवनाचे दर्शन घडते. विविध प्रकारचा आशय या ओव्यांतून व्यक्त होत असतो. या ओव्यांच्या निर्मितीत स्त्रीयांचा मोठा वाटा आहे. खरेतर ह्या ओव्या म्हणजे स्त्रीधनच आहे. हे स्त्रीधन साक्री तालुक्यातील अशिक्षित स्त्रीयांनी मौखिक परंपरेने आज देखील जतन केलेले आहे. या ओव्यांतून स्त्री जीवनाच्या विविध पैलूंवर प्रकाश टाकलेला आहे. मानवी विविध नात्यांना या ओव्यांमध्ये विशिष्ट स्थान आहे. या नात्यांमधील विविध भूमिका, कर्तव्य, पावित्र्य त्यातील सुख-दुःख, राग-लोभ, वात्सल्यभाव, आदरभाव, स्नेहभाव अशा अनेकविध भावनांच्या हृदयस्पर्शा अविष्कार या ओव्यात झालेला आढळतो. कौटुंबिक नात्यातील विविध भावसंबंधांचे अत्यंत भावस्पर्शी चित्रण या ओव्यांमध्ये केलेले असते. म्हणून नात्या-नात्यातील जिव्हाळा, प्रेम, आपुलकी आजही टिकून आहे. अंतरीच्या उमाळ्यातून या ओव्यांची निर्मिती झालेली असल्यामुळे त्या ओव्या भावस्पर्शी आहेत.

साक्री तालुक्यातील अहिराणी बोलीच्या ह्या ओव्यांमध्ये माता-पित्याचे स्थान अनन्य साधारण आहे. आई-वडीलांविषयी कृतज्ञताभाव आणि प्रेमभाव या ओव्यातून व्यक्त होतो. स्त्री ही लग्न होईपर्यंत आई-वडीलांकडेच असते त्यावेळी आई-वडीलांनी तिला दिलेले प्रेम, माया, वात्सल्य तिच्यावर केलेले संस्कार या गोष्टी ती कदापी विसरू शकत नाही म्हणून वडीलांना ती 'समुद्राची' उपमा देते विशालकाय समुद्रासारखे हृदय असलेला बाप सर्व सृष्टीमध्ये दुसरा कोणी नसतो हे ती पुढील ओव्यातून सांगते -

"समदीर समदीर, समदीर सारखा साठ जई
घाली सिरष्टी पावंदये, आयबा सारखं कोणी नई"

मात्र मुलीचे लग्न झाल्यावर तिच्या बापापेक्षा तिला पतीचे राज्य हे लाखमोलाचे असते. कारण पतीच्या राज्यात म्हणजे 'राम' राज्यात तीला सर्व अधिकार प्राप्त झालेले असतात. त्यातच ती सुखी असते आणि त्या सुखाचे वर्णन ती पुढील ओव्यातून करते -

"भरतानं राज, कोरा रांजननं पानी
ऊपसू दोन्ही हाते, माले वरजेना कोनी"

नवऱ्या घरची परिस्थिती गरीबीची जरी असेल तरी गरीबीत मी माझा संसार सुखाने चालवीन म्हणून ती देवाला विनंती करते की, हे देवा, माझी परिस्थिती जरी गरीबीची असेल तरी चालेल पण माझ्या पतीचे आयुष्य वाढू दे अशी विनंती ती पुढील ओव्यातून करते -

"आरे आरे देवा माले दुबय राहू दे
कपायना कुकुमना जलमे जावू दे"

मुलीचे लग्न कितीही चांगल्या श्रीमंत घरातील मुलाशी लाऊन दिले मात्र तीच नशिबच खोट असेल तर तीच्या आई-वडीलांचा काय दोष? हे ती पुढील ओव्यातून सांगते-

"दैवं दैवं करी, दैवं चंदननी खाप
खोटा नशिबले, काय करथी माय-बाप"

मात्र तिचे सासर श्रीमंत असेल तर तिचाही हावरटपणा वाढून जातो पण कुठेही जा सर्वांकडे सारखे असते याचे वर्णन ती पुढील ओव्यातून करते -

"नेका करु नारी, नको करु मन-मनं
जठे जाशी तठे, पयसाले पाने तीन"

आपल्या जवळील धन-दौलतीला कोणीच विचारत नाही मात्र आल्या-गेल्या पाहुण्यांचा आदर सत्कार केल्यास आपली कौर्ती वाढते हे ती पुढील ओव्यातून सांगते-

"कोणी नई सोदत, धन संपत्ती अती रेती
अभ्रीत भोजन, दोन घासनी किरती"

आपले धनदौलत संपत्ती ही आपली मुलेच असतात म्हणून ती देवाकडे मुलगा होण्याची विनंती करते त्यावेळेस ती पुढील ओव्यात म्हणते -

"दिसी रे देवाजी, संपत्तीना सरवा साज
आंगनले गाडाघोडा, वसरीले बायराज"

पोटचा मुलगाच आई-वडीलांना म्हातारपणी सांभाळतो, कुणाचेच दीर-जेठ कुणालाच होत नाहीत उलट ते आपल्या धन-संपत्तीचे, इस्टेटीचे वाटेकरी असतात हे ती पुढील ओव्यातून सांगते -

"पोरे पुतरु महिना फार, पोटे पुतरु महिमा फार
कोना नईथीन देरजेठ, धन-संपत्तीना हिस्सेदार"

मात्र देवाकडे नवसाने मागीतलेला हा मुलगा लग्न झाल्यावर जेव्हा पत्नीचे ऐकून आईला हिनकस वागवणूक देतो तेव्हा ती मुलाला स्पष्टपणे जाबही विचारते -

"माय माय करी, मावल्या माया किती

लेक तुले न्हाणाना म्होटा कया, तवय तुम्ही आस्तुरी कोठे व्हती?" .

नऊ महिने पोटात वाढवले सहा महिने मांडीवर खेळवले याची आठवणही ती त्याला करून देतांना म्हणते -

"माले जलम दिधा, माय मनी मंडोधर

नव महिना बंझ वागं, सव महिना मांडीवर"

मुलाला वेळप्रसंगी जाब विचारणारी ही आई, आयुष्याच्या शेवटी उतारवयात थकलेली आहे. तिला आजारपण आलेले आहे. त्यावेळी तीच्या जीवाच्या वेदना कोणी जाणून घेत नाही म्हणून देहरूपी नगर सोडून माझा जीव देवाघरी निघून जायला पाहीजे असे तिला वाटते यांचे वर्णन ती पुढील ओव्यातून करते -

"झाडले भिरूड, झाड टाकवा तोडूनी

उबगीला जीव, जावा नगर सोडूनी"

स्त्री मेल्यावर तीला शेवटची बोळावन भावाकडची असते मात्र ती चांगली आण, माइया भाऊबंदकीतल्या आयाबाया पाहतील त्यांनी बोळावणीला नाव ठेवायला नको माइया माहेरचे नाव जायला नको असे ती भावाला पुढील ओव्यातून सांगते -

"निदाननी येये, धाव घालसी बंधुराया

सरती बोयावन जोथी, मन्या नगरीन्या बाया"

ज्या पतीच्या छत्रछायेत ती आपले सर्व आयुष्य घालवते तोच पती तीच्या अंतयात्रेत तीच्या प्रेतावर छत्री धरून सावली देण्याचे काम करतो म्हणजे स्त्रीच्या आयुष्यात पतीच महत्त्वाचा असतो याचे मार्मिक वर्णन ती पुढील ओव्यात करते-

"निदाननी येये, किडीबाईले फुटा घाम

आग्या खांद्या देर जेट, वर छतरी धरे राम"

अशा प्रकारे अहिराणी बोलीच्या ओव्यातून स्त्री मनाचे, तिच्या भावभावनांचे व जीवनाचे दर्शन घडते. तसेच सक्षमीकरणाची संकल्पना व्यक्तिच्या मानसिकतेस जोडल्यास त्या-त्या काळातील स्त्रीयांनी विविध प्रकारच्या संकटांशी स्वबळवर संघर्ष केलेला आहे. सदर संघर्षाची जाणीव ह्या ओव्यातून पदोपदी जाणवते.

ओव्यांची प्राप्ती :

श्रीमती मंदोदराबाई श्रीराम साळुंके, रा. शेवाळी, ता. साक्री, जि. धुळे.

**Vidya Vikas Mandals
Sitaram Govind Patil Arts,
Science and Commerce College,
Sakri Tal. Sakri Dist. Dhule 424 304**



**NAAC
ACCREDITED**

**विद्या विकास मंडळाचे,
सिताराम गोविंद पाटील कला,
विज्ञान आणि वाणिज्य महाविद्यालय,
साक्री ता. साक्री जि. धुळे ४२४ ३०४**

Affiliated to Kavayitri Bahinabai Chaudhari North Maharashtra University, Jalgaon

Website : www.sgpcsakri.com

Email : vidyavikas2006@rediffmail.com

Ph : 02568-242323

3.3.2.1 Research Paper Published in UGC Care Listed Journals

Role in Prevention of Corona Virus Infection

S.J. Nandre

Dept. of Physics, Uttamrao Patil
Arts and Science
College, Dahiwal, (Dhule)

N.B. Sonawane

Dept. of Physics, Karm.
A.M. Patil Arts, Comm. and
N.K. Patil Science College,
Pimpalner (Dhule)

R.R. Ahire

Dept. of Physics, S.G. Patil
Arts, Comm. and Science
College, Sakri, (Dhule)

Abstract -

Corona virus disease 2019 (COVID-19) is an infectious disease caused by severe acute respiratory syndrome corona virus 2 (SARS-CoV-2). It was first identified in December 2019 in Wuhan, China, and has since spread globally, resulting in an ongoing pandemic. As of 10 May 2020, more than 4.02 million cases have been reported across 187 countries and territories, resulting in more than 279,000 deaths. More than 1.37 million people have recovered. Common symptoms include fever, cough, fatigue, shortness of breath, and loss of smell and taste. While the majority of cases result in mild symptoms, some progress to acute respiratory distress syndrome (ARDS), multi-organ failure, septic shock, and blood clots. The time from exposure to onset of symptoms is typically around five days but may range from two to fourteen days.

Introduction -

The virus is primarily spread between people during close contact, most often via small droplets produced by coughing, sneezing, and talking. The droplets usually fall to the ground or onto surfaces rather than travelling through air over long distances. Less commonly, people may also become infected by touching a contaminated surface and then touching their face. It is most contagious during the first three days after the onset of symptoms, although spread may be possible before symptoms appear and in later stages of the disease. The standard method of diagnosis is by real-time reverse transcription polymerase chain reaction (rRT-PCR) from a nasopharyngeal swab. Chest CT imaging may also be helpful for diagnosis in individuals where there is a high suspicion of infection based on symptoms and risk factors; however, guidelines do not recommend using it for routine screening.

Recommended measures to prevent infection

include frequent hand washing, maintaining physical distance from others (especially from those with symptoms), quarantine, covering coughs, and keeping unwashed hands away from the face. In addition, the use of a face covering is recommended for those who suspect they have the virus and their caregivers. Recommendations for face covering use by the general public vary, with some authorities recommending, some recommending against, and others requiring their use. There is limited evidence for or against the use of masks (medical or other) in healthy individuals in the wider community.

According to the World Health Organization, there are no available vaccines nor specific antiviral treatments for COVID-19. On 1 May 2020, the United States gave Emergency Use Authorization to the antiviral remdesivir for people hospitalized with severe COVID-19. Management involves the treatment of symptoms, supportive care, isolation, and measures. The World Health Organization (WHO) declared the COVID-19 outbreak a Public Health Emergency of International Concern (PHEIC) on 30 January 2020 and a pandemic on 11 March 2020. Local transmission of the disease has occurred in most countries across all six WHO regions. It is important to note that no fortune teller, astrologer or architect has predicted the corona at the Indian or international level. The important task in the future is to rid the masses of those who propagate and spread unscientific things. Corona urges us to take a positive view of science and research. The name 'Corona' is now well known. Certainly not in a good sense. Today, the whole world is shocked by the disease 'Covid-19' caused by the corona virus. He has never crossed the boundaries of caste, religion, gender, country. I also put 'direction' in it. In all directions, the Corona has penetrated villages and homes. The architect and the person who built the house on his advice are no exception. I don't think anyone would be

upset about that. It should be noted that no fortune teller, astrologer or architect has predicted the corona at the Indian or international level. I say this internationally because the so-called world astrologer Nostradamus or Vedokta astrologer is likely to publish something in the future, so I make it clear at the outset. Evidence of Shlokas, Vedas, Puranas is also likely to be given for this prophecy. A corona is a natural disaster that has hit the entire world. Although it originated in China, it is not officially recognized as a Chinese product. It is irresponsible to make any statement without evidence, so China has not yet been officially reprimanded.

Signs and symptoms -

Fever is the most common symptom, although some older people and those with other health problems experience fever later in the disease. In one study, 44% of people had fever when they presented to the hospital, while 89% went on to develop fever at some point during their hospitalization. Other common symptoms include cough, loss of appetite, fatigue, shortness of breath, sputum production, and muscle and joint pains. Symptoms such as nausea, vomiting, and diarrhea have been observed in varying percentages. Less common symptoms include sneezing, runny nose, or sore throat. Some cases in China initially presented with only chest tightness and palpitations. A decreased sense of smell or disturbances in taste may occur. Loss was a presenting symptom in 30% of confirmed cases in South Korea. As is common with infections, there is a delay between the moment a person is first infected and the time he or she develops symptoms. This is called the incubation period. The incubation period for COVID 19 is typically five to six days but may range from two to 14 days, although 97.5% of people who develop symptoms will do so within 11.5 days of infection.

Prevention -

Preventive measures to reduce the chances of infection include staying at home, avoiding crowded places, keeping distance from others, washing hands with soap and water often and for at least 20 seconds, practicing good respiratory hygiene, and avoiding touching the eyes, nose, or mouth with unwashed hands. The CDC recommends covering the mouth and nose with a

tissue when coughing or sneezing and recommends using the inside of the elbow if no tissue is available. Proper hand hygiene after any cough or sneeze is encouraged. The CDC has recommended the use of cloth face coverings in public settings where other social distancing measures are difficult to maintain, in part to limit transmission by asymptomatic individuals. The U.S. National Institutes of Health guidelines do not recommend any medication for prevention of COVID 19, before or after exposure to the SARS-CoV-2 virus, outside of the setting of a clinical trial. Social distancing strategies aim to reduce contact of infected persons with large groups by closing schools and workplaces, restricting travel, and cancelling large public gatherings. Distancing guidelines also include that people stay at least 6 feet (1.8 m) apart. There is no medication known to be effective at preventing COVID 19. After the implementation of social distancing and stay-at-home orders, many regions have been able to sustain an effective transmission rate ("R_t") of less than one, meaning the disease is in remission in those areas.

As a vaccine is not expected until 2021 at the earliest, a key part of managing COVID 19 is trying to decrease and delay the epidemic peak, known as "flattening the curve". This is done by slowing the infection rate to decrease the risk of health services being overwhelmed, allowing for better treatment of current cases, and delaying additional cases until effective treatments or a vaccine become available. According to the WHO, the use of masks is recommended only if a person is coughing or sneezing or when one is taking care of someone with a suspected infection. For the European Centre for Disease Prevention and Control (ECDC) face masks could be considered especially when visiting busy closed spaces but only as a complementary measure. Several countries have recommended that healthy individuals wear face masks or cloth face coverings (like scarves or bandanas) at least in certain public settings, including China, Hong Kong, Spain, Italy (Lombardy region), Russia, and the United States.

Those diagnosed with COVID 19 or who believe they may be infected are advised by the CDC to stay home except to get medical care, call ahead before visiting a healthcare provider, wear a face mask before entering the healthcare provider's

office and when in any room or vehicle with another person, cover coughs and sneezes with a tissue, regularly wash hands with soap and water and avoid sharing personal household items. The CDC also recommends that individuals wash hands often with soap and water for at least 20 seconds, especially after going to the toilet or when hands are visibly dirty, before eating and after blowing one's nose, coughing or sneezing. It further recommends using an alcohol-based hand sanitizer with at least 60% alcohol, but only when soap and water are not readily available.

Here are the measures you need to take to keep the virus at bay:

1. Avoid close contact with people who are sick. Maintain at least three feet distance between yourself and anyone who is coughing or sneezing.
2. Avoid touching your eyes, nose, and mouth.
3. Stay home when you are sick.
4. Cover your cough or sneeze with a tissue, then dispose of the tissue safely.
5. Clean and disinfect frequently-touched objects and surfaces using a regular household cleaning spray or wipe.
6. Wearing a mask is not necessary unless you are taking care of an infected person. The Centers for Disease Control (CDC) does recommend that only infected people wear masks to prevent the spread of the virus.
7. Wash your hands often with soap and water for at least 20 seconds, especially after going to the bathroom, before eating, and after blowing your nose, coughing, or sneezing.
8. If soap and water are not readily available, use an alcohol-based hand sanitizer with at least 60% alcohol. Always wash hands with soap and water when hands are visibly dirty.
9. If you have a fever, cough and difficulty breathing, seek medical attention immediately.
10. Keep in mind the travel advisory set out by the Ministry of Health and Welfare.

Result -

- 1) Corona in our country. In the new world a

virus that will linger in our minds for a long time. Two things that are very important for it are good health and safe perfume. Now your fight is with Corona for at least a year. 'LOCKDOWN' Whether or not you want to go to the critical stage of corona disease, then the following suggestions are very important because if you do not want the infection to be critical, then two things are important immunity and viral load.

- 2) Corona spreads through the respiratory tract, just as the surface is spread through body clothes, hand objects, mobiles, watches. There is seeing this, I felt it was my responsibility to write this article as a doctor.
- 3) The first point is better health Eating on time for good health, like eight hours of good sleep, one hour of light exercise at home Keep yourself happy with yoga, rope jumping, spot jogging, pranayama, kapalbhati, anulom-vilom (there are many videos available for this on YouTube). Don't let the stress of studying put pressure on the children at home.
- 4) Second issue 'Social Distance'. Today we will understand the meaning of this word which is not new to anyone. There should be at least one meter distance between two persons. Afterwards, when I went to a grocery store to buy groceries, there was a very disturbing picture. The shopkeeper and his three colleagues wore masks around their necks for the show without putting a mask on their faces. There was a bottle of sterlium .Some people didn't even bother to wear a mask .Some even took a packet of chips and started eating. At that moment, the shop seemed to be a hot spot for me. What did I have to do in such a situation??? Get out only if the first thing is necessary.

References -

- 1) Chen N, Zhou M, Dong X, Qu J, Gong F, Han Y, et al. (February 2020). "Epidemiological and clinical characteristics of 99 cases of 2019 novel coronavirus pneumonia in Wuhan, China: a descriptive study". *Lancet*. 395 (10223):

507-513. doi:10.1016/S0140-6736(20)30211-7. PMC 7135076. PMID 32007143.

2) Han X, Cao Y, Jang N, Chen Y, Alwalid O, Zhang X, et al. (March 2020). "Novel Coronavirus Pneumonia (COVID-19) Progression Course in 17 Discharged Patients: Comparison of Clinical and Thin-Section CT Features

During Recovery". *Clinical Infectious Diseases*. doi:10.1093/cid/ciaa271. PMC 7184369. PMID 32227091.

3) "Symptoms of Coronavirus". U.S. Centers for Disease Control and Prevention (CDC). 20 March 2020. Archived from the original on 30 January 2020.



Thermal and Morphological Study of Transition Metal Cobalt Oxalate Crystal Grown By Agar-Agar Gel Technique

H. S. Pawar¹, S. J. Nandre², S. D. Chavhan³ and R. R. Ahire³

¹V.J.N.T. Late Dalpatbhau Rathod Junior College, Mordadtanda (Dhule) M.S

²Department of Physics, Uttamrao Patil Arts and Science College, Dahiwel, (Dhule) M.S

³Department of Physics S.G. Patil Art's, Commerce and Science College, Sakri (Dhule) M.S

ABSTRACT

In this article, we have reported fabrication of various morphological of cobalt oxalate. Cobalt oxalate crystals were grown by agar-agar gel through the single diffusion technique. The tendency of cobalt oxalate crystals to spherulites growth was demonstrated. Also Liesegang ring are observed. The cobalt oxalate preparation method was played crucial role on the crystal structure and its morphology. The optimum growth conditions cobalt oxalate was achieved by controlling the parameters like, concentration of gel, concentration of reactants, aging period and reversing of reactants. The crystal structure of grown material was determined by TGA, DTA and EDAX.

Keywords: Crystal growth, cobalt oxalate, TGA, DTA and EDAX.

Introduction:

Growth of crystal ranges from a small inexpensive technique to a complex sophisticated expensive process and crystallization time ranges from minutes, hours, days and to months. The starting points are the historical works of the inventors of several important crystal growth techniques and their original aim. Crystals are used in semiconductor physics, engineering, as electro-optic devices etc., so there is an increasing demand for crystal [1-5]. For years, Natural specimens were the only source of large, well-formed crystals. The growth of crystals generally occurs by means of following sequence of process. Diffusion of the molecules of the crystallizing substance through the surrounding environment. Diffusion of these molecules over the surface of the crystal to special sites on the surface. Today almost all naturally occurring crystals of interest have been synthesized successfully in the laboratory [6-9]. It is now possible only by crystal growth techniques.

Synthesis of Cobalt Oxalate Crystal in Agar Agar Gel

H.S.Pawar¹, S.J.Nandre², N.B.Sonawane³ and P.R.Ahirc⁴

¹V.J.N.T. Late Delpethben Rathod Junior College, Morchastande (Dhule)

²Department of Physics, Dhanrao Patil Arts and Science College, Dahiwal, (Dhule) M.S

³Department of Physics, Karm A.M.Patil Arts, Commerce and Science College, Fimpalur (Dhule)

⁴Department of Physics S.G.Patil Art's, Commerce and Science College, Sakri (Dhule) M.S

ABSTRACT

Cobalt oxalate crystals were prepared by gel method using agar-agar gel. In the present investigation, the cobalt oxalate was grown by single diffusion techniques. Applying different parameter, the effect on growth of cobalt oxalate was studied. The parameters like, concentration of gel, concentration of reactants, aging period, reversing of reactants found affecting the growth. [1] The growth was also studied by using different sizes of the test tubes. The nucleation was controlled by using such parameters and optimum conditions are obtained. Such grown crystals were found in different shape and transparency. The Surface morphology was studied by optical microscopy.

Keywords: Crystal growth, Gel method, Agar agar gel, Optical microscopy

Introduction

It has long been appreciated that advances in solid state science depends critically on the availability of defect free single crystal specimens. As a result, an enormous amount of labour and care has been lavished on the development of growth techniques. In terms of crystal size, purity and perfection, all the techniques used for the growth of single crystals from melt, vapour, and solution have their own inherent constraints. In spite of the technological advancement in condensed matter physics, crystal growing is still an extremely difficult task requiring great expertise and skill. This method is useful to grow the oxalates because they are insoluble in water and decompose before melting point. Many researchers have grown these crystals by using this technique in silica gel [2 -7] and gelatin gel, however very few researchers used the agar agar gel. The agar agar gel is not pH dependent and again makes the method simple. Khan et al in 1976 reported the growth of transition metal cobalt oxalate in silica gel.

In these context, the gel technique is found to be promising one, for getting good quality single crystals which has an advanced technological application in the fields of optics, acousto-optics, optoelectronics and electronics, etc. The crystals which cannot be satisfactorily grown from melt and vapour are grown successfully by this method. A complete survey made by Henisch in this field gave a fantastic idea to the crystal growers to grow crystals using gel technique. The art and science of growing crystals in gel is historically an old phenomenon. In the early days the gel was not chosen as a medium of crystal growth, but only used to study the Liesegang ring phenomenon which is in no other way separable from the process of crystallization.

Experimental Details

Test tubes were used as crystallizing vessels, for single diffusion, the test tubes were filled by the first reactant (cobalt chloride) of desired volume and morality. Hot agar agar gel was poured in the test tubes and was kept for setting. The second reactant oxalic acid (0.5 M to 1.0M) of desired volume and morality was gently poured along the walls of test tube on the set gel and allowed to diffuse into the gel medium. The open end of tube was closed with cotton plugs and kept undisturbed at room temperature. The ions of supernatant solution reacted with ions of first reactant through capillaries formed in gel medium. After 6 to 7 day some nucleation was observed near the gel solution interface then some opaque crystal some diamond shape crystals were observed in test tube. The crystals were harvested by washing them carefully with acetone. As grown crystals were collected and observed.

In single diffusion test tubes were filled by first reactant oxalic acid, then poured hot agar agar gel in the test tube, after setting the gel then insert the cobalt chloride (0.5M to 1.0M) solution in test, after 7 to 8 day some nucleation is seen on the interface of test tube, then after few days some shiny crystal are observed.

The chemical reactions inside the gel can be expressed as-



The various optimum conditions for growing crystals were found and are given in table 1. Different parameters such as concentration of reactants, gel concentration, etc have considerable effect on the growth rate. In the steady state of concentration gradient, growth rate also becomes steady which favors growth of well-developed crystals, however, very slow rate of growth along one direction results in the platy crystals. Fast growth rate in one

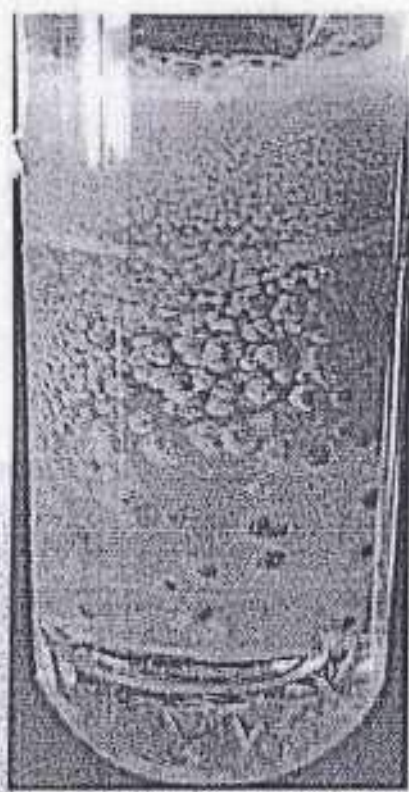
particular direction leads formation of elongated crystals like dendrites. All types of cobalt oxalate crystals show the phenomenon of efflorescence, i.e. due to dehydration, even at room temperature, transparent crystals become opaque.

Effect of Concentration of reactants

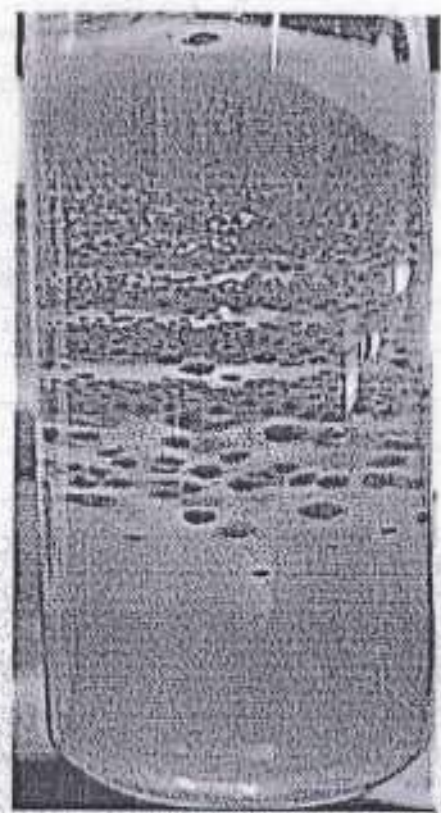
To observe the effect of concentration of reactants on the growth of cobalt oxalate crystals, the Both reactants were prepared in the concentrations of 0.5M, 0.6, 0.7 ..., 1.0M, while the other growth parameters were kept constant, such as gel concentration (0.5%), aging period (4 days) and volume of first reactant (5 ml) and volume of second reactant (15 ml). It was found that the number of nucleation was decreased by decreasing the concentrations of both reactants such as 0.7M and 1M respectively. The same result was observed in single diffusion methods. Meanwhile it was observed that if both reactants were of same concentration (more or less) the rate of diffusion was same and nucleations were found to be 1 cm below interface. In this 1 cm region of nucleation again it was found that when the concentration was of reactants was less but in a equal proportion the crystals were widely separated. For different concentrations it was observed that, the diffusion rate was faster for higher concentration of second reactant to that of first reactant. The best result was obtained when the percentage of gel was at 0.50% and the morality of first reactant was 0.7M and concentration of second reactant was decreased up to 1M, the nucleation growth was controlled and large size cobalt oxalate crystals was obtained.

Effect of percentage of gel

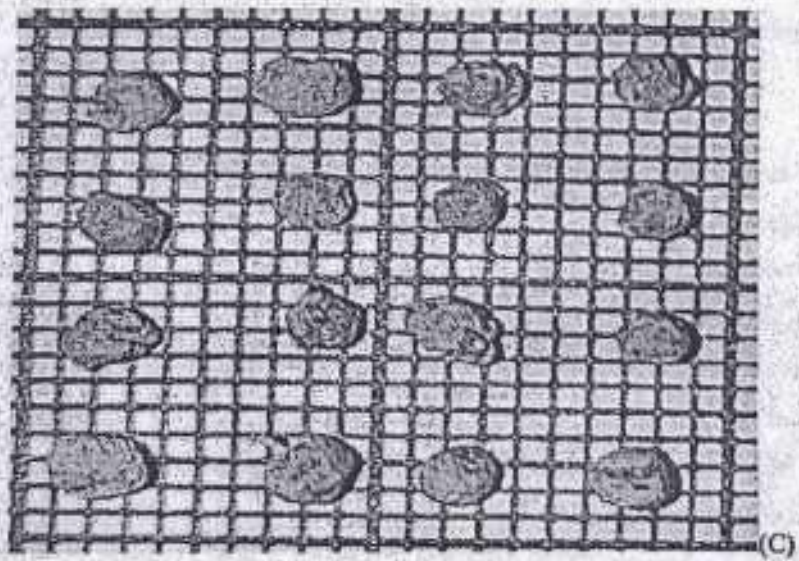
To observe the effect of gel percentage, other parameters such as concentration of first and second reactants, ageing period, setting period as well as size of test tubes were keep constant. Figure 2 shows the effect on growth of cobalt oxalate crystals with variation in percentage of agar gel. It was found that for lower percentage (0.5%) of gel the growth was near the interface and like spikes which after about 34 hours covert into small particles. Such particles were large in number and their size was found very small as show in fig 2(a). When percentage of gel increased to 2.0% and 2.5% dendrite growth was observed nearly spherical in shape at its diameter is about 1cm, below the interface four layer is observed and spherical shape crystal as shown in fig 2(b) and fig 2(c). The size sphericlated and colour is light brown of growing crystals found more precise for 2.0 percentage gel as compare to 2.5 % gel. The optimum condition obtained is as shown in table 1.



(a)



(b)



(c)

Table: 1. The optimum condition for cobalt oxalate crystals.

Sr.No	Condition Single Diffusion	Condition Single Diffusion
1	Percentage of gel	2.0 %
2	Concentration of cobalt chloride	1.0M
3	Concentration of oxalic acid	1.0M
4	Volume of cobalt chloride	5.0 ml
5	Volume of oxalic acid	15 ml
6	Gel setting period	34 Hours
7	Gel aging period	4 days

Conclusion:

Spherical, well sized and shaped cobalt oxalate crystals can be grown by the gel method using agar agar gel with single diffusion technique by applying various parameters such as change of ageing period, method of reversing reactants, change of concentration of first and second reactant alternate change,. The best result is obtained in single diffusion method for 2 % agar gel and reactants of concentration 2M.

Acknowledgement:

Authors are thankful to the Principal, V.V.M's,S.G.Patil Arts, Commerce and Science College, for offering laboratory Facilities

References

1. H. K. Henisch, Crystals in Gels & Liesegang Rings, Cambridge University Press, Cambridge, UK, 1988.
2. B. B. Parekh, M. J. Joshi, and A. D. B. Vaidya, Current Science, vol. 93, no. 3, pp. 373-378, 2007.
3. P. V. Dalal, Indian Journal of Materials Science, Volume 2013 (2013), Article ID 682950.
4. Khunur, M.Misbah; Wahyuni, Dini Tri; PoncoPranantoYuniar , Advances in Natural & Applied Sciences;2011, Vol. 5 Issue 5, p467
5. H.M.Patil, D.K. Sawant , D.S, Bhavsar, J.H. Patil and K.D.Girase, J. Th. Ana.& Calo.,Mar2012, Vol. 107 Issue 3, p1031

6. S. Pandita, R. Tickoo, K. Khamrai, P. N. Kuroo and N. Sahni, *Bull. Mater. Sci.*, Vol. 24, No. 5, October 2001, pp. 435-440. © Indian Academy of Sciences-435
7. A.S. Khan, T.C. Davies, and W.F. Read (1976), *Journal of Crystal Growth*, 35(3): 337-339.



Growth and Characterization of Cobalt Oxalate Crystal by Ager-Ager Gel Method

H.S.Pawar¹, S.J. Nandre², N.B.Sonawane³, S. D. Chavhan⁴ and R.R.Ahire⁵

¹V.J.N.T. Late Dalpatbhau Rathod Junior College, Mordadtanda (Dhule)

²Department of Physics, Uttamrao Patil Arts and Science College, Dahiwel, (Dhule) M.S

³Department of Physics, Karm. A.M. Patil Arts, Commerce and Science College, Pimplaner (Dhule) M.S

^{4,5}Department of Physics S.G. Patil Art's, Commerce and Science College, Sakri (Dhule) M.S

Abstract

We have grown the cobalt oxalate crystals by adopting single diffusion technique via agar-agar gel. The tendency of cobalt oxalate crystals to form splices, twins, spherulites and dendrites was demonstrated. The growth dynamic of cobalt oxalate was studied by controlling the parameters like, concentration of gel, concentration of reactants, aging period and reversing of reactants. Physical properties of the grown crystals were analyzed by XRD, and FTIR techniques and the results are discussed.

KEYWORDS: Gel, Crystal, Gel Growth, Crystal Growth, XRD, and FTIR

Introduction

Crystals grown by the gel method has gained interest in the research community because it is cheap and easy to grow single crystals of alkaline-earth metal oxalates[1] and transition metal oxalates [2]. These materials have interesting properties like low solubility in water [3], decomposition before freezing point [4], interesting optoelectronic properties. Their role in analytical chemistry and subsequently in industries [5, 6] has created an opportunity for the researcher to investigate every scientific aspect of these materials. Therefore, efforts are being made to investigate and study the physical and chemical properties of these materials. Recently, there are reports on the growth of mixed-ligand complex formation using cadmium oxalate [7]. In the present study, we have presented the optimization of growth parameters to grow the cobalt oxalate single crystals using the agar gel method.

Materials and Methods

Materials used to grow the cobalt oxalate crystals are cobalt chloride, oxalic acid, and agar-agar gel. All the chemicals used for the experiment were used without any further purification. Sodium silicate glass test-tubes were used as crystallizing vessels. The test-tubes were filled with the first reactant (cobalt chloride) of desired volume and molarity. The second reactant, oxalic acid having a concentration range of 0.5 to 1.0 M, was poured along the walls of the test-tube into the set-gel, and allowed to diffuse into the gel medium. The open end of the tube was closed with cotton plugs and kept undisturbed. The said procedure was carried out at room temperature. The ions of the supernatant solution reacted with ions of the first reactant via capillaries formed in gel medium. After six to seven days, nucleation kick-started at the gel-solution interface. The chemical reaction that occurred between the two reactants is given as follows:



The diamond-shaped opaque crystals were obtained in the test-tube. The crystals were harvested by washing them carefully with acetone and collected for further characterization. Table 1 shows the optimized crystal growth parameters for the cobalt oxalate crystals.

Sr.No	Condition Single Diffusion	Condition Single Diffusion
1	Percentage of gel	2.0 %
2	Concentration of cobalt chloride	1.0M
3	Concentration of oxalic acid	1.0M
4	Volume of cobalt chloride	5.0 ml
5	Volume of oxalic acid	15 ml
6	Gel setting period	34 Hours
7	Gel aging period	4 days

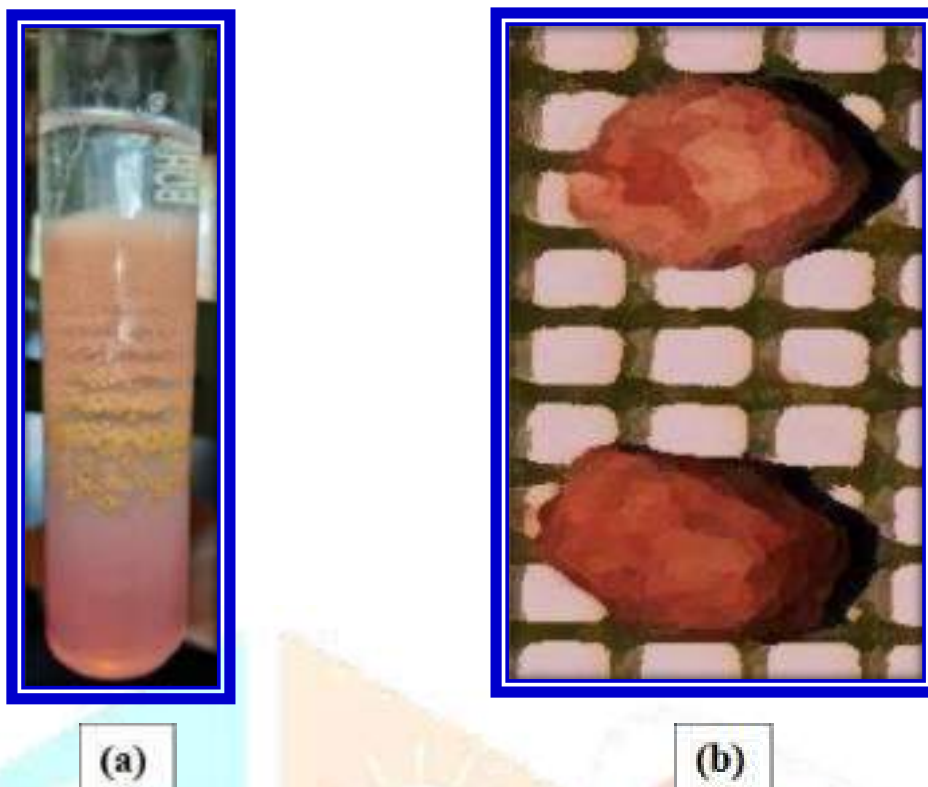


Figure 1:(a) in situ growth of Cobalt oxalate crystals in test-tube and (b) optical photograph of cobalt oxalate crystals

Result and discussion

The crystal structure analysis of the grown cobalt oxalate crystal was done via X-ray diffraction. X-ray pattern was recorded from the range of 10 to 80 degrees. The occurrence of highly resolved intense peaks at specific Bragg angles 2θ indicates the high crystallinity of the grown material and revealed monoclinic structure. The obtained crystal data has been compared with the JCPDS data and it closely matched with the reported JCPDS no. 037-0719. The unit cell parameters ($a' = 5.39820 \text{ \AA}$, $b' = 5.03100 \text{ \AA}$, and $c' = 5.73590 \text{ \AA}$) are close to the reported cell parameters of $\text{CoC}_2\text{O}_4 \cdot 2\text{H}_2\text{O}$, indicating the monoclinic phase of cobalt oxalate crystal. Comparative data is tabulated in Table 2 for the gel-grown cobalt oxalate crystal.

Table 2. Comparison of unit cell parameters of cobalt oxalate.

Parameters	Calculated	JCPDS data
System	Monoclinic (P)	Monoclinic
a	9.67638 \AA	6.4534 \AA
b	6.7156 \AA	7.5009 \AA
c	8.6822 \AA	10.940 \AA

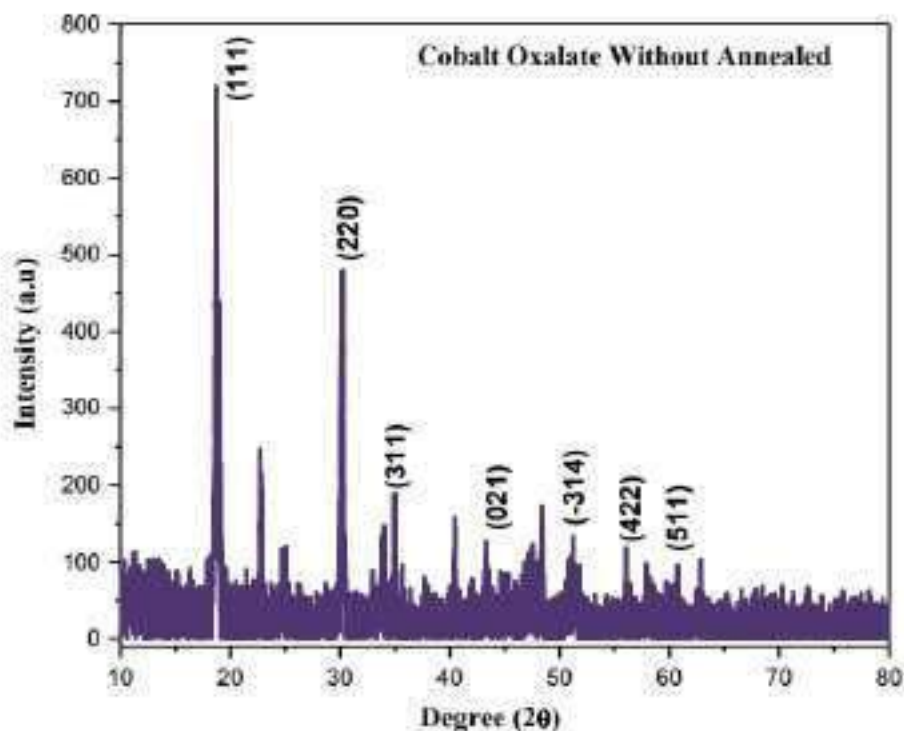


Figure 2: X-ray diffraction pattern of gel-grown cobalt oxalate crystal.

4.2 Fourier transform infrared (FTIR) Spectra

The Fourier transform infrared (FTIR) spectrum of cobalt oxalate was recorded at room temperature in the spectral range $500 - 4500\text{cm}^{-1}$ by KBr pellet method using SHIMADZU spectrophotometer at the department of Physics, Shivaji University Kolhapur. Figure 3 shows the FTIR spectrum of cobalt oxalate. The spectrum shows various frequencies of vibrational modes which confirm the presence of oxalate in the crystal.

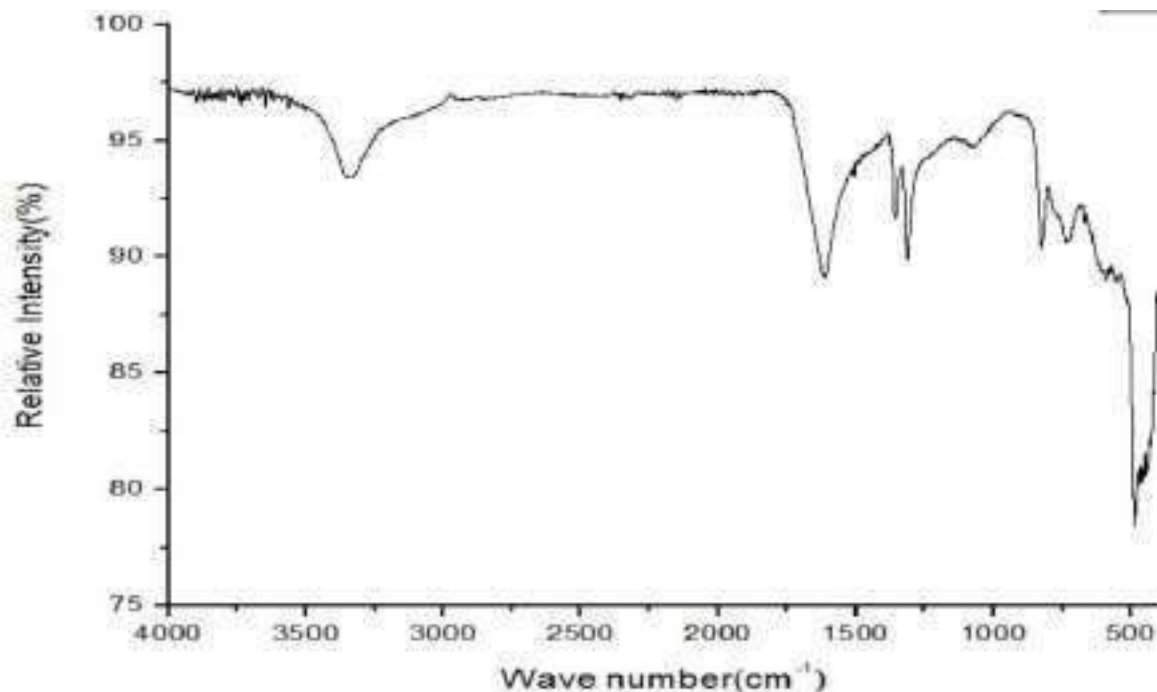


Figure 3: FTIR of Cobalt oxalate grown crystal

The sharp peak at 3300.18 cm^{-1} is attributed to the stretching of O–H group, indicating the presence of water of crystallization or water of hydration. However the peak at 1710.00 cm^{-1} to 1665.00 cm^{-1} correspond to α,β -unsaturated aldehydes, and ketones. The two identical sharp peaks around 1367.93 and 1327.43 cm^{-1} correspond to an asymmetric and symmetric stretch of C–H rock, respectively. Thus the FTIR spectroscopy confirmed the growth of cobalt oxalate crystals due to the presence of water of crystallization.

Conclusions

Cobalt oxalate crystals were grown by gel method using agar- agar gel in well size and shape. XRD powder diffraction patterns and analysis shows the crystalline nature of crystal with monoclinic phase. Different functional groups revealed by FTIR show the metal bond and different vibrations in the sample.

Acknowledgements

The authors are grateful to principal Dr. R. R. Ahire, V.V.M's, S. G. Patil college, Sakri, for providing laboratory facilities. Our special thanks are to Prof Mukesh Padvi, Department of Physics, Shivaji University Kolhapur, for providing facility for XRD and FTIR characterizations One of the authors (SJN) is thankful to Dr. B. D. Borse, principal, Uttamrao Patil College Dahivel for his inspiring suggestions.

References

- [1] A. Pactor, *Kristall und Technik*, vol.12,no.7,pp.729–735, 1977.
- [2] S.K.Arora and T.Abraham, *Journal of Crystal Growth*,vol.52,no.2,pp.851–857,1981.
- [3] J. Dennis and H. K. Henisch, *Journal of The Electrochemical Society*,vol.114,no.3,pp.263–266, 1967.
- [4]N.V.Prasad,G.Prasad,T.Bhimasankaram,S.V.Surya-narayana, and G. S. Kumar, *Bulletin of Materials Science*,vol. 19, no. 4, pp. 639–643, 1996.
- [5] M. I. Diaz-Guemes, A. S. Bhatti, and D. Dollimore, *Thermochimica Acta*,vol.106,pp.125–132,1986.
- [6] Y. Okamoto and W. Brenner,*Organic Semiconductors*,ReinholdPublishing, Chapman & Hall, London, UK, 1964.
- [7] W. B. Schaap and D. L. McMasters, *Journal of the American Chemical Society*, vol.83, no.23, pp.4699–4706, 1961.
- [8] S.J.Nandre, S.S.Sonawane,R.R.Ahire and S.J.Shitole, *Der Pharma Chemica*, 2014, 6(3), PP.33-38.
- [9] S.J.Nandre, S.S.Sonawane, R.R.Ahire and S.J.Shitole, *Journal of Scientific Review*, 2014,1(1),1-6.
- [10] S.J.Nandre, S.S.Sonawane, R.R.Ahire and S.J.Shitole *Renewable Research Journal*, 2014, 3(1),PP. 47-52.
- [11] S.J.Nandre, S.J.Shitole, and R.R.Ahire, *International Journal of Chemical and Physical Sciences*, 2014, 1,PP.123-130.
- [10] AnilkumarKodge et al.,*Int.J.ofEng.Sci.and Tech.*,2011,3(8), 6381–6390. [11] Paul Bowen et al., *Nanoscale*, 2010, 2, 2470–2477.
- [12] Ren, L et al. *B. Q. Chem. Phys. Lett.* 2009, 476, 78–83.
- [13] R. L. Frost et al.*Chinese Science Bulletin*,2003, 48(17), 1844-1852.
- [14] Joanne Hayley Smith, Ph.D.Thesis, University of Natal.2001. [15] E Romero et al. *J.cond.-mat.mtrl –sci*, 2010,
- [15] S. J. Joshi, K. P. Tank, B. B. Parekh, M. J. Joshi, *Cryst. Res. Technol.* 45, No. 3, 303 – 310, 2010.
- [16] J. J. de Yoreo and P. Vekilov, *Crystal Growth*, vol. 35, pp. 24–30, 2008.
- [33] S. M. Arifuzzaman and S. Rohani, *Journal of Crystal Growth*, vol. 267, no.3-4, pp. 624–634, 2004.



Physical and Optical Study of Cobalt Oxalate Single Crystals Grown by Agar-Agar Gel Method

H. S. Pawar^{*1}, S. J. Nandre², N. B. Sonawane³, R. R. Ahire⁴

^{*1}V.J.N.T. Late Dalpatbhau Rathod Arts and Science College, Mordadtanda (Dhule) M.S, pawar.hs1188@gmail.com

²Department of Physics, Uttamrao Patil Arts and Science College, Dahiwel (Dhule) M.S

³Department of Physic, Karm. A. M. Patil Arts, Commerce and Science College, Pimplaner (Dhule) M.S

⁴Department of Physics, S. G. Patil Arts, Commerce and Science College, Sakri (Dhule) M.S

Abstract: The cobalt oxalate single crystals were grown in agar-agar using gel method. In the present investigation, the cobalt oxalate single crystals were grown by single diffusion technique, such grown crystals were found in different size and colour. The physical and optical properties of cobalt oxalate crystals were characterized by different techniques such as SEM and UV-Vis spectroscopy and results are discussed.

Index Terms: Cobalt oxalate, Crystal growth, Optical properties, SEM and Single diffusion.

I. INTRODUCTION

Single crystal growth is the rapid growing field in research because of increase in demand of single crystals for many applications there are various types of crystals which can be grown by gel method. It is simple and inexpensive technique. We have turned our attention towards the oxalates are having good application can be synthesized by gel method. Many research has grown the series of pure and mixed crystals to find out the new materials for various purpose (Bacchhav S. K. et al.,2014; Jhon M.V., et al.,2001; Gao P.,2008). There are various techniques for growing crystals like melt growth, Vapour growth, solution growth and etc. the gel technique attracted more attention towards it because of its simplicity and cost effectiveness. The crystals can be grown at ambient temperature.

Cobalt oxalate is quite interesting compound as they are having good application. The cobalt oxalate crystals have been grown by the single diffusion and double diffusion technique using silica gel and also studied as precursor of Co_4O_4 nano particles (Yuniar P.,2012). In the present work of investigation, the cobalt oxalate single crystals were synthesized using single diffusion technique at room temperature and their characterization by EDAX, Powder XR, FT-IR and TGA-DTA. The work has been already published

by the author (Pawar H.et al.,2021; Pawar H.et al.,2021).The crystals were analyzed by various characterization techniques. The physical and optical properties were studies by Scanning electron microscope (SEM) and UV-Vis Spectroscopy.

II. EXPERIMENTAL

A. Crystal Growth

The growth of cobalt oxalate crystals has been carried out by single diffusion technique using gel method. The glass test tube of 25 mm diameter and 250mm length were used as crystal growth apparatus. 1% of agar gel was prepared by adding 1gm of agar powder into hot water. The solution of cobalt chloride (first reactant) and oxalic acid (second reactant) of 0.5, 1.0, 1.5 and 2.0M concentration were prepared and store in clean glassware. Cobalt chloride solution and oxalic acid solution were used as first reactant and second reactant respectively. The solution of first reactant (oxalic acid) was taken in a test tube and 2% of hot agar gel was poured along the wall. Then test tubes were kept undisturbed for setting and aging gel, after setting and aging, 1M of second reactant (cobalt chloride) solution was gently poured over set gel. The open end of test tubes was closed with cotton plug to prevent evaporation and contamination of the exposed surface by dust particles and impurities of atmosphere and were kept undisturbed. After 28 to 42 days the good quality and different morphological crystals were grown and harvest them. The figures 1 (a) with working reaction during crystal growth in test tube and (b) shows that some good quality harvested cobalt oxalate crystals.

The reaction between cobalt chloride and oxalic acid in agar – agar gel medium resulted in the growth of cobalt oxalate crystals. As grown crystals were characterized for structural, morphological, physical and optical properties. Growth of cobalt

oxalate crystals are gained by reacting the components cobalt chloride (CoCl_2) and oxalic acid ($\text{H}_2\text{C}_2\text{O}_4$). The expected reaction taking place in this work is as follows

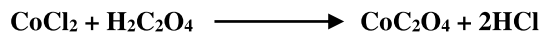


Fig. 1 (a) working reaction during crystal growth in test tube



Fig. 1 (b) Harvested crystals of cobalt oxalate

III. RESULTS AND DISCUSSIONS

A. Scanning Electron Microscopy (SEM)

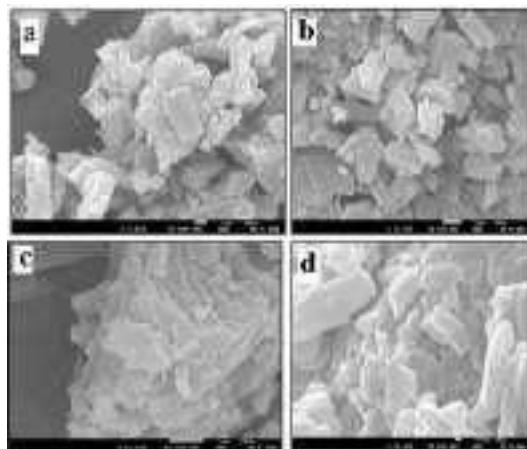


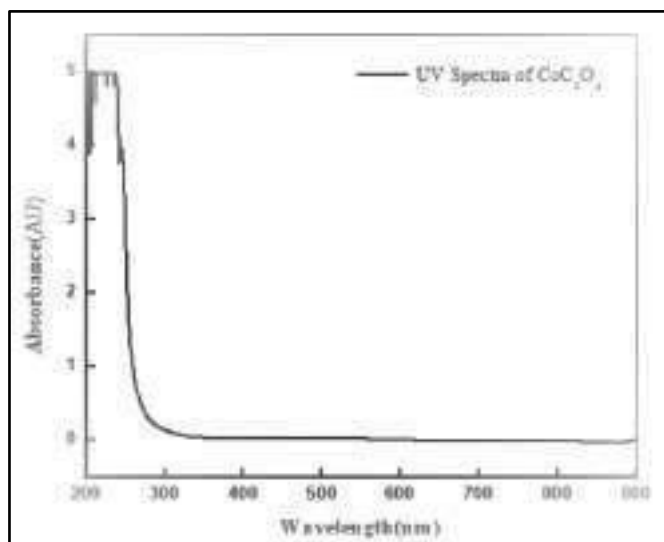
Fig. 2 (a), (b), (c) and (d) SEM images of as grown cobalt oxalate crystal

SEM images give the information about the nature and suitability for device applications and also it is used to check the presence of imperfections. SEM analysis was carried out using JEOL, JSM 7001F scanning electron microscope. The morphology and particles size were observed by scanning electron microscopy. Fig 2(a), (b) and (c) Shows typical SEM images of the cobalt oxalate at resolution X5000, X1000, X15000 and X30000 respectively.

SEM images revealed that the growth of cobalt oxalate crystals was composed of many rectangular sheets approximately greater than $5\mu\text{m}$ in length and of the thickness more than $5\mu\text{m}$. However, in the high magnification of samples as shown in figure 2 (c) and (d). It revealed that the rods are actually bundle of rectangular plates those are in hexagon shape, which were stacked in parallel fashion. (Usha R.et al.,2012). Figure 2 (a), (b), (c) and (d) illustrate the SEM images of same sample.

B. UV-Vis Spectroscopy

Absorption spectrum of cobalt oxalate crystals was obtained by a SHIMADZU UV-2450, UV- Vis spectrophotometer. Figure 5.15 shows UV-Vis absorption spectrum of cobalt oxalate crystal. The lower cutoff wavelength for CoC_2O_4 crystals was found to be 300.31 nm were shows in fig.3 form the graph the value of band gap was found 4.12 eV. The absorption coefficient is high at low wavelength and low at high wavelength. Hence it is wide transparent crystal for wide range of wavelength (300-900). The wide band gap of CoC_2O_4 crystals confirms the less absorbance in visible region (Arun K.et al., 2008; Want B.,2006; Rohit P.S.,2020). The cobalt oxalate crystal can be used for the nonlinear optoelectronic device fabricating applications. The band gap energy of Cobalt oxalate crystals is found to be 4.12 electron volt.



IV. CONCLUSION

The present work reports the growth and characterization of cobalt oxalate single crystals grown by single diffusion technique

using agar-agar gel as a medium of growth. Scanning electron microscopic (SEM) analysis revealed that it consists of many rectangular sheets, those are in hexagonal shape and stacked in a parallel fashion. UV-Vis studies shows that the crystals have a wide transparency window from 300nm to 900nm enables it to good candidate for second harmonic generation.

ACKNOWLEDGMENT

The author is grateful to research guide Dr. S. J. Nandre, Uttamrao Patil Arts and Science college, Dahiwel (Dhule) M.S. also thankful to Prof. Mukesh Padvi, Department of Physics, Shivaji University, Kolhapur and Mr. Rushikesh P. Dhavale, Department of material Science and Engineering, Yensei University, Seoul Republic of Korea for providing characterization facilities.

REFERENCES

- Arun K. J. and S. Jayalekshmi, (2008), "*Optoelectronics and Advanced Materials*", vol-2, pp701-706.
- Bacchhav S. K., N. S. Patil, M. S. Kale and D. S. Bhavsar, (2014) "*Int. Journal of Engineering Research and Application*", vol-4, pp108-112.
- Gao P., Mu.Ga And Xiao, Lui-lou, (2008)"*Cryst. Res. Technology*", vol-43, pp496.
- Jhon M. V. and M. A. Ittayachen, (2001) "*Crystals Res. Technology*", vol-36, pp141-146
- Pawar H. S., S. J. Nandre, N. B. Sonawane, S. D. Chavhan, R. R. Ahire, (2021) "*International Journal of Creative Research Thoughts*", vol-9, pp1343-1348.
- Pawar H. S., S. J. Nandre, N. B. Sonawane, S. D. Chavhan and R. R. Ahire, (2021) "*International Journal of Creative Research Thoughts*", vol-9, pp349-355
- Rohit P. S., N. Jagannatha and K. V. Pradipkumar, (2020). *AIP Conference Proceeding, 2020, 060003*.
- Usha R. J., J. A. M. Mani, P. Sagayaraj and V. Joseph, (2012). "*Archives of Applied Science Research*", vol-4, pp1545-1552.
- Want B., F. Ahmad and P. N. Kotru, (2006) "*Cryst. Res. Technology*", vol-41, pp-1167.
- Yuniar p. et.al. (2012) "*Bulletin of chemical Reaction Eng. and Cat.*"



Comparative Thermal Analysis Studies on Gel Grown Crystals of Li, Cu and Mixed Li-Cu tartrate

D. V. Sonawane ^{*1}, S. J. Nandre ², R.R. Ahire³

^{*1} J.E. S'S Arts, Science and Commerce College, Nandurbar (MS) India, Dvsonawane68@rediffmail.com

² Uttamrao Patil Art's Commerce and Science college, Dahiwel, Tal. Sakri, Dist.-Dhule (MS) India

³S.G. Patil Art's Commerce and Science College, Sakri, Dist.-Dhule (MS) India

Abstract: The Natural as well as Gel grown crystals plays an important role in modern technology development. Gel method for the growth of crystals which are insoluble or sparingly soluble in water is the best alternative for the growth of many crystals. Crystals grown by gel method are relatively perfect compared to the other methods. In the present investigation crystals of Li- tartrate, Cu-tartrate and Mixed crystals of Li-Cu tartrate have been grown by single diffusion gel technique. The Thermal Analysis studies of these crystals are carried out in this work. The Thermal Analysis studies on these crystals.

Index Terms: Gel method, Thermal Analysis, Li, Cu and mixed tartrate.

I. INTRODUCTION

It is well established that there is extensive study on tartrate-based crystal grown by gel technique, however, we have found that there are few reports on the lithium tartrate-based crystal because of its chemical properties (Henisch H.,1970; Henisch H.,1986; Sawant D., et al., 2011; Patil H., et al.,2012). Therefore, in the present study, we have investigated the growth mechanism of lithium tartrate, copper tartrate and mixed lithium-copper tartrate crystals. All the three types of crystals were grown by gel method by using single diffusion techniques, the crystal growth procedures and various different parameters affecting the growth of the crystals are discussed. The present paper contains the comparative study of all crystals under investigation regarding their growth and Thermal Analysis study. All results obtained are put at a glance in present paper.

II. GROWTH OF CRYSTALS

In The crystals of lithium tartrate, copper tartrate, and lithium-

copper tartrate were grown by gel method by using single diffusion technique.

Table 1 gives details regarding method and chemicals used, different habits of crystals obtained and their transparency etc. In the present work, we obtained semitransparent, shiny and star shaped lithium tartrate crystals. The copper tartrate crystals were of diamond shaped with bluish color, while the mixed lithium-copper tartrate crystals were whitish blue in color and having a cubic shape. The adopted single diffusion gel technique proved to be beneficial because of it only we successfully obtained well-shaped and good quality crystals. All the well-defined good quality crystals were found below 2 to 3 cm in the gel interface (Krishnakumar V., et al.,2009; Sawant. D.,2012; Sonawane S.,2015; Ahmad N.,2014).

The optimum growth conditions for gel grown crystals established by varying the different parameters like pH of gel, gel setting time, gel density, room temperature etc. are reported in the Table 2 for the all these three crystals. The suitable value of gel density is found to be 1.04 gm /cm³ and the pH value is 4 to 4.2.

III. THERMAL ANALYSIS

Thermal analysis is the measurement of how specific physical or chemical properties of a substance changes with temperature. It measures the change in weight of the substance with respect to applied temperature. In present work, thermogravimetric analysis of lithium tartrate, copper tartrate and mixed lithium-copper tartrate crystals was done. It was noticed that the pure lithium tartrate crystal was more stable at high temperature than the copper tartrate and mixed lithium-copper tartrate crystals. We observed 60 % weight loss in the temperature range of 200-212 °C for copper tartrate crystals, whereas for

* Corresponding Author

lithium tartrate crystal, weight loss is only about 28% in the same range of temperature. (Nandre S.,2013; Sawant D., et al.,2011; Yanes A., et al.,1996; Lopez T., et al.,1995). The details of weight loss with respect to temperature for all three the details of weight crystals is summarized in Table 3.1.

loss with respect to temperature for all three Similarly, for mixed lithium-copper crystals the total loss of weight was around 68 % in the temperature range of 0-310 °C.

Table 1 Summary of lithium, copper and lithium-copper tartrate crystals grown by gel technique

Sr.No.	Type	Method	Chemicals Used	Solvent	Quality	Size (mm)
1	Lithium Tartrate	Gel method using single diffusion techniques	Na ₂ SiO ₃ , C ₄ H ₆ O ₆ LiCl	Methanol or Ethanol	Opaque, Transparent Good	3 x 1 x 1
2	Copper tartrate	Gel method using single diffusion techniques	Na ₂ SiO ₃ , C ₄ H ₆ O ₆ CuCl ₂	Distilled water	Opaque, bluish color	2.5 x 2 x 1
3	Lithium -copper Tartrate	Gel method using single diffusion techniques	Na ₂ SiO ₃ , C ₄ H ₆ O ₆ CuCl + 2LiCl	Methanol or Ethanol	Opaque, good	2 x 2 x 1.5

Table 2. Optimum growth conditions for gel grown tartrate crystals

Sr.No.	Parameter	Lithium tartrate	Copper tartrate	Copper – lithium tartrate
1	Concentration of tartaric acid	1M, 7ml	1 M, 7ml	1M, 5ml
2	pH of the mixture	4 to 4.2	4.2	3.8 to 4.2
3	Temperature	25 to 30°C	25 to 30°C	20 to 30°C
4	Gel setting time	120 hours	96 hours	96 hours
5	Density of sodium metasilicate solution	1.04 gm/cm ³	1.04 gm/cm ³	1.04 gm/cm ³
6	Period of growth	4 weeks	3-4 weeks	4 weeks
7	solvent	Ethanol	Water	Ethanol or Methanol

Table.3. Kinetic data of TGA analysis for lithium tartrate, copper tartrate and lithium-copper tartrate crystals.

Compound	Steps	Temp. range °C	Observed Weight loss %	Calculated weight loss %	Loss of Molecule
Lithium tartrate	I	25-95	18	18.18	2H ₂ O
	II	95-260	10	11.90	2H ₂ O
	III	260-750	15	15.50	2CO
	IV	750-950	30	32.10	2CO ₂
Copper tartrate	I	25-210	2.15	2.50	5H ₂ O
	II	210-240	65.80	66.15	2H ₂ O
Mixed Lithium-Copper Tartrate	I	30-100	18	19.8	3H ₂ O
	II	100-210	1.5	2.0	CO
	III	210-320	49.5	50.42	CO ₂ , 2H ₂ O

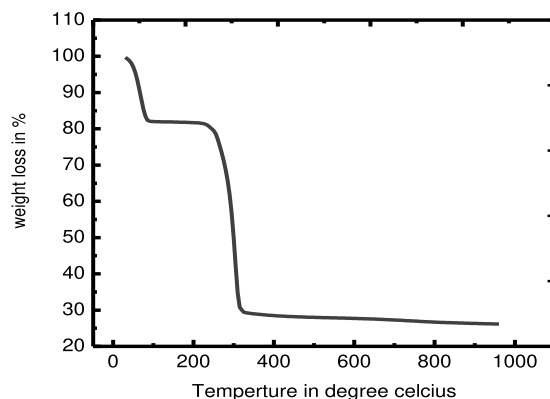
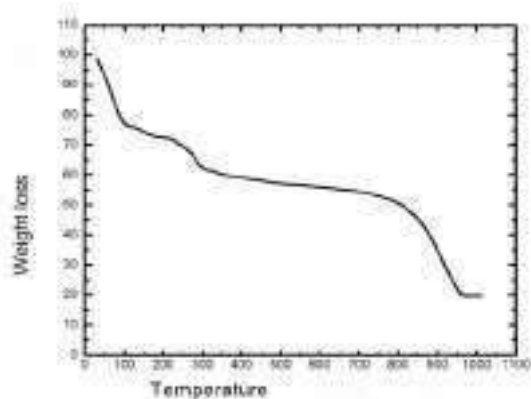


Fig. 1 TGA spectrum of lithium tartrate crystal.

Fig.2 TGA-DTA graph depicting the decomposition of lithium – copper tartrate crystal with respect to temperature

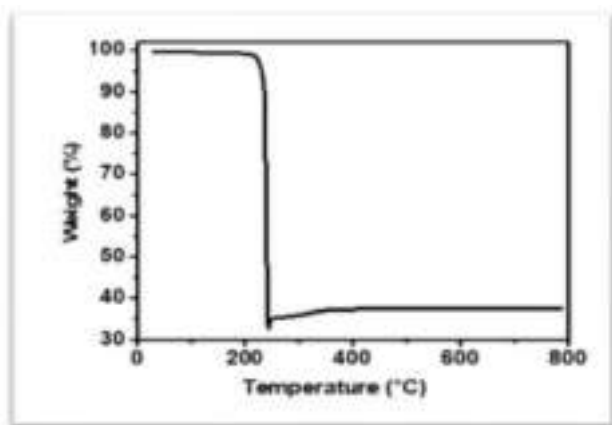


Fig. 3 TGA -DTA graph depicting the decomposition of lithium – copper tartrate crystal with respect to temperature

CONCLUSIONS

The Thermal Analysis revealed the crystallinity of the grown crystals. Thermal analysis is the measurement of how specific physical or chemical properties of a substance changes with temperature. It measures the change in weight of the substance with respect to applied temperature. In present work, thermogravimetric analysis of lithium tartrate, copper tartrate and mixed lithium-copper tartrate crystals was done.

REFERENCES

- Ahmad Nazir and Kotru P.N., (2014), Single crystal growth by gel technique and characterization of lithium hydrogen tartrate, *Journal of Crystal Growth* Accepted Article 24.
- Henisch H.K Patel, A.R., Venkateshwara Rao, (1982) A. Crystal growth in gel media. *Bull. Mater. Sci.* **4**, 527–548.
- Henisch H.K.,(2009), Growth and Characterization Studies of SrCaMHP Single Crystal in Silica Gel Medium and Laser Induced Nucleation Reduction Strategy, *Journal of Minerals and Materials Characterization and Engineering*, **8**,1.
- Krishnakumar Vand Dheivanalar S. (2009), First and second-order Raman scattering of B₆O, “*Journal Raman Spectroscopy*”. **40** ,627-631.
- Lopez T, Stockel J,Peraza J.F and Torres M.E.,(1995) ,Structural Characterization of Doped Calcium Tartrate Tetrahydrate, “*Crys Res.Technol*” **30** (1995) 677.
- Nandre S.J. Ph.D. Thesis North Maharashtra University Jalgaon (2013).

Patil H.M, Sawant D.K, Bhavsar D.S, Patil J.Hand Girase K.D.“*Journal of Therm. Anal. Calorim,*” **107** (2012) 1031.

Sawant D.K, Patil H.M, Bhavsar,D.S., Patil J.H and Girase K.D.“*Journal of Scholars Research Library*”**3** (2011) 404-413.

Sawant D.K, Patil H.M, Bhavsar.D.S, Patil. J.H and Girase K.D. “*Scholars Research Library Archives of Physics Research*”,**2** (2011) 67-73.

Sawant. D. K.; Ph. D. Thesis; (2012), North Maharashtra University, Jalgaon.

Sonawane S.S. Ph.D. Thesis (2015), J.J.T. University Rajasthan.

Yanes A.C, Topez T, Stockel J,Peraza J.F and Torres M.E. (1996) “*Journal Mater Sci.*” **31**,2683.

Growth and Characterization of Barium Oxalate Crystals by Single Diffusion Gel Method

H. S. Pawar¹, S. J. Nandre², S. D. Chavhan³ and R. R. Ahire³

¹V.J.N.T. Late Dalpatbhau Rathod Junior College, Mordadtanda (Dhule) M.S

²Department of Physics, Uttamrao Patil Arts and Science College, Dahiwel, (Dhule) M.S

³Department of Physics S.G. Patil Art's, Commerce and Science College, Sakri (Dhule) M.S

ABSTRACT

Barium oxalate crystals were grown by agar-agar gel through the single diffusion technique. The tendency of barium oxalate crystals to cylindrical growth was demonstrated. The optimum growth conditions barium oxalate was achieved by controlling the parameters like, concentration of gel, concentration of reactants, aging period and reversing of reactants. The crystal structure of grown material was determined by X-ray diffraction technique and was found to be monoclinic with lattice parameters 'a' = 6.6562 Å, b = 8.0464 Å, c = 2.8090 Å, $\beta = 96.832^\circ$, and $V = 149.38 \text{ \AA}^3$. The FTIR spectrum indicates OH and carbonyl group along with the presence of metal-oxygen bond. Morphology of grown crystals, investigated by scanning electron microscopy, exhibited compact grains including small and large sizes. Since the grown crystals are transparent, they show strong absorption in the ultra violet region above 290 nm wavelength.

Keywords: Crystal growth, Barium oxalate, X-ray spectroscopy, FTIR, and SEM.

1. Introduction

A solid which consist of atoms or other microscopic particles arranged in a periodic manner in all directions is called as a crystal. The strong influence of single crystals in the present day technology is evident from the recent advancements ultra-small electronic gadgets. Crystals of different materials have several applications such as they are used in semiconductor devices like electrical diodes, photodiodes, transistors, integrated circuits, magnetic devices like tape heads, transformer cores, superconductors, optoelectronics, quantum electronics, quantum and nonlinear optics, telecommunication etc. hence today's demand is to grow large crystals with good quality, high purity and symmetry. With this demanding requirement it is important to study the growth of single crystals and hence, investigation of their physical properties towards the fulfillment of device fabrication is crucial for both academic as well as applied research. Therefore, enormous amount of toil and treasure has been lavished on the development of crystal growth techniques. The in-depth explanation of various techniques can be obtained in the literature [1-6]. There are three major stages involved in this research. The first is the production of pure materials and improved equipment's associated with the preparation of these materials.

Second one is the production of single crystals first in the laboratory and then extending it to commercial level. The third is the characterization and utilization of these crystals in devices.

In present study, we have adopted the agar-agar gel technique to grow the barium oxalate single crystals. We have successfully grown the cylindrical transparent barium oxalate single crystals and studied their physical properties.

2. Experimental

In the present work, barium oxalate crystals were grown by single diffusion technique. The growth of barium oxalate crystals was carried out in agar-agar gel by adopting the similar technique as reported (Dalal and Saraf 2009) [10]. Barium chloride (BaCl_2 , 99.9%), oxalic acid ($\text{H}_2\text{C}_2\text{O}_4$, 99%), Agar-Agar powder ($\text{C}_{14}\text{H}_{24}\text{O}_9$) were used as the starting materials. All chemicals were of AR grade. The borosilicate glass tubes were used as crystallization apparatus. The glass tubes used for single diffusion were of 25 cm in length having outer diameter of 2.5cm outer diameter and 250ml beaker. The solution of 0.5, 1.0, 1.2, 1.5, and 2M concentrations were prepared and stored in clean glassware. Agar-agar gel was prepared by mixing (0.5 to 2.0gm) of agar powder in 100ml double distilled water at boiling temperature. Barium chloride of concentration 0.5 to 2M and oxalic acid of concentration 0.5 to 2M were used as reactants.

The prepared solution of oxalic acid were transferred into the test tube followed by addition of appropriate volume of agar gel and then kept undisturbed for aging period of few days. After setting and aging over the set-gel, the solution of barium chloride (desire volume and molarity) which is the reactant, was poured gently along the wall and allowed to diffuse into the gel medium. The open end of test tube was closed with cotton plug to protect from dust particles and kept undisturbed at room temperature.

We keenly observed the reaction and noticed that a thin precipitation layer was formed on the surface of the gel. This precipitate band increased gradually and diffusion proceeded into the gel. After 5 to 6 days nucleation process observed at the interstitial sides inside the test tube and then some transparent, star, platy shapes crystals were noticed. The crystals were harvested by washing them carefully with acetone. Prismatic, opaque, and platy shaped crystals were obtained with maximum size of a $3 \times 4 \times 2 \text{ mm}^3$.

The reaction which leads to the growth of crystals is expressed as



The optimum conditions for growing a well-defined crystals are given in table 1.

Table 1. The optimum condition established for growth of barium oxalate crystals

Sr. No	Conditions	Single Diffusion
1	Percentage of gel	1%
2	Con. of Barium Chloride	1M
3	Volume of Barium Chloride	5 ml
4	Con. of Oxalic acid	1M
5	Volume of oxalic acid	10 ml
6	Gel setting period	24 hours
7	Gel aging period	32 days
8	Temperature	Room temperature
9	Quality	Star shaped, Needle shaped, Platy shaped
10	Size	1 to 5 cubic mm

3. Growth kinetics

The growth of barium chloride was observed while growing in a test tube and effect of various parameters such as percentage of gel, concentration of first and second reactants, reversing and aging periods were studied.

3.1 Effect of aging period

To observe the effect of aging period on the growth of barium oxalate crystals. The aging period changes from 24 to 48 hours, while other parameters kept constant. We have found 24 hours aging period indicating the fast growth rate.

3.2 Effect of percentage of gel

To observe the effect of percentage of gel on the growth of crystals, all other parameters were kept constant except the percentage of the gel. It was found that for lower percentage (0.5%) of gel, the growth was slow and form small particles which were in large in number. When percentage of gel increased from 1.0 to 1.5% dendrite shaped crystals growth was observed. The size and appearance of growing crystals found more precise for 1.0% of gel as compare to other percentage of gel. As shown in Fig.1 (a)–(e) good, transparent crystals of barium oxalate having cubic to cylindrical shaped crystals were obtained.



Fig1 (a)



Fig1 (b)



Fig1 (c)

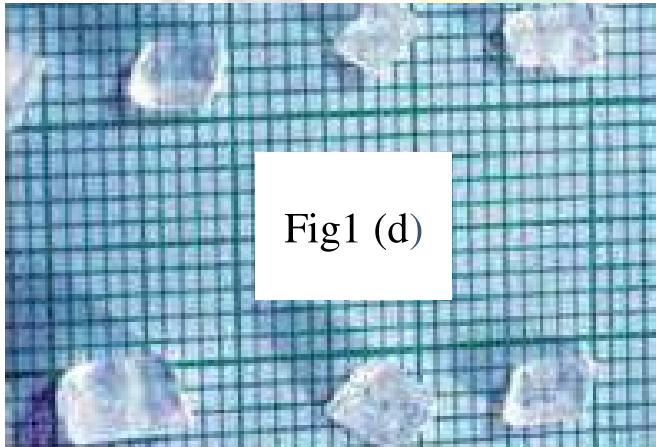


Fig1 (d)

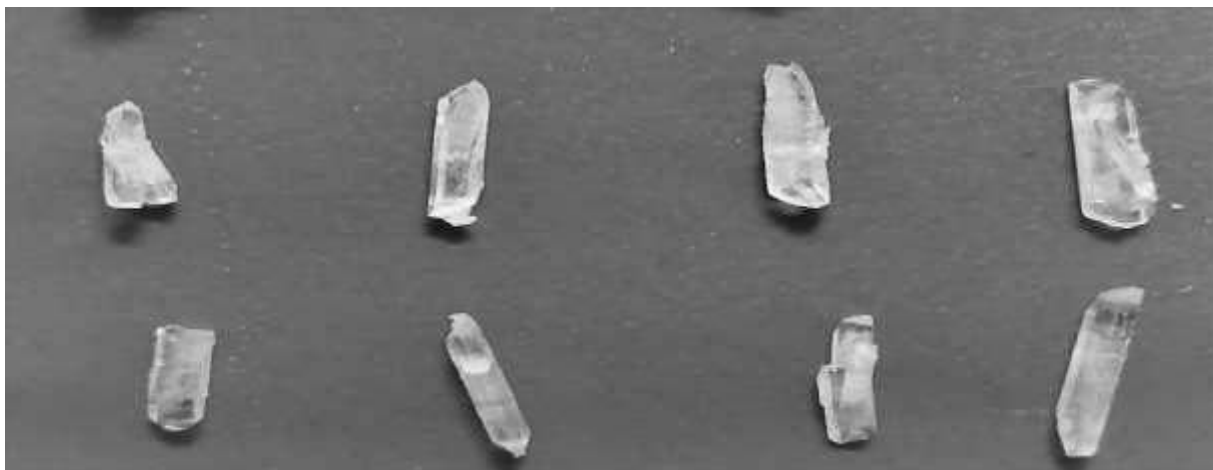


Fig 1(e)

Figure 1 (a-e): Photographs of barium oxalate grown crystals.

4. Result and discussion

4.1 X-ray diffraction studies

X-ray diffractogram is useful method to analyze the crystal structure of unknown material. X-ray diffractogram of gel grown barium oxalate crystals was recorded using powder rotation photograph method on Minislex Regaku X-ray diffract meter at Dept. of Physics at Shivaji University Kolhapur. The sample was rotated in the range 10° - 80° (2θ), scanning speed was kept $2^{\circ}/\text{min}$ and chart speed was $2\text{ cm}/\text{min}$. X-ray diffractogram of barium oxalate is shown in fig. 2.

From the diffraction pattern, “d” values and (h, k, l) planes were computed. Calculated “d” values are well matched with the reported ones. The unit cell parameters and system calculated by the computed program are given in table 2. These parameters satisfy the conditions for monoclinic system. i.e. $a \neq b \neq c$ & $\alpha \neq \beta \neq \gamma$.

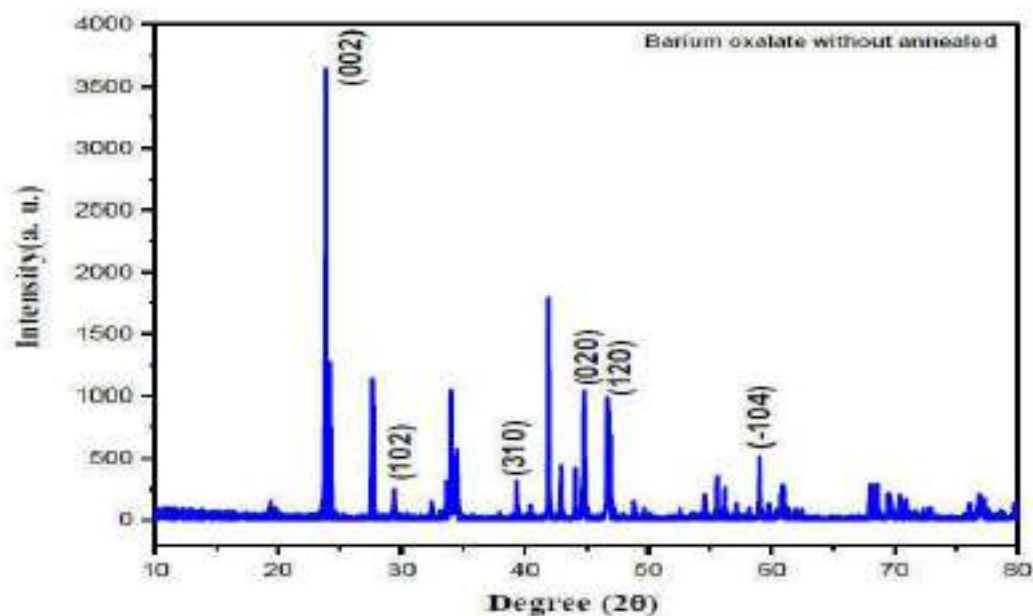


Figure 2: X-ray diffraction pattern of as grown barium oxalate single crystal.

4.2 Fourier transform infrared (FTIR)

The Fourier transform infrared (FT-IR) spectrum of barium oxalate was recorded at room temperature in the spectral range of $500 - 4500 \text{ cm}^{-1}$ by KBr pellet method using SHIMADZU spectrophotometer at the department of Physics, Shivaji University Kolhapur. Figure 3 shows the FTIR spectrum of barium oxalate. A few of the prominent vibrational modes are empirically assigned here. The bands around 2950 to 3650 cm^{-1} are attributed to asymmetric and symmetric $-\text{OH}$ stretching of water. The $-\text{OH}$ stretching frequency of barium oxalate appeared at 2923 cm^{-1} . The moderate absorption around the 3500 to 3200 cm^{-1} is probably due to stretching of alcohol group. The fundamental FT-IR frequencies observed in all barium oxalate crystals [11]. Table 3 shows FTIR spectral and vibrational assignments of barium oxalate.

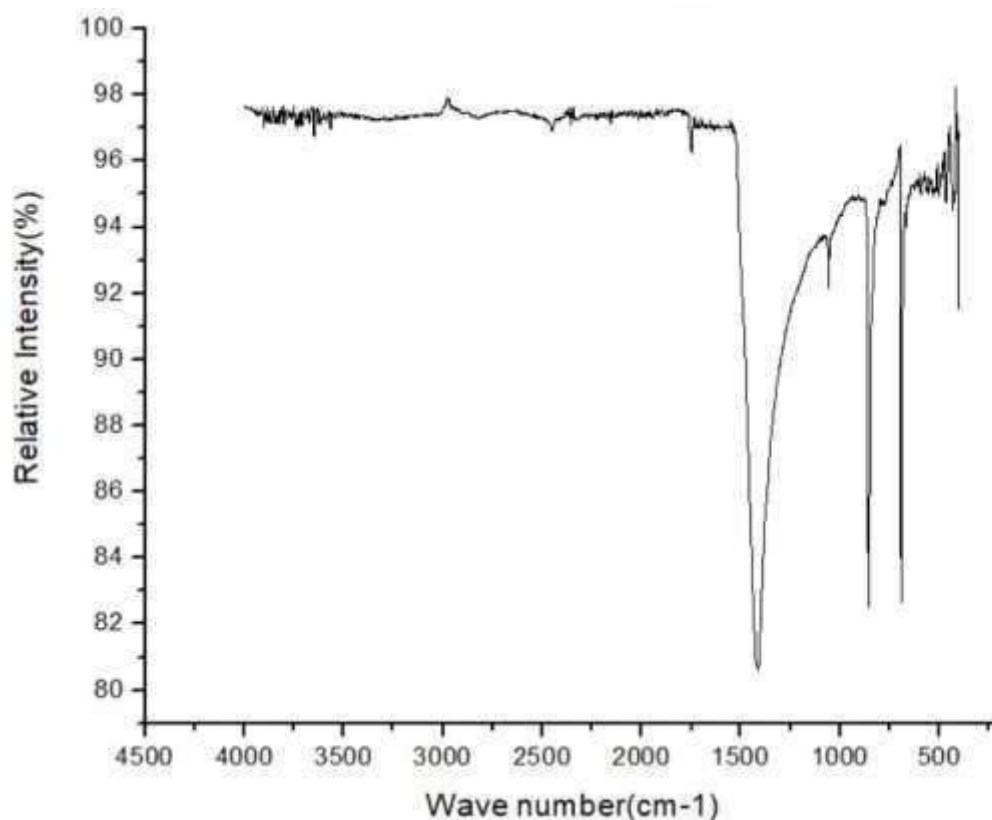


Figure 3. FTIR of Barium oxalate crystal

Table 3. FT – IR spectral and vibrational assignments of barium oxalate.

Wave number cm^{-1}	Intensity	Assignments
3640 - 3610	S,sh	O – H Stretch
3500 – 3200	S,b	O–H Stretch
3330 - 3270	n,s	C=C -H Stretch
3300 – 2500	m	O –H Stretch
3000 - 2850	m	H-C = O Stretch
1710 - 1665	s	C = O stretch
1370 -1350	s	C – H rock
1000 -650	m	= C- H bend
700 - 610	b	C –H bend

m= medium, W = weak, S = strong, B = broad, Sh = sharp, n = normal.

Scanning Electron Microscopy (SEM)

In the present work powdered sample of barium oxalate crystals was examined by using SEM technique at the Dept. of Physics Shivaji University Kolhapur. The study of the surface of the crystal gives valuable information about its internal structure. Figure 4 (a) illustrates SEM photographs of single crystals of barium oxalate crystal. High resolution SEM image is shown in Figure 4 (b). It is observed that due to growth conditions voids are created at the grain boundary. SEM images revealed that the growth of barium oxalate crystals consist of flat layered particles as well as spherical small grains. The individual flat grains possessed sharp edge [13].

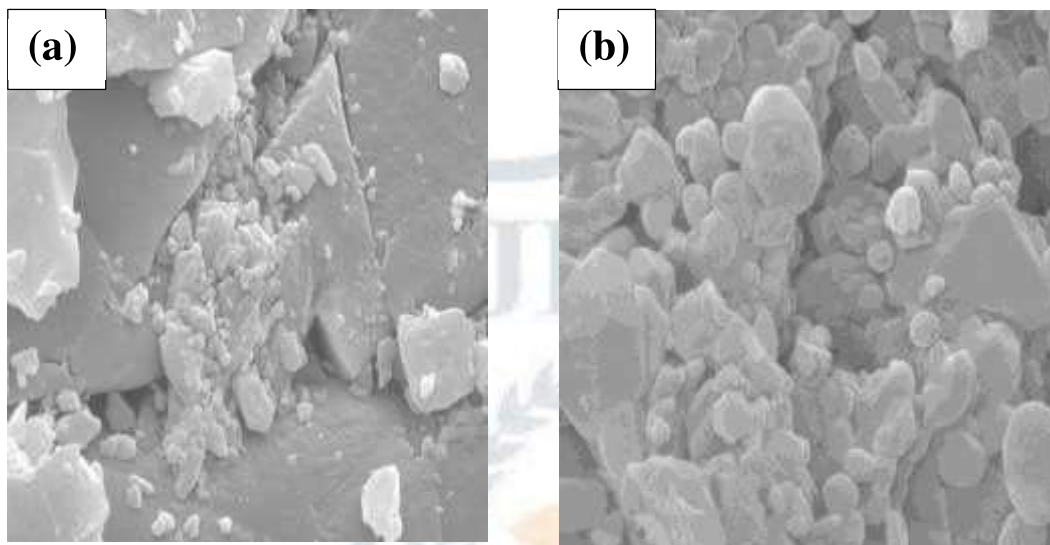


Figure 4: SEM images of as grown (a) barium oxalate crystal and (b) high resolution image.

UV-Vis Absorption spectroscopy

Absorption spectrum of barium oxalate crystals was obtained by a SHIMADZU UV-2450, UV-Vis spectrophotometer at the Dept. of Physics Shivaji University Kolhapur. Figure 5 shows UV-Vis absorption spectrum of barium oxalate crystal. Spectrum shows that the barium oxalate crystal allows to pass the entire visible and IR wavelengths and absorbs only ultra-violet wavelengths and therefore, the absorption coefficient is high at low wavelengths and high at short wavelengths. Since it is transparent crystal for wide range of wavelength (350-900 nm), the barium oxalate crystals can be used for second and third harmonic generations of the 1064 nm radiation [14-15]. Optical band gap energy of the as-grown barium oxalate crystals is calculated using the following simple conversion equation;

$$\text{Band gap energy (eV)} = \frac{1240}{\lambda \text{ (nm)}}$$

The band gap energy of barium oxalate crystal is found to be 4.06eV and tabulated in table 4.

Table 4: the band gap energy of Barium oxalate crystals.

Crystal	λ (nm)	Band gap Energy(ev)
Barium oxalate	305.00	4.06

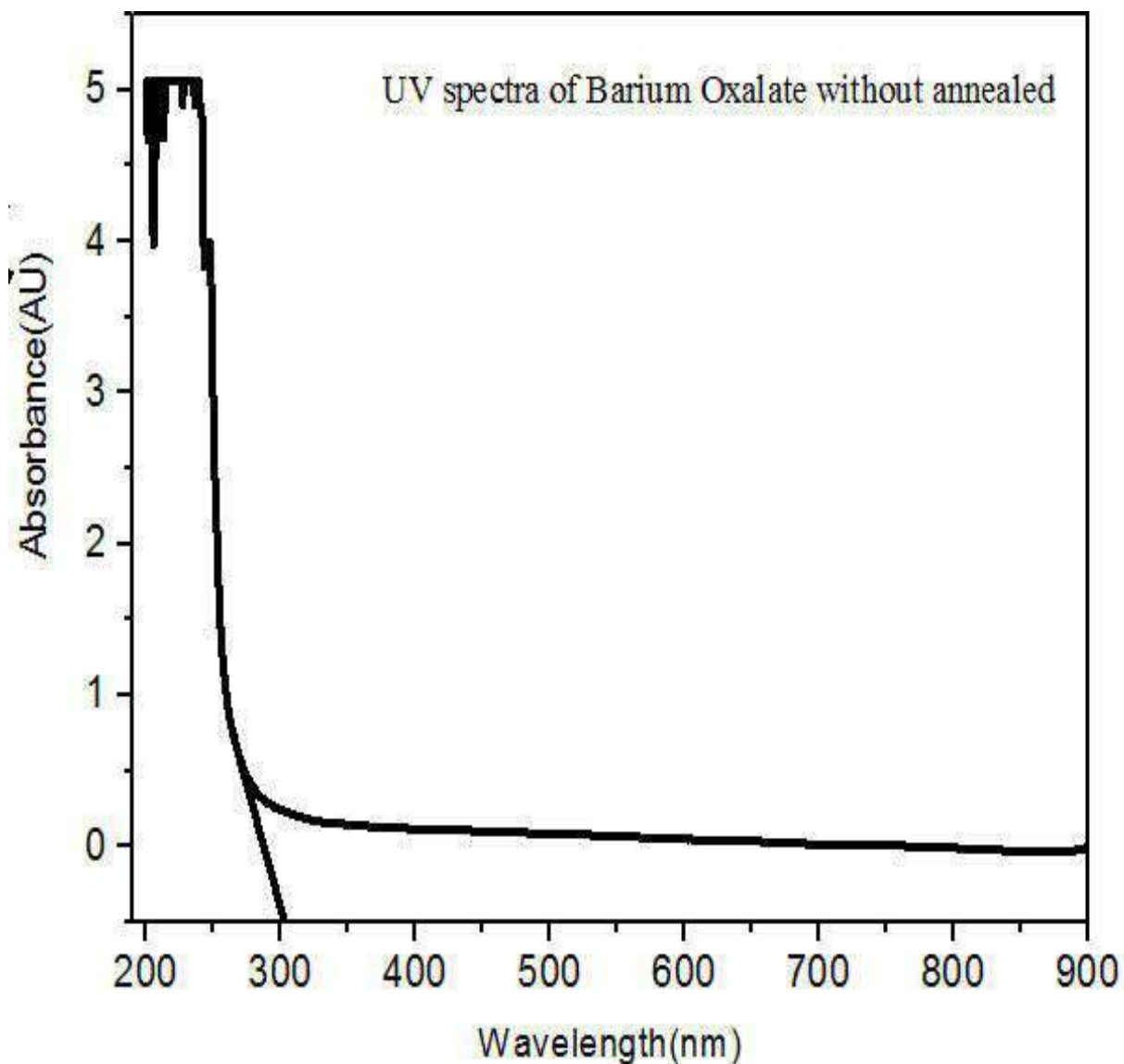


Figure 5: Optical absorption spectra of as-grown barium oxalate crystal.

5 Conclusions

From systematic investigation on the single diffusion gel growth of the barium oxalate crystals. Best conditions have been established to get good crystals.

- 1) Gel method is found suitable for growing barium oxalate crystals.

- 2) The growth of barium oxalate crystals was accomplished by allowing diffusion of barium chloride solution through agar-agar gel impregnated with oxalic acid in single diffusion gel tube system, with all growth conditions. Barium oxalate crystals possessed cubic and cylindrical shapes
- 3) The crystals obtained in agar-agar gel with average size of $3 \times 4 \times 2 \text{ mm}^3$ in single diffusion.
- 4) Different habits of barium oxalate crystals can be obtained by changing parameters like gel density, gel aging pH of gel, concentration of reactant etc.
- 5) The 'd' values of grown material obtained from the XRD are well matches with POWD Programmed.
- 6) The FTIR, studies suggested different characteristics features and morphology of grown crystals.
- 7) UV-Vis absorption spectra of barium oxalate crystal showed 4.06 eV optical band gap energy.

Acknowledgements

The authors are grateful to Principal Dr. R. R. Ahire, V.V.M's S. G. Patil College, Sakri, for providing laboratory facilities. Our special thanks to Prof. Mukesh Padvi, Department of Physics, Shivaji University Kolhapur, for providing characterization facilities like XRD, FTIR and SEM. One of the authors (SJN) is thankful to Dr. B. D. Borse, Principal, Uttamrao Patil College Dahivel for his inspiring suggestions.

References

- [1] H.K. Henisch; In crystal growth in gels, Pennsylvania state university press. **20**(1973).
- [2] H.K. Henisch; In crystals in gel and lies gang rings, Cambridge university press, Cambridge ;(1988).
- [3] H. W. Liaw, J. W. Faust; Jr. In American conference on crystal growth, Gaithersburg, Maryland (1969).
- [4] H.W.Liaw,J.W.Faust;Jr. J. Cryst. Growth **13-14**, 471(1972).
- [5] A.R.Patel and A.V.Rao; J.Cryst.Growth **43**, 351(1978).
- [6] K.V.Kurian and M.A.Ittyachen; J. Mater, Sci. **15**, 1724(1980).
- [7] K.Suryanarayana and S.M.Dharamaprakash; Mater.Chem.Phys.**42**, 92(2000).
- [8] S.K.Arora; Advanced in gel growth,A review progress in crystal growth and characterization of materials **4**, 345(1981).
- [9] S.K. Arora, Vipul Patel,Kothari and Brijesh Amin; Crystal growth and design **343-349**,4(2004).
- [10] S.A. Firdous, I. Quasim,M.M.Ahmad and P.N.Kotru;Bull.Mater.Sci.**377 – 382**,33 (2010).

- [11] K. Nakamoto 1970 'Infrared Spectra of inorganic and co-ordination Compounds' (New York;John wiley and sons Inc) 2nd edn..
- [12] S.J.Nandre, S.J.Shitole and R.R.Ahire, Archives of Physics Research, 2012, 3(1) PP70-77.
- [13] S.J.Nandre, S.J.Shitole, S.S.Sonawane and R.R.Ahire, International Journal of Basic and Applied Research, special issue 2012, 125-128.
- [14] Nisha Santha kumaria, P. Kalainathan, S. Cryst.Res. Technol.4 (2008)317.
- [15] Kalaisevi. D., Mohan Kumar. R, and R Jayavel, Cryst.Res.Technol.8 (2008)851.



Physical and Morphological Study of Barium Oxalate Crystals Grown by Agar-Agar Gel Method

H. S. Pawar¹, S. J. Nandre², S. D. Chavhan³ and R. R. Ahire³

¹V.J.N.T. Late Dalpatbhau Rathod Junior College, Mordadtanda (Dhule) M.S

²Department of Physics, Uttamrao Patil Arts and Science College, Dahiwel, (Dhule) M.S

³Department of

Physics S.G. Patil Art's, Commerce and Science College, Sakri (Dhule) M.S

ABSTRACT

Barium oxalate crystals were grown by agar-agar gel through the single diffusion technique. The tendency of barium oxalate crystals to cylindrical growth was demonstrated. The optimum growth conditions barium oxalate was achieved by controlling the parameters like, concentration of gel, concentration of reactants, aging period and reversing of reactants. The crystal structure of grown material was determined by TGA, DTA, DSC and EDAX.

Keywords: Crystal growth, Barium oxalate, TGA, DTA, DSC, and EDAX.

Introduction

The growth of crystal occurs not only in the crust of Earth or in laboratory but also in a living body. Many crystals, particularly, bio-materials and proteins, cause various ailments and health related problems. The urinary stones are usually composed of either pure or mixed crystals of calcium oxalate, brushite, struvite, and hydroxyapatite and carbonate apatite [1]. Arthropathies, i.e., bone and joint diseases, are caused by crystals such as hydroxyapatite, calcium pyrophosphate and monosodium urate monohydrate [2]. There are other crystals which play important role in various ailments, for instance, f.c.c. type ferritin crystals in development of cataract [3] and cholesterol crystals for cardiovascular diseases and gall stones [4]. This bio-crystallization occurring in human body causes suffering and it is not desirable to occur. This has been discussed in detail by the predecessors of the present author [5-7]. There are several micro-organisms which synthesize crystals, for example, magneto-tactic bacteria synthesizing magnetite [8], chrysophytes [9] diatoms and act in opoda synthesizing siliconous materials and S. layer bacteria synthesizing gypsum and calcium carbonate surface layers [10]. Calcite crystals are found in mollusk shells [11] and as a component in gall stones [12]. The earlier crystal growth study was divided into two parts :(1) The study of the equilibrium between the crystal and surrounding medium(2) The study of the kinetics of growth.

Experimental

Experimental procedure 5 gm of agar-agar powder was dissolved in to hot double distilled water mixed with 0.5 M to 1 M barium chloride solution was incorporated then again the mixture was stirred to make homogenous mixture. The crystallizing vessel were used essentially consist of standard glass tube having inner diameter 2.5 cm and the length 25 cm. Gelling mixture poured in glass test tubes. These tubes were hermitically sealed to prevent evaporation and contamination of the exposed surface by dust particles of atmosphere or atmospheric

impurities and were kept undisturbed. Usually in 3 to 4 days the gel was to be set which depends on the environmental temperature. It was observed that the mixture in a glass tube was initially transparent and slowly turned light white. The water slowly evaporated and gel was completely set. After ensuring firm gel setting, it was kept for aging for 3 to 4 days. After that 0.5 M to 1 M solution of oxalic acid was added as a supernatant over the set gel. Nucleation was observed after 5 to 6 days and crystals started to grow. White color, larger size, transparent and shining crystals were obtained in the gel, as shown in fig.1, Optimum condition tabulated in table 1, [13].

Table 1 Optimum conditions for barium oxalate crystal grown by agar-agar gel method

Concentration of agar-agar gel	5 %
Concentration of reactant, strontium chloride	1M
Concentration of supernatant, oxalic acid	1 M
Room temperature	27 ⁰ C
Gel aging period	4 days
Growth period	25 - 40 days
Quality of crystals	White colour, larger size (1mm × 1mm) transparent, shining crystals

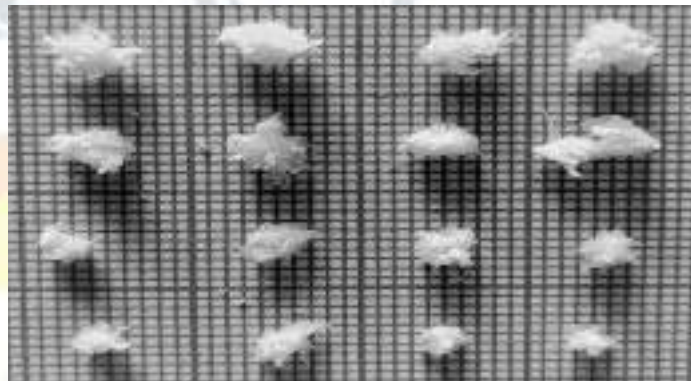


Fig.1 (a) Barium crystal inside the test tube (b) Opaque and shiny crystals

Result and Discussion-

Thermo-Gravimetric Analysis (TGA)

TGA was carried out at Department of Physics, Shivaji University Kolhapur, TGA curve for barium oxalate is shown in figure.2. From the thermo gram of barium oxalate one can observe that

- i) The compound is stable up to 50⁰C.
- ii) 5.165% weight loss in temperature range 50⁰C. To 172⁰C may be due to dehydration of water molecule and up to 172⁰C there is no further loss of weight.
- iii) 25.68% weight loss in temperature range 172⁰C to 277⁰C from the dehydrated compound corresponds to loss of CO.
- iv) 36.68% weight loss in temperature range 277⁰C to 435⁰C corresponds to loss of CO₂.
- v) 13.45% weight loss in temperature range 435⁰C to 478⁰C.
- v) The residue remains stable from 478⁰C and decompose the material. [14-16].

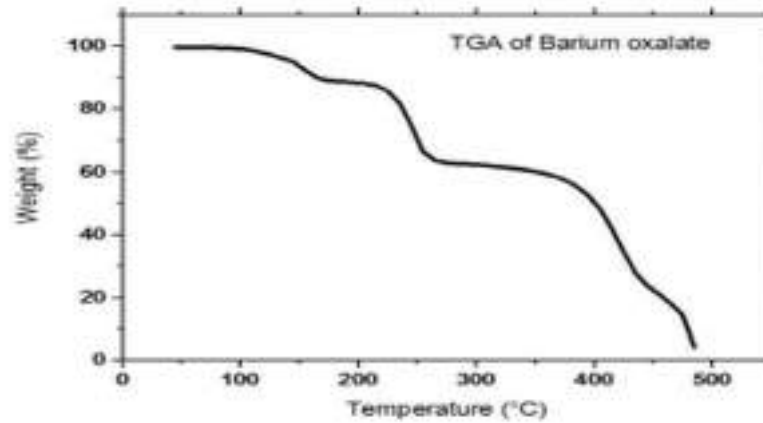


Figure 2 TGA of Barium oxalate crystal grown by agar-agar gel

TGA data indicates that the grown crystals contains water molecule,

Table 2 TGA Data of Barium oxalate

Stage	Temperature range	Observed % weight loss	Calculated % weight loss	Loss of molecule in stage
I	50 ⁰ C-172 ⁰ C	5.165%	5.045%	H ₂ O
II	172 ⁰ C-277 ⁰ C	25.68%	25.8%	It may be CO
III	277 ⁰ C-435 ⁰ C	36.68%	35.99%	CO ₂
IV	435 ⁰ C-478 ⁰ C	13.45%	13.56%	-

Differential Thermal Analysis (DTA)

DTA was carried out at Department of Physics, Shivaji University Kolhapur. DTA curve for barium oxalate is shown in figure 3. From the thermo gram of barium oxalate one can observe that.

In DTA curve of barium oxalate by agar-agar gel at 37.51⁰C an endothermic peak is observed due to the loss of bulk of water of crystallization. The decomposition of oxalate is observed at the onset due to complete dehydration. In DTA curve the exothermic peaks at 153.⁰C to 154.54⁰C shows the decomposition of oxalate. Loss of weight at the temperature range 153.⁰C relates to the loss of water of crystallization which is endothermic in character.

Loss of weight at the temperature 250.07⁰C endothermic peak is observed that means the weight loss with respect to temperature of the grown crystals was further supported by

DTA results. DTA data is shown in table- 3

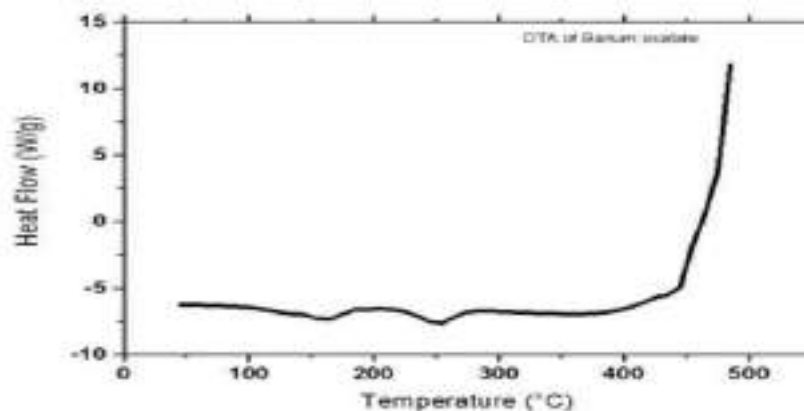


Figure 3 DTA of Barium oxalate

Table no.3 DTA data of barium oxalate

Peak recorded	Peak height	Nature	$\Delta H(J/gm)$
37.51 ⁰ C	-0.600	Endothermic	-0.6406
154.54 ⁰ c	-0.5	Exothermic	-0.5344
250.07 ⁰ c	-0.4	Endothermic	-0.4613

Differential Scanning Calorimeter (DSC)

DSC was carried out at Department of Physics, Shivaji University Kolhapur, The DSC thermogram was recorded in the temperature range from 25⁰C to 450⁰C. Microcrystalline (powdered) samples of barium oxalate crystals were taken for DSC studies and the weight of the sample 8.5230mg. The sample was held for 10 min in air to evaporate water due to moisture and then heated from 25⁰C to 450⁰C. at the rate 10c/min in Air. After reaching the temperature of 450⁰C, the sample was hold for I minute at 450⁰C and then again cooled from 450⁰C to 25⁰C at the rate of 10C/min in Air.

The DSC curve for barium oxalate gel grown crystal shown in figure 4. And the DSC data collected from this curve is tabulated in the table 4.

Step-I

i) The initiation temperature is 225⁰C and equilibrium temperature 277⁰C. At 225⁰C (initiation temperature) initiation of phase change start & is completed at peak endo-down temperature of 250.07⁰C (transition temperature). The temperature at which the sample and the reference come to the thermal equilibrium by thermal diffusion appears to be at 277⁰C. The peak appeared in the DSC curve at 154.54⁰C indicates the phase transformation due to loss of water molecules and formation of stable anhydrous barium oxalate. This is the good agreement with the TGA curve,

ii) Area under the curve is 5707.384 mJ.

iii) Heat of transition ΔH i.e. enthalpy change of transition 517.56 J/g which 0.51756 kJ/mole. Since molecular weight is 1 g/mole, $\Delta H_{tr} = \Delta H_f$ i.e. heat of phase transformation is also 0.5756 kJ/mole, where ΔH_f is enthalpy change of new phase transformation or it is called heat of phase formation.

Step-II

- i) The initiation temperature is 430⁰C and equilibrium temperature is 450⁰C. At 430⁰C (initiation temperature) initiation of phase change starts and is completed at peak endo- down temperature of 438.76⁰C (transition temperature). The temperature at which the sample and the reference come to the thermal equilibrium diffusion appears to be 450⁰C. The further phase transition occurs at temperature 438.76⁰C due to the loss of carbon and H₂O and formation of stable barium oxalate. This is good agreement with TGA Curve.
- ii) Area under the curve is 232.43 mJ.
- iii) Heat of transition ΔH i.e. enthalpy change of transition 21.99 J/g which is 0.02199 kJ/mole. Since molecular weight is 1 g/mole, Hence $\Delta H_{tr} = \Delta H_f$ i.e. heat of phase transformation is also 0.02199 kJ/mole. Where ΔH_f enthalpy change of new phase transformation or it is called heat of phase formation. DSC data is shown in table- 4.

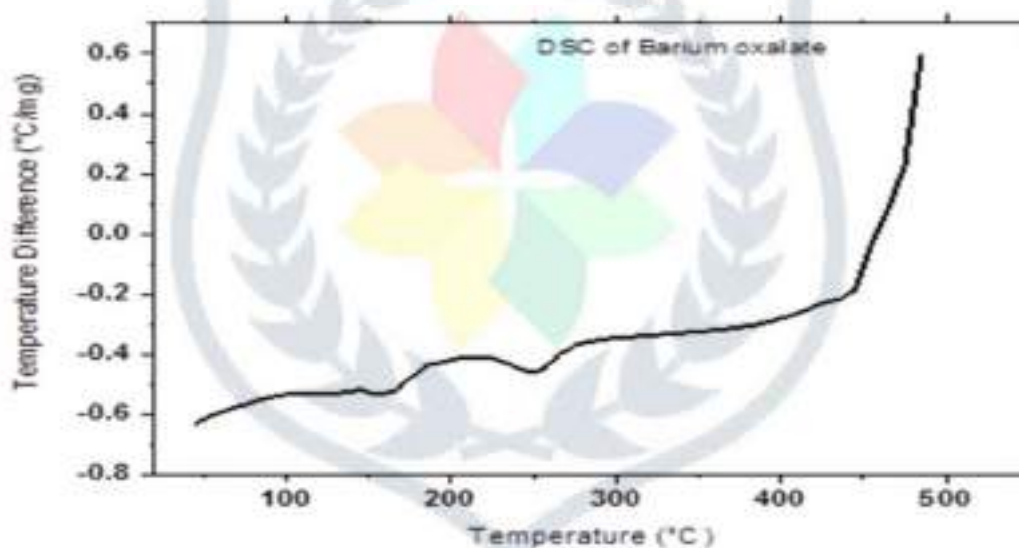


Figure 4 DSC curve for Barium oxalate

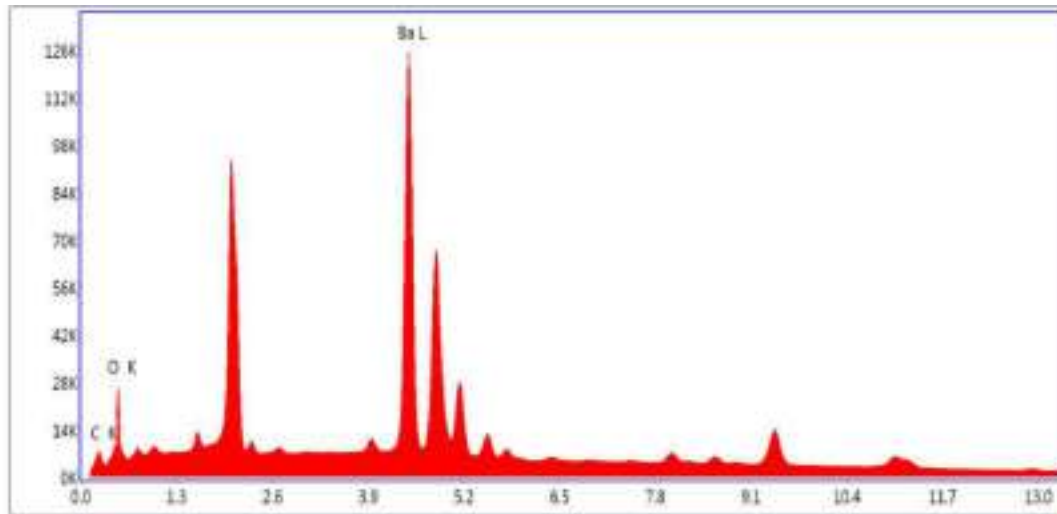
DSC data is shown in table- 4

Sample	Weight of the sample	Stage	Change in the enthalpy(ΔH)	Transition temperature (Tr)
Barium oxalate	0.8523 gm	I	0.51756 kJ/mole	250.07 ⁰ C
		II	0.02199 kJ/mole	438.76 ⁰ C

Energy Dispersive Analysis by X-rays (EDAX) –

Energy Dispersive analysis by X-ray (EDAX) is used for the quantitative analysis of barium oxalate and is also called as elemental analysis. Fig 5 & Table No 5 shows, in present work elemental analysis of gel grown barium oxalate crystals was Department of Physics, Shivaji University Kolhapur. It conclude that the (weight

& atomic %) of copper (Cu) in the grown crystal measured by EDAX are very close with the values calculated from the molecular formula.[17-20]



eZAF smaryt quant Results

Element	Weight%	Atomic%	Net.Int	Error	%	K ratio	Z	R	A	F
Ck	7.36	34.64	443.18	7.82	0.05	0.05	1.47	0.75	0.47	1.00
Ok	8.71	30.80	991.30	7.87	0.05	0.05	1.42	0.77	0.39	1.00
Barium	83.93	34.56	5594.20	2.05	0.80	0.80	0.91	1.07	1.03	1.03

Conclusions —

The present work reports the growth and characterization of barium oxalate single crystals. We have demonstrated the formation of barium oxalate single crystals in agar-agar gels. Barium oxalates exhibits micro-rod-like and spherulites growth (flower) shape are observed. Further to obtain good quality single crystals of barium oxalate, both reactants –barium chloride and oxalic acid were interchanged. With barium chloride incorporated gels result only fibers. These facts have been explained by taking in account the interaction of the reactants ions with the sodium and silica ions. The effect of temperature on growth of barium oxalate crystals showed that there is a decrease in nucleation density at higher temperature which is due to the increases of the aqueous solubility of barium oxalate.

References

- [1] M. Menon, B. G. Parulkar and G. W. Drach; Campbell's Urology, W. B. Saunders, New York, 9th Edition,3 (1998) 2662-2676.
- [2] S. J. Gupta; J. Indian Rheumatol Assoc., 10(2002) 5-13.
- [3] D. G. Brooks, K. Manova-Todorova, J. Farmer, L. Lobmayr, R. B. Wilson, R. C. Eagle, Jr., T. G. St. Pierre and D. Stambolian; Invest. Ophthalmol. Vis. Sci., 43(2002)1121.
- [4] S. P. Wrenn; "Engineering Approaches to Cholesterol-Linked Diseases", (2001).

- [5] V. S. Joshi; Ph. D. Thesis, Saurashtra University, Rajkot (2001).
- [6] K. C. Joseph; Ph.D. Thesis, Saurashtra University, Rajkot, (2005).
- [7] B. B. Parekh; Ph. D. Thesis, Saurashtra University, Rajkot (2006).
- [8] R. B. Frankel and R. P. Blakemore; “Eds in Iron Biominerals, Plenum”, New York, (1991).
- [9] J. Kristiansen and R. A. Andersen; “Eds in Chrysophytes Aspects and Problems”, Cambridge University Press, Cambridge (1986).
- [10] M. Sarikaya; Proc. Natl. Acad. Sci. USA, B96(1999) 14183.
- [11] C. E. Bowen and H. Tang; Comp. Biochem. Physiol., 115A(4)(1996)269.
- [12] D. S. June and E.S. Weley; Science, 159 (1968)1113.
- [13] P.V.Dalal and K.B.Saraf ,:”Bull.Mater.Sci” Vol.29 N0.5,2006 421-425.
- [14] K.S.Raju,Johan Varughese and M.A.Ittyachen; “ Bull. Mater.Sci.” 21(1998)375.
- [15] D.K.Sawant,H.E.Patil,D.S.Bhavsar,K.D.Girase and J.H.Patil; “Journal of Thermal Analysis and Calorimetry,” 107 (2012)3.
- [16]N. S. Patil, P. A. Savale. S. K. Bachhav and S. T. Pawar ; ‘ Archive of physics research’, Vol2(1), (2011). 39-47,
- [17]D. K. Sawant., H. M. Patil and D. S. Bhavsar., ‘Pelagia research Library, DCS’ Vol2(3), (2011) 63,
- [18]D. K. Sawant., H. M. Patil and D. S. Bhavsar., ‘Scholars Research Library Archives of Physics Research’, Vol2(2), (2011). 67.
- [19] S.J.Nandre,S.J.Shitole and R.R.Ahire; “Journal of Nano and Electronic Physics”Vol.4,4,(2012)4013.
- [20] M.Selvapandiyam, S. Sudhakar and M.Prasath; “Int. Journal of Engineering Research and Application”, Vol. 7,8,(3) (2017), 65-72.

Influence of Mn²⁺ Magnetic Ions on the Properties of Cd_{1-x}Mn_xS Thin Films Synthesized by Chemical Bath Deposition

A.E. Mali^{1*}, A.S. Gaikwad¹, S.V. Borse², R.R. Ahire³

¹ Department of Physics, SPDM College, Shirpur, Dist. Dhule (MS) 425405, India

² Department of Physics, SSVPS College, Shindkheda, Dist. Dhule (MS) 425406, India

³ Department of Physics, SG Patil College, Sakri, Dist. Dhule (MS) 424304, India

(Received 26 November 2020; revised manuscript received 15 February 2021; published online 25 February 2021)

II-VI semiconductor based ternary CdMnS compound material has received more attention due to its wide area of applications in semiconductor technology. Cd_{1-x}Mn_xS ($x = 0, 0.2, 0.4, 0.6, 0.8$ and 1.0) thin films were successfully prepared by chemical bath deposition technique on non-conducting glass substrates. Thin films were deposited at a bath temperature of 80 °C and pH = 11 by using the chemical bath reaction of cadmium chloride (CdCl₂) and manganese chloride (MnCl₂) with thiourea (NH₂)₂S in an aqueous solution. Further, the prepared samples were characterized by UV-visible spectroscopy, photoluminescence, XRD, SEM and EDAX to study the optical, structural, surface, and chemical properties. Effect of Mn²⁺ ions on the film thickness of Cd_{1-x}Mn_xS films was investigated using weight difference technique. The film thickness of Cd_{1-x}Mn_xS films decreases as Mn²⁺ ions increase in the bath solution. The polycrystalline nature with hexagonal and cubic structures of the as-deposited films was confirmed by XRD. The band gap value of the deposited films was observed to increase with increasing Mn²⁺ ion concentration, this might be ascribed to the fact that Cd atom was substituted by Mn atom in the CdS structure. EDAX analysis confirmed the deposition of Cd, Mn and S elements in the films. Photoluminescence spectra of Cd_{1-x}Mn_xS with different values of the composition parameter x exhibited two emission peaks with different intensities. The measurement of the electrical resistivity of Cd_{1-x}Mn_xS films was performed at room temperature using two probe methods. The variation in electrical resistivity values with compositional parameters was discussed based on deposition parameters. The investigated polycrystalline Cd_{1-x}Mn_xS thin films show promising technological applications in semiconductor industry.

Keywords: CdMnS films, Optical properties, Electrical properties, Chemical bath deposition, Mn²⁺ ion.

DOI: 10.21272/jnep.13(1).01004

PACS numbers: 68.55.eg, 68.55.jd, 81.10.Ba, 68.37.Hk, 78.66.Hf

1. INTRODUCTION

The *n*-type CdS [1] (band gap ~ 2.42 eV) and *p*-type MnS [2] (band gap ~ 3.88 eV) are important materials of group II-VI semiconductors and they have potential application prospect in electronics and optoelectronic devices, sensors, lasers and thin film based devices in semiconductor industries [3]. The CdS structure has high electrical resistivity values and the energy gap of CdS is narrow [4]. Hence, the use of CdS alone is not enough for future hopes. To do this, unlike earlier reports, we have incorporated here Mn²⁺ ions into the CdS structure to produce CdMnS thin films in a wide range of composition ($x = 0.0$ to 1.0). Doping of CdS with Mn²⁺ ions has been made to achieve improved structural, electrical and optical properties. Most of the research done so far has focused extensively on structural, optical and electrical properties of Cd_{1-x}Mn_xS thin films. However, the study of the influence of Mn²⁺ ions on various properties of Cd_{1-x}Mn_xS thin films is rare in the literature.

A variety of techniques like spray pyrolysis, thermal evaporation, molecular beam epitaxy, sputtering, chemical vapor deposition, pulsed laser deposition, chemical bath deposition (CBD) etc. have been used in the synthesis of CdMnS thin films [5, 6]. Among these, CBD is one of the important techniques. CBD can provide simplicity, cost effectiveness, ease of handling and requires low cost equipment. It can be performed using a range of precursors and synthesis conditions like

temperature, time, concentration of reactants etc. The technique is simple, inexpensive and has a high yield, reproducible on large-area thin films [7, 8].

This paper attempts to use a CBD technique for the deposition of Cd_{1-x}Mn_xS thin films for different values of the composition x and systematic study of the influence of Mn²⁺ ions on various characterization properties of Cd_{1-x}Mn_xS thin films.

2. EXPERIMENTAL DETAILS

Cd_{1-x}Mn_xS thin films were deposited using CBD technique. Cadmium chloride (CdCl₂), manganese chloride (MnCl₂) and thiourea (CH₄N₂S) were used as Cd²⁺, Mn²⁺ and S²⁻ ion sources, respectively. The stock solutions of CdCl₂ (1 M), MnCl₂ (1 M) and thiourea (1 M) all of AR grade were prepared using distilled water. The experimental solutions of CdCl₂ and MnCl₂ were dissolved in high purity DI water in 50 ml glass beaker. Subsequently, thiourea was added dropwise to the solution with continuous stirring until a volume of 50 ml reached. Ammonia solution was added until the pH reached 11 and stirred for few minutes. The microscopic non-conducting glass substrate was cleaned with distilled water and liquid soap, soaked in dilute HCl for one day, washed with acetone and finally with distilled water. Then the substrate was kept vertically inclined into the chemical bath. The chemical bath maintained at 80 °C for one hour. Finally, deposited samples were taken out of the solution cleaned with DI water and

*aemalispdm@gmail.com

dried in air at room temperature. To study the influence of Mn^{2+} on various properties of $Cd_{1-x}Mn_xS$ thin films, the CBD parameters, such as complexing agent, deposition time, temperature and pH of the solution were firstly optimized in the present procedure to achieve good quality films. Fig. 1 shows the schematic sketches of the sample preparation process.

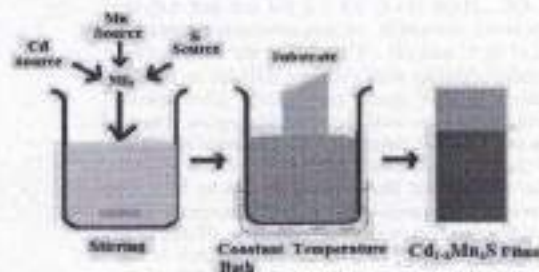
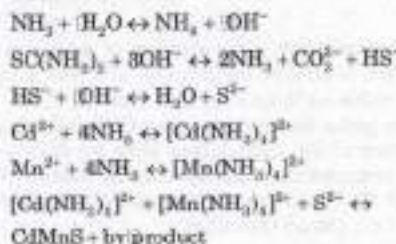


Fig. 1 – Process flow for deposition of $Cd_{1-x}Mn_xS$ films

The deposited $CdMnS$ thin film exhibits yellowish to yellow brownish color with variation in Mn^{2+} ion concentration.

The chemical reaction for the deposition of $CdMnS$ by CBD is as shown below



3. RESULTS AND DISCUSSION

The as-deposited films were characterized by different techniques. The film thickness was measured using gravimetric weight difference method. The XRD of the films was recorded using Bruker AXS D8 advance spectrophotometer. The surface morphology of the $CdMnS$ films was analyzed by FESEM (SEM Hitachi S-47009). The compositional purity of the films was confirmed by EDAX analysis. The UV-visible spectrum was recorded by the spectrophotometer in the wavelength range 300–900 nm. The room temperature PL spectrum was recorded by Perkin Elmer LS55 using laser source at a wavelength of 390 nm. The dc electrical transport properties have been studied at room temperature by two-probe dc electrical conductivity equipment.

3.1 Thickness Measurement

The as-deposited film thickness of $Cd_{1-x}Mn_xS$ samples was measured by gravimetric weight difference method using a high-precision electric balance. This method gives an appropriate value of the thickness of the deposited films. The thickness of the film can be determined using the equation [9]

$$t = \frac{(w_2 - w_1)}{A\rho} \times 10^{-4} \mu m$$

where w_1 and w_2 are the weights of the substrate before and after film deposition in grams, A is the area of the deposited film in cm^2 and ρ is the theoretical density of the deposited material.

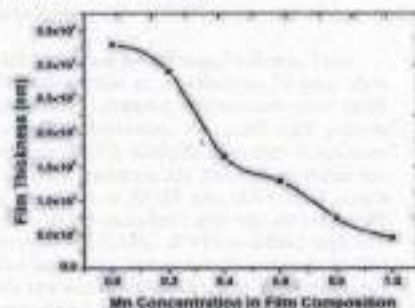


Fig. 2 – Variation in film thickness as a function of Mn concentration

Fig. 2 shows the variation in film thickness versus Mn^{2+} ion concentration in the CdS structure. It is seen that the thickness of the film decreases with the addition of Mn^{2+} ions to the CBD solution. It can be ascribed to the fact that Mn^{2+} ion has smaller atomic/ionic radius (117/80 pm) than that of Cd^{2+} (154/97 pm). As Mn^{2+} ion concentration in the bath solution increases, the film (Mn^{2+}) content also increases. Further, substitution of Cd^{2+} by Mn^{2+} atoms is easily possible in the chemical bath.

3.2 Characterization Using XRD

The crystal structure of the as-deposited films has been investigated by XRD patterns which are shown in Fig. 3. The diffractogram illustrated in the figure clearly shows that the as-deposited films are polycrystalline in nature. The analysis of these diffractograms was done and the corresponding data (interplanar distance d , hkl planes, grain size etc.) were determined. There are six prominent reflections at d values equal to 3.577 Å, 3.351 Å, 3.164 Å, 2.066 Å, 1.890 Å and 1.760 Å that correspond to the (100), (002), (101) (110), (103) and (200) reflections, respectively. XRD pattern of the films indicates that they are polycrystalline with both the hexagonal wurtzite type structure (JCPDS card No. 772306 for CdS and card No. 894953 for MnS) and cubic structure with preferential growth along the (002) direction. The addition of Mn^{2+} to the CdS matrix showed the formation of a solid solution up to $x = 0.8$. The further incorporation of Mn^{2+} resulted in phase separation of both CdS and MnS .

The average grain size enhanced with the addition of Mn^{2+} ions into the bath solution. A plot showing grain size versus concentration is represented in Fig. 4. When Mn^{2+} ions are added to the host lattice of CdS , Mn atoms substitutionally occupy Cd atom sites instead of forming a separate MnS phase. The effect of Mn^{2+} ions on grain size of the obtained films is shown in Fig. 4.

This caused improved crystallinity, especially for $x = 0.2$. Above the composition $x = 0.4$, phase separation started resulting in deterioration of crystallinity for films with $x = 0.6$ and $x = 0.8$. Films with $x = 1.0$ represent amorphous nature with dominant MnS phase [10].

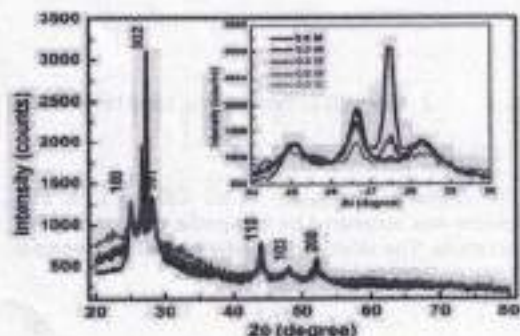


Fig. 3 – X-ray diffraction spectra of CdMnS films. The inset shows intense peaks

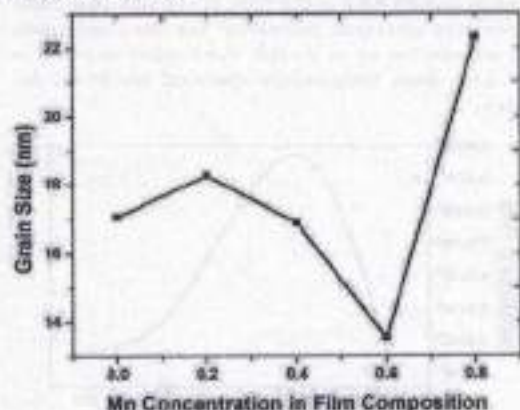


Fig. 4 – Effect of Mn concentration in the film composition on grain size

Table 1 – Observed and standard 2θ and d values for respective hkl planes

Sr. No.	2θ , degrees		d , Å		Planes (hkl)
	Observed	Standard	Observed	Standard	
1	24.90	25.18	3.5775	3.5380	(100)
2	26.61	26.91	3.3514	3.3147	(002)
3	28.21	28.61	3.1648	3.1215	(101)
4	43.84	44.36	2.0680	2.0430	(110)
5	48.15	48.60	1.8906	1.8716	(103)
6	51.96	51.69	1.7606	1.7692	(200)

The XRD data are given in Table 1. The average grain size in the deposited films is estimated using Scherrer relation:

$$D = \frac{k\lambda}{\beta \cos\theta} \quad (2)$$

where k is the Scherrer constant, λ is the wavelength of X-rays, β is the full width at half maximum (FWHM) in radians and θ is the Bragg angle.

3.3 SEM Analysis

The surface morphology of $Cd_{1-x}Mn_xS$ thin films was investigated by FESEM. Fig. 5 shows variations in the surface morphology of $Cd_{1-x}Mn_xS$ ($x = 0.0, 0.2, 0.4,$

$0.6, 0.8, 1.0$) films with respect to increase in Mn^{2+} ion concentration in the coating solution. All the films were scanned at 20 K magnification.



Fig. 5 – FESEM images of the films: a) CdS, b) $Cd_{0.2}Mn_{0.8}S$, c) $Cd_{0.4}Mn_{0.6}S$, d) $Cd_{0.6}Mn_{0.4}S$, e) $Cd_{0.8}Mn_{0.2}S$, f) MnS

The micrographs show the uniform deposition of $Cd_{1-x}Mn_xS$ films without any pinholes. Pure CdS has a flower-like structure and is shown in Fig. 5a. As we incorporate Mn^{2+} ions into CdS coating solution, Mn atoms interact with CdS molecules. This interaction slightly changes the film surface morphology, which is confirmed by Fig. 5b. Further increase in Mn^{2+} ion concentration in the coating solution resulted in the formation of nanocrystalline CdMnS compounds that is shown in Fig. 5c-e. When concentration of Mn^{2+} ions reaches the highest level, Cd atoms are replaced by Mn atoms and this gives us the pure form of MnS films. The nanocrystalline morphology of pure MnS films is shown in Fig. 5f.

3.4 EDAX Analysis

To confirm the elemental composition of Cd, Mn and S in CdMnS thin films, EDAX is carried out. Table 2 shows EDAX data of the deposited $Cd_{1-x}Mn_xS$ ($x = 0.4$) thin films. It also confirms the presence of Cd^{2+} , Mn^{2+} and S^{2-} in the obtained film matrix.

Table 2 – EDAX data for $Cd_{1-x}Mn_xS$ ($x = 0.4$) films

Element	Atomic number	Series	Atomic percent (%)
S	16	K-series	42.22
Mn	25	K-series	17.26
Cd	48	L-series	40.52
Total			100

3.5 UV-visible Spectrophotometer

The optical absorbance data of CdMnS thin films were recorded using UV-visible spectrophotometer. The absorbance spectra were used to estimate the energy band gap (E_g) by Tauc plot method. It is found that the optical band gap has been enhanced with composition. This is shown in Fig. 6. With an increase in Mn^{2+} ions, the strain was induced by Mn^{2+} ions, and therefore the lattice structure became highly distorted tending towards amorphousness of the material that caused the band gap to be enhanced. This enhancement in the

band gap is in good agreement with previous results. The band gap values vary from 2.05 to 2.82 eV which is consistent with the values reported for thin films obtained by CBD [5, 11].

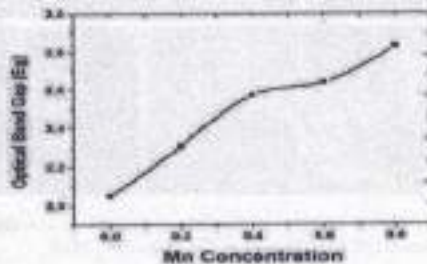


Fig. 6 – Effect of Mn concentration on band gap

The dependence of the optical band gap on the Mn^{2+} ion concentration can be attributed to Mn atoms in the CdS structure [12, 13]. The difference in the band gap values is clearly indicated by the color of the thin film, the yellow color turned to dark yellowish or orange color as Mn^{2+} ions increase.

3.6 Photoluminescence Analysis

Photoluminescence (PL) is an efficient, non-contact and non-destructive method to probe the electronic structure of different materials, which can also be used to determine the band gap, impurity levels, defects etc. Fig. 7 represents the room temperature PL spectra of $Cd_{1-x}Mn_xS$ thin films, showing two broad emission peaks at 525 and 589 nm. The emission peak at 525 nm corresponds to the green band; it is due to the donor-acceptor transition and is attributed to the radiative recombination of a hole in the valence band and of an electron in the conduction band. In addition, the unshifted peak positions indicate that the crystallite sizes are almost the same for all samples. Our XRD studies shed light on these observations. Another well-known emission peak at 589 nm (2.1 eV, red band) corresponds to the ${}^6T_1 \rightarrow A_1$ transitions of Mn^{2+} d-states in CdS nanocrystals.

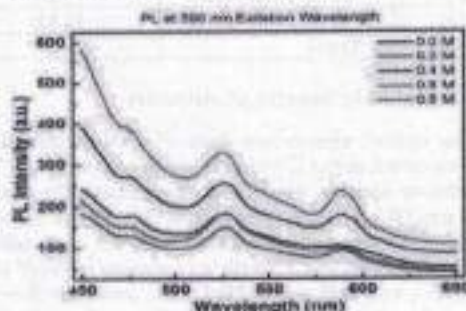


Fig. 7 – Photoluminescence spectra of CdMnS films

The vacancies created by Cd atom (surface defects) can either act as traps or as non-radiative recombination centers. Thus, PL analysis indicated that Mn^{2+} ions are distributed on the surface of the CdS lattice and fill the vacancies of Cd atoms.

3.7 Electrical Properties

The electrical resistivity of all CdMnS thin film structures was measured by two-probe method at room temperature. The electrical resistivity (ρ) of the sample has been determined using the relation

$$\rho = \frac{RA}{t} \quad (3)$$

where R is the resistance, t is the thickness, and A is the cross section area of the film. It is found that room temperature electrical resistivity has been enhanced with composition up to $x = 0.2$. For further increase in Mn^{2+} ions, room temperature electrical resistivity decreases.

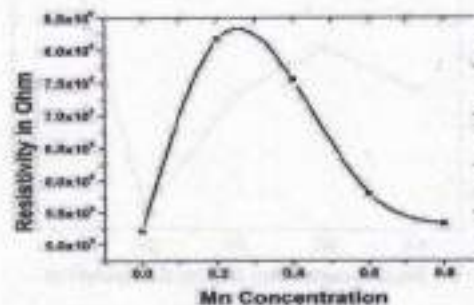


Fig. 8 – Effect of Mn concentration on resistivity of CdMnS films

This is shown in Fig. 8. The resistivity modulation by incorporation of Mn^{2+} ions into CdS lattice can be explained based on the following facts: Cd^{2+} and Mn^{2+} are co-deposited simultaneously and substitution of Cd^{2+} ions by Mn^{2+} is the predominant mechanism under this situation. The EDAX analysis of $Cd_{1-x}Mn_xS$ films also supported these observations. Also, as we add Mn^{2+} ions into CdS lattice, initially they do not react with CdS and do not form CdMnS alloy. Since the volume of Cd atom is greater than that of Mn atom, hence Mn^{2+} ions settle down at the interstitial sites of the CdS lattice. This, in turn, increases the number of scattering centers in the material, hence the resistivity. With further addition of Mn^{2+} to CdS lattice, some Mn atoms settle down at the interstitial sites of the CdS lattice, while other atoms form CdS as well as CdMnS. As a result, CdMnS dominates in the film, and hence the numbers of scattering centers reduces resulting in a decrease in resistivity. Thus, by the addition of Mn^{2+} ions into CdS films, resistivity values decrease. This property is more beneficial in designing solar cells.

4. CONCLUSIONS

The optimum condition with a bath temperature of 80 °C and pH = 1 yielded good quality thin films of $Cd_{1-x}Mn_xS$ using CBD technique. The effect of Mn^{2+} ion concentration on the optical, structural, morphological and electrical properties has been investigated by various analysis techniques. The structural characterization reveals the polycrystalline nature in mixed phases (hexagonal and cubic), and grain sizes are of the order of few nm. It is found that grain sizes are almost

the same for all $Cd_{1-x}Mn_xS$ thin films with variation in Mn^{2+} ion concentration. The optical study reveals the increase in the band gap value with Mn^{2+} incorporation. The electrical resistivity was found to be enhanced with x up to 0.2 and then decreased with further increase in Mn^{2+} ion concentration. The photoluminescence result confirms that Mn^{2+} ions induce luminescence, exhibiting two broad peaks at 525 and 589 nm. Surface morphology also confirms almost uniform grain size of the crystals. EDAX analysis of the films shows that as Mn^{2+} ion concentration changes, the films become almost stoichiometric. Overall, the obtained $Cd_{1-x}Mn_xS$ thin films demonstrate the potential for use as a promising material for technological applications.

ACKNOWLEDGEMENTS

REFERENCES

1. Woodhead Publishing Series in Electronic and Optical Materials, Semiconductor Nanowires (Ed. by J. Arbiol, Q. Xiong) (Woodhead Publishing: 2015).
2. C. Gümüç, C. Uluçay, Y. Ufuktepe, *Opt. Mater.* 29 No 9, 1183 (2007).
3. R.N. Bhargava, *J. Cryst. Growth* 86, 873 (1988).
4. L. Huang, Z.L. Wei, F.M. Zhang, X.S. Wu, *J. Alloy. Compd.* 648, 501 (2015).
5. F. Iacomi, I. Salacru, N. Apetresei, A. Vasile, C.M. Teodorescu, D. Macovei, *J. Optoelectron. Adv. M.* 8, 266 (2000).
6. H. Sekhar, G.T. Rao, P.H. Reddy, D.N. Rao, *J. Alloy. Compd.* 562, 38 (2013).
7. J. Cheng, D. Fan, H. Wang, B. Liu, Y. Zhang, H. Yan, *Semicond. Sci. Technol.* 18 No 7, 676 (2003).
8. D. Mugle, G. Jadhav, *AIP Conf. Proc.* 1728, 020097 (2016).
9. C. Lai, X. Li, C. Liu, X. Guo, Z. Xiang, B. Xie, L. Zou, *Mater. Sci. Semicond. Process* 26, 501 (2014).
10. M.P. Gonullu, S. Kose, *Metal. Mater. Trans. A* 48 No 3, 1321 (2017).
11. S.M. Al-Jawad, *Int. J. Appl. Innov. Eng. Manag.* 3, 325 (2014).
12. M. Ikeda, K. Itoh, H. Sato, *J. Phys. Soc. Jpn.* 25, 455 (1966).
13. C.T. Tsai, S.H. Chen, D.S. Chuu, W.C. Chou, *Phys. Rev. B* 54, 11555 (1996).

This work was supported by University Grants Commission (UGC, WRO), India, under minor research project scheme (File No.47-1066/14(WRO) dated 08/01/2016). Authors are thankful to the Principal, Dr. S.N. Patel, SPDM College, Shirpur for providing necessary college level facilities. Authors are also thankful to Dr. P.K. Baviskar, PostDoc Fellow, SPPU, Pune, who helped in various ways during this work.

AUTHOR CONTRIBUTIONS

Ashok E. Mali and Anil S. Gaikwad equally contributed in manuscript preparation, designing experimental setup, carrying out measurements and analysis part, Sanjay V. Borse and Rajendra R. Ahire contributed in composition of manuscript and result analysis.



Modification effect of hole injection layer on efficiency performance of wet-processed blue organic light emitting diodes

Cheng-Chieh Lo^{a,b}, Sujith Sudheendran Swayamprabha^a, Tsung-Chia Hsueh^a,
Sudam D. Chavhan^{b,1}, Rohit Ashok Kumar Yadav^a, Jia-Ren Lee^b, Kiran Kishore Kesavan^a,
Sun-Zen Chen^c, Ching-Wu Wang^d, Jwo-Huei Jou^{a,*}

^a Department of Materials Science and Engineering, National Tsing Hua University, Hsinchu, 30013, Taiwan, Republic of China

^b Department of Physics, National Kaohsiung Normal University, Kaohsiung, 82444, Taiwan, Republic of China

^c Center for Nanotechnology, Materials Science and Microsystems, National Tsing Hua University, Hsinchu, 30013, Taiwan, Republic of China

^d Graduate Institute of Opto-Mechatronics, Department of Mechanical Engineering, National Chung Cheng University, Chiayi, 62102, Taiwan

ARTICLE INFO

Keywords:

Blue OLED
Hole injection layer
Modification

ABSTRACT

We examined the performance of solution-processed organic light emitting diodes (OLEDs) by modifying the hole injection layer (HIL), poly(3,4-ethylenedioxythiophene) polystyrene sulfonate (PEDOT: PSS). Atomic force microscopy (AFM) showed morphological changes with surface roughness (R_{RMS}) of 1.47, 1.73, and 1.37 nm for pristine PEDOT: PSS, PEDOT: PSS modified with a 40 v% deionized water and with a 30 v% acetone, respectively. The surface hydrophobicity of the acetone modified PEDOT:PSS HIL layer was decreased by 34% as comparing with the water modified counterpart. Electrical conductivity was increased to two orders of magnitude for the water and acetone modified PEDOT:PSS as compared to pristine. We observed a low refractive index and high transmittance for the modified HILs. We fabricated and explored electroluminescent properties of bis[2-(4,6-difluorophenyl)pyridinato-C2,N](picolinato)iridium(III) (FIrpic) based sky blue device by utilizing HIL with and without modification. The changes in electrical conductivity, surface roughness, refractive index, and transmittance of the modified HILs strongly influenced the performance of devices. By utilizing a 30% acetone modified HIL, the power efficiency was increased from 14.2 to 24.2 lm/W, an increment of 70% and the EQE from 8.5 to 13.1% at 100 cd/m², an increment of 54%. The maximum luminance also increased from 11,780 to 18,190 cd/m². The findings revealed herein would be helpful in designing and fabricating high efficiency solution processed OLEDs.

1. Introduction

OLEDs are extensively used both in displays technology and making entry into healthy indoor lighting applications [1] [–] [4]. Examples include smartphone displays, television screens, computer monitors, MP3 players, and GPS devices, etc. [5,6]. OLEDs are not only superior in terms of physical properties but also allow to fabricate devices via solution process that is advantageous over existing technologies and might reduce the production cost [7]. The solution process technology has a degree of freedom over the physical deposition techniques, that permits to fabricate OLED devices via a roll to roll process, inkjet printing, and slot die coating methods, incredibly enhancing the scale-up feasibility of

OLED devices on a large area and profoundly reducing the product cost [6]. Moreover, these techniques are more compatible with the flexible substrates, which are tempting to develop attractive electronic gadgets [8,9]. Fabricating high-efficiency OLED devices via solution process techniques is hence vitally important.

In general, a typical solution processed OLED device structure is made up of hole injection and transport layers (HIL/HTL), emissive layer (EML) and electron transport layer (ETL) excluding anode and cathode electrodes [10,11]. To fabricate highly efficient OLED devices, one has a wide variety of choices to select the EML and ETL materials according to requirements. However, very few choices are left in selecting appropriate molecule HTLs because of their high solubility in commonly used

* Corresponding author.

E-mail address: jjou@mx.nthu.edu.tw (J.-H. Jou).

¹ Present address: Department of Physics, V.V.M.'s S.G. Patil ACS College Sakri, Dist. Dhule, 424304, Affiliated to K.B.C. North Maharashtra University, Jalgaon, India.

solvents making them more difficult to deposit the layers one over another [12]. To date, PEDOT: PSS is the widely used HIL in solution processed OLED devices due to its compatibility with the organic solvent along with excellent electronic properties [13] [–] [15]. An alternative to PEDOT:PSS is p-type metal oxide semiconductor materials, but many of these materials require high processing temperature and hence unfit to fabricate flexible OLED devices [12]. Moreover, most of metal oxide semiconductors possess low hole-mobility as compared to PEDOT:PSS and forbid to deposit a HTL layer more than few nanometers. On the other hand, PEDOT:PSS is available in aqueous form and readily used to deposit at room temperature and having superior electronic properties and more importantly, its chemical composition can be easily tailored according to the requirement of application [13]. Therefore, PEDOT:PSS is emerged as one of the most suitable material to fabricate highly efficient solution processed OLED devices [16,17]. PEDOT: PSS is an intricate material, from chemical, morphological and electronic point of view. Favorable alteration of these properties can influence the optoelectronic device performances [18] [–] [20].

There are many studies discussing the physical properties changes of PEDOT: PSS with the addition of co-solvents [21] [–] [25]. De Kok et al. reported that with increasing the pH of PEDOT: PSS, the device lifetime diminished [26]. According to Snaith et al. addition of glycerol to PEDOT: PSS solution prior to spin coating reduced the sheet resistivity of thin film [27]. Syed et al. employed sodium citrate modified PEDOT: PSS as a hole transporting layer for the efficiency enhancement of solar cell [28]. Zhang et al. investigated the change in thermoelectric properties with the addition of both organic solvents and water as co-solvent in PEDOT: PSS [29]. Pathak et al. examined the conductivity increment with the addition of graphene oxide and solvents, and found the solvent addition to wash away insulating PSS from the substrate surface after spin coating and annealing [30].

Some studies revealed the performance of the solution processed devices, in which the HIL is metal oxide blended or bilayer with PEDOT: PSS. Zhang et al. reported an efficient ultraviolet (UV) OLED with PEDOT:PSS/MO_x, the device showed an external quantum efficiency (EQE) of 4.6% [31]. Zheng et al. reported a UV OLED with an EQE of 4.4% by utilizing PEDOT:PSS blended with MoO_x as the HIL [32]. Lian et al. utilized blend of magnetic nano particles PEDOT:PSS to fabricate efficient OLEDs [33]. Yadav et al. reported a blend of V₂O₅-PEDOT:PSS HIL for high efficiency OLEDs [34].

“Hole carrier mobility is one of the key parameters to achieve an efficient blue OLED device. Apart from the hole mobility of hole injection/transport material, triplet energy, work function, molecular orbital energy levels, charge injection/migration barrier, recombination, and exciton generation process across the successive layers significantly contributing to the overall device performance [35] [–] [37]. In 2015, Kim et al. proposed high hole mobility and compatible molecular orbital level (5.1 eV) that been important for excellent hole injection layer (HIL) in the OLED applications [38]. Lee and coworkers demonstrated an improved hole injection for blue phosphorescent OLEDs using solution deposited SnO_x NPs decorated ITO anodes with enhanced work function and hole injection capability [39]. Liu et al. demonstrated improved deep-blue PLED efficiencies with the optimization of both the optical and electrical performance through an optimal top-to-bottom HOMO energy level arrangement and improved hole mobility [40]. Furthermore, the studied device shows improved device performance because high hole mobility causes accumulation of holes near the EML/ETL interface, resulting in triplet-polaron or triplet-triplet annihilation leads to enhanced blue efficiency [41–43].

In the present study, we tuned the electrical conductivity, surface roughness, refractive index, transmittance, and film-forming property of PEDOT: PSS by the addition of deionized water and acetone. The modified PEDOT: PSS was employed as HIL in phosphorescent sky blue OLED device structure to study its effect on electroluminescence properties. The reason for selecting FIrpic as emissive material is because of the sky blue emission. The demand for efficient and long lifetime blue

Table 1
Resistivity and Conductivity measurement of pristine and modified PEDOT: PSS.

HIL	Resistivity ($\Omega \cdot \text{cm}$)	Conductivity (S/cm)
Pristine	1.13×10^{-2}	8.84×10^1
40 v% DI water	2.47×10^{-4}	4.05×10^3
30 v% ACE	2.58×10^{-4}	1.13×10^3

OLEDs are always increasing. All the devices that consist of the modified HIL showed better performance compared to the pristine counterpart. The best EL properties were observed in a device with a 30% acetone in HIL. The power efficiency was increased from 14.2 to 24.2 lm/W, an increment of 70% and the EQE from 8.5 to 13.1% at 100 cd/m², an increment of 54%. The maximum luminance also increased from 11,780 to 18,190 cd/m².

2. Experimental

PEDOT: PSS aqueous solution [CLEVIOS P VP AI4083] was purchased from Heraeus. The modification of PEDOT:PSS was done by adding optimized amount of deionized water (DI water, 40 v%) and acetone (ACE, 30 v%) [ECHO Chemical Co., Ltd.]. Electrical conductivity of modified PEDOT:PSS solution was investigated by EUTECH PC300 CyberScan Portable pH/Conductivity/TDS Meter. Surface morphology analysis of modified and pristine HILs was characterized by using atomic force microscopy (AFM, Bruker) under tapping mode. The water contact angles of thin films were measured by First-Ten-Angstroms FTA-100 series (Chi 608) instrument using deionized water droplets of about 6 μL . Ellipsometer was used to determine the refractive index (n) [Radiation Technology Co., Ltd.] of pristine and modified PEDOT:PSS layer.

The OLED device fabrication process was started with spin coating of pristine and modified PEDOT: PSS at 4000 rpm for 20 s on a pre-cleaned indium tin oxide (ITO) anode. The emissive layer solution was prepared by dissolving the host Tris(4-carbazoyl-9-ylphenyl)amine (TCTA) and guest (FIrpic 20%) molecules in toluene solvent at 50 °C for 90 min with stirring using a magnetic stirrer. The prepared solution was spin coated at 2500 rpm for 20 s inside a nitrogen-filled glove box. The electron transporting layer (2,2',2''-(1,3,5-Benzinetriyl)-tris(1-phenyl-1-*H*-benzimidazole), (TPBi) bought from, Shine Materials Technology Co., Ltd), electron injection layer of lithium fluoride (LiF, Shine Materials Technology Co., Ltd) and aluminum as a cathode electrode (Guv Team International Co., Ltd.), were deposited via thermal evaporation under less than 10^{-6} Torr.

OLED characteristics of all the fabricated devices were investigated in ambient atmosphere without encapsulation. Luminance, CIE chromatic coordinates and electroluminescence spectrum of the resulting sky-blue OLEDs were measured using Photo Research PR-655 spectra scan. Keithley 2400 electrometer with minol was used to measure the current-voltage (I - V) characteristics. The emission area of the devices was kept to 9 mm², and the luminance in the forward direction was measured.

3. Results and discussion

3.1. Characterizations of pristine and modified PEDOT: PSS

The electronic properties of pristine and modified PEDOT: PSS were examined via a resistivity and conductivity measurement. Electrical conductivity and resistivity of the modified and pristine PEDOT: PSS tabulated in Table 1. The measured electrical conductivities were found to be 8.84×10^1 , 4.05×10^3 , and 1.13×10^3 S cm⁻¹ for pristine, modified with 40 v% DI water and 30 v % PEDOT: PSS HIL., respectively. The electrical conductivity of PEDOT: PSS increased with the addition of water and acetone. The electrical conductivity of PEDOT:PSS is increasing with the addition of polar cosolvents. Lee and Na et al.

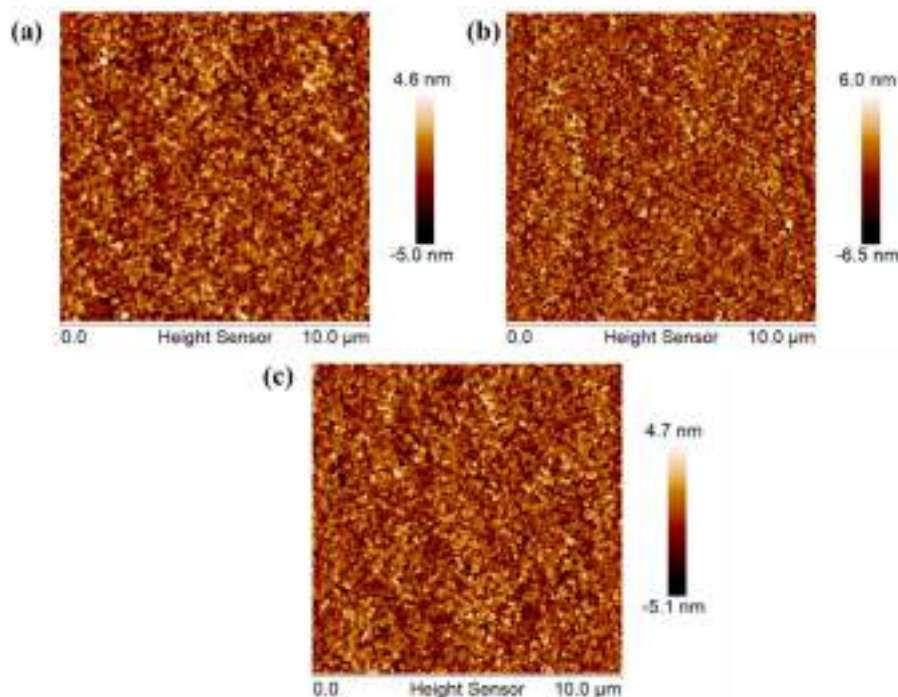


Fig. 1. Surface morphologies of the layer of PEDOT: PSS (a) without modification (b) modified by adding 40 v% DI water and (c) modified by adding 30 v% ACE.

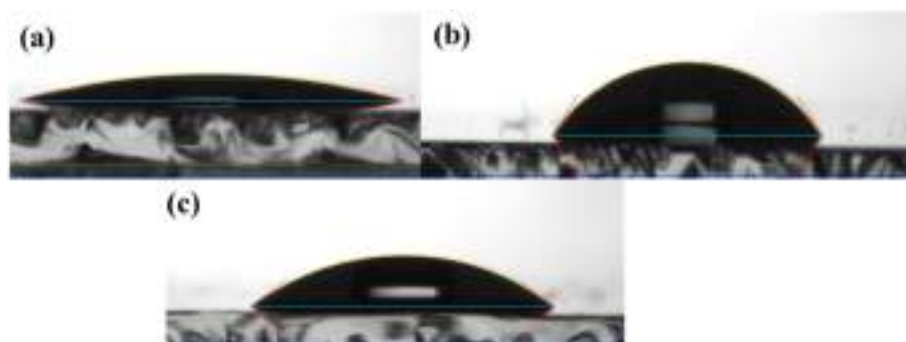


Fig. 2. Static contact angles of water drop on thin films (a) Pristine PEDOT: PSS, (b) PEDOT: PSS modified with DI water, and (c) PEDOT: PSS modified with acetone.

fabricated a highly conductive PEDOT:PSS thin film by adding DMSO as a cosolvent in their independent research works [44,45]. Palumbiny et al. improved the electrical conductivity of PEDOT:PSS by the addition of ethylene glycol cosolvent [46]. Solvation plays a crucial role in the conductivity increment. Acetone solvates PEDOT and water solvates PSS chain selectively, which results in synergetic effect and subsequently reduces the Coulombic repulsions and increases the conductivity [47].

The surface morphologies of thin films; pristine modified with 40 v% deionized water and with 30 v% acetone PEDOT:PSS HIL are shown in Fig. 1. The film showed surface roughness of (R_{RMS}) 1.47, 1.73, and 1.37 nm for pristine, modified with 40 v% DI water and with 30 v% acetone PEDOT: PSS layer, respectively. The film surface morphologies are not showing any drastic change after modification.

We examined the water contact angles in order to measure the hydrophilic property and spread-ability of pristine and modified PEDOT: PSS on ITO. Fig. 2 shows the static contact angles of water drop on the thin films of both pristine and modified PEDOT: PSS thin films. The contact angle measurement showed 15°, 58°, and 38°, respectively, for pristine PEDOT: PSS, PEDOT: PSS modified with 40 v% DI water and 30 v% acetone. This means, the DI water modified PEDOT: PSS (Fig. 2(b)) is more hydrophobic compared to pristine and acetone modified PEDOT: PSS. The spreading ability of pristine and 30 v% acetone modified

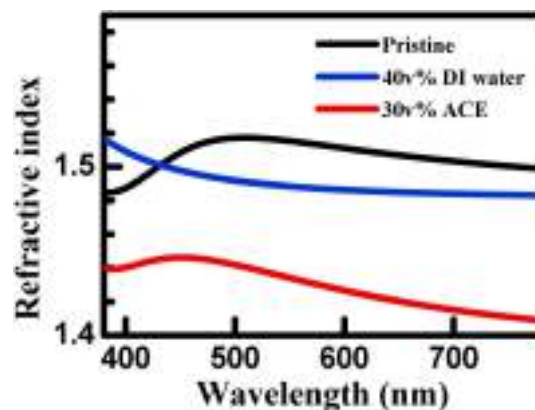


Fig. 3. Refractive indices of pristine and modified PEDOT: PSS thin films.

PEDOT: PSS is higher compared to DI water modified PEDOT: PSS, low water contact angle indicates the hydrophilic property of HIL that enhances the film forming property.

Fig. 3 shows the refractive indices of the pristine, modified with 40 v

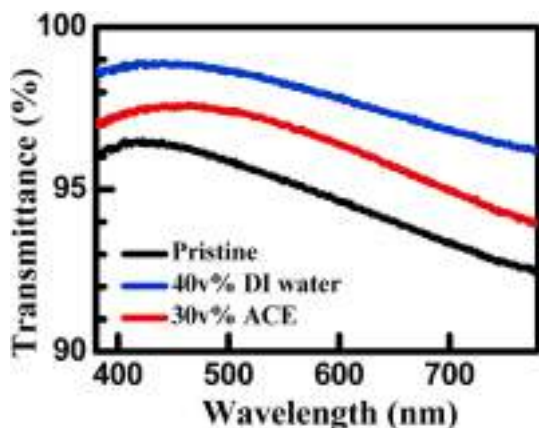


Fig. 4. Transmittance of thin films with and without modification of PEDOT: PSS.

% of DI water, and 30 v % of acetone PEDOT:PSS HIL. High refractive indices of pristine PEDOT:PSS are noticed in the visible region. Refractive indices of 30 v% acetone added PEDOT:PSS decrease drastically as compared to DI water modified PEDOT:PSS.

Fig. 4 shows transmittance spectra recorded in the visible region for pristine and modified PEDOT:PSS thin films. It is very clear from the experimental data that 40 v% DI water and 30 v% acetone modified PEDOT: PSS evince higher transmittance compared to pristine PEDOT: PSS over the visible wavelengths region. At lower wavelengths between 400 and 450 nm, the transmittance is higher. The thin films showed 96, 98.5 and 97% transmittance respectively for pristine PEDOT: PSS, 40 v% DI water modified PEDOT: PSS, and 30 v% acetone modified PEDOT: PSS. The transmittance increased with decrease in film thickness. The

thickness was 35, 25, and 29 nm respectively for pristine PEDOT:PSS, DI water modified PEDOT:PSS and acetone modified PEDOT:PSS.

3.2. Electroluminescent properties

To investigate the influence of physical and optical properties of modified PEDOT:PSS, blue OLED devices were fabricated. Fig. 5 show a schematic representation of a modification of PEDOT: PSS and energy level diagrams of blue OLEDs devices. D1 was fabricated with pristine PEDOT: PSS HIL and other two devices by utilizing modified PEDOT: PSS i.e. D2 was fabricated by employing PEDOT: PSS modified with 40 v % of DI water and D3 was fabricated with PEDOT: PSS modified with 30 v% of acetone., The pristine and modified HIL layers were deposited via spin coating on ITO substrate. Effect of modification of the HIL layer on electroluminescence parameters of fabricated blue OLED devices is summarized in Table 2. Performance of OLED devices with different ratios of water and acetone modified PEDOT:PSS as HIL showed in Table S2.

Addition of solvents strongly influenced the device performance. Optimum addition of DI water (40% DI water, D2) showed better performance compared to the reference device, D1. The device showed PE increment of 40% from 14.2 to 19.9 lm/W, external quantum efficiency (EQE) showed an increment of 24%, from 8.5 to 10.6% at 100 cd/m², compared to the reference device, D1. D2 showed a low operating voltage of 4.2 V compared to D1, 4.4 V. Among all devices, PEDOT: PSS modified with 30% acetone (D3) showed the best performance both at low luminance and higher luminance, compared to all other devices fabricated. In D3 the power efficiency increased from 14.2 to 24.2 lm/W, an increment of 70%, EQE showed an increment of 54%, from 8.5 to 13.1% at 100 cd/m², comparing to the device without HIL modification. The maximum luminance also showed an increment from 11,780 to 18,190 cd/m².

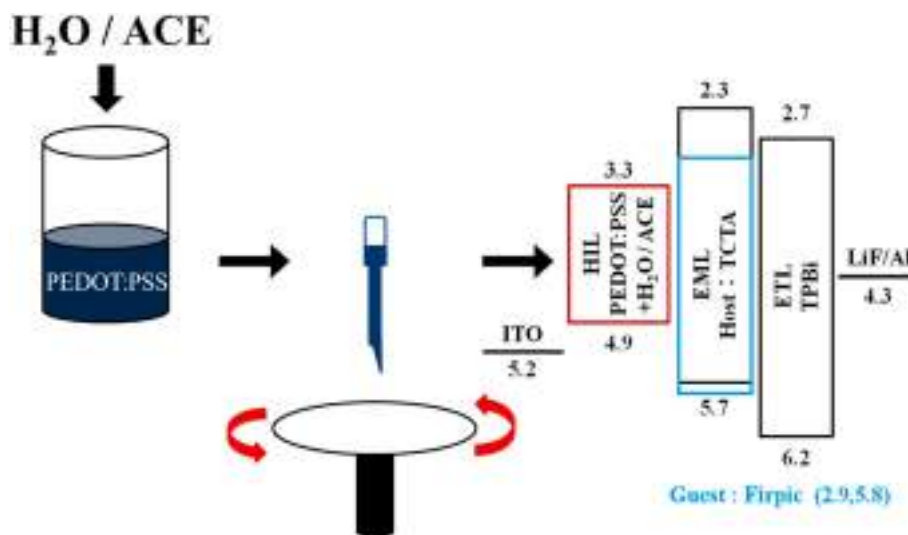


Fig. 5. Schematic diagram of the energy-levels of a sky-blue OLED containing PEDOT: PSS as hole injection material, whose solution is modified by adding either deionized water or acetone. (For interpretation of the references to colour in this figure legend, the reader is referred to the Web version of this article.)

Table 2

Effect of modified hole injection layer on the operation voltage(OV), power efficiency(PE), current efficiency(CE), external quantum efficiency (EQE), CIE coordinates, and maximum luminance of the studied sky-blue OLEDs.

Device	DI H ₂ O [ratio%]	ACE [ratio%]	OV [V] @100/1000/10000 cd/m ²	PE [lm/W]	CE [cd/A]	EQE [%]	CIE coordinates [cd/m ²]	Max Luminance
D1	-	-	4.4/4.9/7.3	14.2/12.8/3.1	20.0/20.0/7.1	8.5/8.6/-	(0.18, 0.40)/(0.18, 0.40)/-	11780
D2	40	-	4.2/4.8/7.0	19.9/14.0/3.7	26.4/21.2/8.3	10.6/8.5/-	(0.18, 0.42)/(0.18, 0.41)/-	12760
D3	-	30	3.9/4.6/6.3	24.2/18.2/6.3	30.5/26.5/12.6	13.1/11.6/5.5	(0.17, 0.39)/(0.17, 0.39)/(0.17, 0.38)	18190

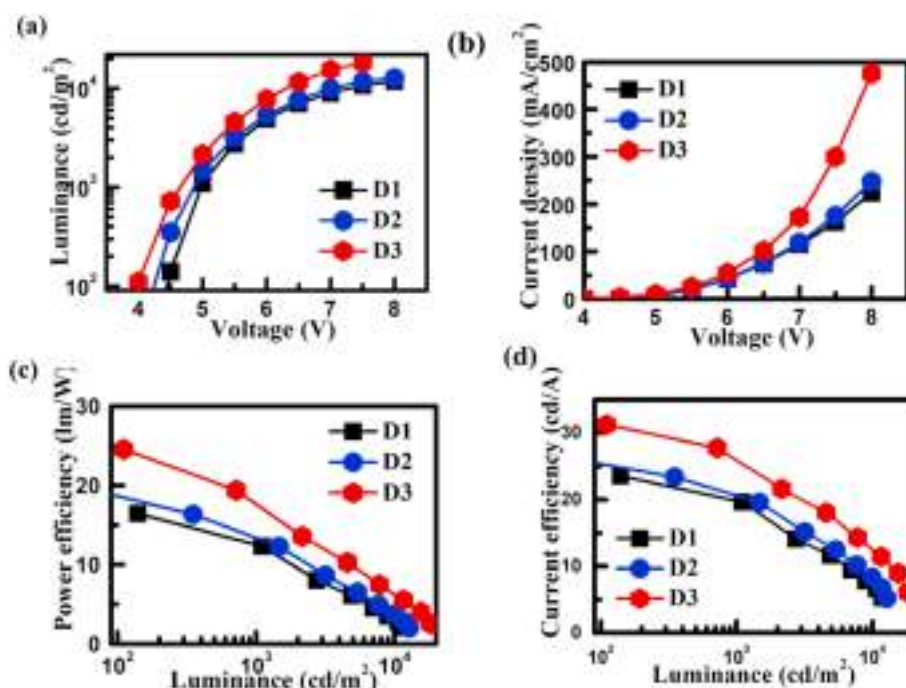


Fig. 6. Electroluminescent characteristics of solution processed OLED devices with pristine or modified HIL (a) current density vs voltage, (b) luminance vs voltage, (c) power efficiency vs luminance, and (d) current efficiency vs luminance.

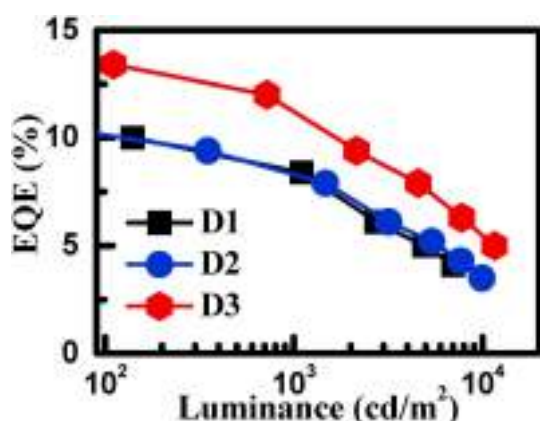


Fig. 7. EQE of solution processed OLEDs with pristine or modified HIL.

Fig. 6 showing the electroluminescent characteristics of solution processed sky blue OLEDs with pristine or modified HIL. From Fig. 6(a), it is clear that, D2 and D3 showed a low turn on voltage compared to D1. The turn on voltage may be influenced by change in conductivity with modification. Current density also following the same trend (Fig. 6(b)). The efficiency roll-off of all the three devices is showed in Fig. 6(c) and (d). Fig. 7 showing the EQE increment with the modification in HIL.

Fig. 8 showing the EL spectra of devices D1, D2 and D3. In the case of deionized water modified HIL, the device showing a slight bathochromic shift compared to the reference device, D1. In the case of acetone modified HIL, the device showing similar emission like reference device D1.

The better performance of device with acetone modified HIL may attributed to different factors. The increment in conductivity of modified HIL influenced the device performance. Hole mobility also improved with the addition of acetone, which may facilitate the exciton formation and thereby improvement in device performance. Compared with the surface roughness of DI water modified HIL, acetone modified HIL showed a less surface roughness. The low surface roughness can reduce

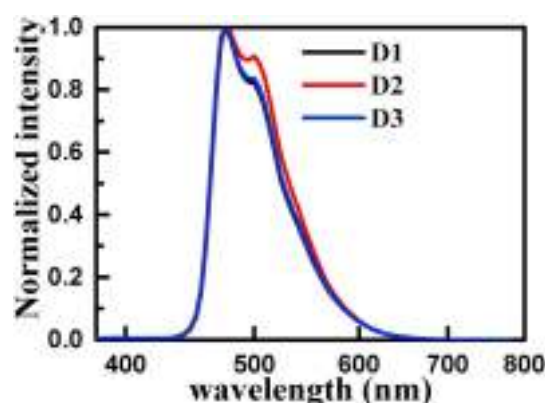


Fig. 8. Modification effect of hole injection layer on the EL spectra at 100 cd/m². EL spectra of the studied sky-blue OLEDs with PEDOT:PSS (HIL) with and without modification. (For interpretation of the references to colour in this figure legend, the reader is referred to the Web version of this article.)

Table 3
Outcoupling efficiency enhancement of acetone modified PEDOT:PSS device performance for various luminescence (100/1000/10000 cd/m²) compared with pristine PEDOT:PSS.

@100/1000/10000 cd/m ²			
Outcoupling Enhancement (%)			
PE [lm/W]	CE [cd/A]	EQE [%]	Max Luminance [cd/m ²]
70.4/42.1/103.2	52.5/32.5/77.4	54.1/34.8/-	54.4

the dielectric breakdown of thin films [48]. Low refractive index of acetone modified HIL is one of the key factor, which improved the device performance [49]. Outcoupling efficiency enhancement of acetone modified PEDOT:PSS device performance for various luminescence (100/1000/10000 cd/m²) compared with pristine PEDOT:PSS shown in Table 3.

Numerous studies have been reported that a film possessing a lower refractive index, a hole-transport layer with reduced optical density but slightly reduced hole-transport characteristics. The device based on reduced-index layer show an improved efficiency compared to reference devices (PEDOT:PSS). It strongly discovers that efficiency improvement is only to some extent due to enhanced outcoupling resulting directly from the reduced refractive index but primarily due to a change of the width of the emission zone [18,49–51].

The transmittance increment of modified HIL, compared to pristine PEDOT: PSS also influenced the device performance. The less water of acetone modified PEDOT:PSS compared to DI water modification also plays a role in the efficiency improvement. The increment in electrical conductivity may played a vital role in the improvement of device performance. Kim et al. utilized a high conductive ZnO/CNT HTL for the performance of OLEDs [52]. Gu et al. also improved the conductivity of PEDOT:PSS by associating it with CNT and ethylene glycol and the device showed a better performance [53].

4. Conclusion

Modified PEDOT:PSS utilized for the fabrication of sky blue OLEDs. PEDOT: PSS modified with 40 v% deionized water and with 30 v% acetone, respectively showed better performance. We fabricated and explored electroluminescent properties of Bis[2-(4,6-difluorophenyl)pyridinato-C₂,N](picolinato)iridium(III) (FIrpic) based sky blue device by utilizing HIL with and without modification. The changes in electrical conductivity, surface roughness, refractive index and transmittance of modified HIL strongly influenced the performance of devices. By utilizing a 30% acetone modified HIL, the power efficiency was increased from 14.2 to 24.2 lm/W, an increment of 70% and the EQE from 8.5 to 13.1% at 100 cd/m², an increment of 54%. The maximum luminance also increased from 11,780 to 18,190 cd/m².

Declaration of competing interest

The authors declare that they have no known competing financial interests or personal relationships that could have appeared to influence the work reported in this paper.

Acknowledgements

This research was funded by grant 106-2119-M-007-011- from Ministry of Science and Technology of Taiwan.

Appendix A. Supplementary data

Supplementary data to this article can be found online at <https://doi.org/10.1016/j.orgel.2021.106084>.

References

- J.-H. Jou, M. Singh, Y.-T. Su, S.-H. Liu, Z.-K. He, Blue-hazard-free candlelight OLED, *JoVE (Journal Vis. Exp.)* (2017), e54644.
- J.-H. Jou, Y.-T. Su, S.-H. Liu, Z.-K. He, S. Sahoo, H.-H. Yu, S.-Z. Chen, C.-W. Wang, J.-R. Lee, Wet-process feasible candlelight OLED, *J. Mater. Chem. C* 4 (2016) 6070–6077.
- S.-M. Lee, J.H. Kwon, S. Kwon, K.C. Choi, A review of flexible OLEDs toward highly durable unusual displays, *IEEE Trans. Electron. Dev.* 64 (2017) 1922–1931.
- N.T. Kalyani, S.J. Dhoble, Organic light emitting diodes: energy saving lighting technology—a review, *Renew. Sustain. Energy Rev.* 16 (2012) 2696–2723.
- J.H. Jou, S. Kumar, A. Agrawal, T.H. Li, S. Sahoo, Approaches for fabricating high efficiency organic light emitting diodes, *J. Mater. Chem. C* (2015), <https://doi.org/10.1039/c4tc02495h>.
- J.H. Jou, S. Sahoo, D.K. Dubey, R.A.K. Yadav, S.S. Swayamprabha, S.D. Chavhan, Molecule-based monochromatic and polychromatic OLEDs with wet-process feasibility, *J. Mater. Chem. C* (2018), <https://doi.org/10.1039/c8tc04203a>.
- M. O'Regan, 40.3: solution processed OLED displays: advances in performance, resolution, lifetime and appearance, in: *SID Symp. Dig. Tech. Pap.*, 2009, pp. 600–602.
- E.G. Jeong, J.H. Kwon, K.S. Kang, S.Y. Jeong, K.C. Choi, A review of highly reliable flexible encapsulation technologies towards rollable and foldable OLEDs, *J. Infect. Dis.* 21 (2020) 19–32.
- F.-S. Yi, Y.-G. Bi, X.-L. Zhang, D. Yin, Y.-F. Liu, J. Feng, H.-B. Sun, Highly flexible and mechanically robust ultrathin Au grid as electrodes for flexible organic light-emitting devices, *IEEE Trans. Nanotechnol.* 18 (2019) 776–780.
- D.K. Dubey, G. Krucaite, S.S. Swayamprabha, R.A.K. Yadav, D. Blazelevicius, J. Tagare, S. Chavhan, T.C. Hsueh, S. Vaidyanathan, S. Grigalevicius, J.H. Jou, Fluorene based amorphous hole transporting materials for solution processed organic light-emitting diodes, *Org. Electron.* 79 (2020) 105633, <https://doi.org/10.1016/j.orgel.2020.105633>.
- D.K. Dubey, S.S. Swayamprabha, R.A.K. Yadav, D. Tavgeniene, D. Volyniuk, S. Grigalevicius, J.-H. Jou, A thermally cross-linkable hole-transporting small-molecule for efficient solution-processed organic light emitting diodes, *Org. Electron.* 73 (2019) 94–101.
- S. Ho, S. Liu, Y. Chen, F. So, Review of recent progress in multilayer solution-processed organic light-emitting diodes, *J. Photon. Energy* 5 (2015) 57611.
- D.J. Lipomi, J.A. Lee, M. Vosgueritchian, B.C.-K. Tee, J.A. Bolander, Z. Bao, Electronic properties of transparent conductive films of PEDOT: PSS on stretchable substrates, *Chem. Mater.* 24 (2012) 373–382.
- A. Benor, S. Takizawa, C. Pérez-Bolivar, P. Anzenbacher Jr., Efficiency improvement of fluorescent OLEDs by tuning the working-function of PEDOT: PSS using UV-ozone exposure, *Org. Electron.* 11 (2010) 938–945.
- M. Petrosino, P. Vacca, R. Miscioscia, G. Nenna, C. Minarini, A. Rubino, Effect of PEDOT: PSS ratio on the electrical and optical properties of OLEDs, *Photonic Mater. Dev. Appl. II* (2007) 659310.
- J. Tagare, S.S. Swayamprabha, D.K. Dubey, R.A.K. Yadav, J.H. Jou, S. Vaidyanathan, Highly twisted tetra-N-phenylbenzidine-phenanthroimidazole based derivatives for blue organic light emitting diodes: experimental and theoretical investigation, *Org. Electron. Phys. Mater. Appl.* (2018), <https://doi.org/10.1016/j.orgel.2018.08.022>.
- R. Komatsu, H. Sasabe, S. Inomata, Y.J. Pu, J. Kido, High efficiency solution processed OLEDs using a thermally activated delayed fluorescence emitter, *Synth. Met.* (2015), <https://doi.org/10.1016/j.synthmet.2015.02.009>.
- G.-F. Wang, X.-M. Tao, R.-X. Wang, Fabrication and characterization of OLEDs using PEDOT: PSS and MWCNT nanocomposites, *Compos. Sci. Technol.* 68 (2008) 2837–2841.
- A.K. Havare, M. Can, S. Demic, M. Kus, S. Icli, The performance of OLEDs based on sorbitol doped PEDOT: PSS, *Synth. Met.* 161 (2012) 2734–2738.
- M.A. Lopez, J.C. Sanchez, M. Estrada, Characterization of PEDOT: PSS dilutions for inkjet printing applied to OLED fabrication, in: *2008 7th Int. Caribb. Conf. Devices, Circuits Syst.*, 2008, pp. 1–4.
- J. Ouyang, Q. Xu, C.-W. Chu, Y. Yang, G. Li, J. Shinar, On the mechanism of conductivity enhancement in poly (3, 4-ethylenedioxythiophene): poly (styrene sulfonate) film through solvent treatment, *Polymer (Guildf)* 45 (2004) 8443–8450.
- C. Song, Z. Zhong, Z. Hu, Y. Luo, L. Wang, J. Wang, Y. Cao, The effect of solvent treatment on the buried PEDOT: PSS layer, *Org. Electron.* 43 (2017) 9–14.
- I. Lee, G.W. Kim, M. Yang, T.-S. Kim, Simultaneously enhancing the cohesion and electrical conductivity of PEDOT: PSS conductive polymer films using DMSO additives, *ACS Appl. Mater. Interfaces.* 8 (2016) 302–310.
- H. Shi, C. Liu, Q. Jiang, J. Xu, Effective approaches to improve the electrical conductivity of PEDOT: PSS: a review, *Adv. Electron. Mater.* 1 (2015) 1500017.
- P. Wilson, C. Lekakou, J.F. Watts, A comparative assessment of surface microstructure and electrical conductivity dependence on co-solvent addition in spin coated and inkjet printed poly (3, 4-ethylenedioxythiophene): polystyrene sulfonate (PEDOT: PSS), *Org. Electron.* 13 (2012) 409–418.
- M.M. De Kok, M. Buechel, S.I.E. Vulto, P. de Weijer, E.A. Meulenlamp, S. De Winter, A.J.G. Mank, H.J.M. Vorstenbosch, C.H.L. Weijtens, V. Van Elsbergen, Modification of PEDOT: PSS as hole injection layer in polymer LEDs, *Phys. Status Solidi.* 201 (2004) 1342–1359.
- H.J. Snaith, H. Kenrick, M. Chiesa, R.H. Friend, Morphological and electronic consequences of modifications to the polymer anode PEDOT: PSS, *Polymer (Guildf)* 46 (2005) 2573–2578.
- A.A. Syed, C.Y. Poon, H.W. Li, F. Zhu, A sodium citrate-modified-PEDOT: PSS hole transporting layer for performance enhancement in inverted planar perovskite solar cells, *J. Mater. Chem. C* 7 (2019) 5260–5266.
- S. Zhang, Z. Fan, X. Wang, Z. Zhang, J. Ouyang, Enhancement of the thermoelectric properties of PEDOT: PSS via one-step treatment with cosolvents or their solutions of organic salts, *J. Mater. Chem. A* 6 (2018) 7080–7087.
- C.S. Pathak, S.S. Gill, P.K. Pathak, R. Singh, Modification in electrical and morphological properties of PEDOT: PSS films with solvents and graphene oxide, *AIP Conf. Proc.* (2018) 30040.
- X. Zhang, F. You, S. Liu, B. Mo, Z. Zhang, J. Xiong, P. Cai, X. Xue, J. Zhang, B. Wei, Exceeding 4% external quantum efficiency in ultraviolet organic light-emitting diode using PEDOT: PSS/MoO_x double-stacked hole injection layer, *Appl. Phys. Lett.* 110 (2017) 43301.
- Q. Zheng, F. You, J. Xu, J. Xiong, X. Xue, P. Cai, X. Zhang, H. Wang, B. Wei, L. Wang, Solution-processed aqueous composite hole injection layer of PEDOT: PSS + MoO_x for efficient ultraviolet organic light-emitting diode, *Org. Electron.* 46 (2017) 7–13.
- H. Lian, Z. Tang, H. Guo, Z. Zhong, J. Wu, Q. Dong, F. Zhu, B. Wei, W.-Y. Wong, Magnetic nanoparticles/PEDOT: PSS composite hole-injection layer for efficient organic light-emitting diodes, *J. Mater. Chem. C* 6 (2018) 4903–4911.
- R.A.K. Yadav, M.R. Nagar, D.K. Dubey, S.S. Swayamprabha, J.-H. Jou, Highly-efficient solution-processed organic light emitting diodes with blend V₂O₅/PEDOT: PSS hole-injection/hole-transport layer, *MRS Adv.* 4 (2019) 1779–1786.

- [35] N. Liu, S. Mei, D. Sun, W. Shi, J. Feng, Y. Zhou, F. Mei, J. Xu, Y. Jiang, X. Cao, Effects of charge transport materials on blue fluorescent organic light-emitting diodes with a host-dopant system, *Micromachines* 10 (2019) 344.
- [36] Z. Wenjin, B. Ran, Z. Hongmei, H. Wei, The effect of the hole injection layer on the performance of single layer organic light-emitting diodes, *J. Appl. Phys.* 116 (2014) 224502.
- [37] S.-W. Wen, M.-T. Lee, C.H. Chen, Recent development of blue fluorescent OLED materials and devices, *J. Disp. Technol.* 1 (2005) 90–99.
- [38] G.W. Kim, R. Lampande, D.C. Choe, H.W. Bae, J.H. Kwon, Efficient hole injection material for low operating voltage blue fluorescent organic light emitting diodes, *Thin Solid Films* 589 (2015) 105–110.
- [39] S. Il Lee, G.J. Yun, J.W. Kim, G. Hanta, K. Liang, L. Kojvic, L.S. Hui, A. Turak, W. Y. Kim, Improved hole injection for blue phosphorescent organic light-emitting diodes using solution deposited tin oxide nano-particles decorated ITO anodes, *Sci. Rep.* 9 (2019) 1–9.
- [40] Z. Liu, L. Xia, Y. Zhang, Y. Lin, W. Zheng, J. Yang, Y. Li, Y. Li, Y. Mo, L. Hou, Improved performance of deep-blue polymer light-emitting diodes by one-step coating self-assembly hole injection/transport nanocomposites with both the optical and electrical optimization, *Org. Electron.* 45 (2017) 285–292.
- [41] H. Lee, J. Kwak, C.-M. Kang, Y.-Y. Lyu, K. Char, C. Lee, Trap-level-engineered common red layer for fabricating red, green, and blue subpixels of full-color organic light-emitting diode displays, *Optic Express* 23 (2015) 11424–11435.
- [42] T. Kim, K.H. Lee, J.Y. Lee, Superb lifetime of blue organic light-emitting diodes through engineering interface carrier blocking layers and adjusting electron leakage and an unusual efficiency variation at low electric field, *J. Mater. Chem. C.* 6 (2018) 8472–8478.
- [43] T.-Y. Cheng, J.-H. Lee, C.-H. Chen, P.-H. Chen, P.-S. Wang, C.-E. Lin, B.-Y. Lin, Y.-H. Lan, Y.-H. Hsieh, J.-J. Huang, others, Carrier transport and recombination mechanism in blue phosphorescent organic light-emitting diode with hosts consisting of cabazole-and triazole-moiety, *Sci. Rep.* 9 (2019) 1–12.
- [44] S.-I. Na, G. Wang, S.-S. Kim, T.-W. Kim, S.-H. Oh, B.-K. Yu, T. Lee, D.-Y. Kim, Evolution of nanomorphology and anisotropic conductivity in solvent-modified PEDOT: PSS films for polymeric anodes of polymer solar cells, *J. Mater. Chem.* 19 (2009) 9045–9053.
- [45] S.H. Lee, J.S. Sohn, S.B. Kulkarni, U.M. Patil, S.C. Jun, J.H. Kim, Modified physico-chemical properties and supercapacitive performance via DMSO inducement to PEDOT: PSS active layer, *Org. Electron.* 15 (2014) 3423–3430.
- [46] C.M. Palumbiny, C. Heller, C.J. Schaffer, V. Köstgens, G. Santoro, S.V. Roth, P. Müller-Buschbaum, Molecular reorientation and structural changes in cosolvent-treated highly conductive PEDOT: PSS electrodes for flexible indium tin oxide-free organic electronics, *J. Phys. Chem. C.* 118 (2014) 13598–13606.
- [47] S.-P. Rwei, Y.-H. Lee, J.-W. Shiu, R. Sasikumar, U.-T. Shyr, Characterization of solvent-treated PEDOT: PSS thin films with enhanced conductivities, *Polymers (Basel)* 11 (2019) 134.
- [48] S. Sudheendran Swayamprabha, D. Kumar Dubey, W.-C. Song, Y.-T. Lin, R. Ashok Kumar Yadav, M. Singh, J.-H. Jou, An approach for measuring the dielectric strength of OLED materials, *Materials (Basel)* 11 (2018) 979.
- [49] A. Köhnen, M.C. Gather, N. Riegel, P. Zacharias, K. Meerholz, Enhanced efficiency of multilayer organic light-emitting diodes with a low-refractive index hole-transport layer: an effect of improved outcoupling? *Appl. Phys. Lett.* 91 (2007), 113501.
- [50] C.H. Park, J.G. Kim, S.-G. Jung, D.J. Lee, Y.W. Park, B.-K. Ju, Optical characteristics of refractive-index-matching diffusion layer in organic light-emitting diodes, *Sci. Rep.* 9 (2019) 1–10.
- [51] P. Predeep, T.A. Shahul Hameed, J. Aneesh, M.R. Baiju, Organic light emitting diodes: effect of annealing the hole injection layer on the electrical and optical properties, *Solid State Phenom.* (2011) 39–50.
- [52] J.S. Park, J.M. Lee, S.K. Hwang, S.H. Lee, H.-J. Lee, B.R. Lee, H. Il Park, J.-S. Kim, S. Yoo, M.H. Song, others, A ZnO/N-doped carbon nanotube nanocomposite charge transport layer for high performance optoelectronics, *J. Mater. Chem.* 22 (2012) 12695–12700.
- [53] Z.-Z. Gu, Y. Tian, H.-Z. Geng, D.S. Rhen, A.S. Ethiraj, X. Zhang, L.-C. Jing, T. Wang, Z.-H. Xu, X.-T. Yuan, Highly conductive sandwich-structured CNT/PEDOT: PSS/CNT transparent conductive films for OLED electrodes, *Appl. Nanosci.* 9 (2019) 1971–1979.

Short Alkyl Chain Engineering Modulation on Naphthalene Flanked Diketopyrrolopyrrole toward High-Performance Single Crystal Transistors and Organic Thin Film Displays

Qian Liu, **Sudam Chavhan**, Hantang Zhang, Huabin Sun, Aidan J. Brock, Sergei Manzhos, Yingqian Chen, Krishna Feron, Steven E. Bottle, John C. McMurtrie, Jwo-Huei Jou, Ho-Shin Chen, Mangey Ram Nagar, Wenping Hu, Yong-Young Noh, Yonggang Zhen, and Prashant Sonar*

Studying multi-purpose applications of a specific material is a challenging topic in the organic electronics community. In this work, through molecular engineering and smart device structure design strategy, high performance in transistors and thin film display devices is simultaneously achieved by applying a simple new dye molecule, naphthalene flanked diketopyrrolopyrrole (DPPN), as the active layer material. Short alkyl chains (hexyl or octyl side groups for H-DPPN and O-DPPN, respectively) are adapted to improve the hole mobility in organic thin film transistors (OTFTs) and single crystal transistors (SCTs). Specifically, H-DPPN shows a similar hole mobility in either OTFTs or SCTs, while O-DPPN exhibits a dramatically enhanced mobility, reaching $0.125 \text{ cm}^2 \text{ V}^{-1} \text{ s}^{-1}$ in SCTs. Additionally, a smart organic light emitting diode (OLED) device is designed by using DPPN molecule as the dopant with a host matrix. The promising external quantum efficiencies of 4.0% and 2.3% are achieved for H-DPPN and O-DPPN fabricated OLEDs. Overall, in this work, it is reported that DPP-based small molecules can simultaneously function well in both transistors and thin film displays with high device performance through molecular and smart device engineering.

1. Introduction

Diketopyrrolopyrrole (DPP) derivatives have proven to be an important class of high-performance organic semiconductors that can be used as active materials in various types of electronic devices.^[1–7] As representative examples, the power conversion efficiency (PCE) of organic photovoltaic (OPV) devices have reached more than 12% by using some DPP derivatives as the active layer materials.^[8,9] In DPP semiconductors for organic thin film transistors (OTFTs), impressive hole mobilities exceeding $10 \text{ cm}^2 \text{ V}^{-1} \text{ s}^{-1}$ have been demonstrated.^[1] Recently, DPP materials are being exploited in more applications like OLEDs, sensors, photodetectors, and memory devices.^[2,10–17] Flanking groups substituted at the 3- and 6-position of the DPP core play significant roles in the


Q. Liu, Dr. A. J. Brock, Prof. S. E. Bottle, Prof. J. C. McMurtrie, Prof. P. Sonar
School of Chemistry and Physics, Science and Engineering Faculty
Queensland University of Technology
Brisbane, QLD 4000, Australia
E-mail: sonar.prashant@qut.edu.au

Dr. S. Chavhan^[†], Prof. J.-H. Jou, Prof. H.-S. Chen, Prof. M. R. Nagar
Department of Materials Science and Engineering
National Tsing-Hua University
101 Sec-2, Kuang-Fu Road, Hsinchu, Taiwan 30013, P. R. China

Dr. H. Zhang
College of Chemistry and Material Science
Shandong Agricultural University
61 Daizong Street, Tai'an, Shandong 271018, P. R. China

Dr. H. Zhang, Prof. Y. Zhen
Institute of Chemistry, Chinese Academy of Sciences
2 North First Street, Zhongguancun, Beijing 100190, P. R. China

Dr. H. Sun, Prof. Y.-Y. Noh
Department of Chemical Engineering
Pohang University of Science and Technology
77 Cheongam-Ro, Nam-Gu, Pohang 37673, Republic of Korea

 The ORCID identification number(s) for the author(s) of this article can be found under <https://doi.org/10.1002/aelm.202000804>.

^[†]Present address: Department of Physics, V. V. M's S. G. Patil ACS College Sakri, Affiliated to K. B. C. NMU Jalgaon (MS) India

Prof. S. Manzhos
Centre Énergie Matériaux Télécommunications
Institut National de la Recherche Scientifique
1650 boulevard Lionel-Boulet, Varennes, QC J3X1S2, Canada

Dr. Y. Chen
Department of Mechanical Engineering
Faculty of Engineering
National University of Singapore
Block EA #07-08, 9 Engineering Drive 1, Singapore 117576, Singapore

Dr. K. Feron
CSIRO Energy Centre
10 Murray Dwyer Circuit, Mayfield West, NSW 2304, Australia

Dr. K. Feron
Centre for Organic Electronics
University of Newcastle
Callaghan, NSW 2308, Australia

Prof. S. E. Bottle, Prof. J. C. McMurtrie, Prof. P. Sonar
Centre for Materials Science
Queensland University of Technology
Brisbane, QLD 4000, Australia

Prof. W. Hu
Tianjin Key Laboratory of Molecular Optoelectronic Sciences
Department of Chemistry, School of Science
Tianjin University
Tianjin 300072, P. R. China

DOI: 10.1002/aelm.202000804

optoelectronic properties of resultant materials.^[18] Flanking moieties such as thiophene, furan, selenophene, thiazol, thienothiophene, phenyl, and pyridyl groups have been reported.^[19,20] Thiophene flanked DPP (DPPT) is one of the most promising building blocks to construct high-performance materials for both OTFTs and OPVs. We previously reported the polymer, PDPP-TNT, consisting of DPPT and naphthalene.^[21,22] The introduction of conjugation-extended naphthalene promoted strong intermolecular interactions and resulted in favorable π stacking between polymer backbones. Thus, a high hole mobility of $\approx 1.0 \text{ cm}^2 \text{ V}^{-1} \text{ s}^{-1}$ was observed in OTFTs and a promising PCE of 4.7% was obtained in OPVs as donor mixing with PC₇₁BM. Simultaneously achieving high performance in both OPVs and OTFTs is feasible, because the good charge carrier transport for a molecule is also a beneficial factor for improving both the short-circuit current (J_{SC}) and fill factor (FF) when it is used in active layer of OPV devices.^[23] In addition to DPPT, other DPP derivatives based semiconductors also successfully demonstrated high performance in electronic devices.^[24–26]

It is worth mentioning that phenyl flanked DPP (DPPh) has been proven to be a great choice of luminescent material for OLEDs and related applications.^[10] One reason making DPPh a promising molecule is that the dihedral angles between the phenyl groups and the DPP core (estimated to be around 40°) to some extent weaken the π stacking which minimizes the fluorescence quenching in solid state.^[27] Recently, we reported novel naphthalene flanked DPP (DPPN) with different alkyl chains as a new member in the DPP family.^[28] Compared with five- or six-membered ring DPPs, the fused aromatic ring of naphthalene resulted in a more extended π -conjugation leading to a larger intermolecular orbital overlap and thus facilitated the charge transport. Our primary attempt has demonstrated that *n*-decyl substituted DPPN (D-DPPN) monomer showed the highest hole mobility of $0.019 \text{ cm}^2 \text{ V}^{-1} \text{ s}^{-1}$ in OTFTs as the active semiconductor directly, without any further functionalization. It is believed that there is still room to further improve the mobility by decreasing the length of side chains. Moreover, shorter chains substituted DPPN monomers are more suitable for growing single crystals, which prompted us to study their intrinsic charge carrier transport behavior by fabricating single crystal transistors (SCTs). Naphthalene, a common acene type of benzene derivative that has been proven to form J-aggregation in solid state, can be used as a building block in materials that can retain efficient emission and thus lead to high photoluminescence quantum yield.^[29] Our DPPNs were observed to show strong luminescence under a laboratory lamp thus could be also promising in related devices like OLEDs.

In this work, *n*-hexyl and *n*-octyl alkylated DPPN compounds, H-DPPN and O-DPPN, were synthesized and their thermal, optical, and electronic properties were studied. The hole mobility of OTFTs was further enhanced by decreasing the length of side chains to *n*-octyl (O-DPPN) but dropped then for shorter *n*-hexyl H-DPPN. Moreover, single crystals for both materials were successfully grown and the fabricated SCTs indicated their high intrinsic hole transporting property. Due to the strong luminescence feature under laboratory UV light, we also fabricated OLED devices by using H-DPPN and O-DPPN as the dopant mixed with tris(4-carbazoyl-9-ylphenyl) amine (TCTA) host and achieved promising performance with

external quantum efficiencies (EQEs) of 4.0% and 2.3% respectively. It is well known that compact packing of molecules can induce strong and plentiful intermolecular interactions that generally facilitate charge transport in OTFTs. However, the interactions will also quench the solid-state luminescence, which makes it difficult to achieve both high mobility in OTFTs and high EQE in OLEDs. Nevertheless, in our current scenario, we have achieved high performance in both OTFTs and OLEDs via smart device and molecular engineering approaches. This is the first report of novel flanking group naphthalene attached DPP based small molecules, which can simultaneously function well in several different electronic devices, and the afforded high performance is encouraging for the future advancement of organic electronics.

2. Results and Discussion

Our previous report on DPPNs has demonstrated that a linear and short side alkyl chain enhances charge carrier mobility; in particular, the obtained hole mobility was higher.^[28] We perform a systematic study to investigate this type of material further, in particular, to find the most suitable side chains for this series of DPPN compounds. In this work, we continuously shorten the side chains to synthesize *n*-hexyl and *n*-octyl substituted DPPN based small molecular materials namely H-DPPN and O-DPPN. Besides, both materials are expected to show versatility for use in various electronic devices considering the structural advantages: i) higher hole mobility is expected according to our previous report; ii) monomers with short side chains are more feasible to grow single crystals, being beneficial for SCTs fabrication; iii) as an analogue of DPPh, H-DPPN, and O-DPPN solutions were observed to be highly fluorescent under the laboratory UV lamp (Figure S1, Supporting Information), demonstrating their potential in OLEDs. As per our previous report, the synthetic route to H-DPPN and O-DPPN is shown in **Figure 1a**.^[30] The alkylation of NH-DPPN was performed in the presence of *n*-hexyl or *n*-octyl bromide, respectively, at 120 °C in dimethylformamide (DMF) with anhydrous potassium carbonate (K_2CO_3) as the base. The purity and structures of H-DPPN and O-DPPN were characterized with ¹H, ¹³C NMR spectra, and high-resolution mass spectrometry (HRMS).

The thermogravimetric analysis (TGA, Figure S2a in the Supporting Information) indicated that both H-DPPN and O-DPPN appear to possess excellent thermal stability with the decomposition temperature (T_d , 5% weight loss) of 340 and 348 °C, respectively. These values are high enough to perform annealing or other thermal processing required for devices fabrication. The differential scanning calorimetry (DSC, Figure S2b–d; Supporting Information) demonstrated that small variation in side chains on DPPN has dramatic influence on their crystallinity. H-DPPN undergoes a classic melting transition at 162 °C (91.22 J g^{-1}) and a crystalline transition at 102 °C (72.74 J g^{-1}). However, O-DPPN shows a different behavior in that an endothermic peak at 119 °C followed by a cold crystallization at 125 °C (18.96 J g^{-1}) was observed before the material was completely melted at 147 °C (79.80 J g^{-1}). This feature is an indication of the melting and secondary recrystallization of the amorphous area. The crystallinity peak is observed at about 84 °C

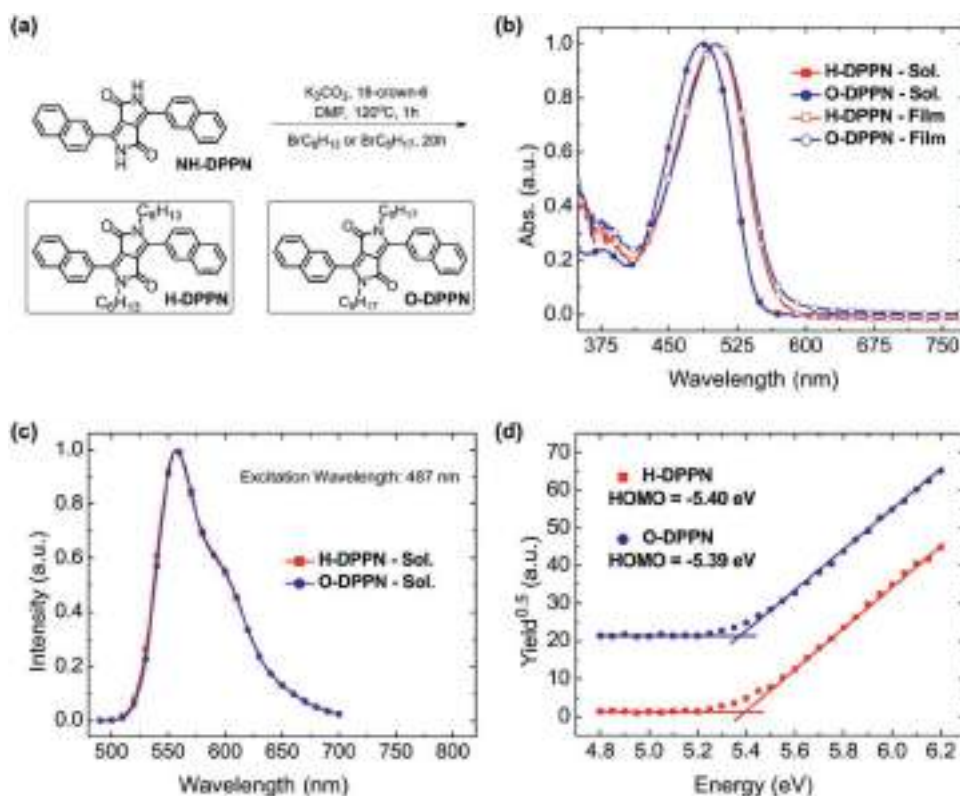


Figure 1. a) The synthetic route to H-DPPN and O-DPPN. b) UV-vis absorption spectra of H-DPPN and O-DPPN in both chloroform solutions and thin films. c) Photoluminescence (PL) spectra of H-DPPN and O-DPPN in chloroform solutions. d) Photoelectron spectroscopy in air (PESA) measurements of H-DPPN and O-DPPN films.

during cooling process with the enthalpy of 29.59 J g^{-1} . The original DSC analysis labelled with enthalpy values are present in Figure S3 in the Supporting Information.

The UV-vis absorption spectra (Figure 1b) of both compounds in solutions are well overlapped due to the similar molecular backbone and the absence of interchain interactions. This observation has also been confirmed by density functional theory (DFT) modelling where both molecules exhibit the same visible peak position (503 nm, Figure S4a: Supporting Information). The measured absorption maximum in solution is located around 487 nm, which is attributed to the intramolecular charge transfer (ICT) from naphthalene to the DPP core. This peak was red-shifted to 502 and 503 nm for H-DPPN and O-DPPN thin films, respectively, due to the molecular aggregation. In thin films, both materials only exhibit H-aggregation which follows a similar trend to that observed in our previous work, namely, that the shorter the side chains, the stronger the H-aggregation.^[28] After annealing the thin films at 100 and 130 °C for 10 min (Figure S5a,b: Supporting Information), the J-aggregation of H-DPPN has been enhanced, whereas for O-DPPN, not only the J-aggregation was enhanced after 100 °C annealing, an extra absorption peak and a red-shifted spectrum are observed. After annealing at 130 °C, the spectrum went back to the dominant H-aggregation, but the red shift remains the same. This phenomenon is consistent with the DSC analysis, since the secondary recrystallization of the amorphous area of O-DPPN promoted further aggregation and caused the change from J- to H-aggregation. The bandgaps of both compounds are

calculated from the onset of thin film spectra (559 and 565 nm for H-DPPN and O-DPPN, respectively) to be 2.22 and 2.19 eV. In solutions, both materials show a strong PL emissive peak at 558 nm (Figure 1c and Figure S5c: Supporting Information). In thin films, aggregation caused quenching was observed for both materials with a dominant emissive peak at 388 and 422 nm for H-DPPN and O-DPPN, respectively, under excitation wavelength of 325 nm. Upon exciting at 502 or 503 nm, both compounds exhibited weak emission with a peak located at around 610 nm (Figure S5d: Supporting Information).

The highest occupied molecular orbital (HOMO) energy levels are determined through photoelectron spectroscopy in air (PESA) measurements to be -5.40 and -5.39 eV respectively as shown in Figure 1d. In our previous publication,^[28] we observed that the side chains on DPPN can have a significant influence on the energy levels (despite of same conjugated backbone) due to the different solid state stacking, which is supported by the significant color variation. However, for H-DPPN and O-DPPN, the HOMOs are only slightly changed. This can be further confirmed from the similar color appearance of both compounds and the similarity of the absorption spectra in solutions and thin films. The lowest unoccupied molecular orbital (LUMO) energy levels are estimated from the difference between optical bandgaps and HOMOs to be -3.18 and -3.20 eV for H-DPPN and O-DPPN, respectively.

DFT calculations were employed to investigate the electronic structure and molecular geometry of H-DPPN and O-DPPN. As shown in Figure S6 (Supporting Information), both molecules

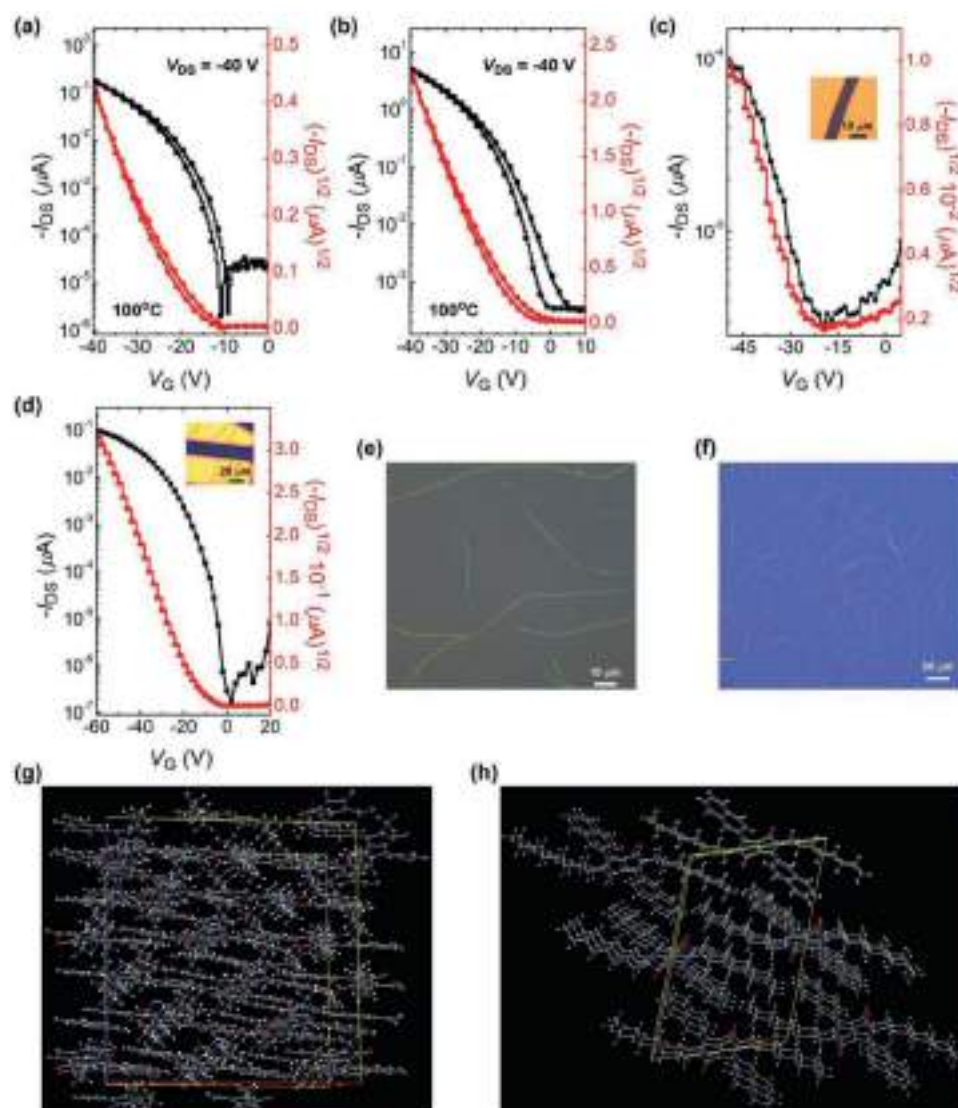


Figure 2. Transfer curves of OTFTs based on a) H-DPPN and b) O-DPPN thin films. Transfer curves of SCTs based on c) H-DPPN and d) O-DPPN crystals with the corresponding optical device structure images in the insets. Optical images of e) H-DPPN and f) O-DPPN single crystals. X-ray determined unit cells of g) H-DPPN and h) O-DPPN crystals.

have same HOMO and LUMO distributions, which are found to be localized at the entire molecular backbone that can be beneficial to facilitate the intramolecular charge carrier transport. The computed molecular HOMO levels are -5.35 eV for both molecules, which is in an excellent agreement with the experimental results. The calculated bandgaps (2.62 eV) and LUMO (-2.73 eV) values are higher than the experimental values which could be attributed to the fact that the measured onset of optical absorption is affected by vibrational broadening while the computed levels are at the equilibrium geometry, as well as errors due to approximations used. The optimized backbone conformation indicates the same dihedral angles of 37° and 31° for both molecules (Figure S6, Supporting Information). Since both H-DPPN and O-DPPN solutions have shown strong fluorescence under a UV lamp, the relatively large dihedral angles can, to some extent, restrain the emission quenching effect in solid state, demonstrating their promise for application in OLEDs.

Top gate bottom contact (TG/BC) OTFT devices were fabricated to evaluate the electrical properties of newly synthesized H-DPPN and O-DPPN semiconductors. The representative device schematic and transfer curves after annealing at 100°C or 120°C are shown in Figure S7 (Supporting Information) and Figure 2a,b. The hole mobility values (μ_{h}), threshold voltage (V_{th}), subthreshold swing (SS) and on/off ratio ($I_{\text{on}}/I_{\text{off}}$) extracted from transfer curves at the saturation regime are summarized in Table 1.

It was found that the devices annealed at 100°C exhibited better performance with a highest hole mobility of $0.01\text{ cm}^2\text{ V}^{-1}\text{ s}^{-1}$ for H-DPPN and $0.05\text{ cm}^2\text{ V}^{-1}\text{ s}^{-1}$ for O-DPPN. This performance is better than some reported alkylated thiophene DPP monomers in solution processed thin film transistors as compared in Table S1 (Supporting Information).^[31] When the thin films were annealed at 120°C , the mobility decreased to 0.006 and $0.001\text{ cm}^2\text{ V}^{-1}\text{ s}^{-1}$, respectively. By comparing with

Table 1. Summary of TG/BC structured OTFT device performance.

Material	$T_{\text{anneal}} [^{\circ}\text{C}]$	$\mu_{\text{h}}^{\text{ave.}} \times 10^{-2} [\text{cm}^2 \text{V}^{-1} \text{s}^{-1}]$	$\mu_{\text{h}}^{\text{max.}} \times 10^{-2} [\text{cm}^2 \text{V}^{-1} \text{s}^{-1}]$	SS [V dec ⁻¹]	V_{th} [V]	$I_{\text{on}}/I_{\text{off}} [\times 10^6]$
H-DPPN	100	0.66 ± 0.27	1.02	0.95 ± 0.20	20.1 ± 4.1	0.43 ± 0.49
	120	0.23 ± 0.19	0.61	0.77 ± 0.17	23.5 ± 1.8	0.54 ± 0.63
O-DPPN	100	4.29 ± 1.38	5.03	-4.70 ± 1.0	-8v.9 ± 2.6	0.63 ± 0.13
	120	0.04 ± 0.06	0.16	5.62 ± 5.60	-	0.13 ± 0.27

our reported compounds, O-DPPN was observed to show the best performance and H-DPPN shows an even worse mobility than D-DPPN ($0.019 \text{ cm}^2 \text{ V}^{-1} \text{ s}^{-1}$).^[28] From the polarized microscopic images shown in Figure S8 (Supporting Information), it is clear that the films of both materials easily form large crystalline domains, which is beneficial for charge carrier transport. However, the H-DPPN film has many defects while the O-DPPN film is smoother that contributed to the higher hole mobility. Upon annealing at 120 °C, the defects become more obvious in H-DPPN film which caused a decreased hole mobility, while the crystal domains did not change much, that is consistent with the high melting point >160 °C observed from the DSC curve. From the AFM (atomic force microscope) images of H-DPPN and O-DPPN films annealed at 120 °C, similar phenomenon is observed as shown in Figure S9 (Supporting Information). For the O-DPPN film, the crystal domains were broken, and a cullet-shaped film was observed. After 120 °C annealing, the amorphous area experienced melting process, which, we assume, caused the broken of crystalline regions of O-DPPN films. This phenomenon can easily cause disconnection along the conducting channel and thus result in a large decrease in mobility. Microstructure, defects, and domain walls are thus critical determinants of mobility in these materials. Computed estimates of charge transfer rates (see the Supporting Information) also point the critical role of domains and microstructure: while the computed single crystal charge hopping rate between neighboring molecules is higher for H-DPPN than for O-DPPN, the packing of H-DPPN favors 1D hopping pathways, while the packing of O-DPPN favors 2D pathways (Figure S10, Supporting Information). The low-dimensional hopping paths imply strong dependence of the measured bulk rate on crystal domain size, whereby domain boundaries are expected to be a significant bottleneck to transport in particular because ideal crystal transport is low-dimensional. The grain boundaries are expected to be a more significant bottleneck in H-DPPN due to 1D transport in the ideal crystal, explaining the better measured mobility with O-DPPN.

To investigate the intrinsic charge transport behavior, transistor devices based on H-DPPN or O-DPPN single crystals were fabricated. By drop-casting a H-DPPN (0.1 mg mL^{-1}) solution in chlorobenzene on bare Si/SiO₂ wafer and after solvent evaporation, well-defined ribbon-shaped crystals were grown in three days (Figure 2e). Since ill-defined clusters of O-DPPN were grown in chlorobenzene, we screened the solvent species and used a mixed solvent (chloroform:ethyl acetate = 1:2) to grow ribbon-shaped crystals (Figure 2f) by drop-casting method (0.05 mg mL^{-1}). The optical images of H-DPPN and O-DPPN single crystals are also present in Figure S11 (Supporting Information) with a same scale plate for better comparison. The single crystals were annealed in vacuum at 80 °C to remove residual solvent before devices fabrication. Drain

and source electrodes (40 nm) were deposited on H-DPPN and O-DPPN crystals by thermal evaporation of a gold film with the “Au stripe mask”.^[32] The transfer curves and optical images (insets) of fabricated devices are shown in Figure 2c,d. The electrical characteristics of all devices were measured under ambient conditions. From the saturation regime of the transfer characteristics, the mobility is calculated by linear fitting of the dependence of $(I_{\text{DS}})^{1/2}$ versus V_{G} . The mobility of the best devices for O-DPPN crystals is up to $0.125 \text{ cm}^2 \text{ V}^{-1} \text{ s}^{-1}$, over ten times higher than that of H-DPPN crystals. The $I_{\text{on}}/I_{\text{off}}$ ratio of the best device for O-DPPN crystals was measured to be 10^6 , five orders of magnitude higher than that of H-DPPN crystals. These results further demonstrated that O-DPPN crystals exhibit much better charge transport behaviors compared with H-DPPN.

To better understand the difference between single crystals for H-DPPN and O-DPPN, we grew H-DPPN and O-DPPN single crystals as shown in Figure S12 (Supporting Information). Their structures and unit cells were determined through X-ray diffraction as shown in Figure S13 (Supporting Information) and Figure 2g,h. H-DPPN and O-DPPN crystallize in the space groups $P2_1/c$ and $P2_1/n$, respectively. In the crystal structure of H-DPPN, the molecules stack in chain to chains, with the principal interaction being an offset face-to-face π - π interaction between adjacent naphthalene units (3.278 Å). In the O-DPPN crystal structure, chains of stacked O-DPPN molecules (vertical offset 2.760 Å) interact with adjacent chains via weak naphthalene CH- π interactions (3.808 Å) between neighboring naphthalene units. CH- π interactions (2.695 Å) are also observed between naphthalene rings and adjacent alkyl chains. Obviously, the favorable backbone stacking in Figure 2h for O-DPPN crystals explained its higher mobility in SCTs. The comparison of single crystal data of H-DPPN and O-DPPN with thiophene, selenophene, and phenyl DPPs (with hexyl side chains) indicate that DPPN compounds exhibit a much closer π stacking than other DPP derivatives as compared in Table S1 (Supporting Information).^[33] That is a highly favorable feature for intermolecular charge carrier transport. We also performed large-scale calculations on crystals and clusters of H-DPPN and O-DPPN to estimate the effect of solid-state packing on electronic properties. First, density functional tight binding (DFTB) and time-dependent DFTB (TD-DFTB) were benchmarked to DFT and TD-DFT in single-molecule calculations. The results are given in Table S2 and Figure S4 (Supporting Information), showing that while (TD)-DFTB results in somewhat different values of the HOMO, LUMO energies, the gap, and the visible absorption peak from DFT (as is expected given that the DFTB parameterization is based on GGA calculations), it can be used for qualitative assessment and is reliable for comparison between the two molecules and between different molecular

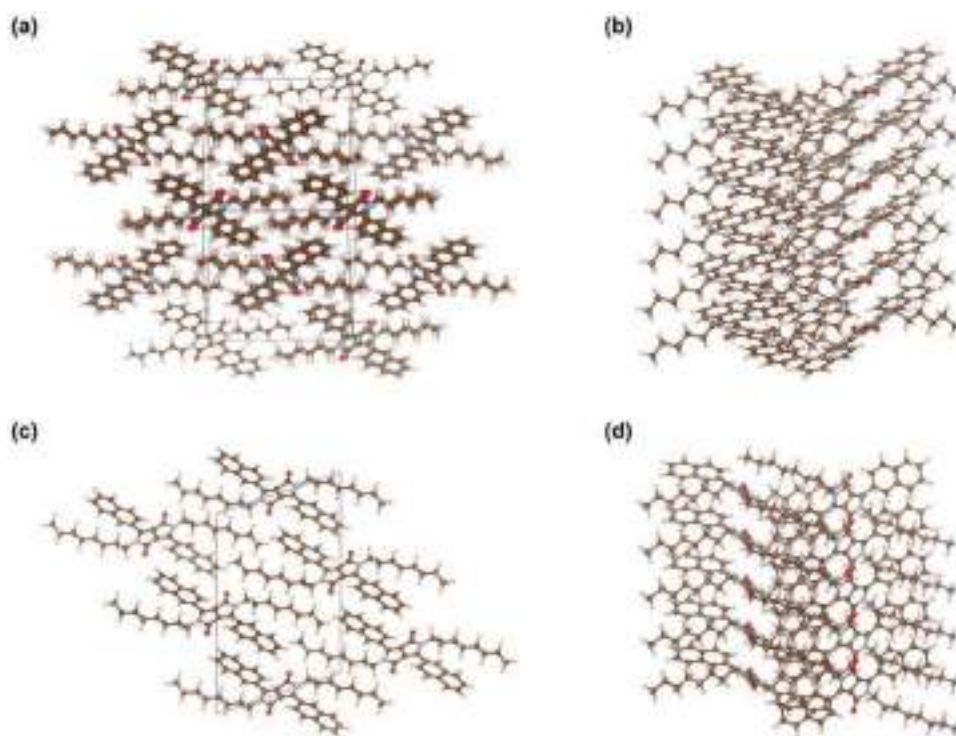


Figure 3. DFTB-computed unit cells (delimited by the box) of crystalline a) H-DPPN and c) O-DPPN. Molecular clusters of b) H-DPPN and d) O-DPPN.

environments. We therefore compared properties computed in periodic crystals and clusters to those of the molecules.

The unit cells of H-DPPN and O-DPPN crystals are shown in **Figure 3a,c**. Experimental structures were used as a starting point of optimizations. Clusters were cut preserving the optimized geometry of the periodic calculation (**Figure 3b,d**). The DFTB-optimized cell parameters are given in Table S3 (Supporting Information). As TD-DFTB calculations had to be done with the Γ point, a supercell with 10 molecules was then optimized for O-DPPN to make Γ point calculations sufficiently accurate (for H-DPPN, the unit cell is big enough for a Γ point calculation). The calculated HOMO, LUMO values and the gap for crystals and clusters are also shown in Table S2 (Supporting Information). For crystals, they show stabilization of the HOMO about 0.3 eV for H-DPPN and ≈ 0.4 eV for O-DPPN. The band gap becomes about 0.3 eV lower in H-DPPN versus O-DPPN, while the HOMO-LUMO gap is practically the same at the single-molecule level. While the absolute values of HOMO and LUMO in periodic systems are generally not directly comparable to molecular levels, changes in the gap are comparable and indicate stronger effects of aggregation on the gap with H-DPPN. The cluster calculations result in higher HOMO values versus single molecules, by 0.2–0.3 eV. They confirm the decrease in the gap in H-DPPN versus O-DPPN due to aggregate state effects, by 0.36 eV, similar to the results of the periodic calculations. Both periodic and cluster calculations indicate a slightly (≈ 0.1 eV) lower HOMO of O-DPPN in solid state versus H-DPPN even though molecular HOMO are nearly identical. The calculations also clearly confirmed the π stacking between naphthalene for O-DPPN, while H-DPPN tends to stack parallel.

A family of DPP molecules is gaining significant importance in OLED technology because of its high fluorescent quantum yield, thermal and photostability.^[10,27] In the present study, H-DPPN and O-DPPN were used to fabricate yellowish orange OLED by using cost-effective solution processing. Specifically, the device structure is shown in **Figure S14** (Supporting Information) where PEDOT:PSS is employed as a hole injecting and transporting layer (HIL/HTL), the emissive layer (EML) is composed of TCTA host doped with 2 wt% H-DPPN or O-DPPN orange emitter, TPBi is used as an electron transporting layer (ETL), and LiF/Al acts as a cathode. The energy level diagram of all used materials is shown in **Figure 4a**. The J - V curve as shown in **Figure 4b** exhibits well-defined diode characteristics, revealing that the fabricated OLED behaves as a rectifying device. The forward bias current for both devices rises with the increase of applied bias voltage, however, the reverse bias current remained significantly low (not shown in J - V curve), suggesting both OLEDs act as rectifying diodes. The rapid increase in forward-bias current is observed for O-DPPN based OLED, implying a small sheet resistance of the device, whereas H-DPPN OLED has a high sheet resistance.

The difference in high forward bias current is attributed to differences in charge carrier mobility of the corresponding molecules.^[34] From the OTFTs and SCTs study, it is confirmed that O-DPPN possesses a higher mobility compared to H-DPPN. The influence of hole mobility is vividly observed in OLED device turn-on voltage as shown in **Figure 4c** which is the plot of luminescence versus applied voltage. The O-DPPN based OLED requires a 3.0 V to emit 10 cd m^{-2} luminescence, whereas to get the same luminescence, 3.8 V is needed for H-DPPN emitter OLED (0.8 V more). However, the power

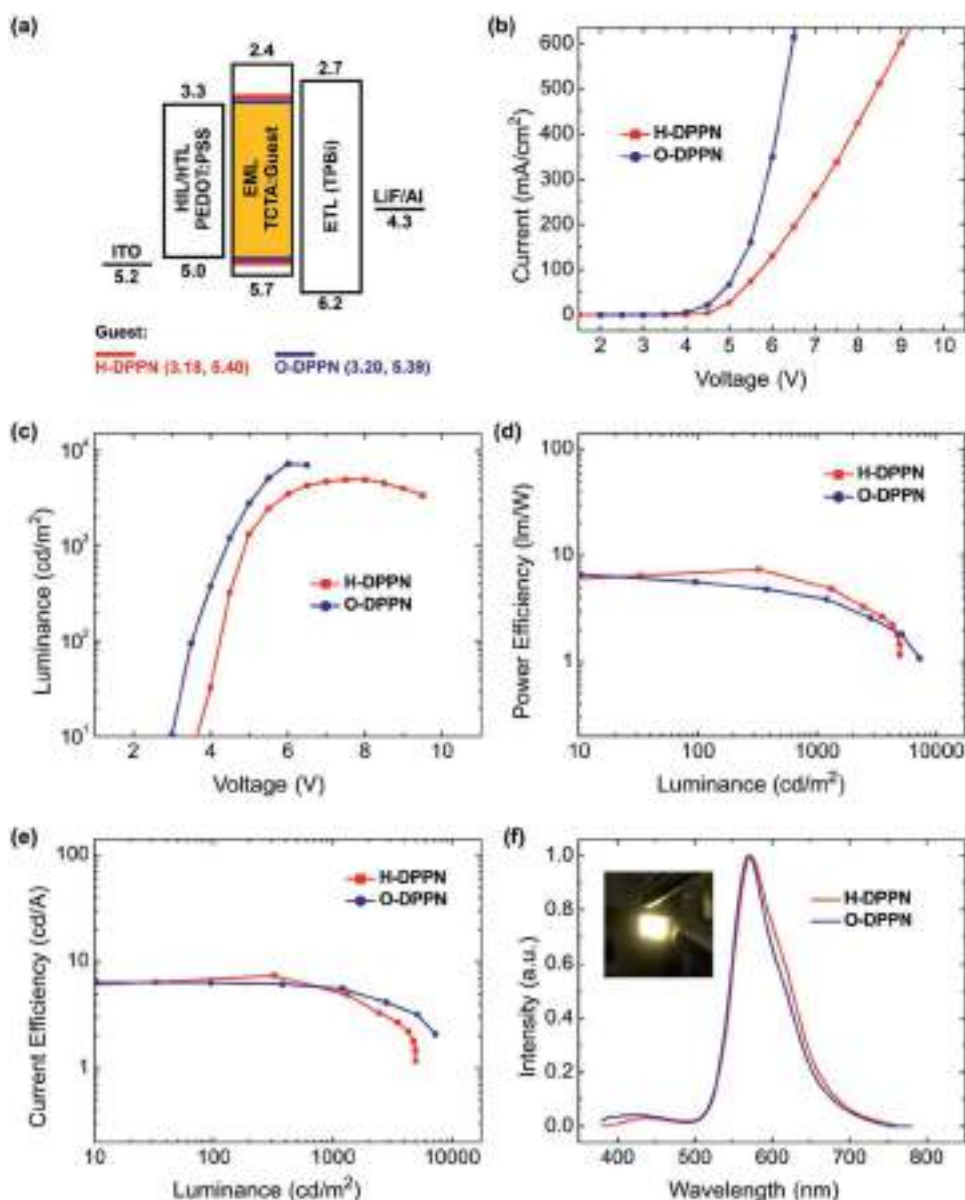


Figure 4. a) Energy level diagram of studied OLED device. b) Current–voltage (J – V), c) luminance, d) power efficiency, and e) current efficiency of studied OLED devices based on TCTA host doped with 2 wt% H-DPPN or O-DPPN molecules. f) Electroluminescence (EL) spectra of the fabricated OLED devices at 100 cd m^{-2} . Inset picture is the photograph of the working O-DPPN based OLED device.

efficiency obtained for H-DPPN OLED is 8.8 lm W^{-1} which is 27% higher than that of O-DPPN (6.5 lm W^{-1}) based device at 100 cd m^{-2} (Figure 4d) and a similar trend is noticed for current efficiency (Figure 4e). **Table 2** details electroluminescent properties of the fabricated OLEDs. The maximum power efficiency, current efficiency, and EQE were found to be 8.3 lm W^{-1} , 11.8 cd A^{-1} , and 4.0%, respectively, at 100 nits, for the H-DPPN based OLED. The overall performance of the H-DPPN OLED is superior to the O-DPPN counterpart, except the maximum luminance. To emphasize the advantage of DPPN compound in OLEDs, we compared the EQE values with other DPP derivatives (Table S1, Supporting Information). Also as the dopant for a host material, the device fabricated with TAPC (4,4'-cyclohexylidenebis[*N,N*-bis(4-methylphenyl)benzenamine])

host doped with 10 wt% furan flanked DPP exhibited a much lower EQE value of 0.7%.^[27] Although this value is

Table 2. OLED device parameters with TCTA host doped with 2 wt% DPPNs.

Dopant ^{a)}	OV [V]	PE [lm W^{-1}]	CE [cd A^{-1}]	EQE [%]	CIE/(x,y)	Max. L [cd m^{-2}]
@100/1000 cd m^{-2}						
H-DPPN	4.5/5.2	8.3/4.7	11.8/7.8	4.0/2.7	(0.50,0.48)/(0.49,0.47)	5371
O-DPPN	3.5/4.5	6.5/4.5	7.3/6.5	2.3/2.0	(0.49,0.48)/(0.48,0.48)	6065

^{a)}OV: Operating Voltage; PE: Power Efficiency; CE: Current Efficiency; EQE: External Quantum Efficiency; CIE 1931 Color Coordinates; Max. L: Maximum Luminance.

further enhanced to 12.1% by introducing a second dopant (9-[2,8]-9-carbazole-[dibenzothiophene-S,S-dioxide]-carbazole, initialized as 2d), it is not competitive since the 2d doped TAPC shows a EQE value of 15%.^[35]

Figure 4f shows the normalized electroluminescent (EL) spectra of two OLED devices. Each one was made with 2 wt% H-DPPN and O-DPPN molecules doped in the TCTA host, obtained at 100 nits. The main emission peak is obtained at 570 nm for both devices, which corresponds to the absorbance band of H-DPPN and O-DPPN molecules, confirming the direct excitation of DPP cores. The CIE (x,y) coordinate of EL spectra (0.50, 0.48) evidences that the fabricated OLED devices generate greenish-yellow light. However, emission noticed at 400–450 nm originates from the TCTA host molecules. The EL spectrum of O-DPPN OLED is narrower than that of the H-DPPN counterpart, suggesting the recombination zone of the injected charge carriers is narrower as compared to H-DPPN based OLED. To explain this behavior, it is important to consider the charge carrier mobility of O-DPPN and H-DPPN. It is a well-known fact that the OLED device with a TCTA host with TPBi ETL is a hole charge carrier-dominated device and therefore the charge carrier recombination zone is mainly available at the interface of the emissive layer (EML) and the electron transporting layer (ETL).^[36] O-DPPN possesses a higher hole mobility allowing for more efficient hole injection and transport through the EML layer up to the ETL interface, resulting in a narrower recombination zone. On the other hand, the H-DPPN molecule has a slightly lower hole-mobility that assists to widen the charge carrier recombination zone up to the interface of the HTL and EML.^[34,37] As a result of this, we have obtained higher power and current efficacy and EQE for H-DPPN based OLED compared to the O-DPPN counterpart.

3. Conclusions

To summarize, we designed and synthesized two naphthalene flanked DPP dye based versatile materials, namely, H-DPPN and O-DPPN. It was found that, through molecular engineering and smart device structure design, high performance can be achieved in both transistors and thin film displays, which is encouraging for researchers working on organic electronics. DPPNs with different side chains were first reported by our group, and in this work, we demonstrated that the octyl side chain is most suitable for this series of molecules due to its highest hole mobility of $0.05 \text{ cm}^2 \text{ V}^{-1} \text{ s}^{-1}$ in OTFTs. The better performance was ascribed to the uniform morphology with a highly crystalline nature. Molecule with short side chains allows growing single crystals for SCTs. O-DPPN shows a largely enhanced performance with mobility of up to $0.125 \text{ cm}^2 \text{ V}^{-1} \text{ s}^{-1}$ which is 10 times higher than that of H-DPPN. This is attributed to the stacking mode suggested by X-ray determined unit cells and DFTB computations. H-DPPN crystals appear to stack in 1D chain with a face to face π - π interaction that lacks favorable backbone stacking for charge carrier transport. However, obvious backbone stacking from X-ray diffraction for O-DPPN crystals and naphthalene-naphthalene stacking from DFTB calculations are observed. This is a favorable feature for better charge carrier transport, explaining its higher hole

mobility in SCTs. Additionally, as the analogue of phenyl DPP, H-DPPN and O-DPPN also exhibit potential in OLEDs. To avoid the emission quenching effect of pristine DPPN film in the active layer, we smartly modified the OLED device structure by using the DPPN molecule as a dopant for TCTA. H-DPPN based OLED shows better performances with maximum power efficiency, current efficiency, and EQE of 8.3 lm W^{-1} , 11.8 cd A^{-1} , and 4.0%, respectively, at 100 nits. Overall, in this work, we have clearly disclosed the versatility of two DPPN molecules in various types of electronic devices. Especially, simultaneously achieving high performance in both transistors and thin film displays through molecular engineering and smart device structure design is a new scenario in organic electronics community which is expected to advance the future development of electronic devices.

Supporting Information

Supporting Information is available from the Wiley Online Library or from the author.

Acknowledgements

Q.L. is thankful to QUT for offering here QUTPRA scholarship to conduct his research. P.S. is thankful to QUT for the financial support from the Australian Research Council (ARC) for the Future Fellowship (FT130101337) and QUT core funding (QUT/322120-0301/07). Some of the data reported in this paper were obtained at the Central Analytical Research Facility (CARF) operated by the Institute for Future Environments (QUT). Access to CARF is supported by generous funding from the Science and Engineering Faculty (QUT). S.M. is supported by the National Sciences and Engineering Research Council of Canada. This research was enabled in part by support provided by Compute Canada. Additionally, this project has received funding from the European Union's Horizon 2020 research and innovation programme under the Marie Skłodowska-Curie grant agreement no. 663830. Parts of this research were undertaken on the MX1 beamline at the Australian Synchrotron, part of ANSTO. The authors thank the synchrotron for travel support and the beamline staff for their assistance. The authors appreciate the help from Dr. Dilini Galpayage Dona in obtaining the enthalpies of melting/crystallinity of both materials from DSC analysis.

Conflict of Interest

The authors declare no conflict of interest.

Author Contributions

Q.L. is responsible for the materials synthesis, properties characterization as well as managing the final manuscript preparation. S.C., J.-H.J., H.-S.C., and M.R.N. are responsible for the OLED device fabrication and characterization. H.Z., Y.Z., and W.H. are responsible for the single crystal transistors fabrication and characterization. H.S. and Y.-Y.N. are responsible for the thin film transistors fabrication and characterization. A.B. and J.M. are responsible for the X-ray determined single crystal data. S.M. and Y.C. are responsible for the DFT and DFTB calculations. K.F. is responsible for the PESA measurement. S.E.B. reviewed and revised the manuscript. P.S. conceived and directed the project. All authors have reviewed or commented on the final version of the manuscript.

Keywords

molecular engineering, naphthalene flanked diketopyrrolopyrrole, smart device structure design, thin film displays, transistors

Received: August 8, 2020

Revised: October 17, 2020

Published online:

- [1] Z. Yi, S. Wang, Y. Liu, *Adv. Mater.* **2015**, *27*, 3589.
- [2] M. Kaur, D. H. Choi, *Chem. Soc. Rev.* **2015**, *44*, 58.
- [3] A. Tang, C. Zhan, J. Yao, E. Zhou, *Adv. Mater.* **2017**, *29*, 1600013.
- [4] Q. Liu, S. E. Bottle, P. Sonar, *Adv. Mater.* **2020**, *32*, 1903882.
- [5] Q. Liu, Y. Wang, A. Kohara, H. Matsumoto, S. Manzhos, K. Feron, S. E. Bottle, J. Bell, T. Michinobu, P. Sonar, *Adv. Funct. Mater.* **2020**, *30*, 1907452.
- [6] Q. Liu, S. Kumagai, S. Manzhos, Y. Chen, I. Angunawela, M. M. Nahid, K. Feron, S. E. Bottle, J. Bell, H. Ade, J. Takeya, P. Sonar, *Adv. Funct. Mater.* **2020**, *30*, 2000489.
- [7] Q. Liu, Y. Wang, Y. Ren, A. Kohara, H. Matsumoto, Y. Chen, S. Manzhos, K. Feron, S. E. Bottle, J. Bell, Y. Zhou, T. Michinobu, P. Sonar, *ACS Appl. Electron. Mater.* **2020**, *2*, 1609.
- [8] K. Gao, S. B. Jo, X. Shi, L. Nian, M. Zhang, Y. Kan, F. Lin, B. Kan, B. Xu, Q. Rong, *Adv. Mater.* **2019**, *31*, 1807842.
- [9] C. Zhao, Y. Guo, Y. Zhang, N. Yan, S. You, W. Li, *J. Mater. Chem. A* **2019**, *7*, 10174.
- [10] A. Leventis, J. Royakkers, A. G. Rapidis, N. Goodeal, M. K. Corpinot, J. M. Frost, D. K. Bucar, M. O. Blunt, F. Cacialli, H. Bronstein, *J. Am. Chem. Soc.* **2018**, *140*, 1622.
- [11] C. Y. Yang, W. L. Jin, J. Wang, Y. F. Ding, S. Nong, K. Shi, Y. Lu, Y. Z. Dai, F. D. Zhuang, T. Lei, C. A. Di, D. Zhu, J. Y. Wang, J. Pei, *Adv. Mater.* **2018**, *30*, 1802850.
- [12] L. Zhang, T. Yang, L. Shen, Y. Fang, L. Dang, N. Zhou, X. Guo, Z. Hong, Y. Yang, H. Wu, J. Huang, Y. Liang, *Adv. Mater.* **2015**, *27*, 6496.
- [13] B. Wang, T. P. Huynh, W. Wu, N. Hayek, T. T. Do, J. C. Cancilla, J. S. Torrecilla, M. M. Nahid, J. M. Colwell, O. M. Gazit, S. R. Puniredd, C. R. McNeill, P. Sonar, H. Haick, *Adv. Mater.* **2016**, *28*, 4012.
- [14] W. Y. Lee, H. C. Wu, C. Lu, B. D. Naab, W. C. Chen, Z. Bao, *Adv. Mater.* **2017**, *29*, 1605166.
- [15] X. J. She, D. Gustafsson, H. Sirringhaus, *Adv. Mater.* **2017**, *29*, 1604769.
- [16] C.-T. Chen, W.-Y. Lee, T.-L. Shen, H.-C. Wu, C.-C. Shih, B.-W. Ye, T.-Y. Lin, W.-C. Chen, Y.-F. Chen, *Adv. Electron. Mater.* **2017**, *3*, 1600548.
- [17] P. P. Kumavat, P. Sonar, D. S. Dalal, *Renewable Sustainable Energy Rev.* **2017**, *78*, 1262.
- [18] L. Shi, Y. Guo, W. Hu, Y. Liu, *Mater. Chem. Front.* **2017**, *1*, 2423.
- [19] Q. Liu, A. Surendran, K. Feron, S. Manzhos, X. Jiao, C. R. McNeill, S. E. Bottle, J. Bell, W. L. Leong, P. Sonar, *New J. Chem.* **2018**, *42*, 4017.
- [20] Q. Liu, H. Sun, S. P. Ponnappa, K. Feron, S. Manzhos, M. W. M. Jones, S. E. Bottle, J. Bell, Y.-Y. Noh, P. Sonar, *Org. Electron.* **2019**, *74*, 290.
- [21] P. Sonar, S. P. Singh, Y. Li, Z.-E. Ooi, T.-j. Ha, I. Wong, M. S. Soh, A. Dodabalapur, *Energy Environ. Sci.* **2011**, *4*, 2288.
- [22] T.-J. Ha, P. Sonar, A. Dodabalapur, *Appl. Phys. Lett.* **2011**, *98*, 253305.
- [23] R. S. Ashraf, I. Meager, M. Nikolka, M. Kirkus, M. Planells, B. C. Schroeder, S. Holliday, M. Hurhangee, C. B. Nielsen, H. Sirringhaus, I. McCulloch, *J. Am. Chem. Soc.* **2015**, *137*, 1314.
- [24] Z. Genene, W. Mammo, E. Wang, M. R. Andersson, *Adv. Mater.* **2019**, *31*, 1807275.
- [25] Z. Ni, H. Wang, H. Dong, Y. Dang, Q. Zhao, X. Zhang, W. Hu, *Nat. Chem.* **2019**, *11*, 271.
- [26] M. A. Naik, S. Patil, *J. Polym. Sci., Part A: Polym. Chem.* **2013**, *51*, 4241.
- [27] P. Data, A. Kurowska, S. Pluczyk, P. Zassowski, P. Pander, R. Jedrysiak, M. Czwartosz, L. Otulakowski, J. Suwinski, M. Lapkowski, A. P. Monkman, *J. Phys. Chem. C* **2016**, *120*, 2070.
- [28] Q. Liu, H. Sun, C. Blaikie, C. Caporale, S. Manzhos, K. Feron, J. M. MacLeod, M. Massi, S. E. Bottle, J. Bell, Y.-Y. Noh, P. Sonar, *New J. Chem.* **2018**, *42*, 12374.
- [29] J. Li, K. Zhou, J. Liu, Y. Zhen, L. Liu, J. Zhang, H. Dong, X. Zhang, L. Jiang, W. Hu, *J. Am. Chem. Soc.* **2017**, *139*, 17261.
- [30] S. P. Ponnappa, Q. Liu, M. Umer, J. MacLeod, J. Jackson, G. Ayoko, M. J. A. Shiddiky, A. P. O'Mullane, P. Sonar, *Polym. Chem.* **2019**, *10*, 3722.
- [31] A. Kovalenko, C. Yumusak, P. Heinrichova, S. Stritesky, L. Fekete, M. Vala, M. Weiter, N. S. Sariciftci, J. Krajcovic, *J. Mater. Chem. C* **2017**, *5*, 4716.
- [32] Q. Tang, Y. Tong, H. Li, Z. Ji, L. Li, W. Hu, Y. Liu, D. Zhu, *Adv. Mater.* **2008**, *20*, 1511.
- [33] J. Dhar, N. Venkatramaiah, A. A. S. Patil, *J. Mater. Chem. C* **2014**, *2*, 3457.
- [34] G. G. Malliaras, J. C. Scott, *J. Appl. Phys.* **1998**, *83*, 5399.
- [35] V. Jankus, P. Data, D. Graves, C. McGuinness, J. Santos, M. R. Bryce, F. B. Dias, A. P. Monkman, *Adv. Funct. Mater.* **2014**, *24*, 6178.
- [36] J.-H. Jou, J.-W. Weng, S. D. Chavhan, R. A. K. Yadav, T.-W. Liang, *J. Phys. D: Appl. Phys.* **2018**, *51*, 454002.
- [37] S. W. Culligan, A. C. A. Chen, J. U. Wallace, K. P. Klubek, C. W. Tang, S. H. Chen, *Adv. Funct. Mater.* **2006**, *16*, 1481.

**Vidya Vikas Mandal's
Sitaram Govind Patil Arts,
Science and Commerce College,
Sakri Tal. Sakri Dist. Dhule 424 304**



**NAAC
ACCREDITED**

**विद्या विकास मंडळाचे,
सिताराम गोविंद पाटील कला,
विज्ञान आणि वाणिज्य महाविद्यालय,
साक्री ता. साक्री जि. धुळे ४२४ ३०४**

Affiliated to Kavayitri Bahinabai Chaudhari North Maharashtra University, Jalgaon

Website : www.sgpcsakri.com

Email : vidyavikas2006@rediffmail.com

Ph : 02568-242323

3.3.2.1 Research Paper Published in UGC Approved Journals

Growth and Characterization of Barium Oxalate Crystals by Single Diffusion Gel Method

H. S. Pawar¹, S. J. Nandre², S. D. Chavhan³ and R. R. Ahire³

¹V.J.N.T. Late Dalpatbhai Rathod Junior College, Mordadtanda (Dhule) M.S

²Department of Physics, Uttamrao Patil Arts and Science College, Dahiwel, (Dhule) M.S

³Department of Physics S.G. Patil Art's, Commerce and Science College, Sakri (Dhule) M.S

ABSTRACT

Barium oxalate crystals were grown by agar-agar gel through the single diffusion technique. The tendency of barium oxalate crystals to cylindrical growth was demonstrated. The optimum growth conditions barium oxalate was achieved by controlling the parameters like, concentration of gel, concentration of reactants, aging period and reversing of reactants. The crystal structure of grown material was determined by X-ray diffraction technique and was found to be monoclinic with lattice parameters 'a' = 6.6562 Å, b = 8.0464 Å, c = 2.8090 Å, $\beta = 96.832^\circ$, and $V = 149.38 \text{ \AA}^3$. The FTIR spectrum indicates OH and carbonyl group along with the presence of metal-oxygen bond. Morphology of grown crystals, investigated by scanning electron microscopy, exhibited compact grains including small and large sizes. Since the grown crystals are transparent, they show strong absorption in the ultra violet region above 290 nm wavelength.

Keywords: Crystal growth, Barium oxalate, X-ray spectroscopy, FTIR, and SEM.

1. Introduction

A solid which consist of atoms or other microscopic particles arranged in a periodic manner in all directions is called as a crystal. The strong influence of single crystals in the present day technology is evident from the recent advancements ultra-small electronic gadgets. Crystals of different materials have several applications such as they are used in semiconductor devices like electrical diodes, photodiodes, transistors, integrated circuits, magnetic devices like tape heads, transformer cores, superconductors, optoelectronics, quantum electronics, quantum and nonlinear optics, telecommunication etc. hence today's demand is to grow large crystals with good quality, high purity and symmetry. With this demanding requirement it is important to study the growth of single crystals and hence, investigation of their physical properties towards the fulfillment of device fabrication is crucial for both academic as well as applied research. Therefore, enormous amount of toil and treasure has been lavished on the development of crystal growth techniques. The in-depth explanation of various techniques can be obtained in the literature [1-6]. There are three major stages involved in this research. The first is the production of pure materials and improved equipment's associated with the preparation of these materials.

Second one is the production of single crystals first in the laboratory and then extending it to commercial level. The third is the characterization and utilization of these crystals in devices.

In present study, we have adopted the agar-agar gel technique to grow the barium oxalate single crystals. We have successfully grown the cylindrical transparent barium oxalate single crystals and studied their physical properties.

2. Experimental

In the present work, barium oxalate crystals were grown by single diffusion technique. The growth of barium oxalate crystals was carried out in agar-agar gel by adopting the similar technique as reported (Dalal and Saraf 2009) [10]. Barium chloride (BaCl_2 , 99.9%), oxalic acid ($\text{H}_2\text{C}_2\text{O}_4$, 99%), Agar-Agar powder ($\text{C}_{14}\text{H}_{24}\text{O}_9$) were used as the starting materials. All chemicals were of AR grade. The borosilicate glass tubes were used as crystallization apparatus. The glass tubes used for single diffusion were of 25 cm in length having outer diameter of 2.5cm outer diameter and 250ml beaker. The solution of 0.5, 1.0, 1.2, 1.5, and 2M concentrations were prepared and stored in clean glassware. Agar-agar gel was prepared by mixing (0.5 to 2.0gm) of agar powder in 100ml double distilled water at boiling temperature. Barium chloride of concentration 0.5 to 2M and oxalic acid of concentration 0.5 to 2M were used as reactants.

The prepared solution of oxalic acid were transferred into the test tube followed by addition of appropriate volume of agar gel and then kept undisturbed for aging period of few days. After setting and aging over the set-gel, the solution of barium chloride (desire volume and molarity) which is the reactant, was poured gently along the wall and allowed to diffuse into the gel medium. The open end of test tube was closed with cotton plug to protect from dust particles and kept undisturbed at room temperature.

We keenly observed the reaction and noticed that a thin precipitation layer was formed on the surface of the gel. This precipitate band increased gradually and diffusion proceeded into the gel. After 5 to 6 days nucleation process observed at the interstitial sides inside the test tube and then some transparent, star, platy shapes crystals were noticed. The crystals were harvested by washing them carefully with acetone. Prismatic, opaque, and platy shaped crystals were obtained with maximum size of a $3 \times 4 \times 2 \text{ mm}^3$.

The reaction which leads to the growth of crystals is expressed as



The optimum conditions for growing a well-defined crystals are given in table 1.

Table 1. The optimum condition established for growth of barium oxalate crystals

Sr. No	Conditions	Single Diffusion
1	Percentage of gel	1%
2	Con. of Barium Chloride	1M
3	Volume of Barium Chloride	5 ml
4	Con. of Oxalic acid	1M
5	Volume of oxalic acid	10 ml
6	Gel setting period	24 hours
7	Gel aging period	32 days
8	Temperature	Room temperature
9	Quality	Star shaped, Needle shaped, Platy shaped
10	Size	1 to 5 cubic mm

3. Growth kinetics

The growth of barium chloride was observed while growing in a test tube and effect of various parameters such as percentage of gel, concentration of first and second reactants, reversing and aging periods were studied.

3.1 Effect of aging period

To observe the effect of aging period on the growth of barium oxalate crystals. The aging period changes from 24 to 48 hours, while other parameters kept constant. We have found 24 hours aging period indicating the fast growth rate.

3.2 Effect of percentage of gel

To observe the effect of percentage of gel on the growth of crystals, all other parameters were kept constant except the percentage of the gel. It was found that for lower percentage (0.5%) of gel, the growth was slow and form small particles which were in large in number. When percentage of gel increased from 1.0 to 1.5% dendrite shaped crystals growth was observed. The size and appearance of growing crystals found more precise for 1.0% of gel as compare to other percentage of gel. As shown in Fig.1 (a)–(e) good, transparent crystals of barium oxalate having cubic to cylindrical shaped crystals were obtained.



Fig1 (a)



Fig1 (b)



Fig1 (c)

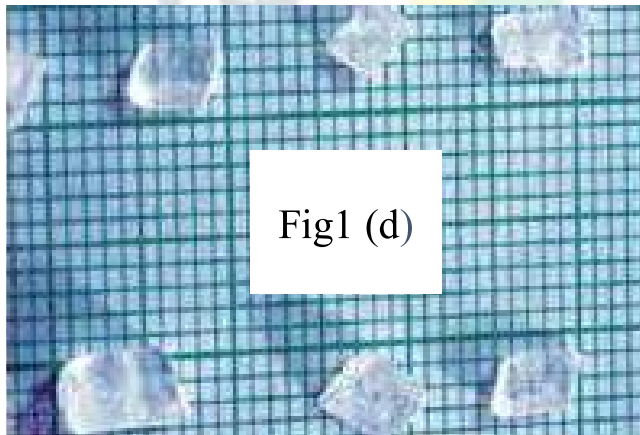


Fig1 (d)

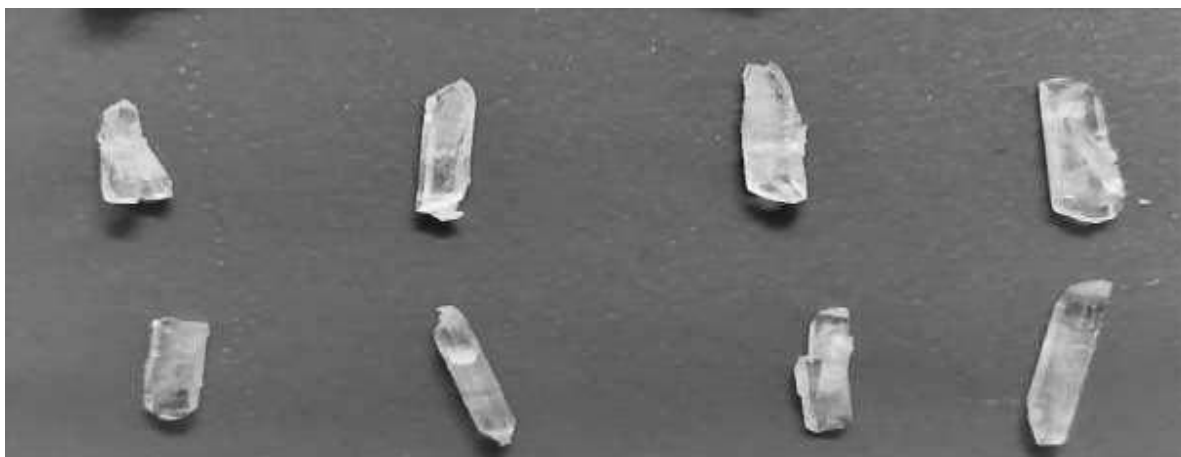


Fig 1(e)

Figure 1 (a-e): Photographs of barium oxalate grown crystals.

4. Result and discussion

4.1 X-ray diffraction studies

X-ray diffractogram is useful method to analyze the crystal structure of unknown material. X-ray diffractogram of gel grown barium oxalate crystals was recorded using powder rotation photograph method on Minislex Regaku X-ray diffract meter at Dept. of Physics at Shivaji University Kolhapur. The sample was rotated in the range 10° - 80° (2θ), scanning speed was kept $2^{\circ}/\text{min}$ and chart speed was $2\text{ cm}/\text{min}$. X-ray diffractogram of barium oxalate is shown in fig. 2.

From the diffraction pattern, “d” values and (h, k, l) planes were computed. Calculated “d” values are well matched with the reported ones. The unit cell parameters and system calculated by the computed program are given in table 2. These parameters satisfy the conditions for monoclinic system. i.e. $a \neq b \neq c$ & $\alpha \neq \beta \neq \gamma$.

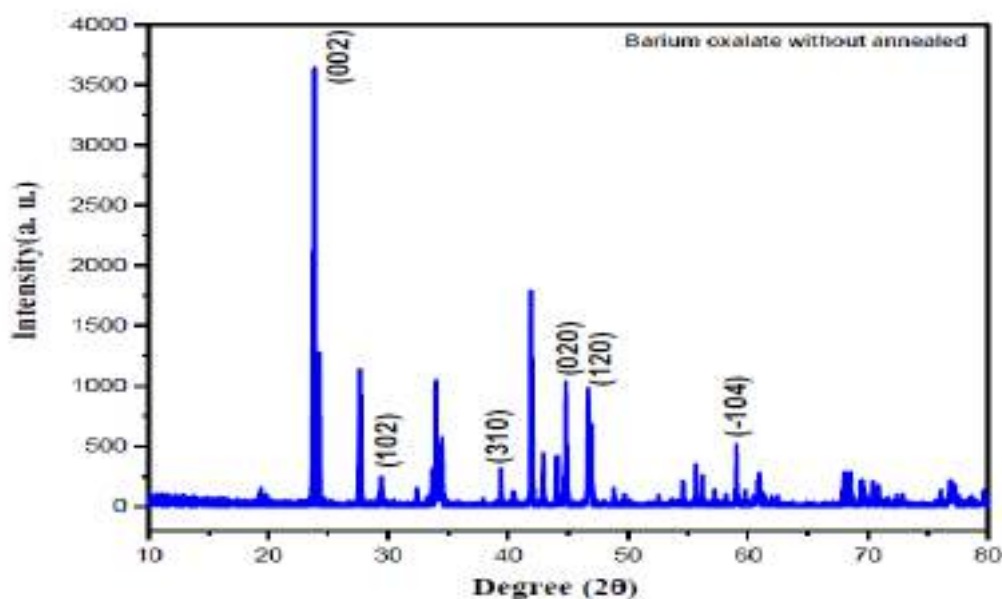


Figure 2: X-ray diffraction pattern of as grown barium oxalate single crystal.

4.2 Fourier transform infrared (FTIR)

The Fourier transform infrared (FT-IR) spectrum of barium oxalate was recorded at room temperature in the spectral range of 500 – 4500 cm^{-1} by KBr pellet method using SHIMADZU spectrophotometer at the department of Physics, Shivaji University Kolhapur. Figure 3 shows the FTIR spectrum of barium oxalate. A few of the prominent vibrational modes are empirically assigned here. The bands around 2950 to 3650 cm^{-1} are attributed to asymmetric and symmetric –OH stretching of water. The –OH stretching frequency of barium oxalate appeared at 2923 cm^{-1} . The moderate absorption around the 3500 to 3200 cm^{-1} is probably due to stretching of alcohol group. The fundamental FT-IR frequencies observed in all barium oxalate crystals [11]. Table 3 shows FTIR spectral and vibrational assignments of barium oxalate.

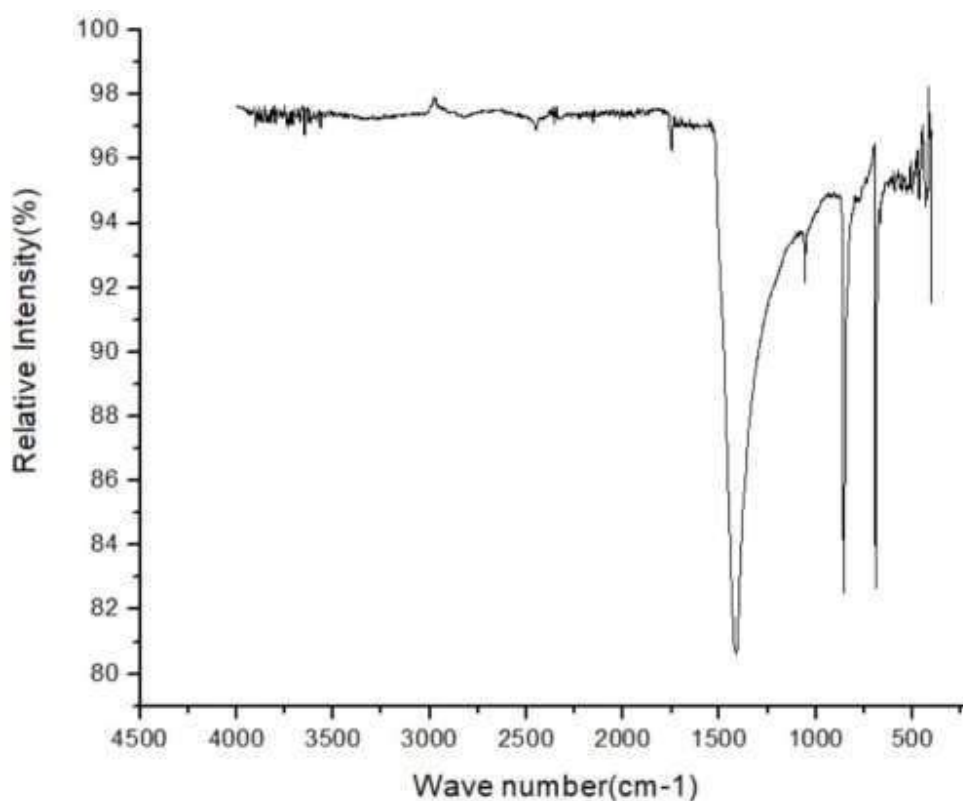


Figure 3. FTIR of Barium oxalate crystal

Table 3. FT – IR spectral and vibrational assignments of barium oxalate.

Wave number cm^{-1}	Intensity	Assignments
3640 - 3610	S,sh	O – H Stretch
3500 – 3200	S,b	O–H Stretch
3330 - 3270	n,s	C=C -H Stretch
3300 – 2500	m	O –H Stretch
3000 - 2850	m	H-C = O Stretch
1710 - 1665	s	C = O stretch
1370 -1350	s	C – H rock
1000 -650	m	= C- H bend
700 - 610	b	C –H bend

m= medium, W = weak, S = strong, B = broad, Sh = sharp, n = normal.

Scanning Electron Microscopy (SEM)

In the present work powdered sample of barium oxalate crystals was examined by using SEM technique at the Dept. of Physics Shivaji University Kolhapur. The study of the surface of the crystal gives valuable information about its internal structure. Figure 4 (a) illustrates SEM photographs of single crystals of barium oxalate crystal. High resolution SEM image is shown in Figure 4 (b). It is observed that due to growth conditions voids are created at the grain boundary. SEM images revealed that the growth of barium oxalate crystals consist of flat layered particles as well as spherical small grains. The individual flat grains possessed sharp edge [13].

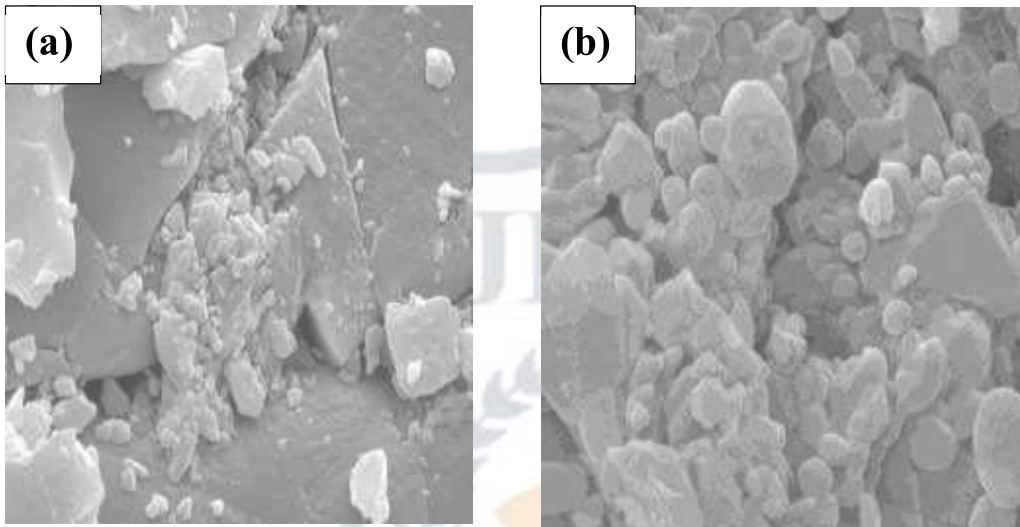


Figure 4: SEM images of as grown (a) barium oxalate crystal and (b) high resolution image.

UV-Vis Absorption spectroscopy

Absorption spectrum of barium oxalate crystals was obtained by a SHIMADZU UV-2450, UV-Vis spectrophotometer at the Dept. of Physics Shivaji University Kolhapur. Figure 5 shows UV-Vis absorption spectrum of barium oxalate crystal. Spectrum shows that the barium oxalate crystal allows to pass the entire visible and IR wavelengths and absorbs only ultra-violet wavelengths and therefore, the absorption coefficient is high at low wavelengths and high at short wavelengths. Since it is transparent crystal for wide range of wavelength (350-900 nm), the barium oxalate crystals can be used for second and third harmonic generations of the 1064 nm radiation [14-15]. Optical band gap energy of the as-grown barium oxalate crystals is calculated using the following simple conversion equation;

$$\text{Band gap energy (eV)} = \frac{1240}{\lambda \text{ (nm)}}$$

The band gap energy of barium oxalate crystal is found to be 4.06eV and tabulated in table 4.

Table 4: the band gap energy of Barium oxalate crystals.

Crystal	λ (nm)	Band gap Energy(ev)
Barium oxalate	305.00	4.06

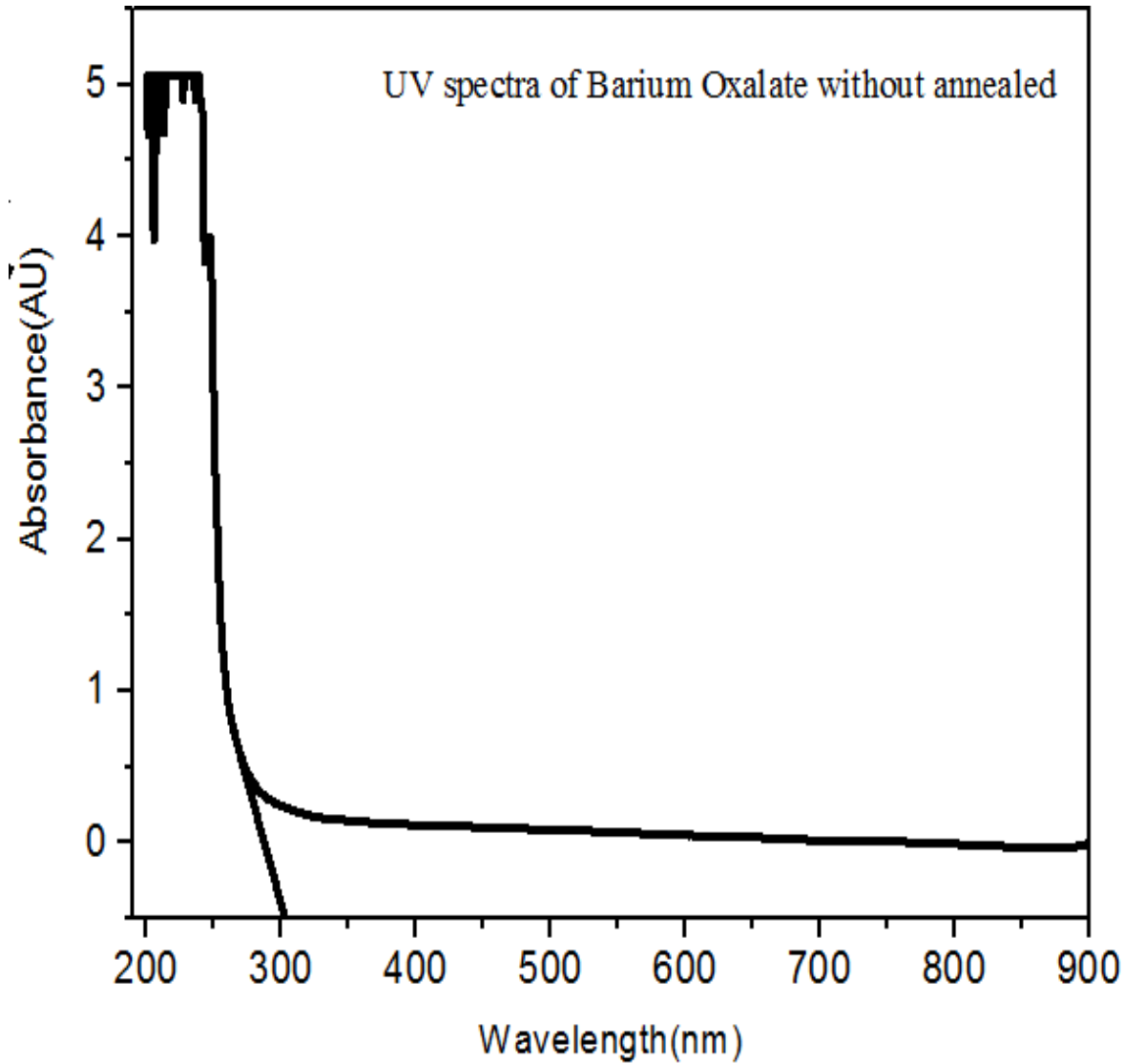


Figure 5: Optical absorption spectra of as-grown barium oxalate crystal.

5 Conclusions

From systematic investigation on the single diffusion gel growth of the barium oxalate crystals. Best conditions have been established to get good crystals.

- 1) Gel method is found suitable for growing barium oxalate crystals.

- 2) The growth of barium oxalate crystals was accomplished by allowing diffusion of barium chloride solution through agar-agar gel impregnated with oxalic acid in single diffusion gel tube system, with all growth conditions. Barium oxalate crystals possessed cubic and cylindrical shapes
- 3) The crystals obtained in agar-agar gel with average size of $3 \times 4 \times 2 \text{ mm}^3$ in single diffusion.
- 4) Different habits of barium oxalate crystals can be obtained by changing parameters like gel density, gel aging pH of gel, concentration of reactant etc.
- 5) The 'd' values of grown material obtained from the XRD are well matches with POWD Programmed.
- 6) The FTIR, studies suggested different characteristics features and morphology of grown crystals.
- 7) UV-Vis absorption spectra of barium oxalate crystal showed 4.06 eV optical band gap energy.

Acknowledgements

The authors are grateful to Principal Dr. R. R. Ahire, V.V.M's S. G. Patil College, Sakri, for providing laboratory facilities. Our special thanks to Prof. Mukesh Padvi, Department of Physics, Shivaji University Kolhapur, for providing characterization facilities like XRD, FTIR and SEM. One of the authors (SJN) is thankful to Dr. B. D. Borse, Principal, Uttamrao Patil College Dahivel for his inspiring suggestions.

References

- [1] H.K. Henisch; In crystal growth in gels, Pennsylvania state university press. **20**(1973).
- [2] H.K. Henisch; In crystals in gel and lies gang rings, Cambridge university press, Cambridge ;(1988).
- [3] H. W. Liaw, J. W. Faust; Jr. In American conference on crystal growth, Gaithersburg, Maryland (1969).
- [4] H.W.Liaw,J.W.Faust;Jr. J. Cryst. Growth **13-14**, 471(1972).
- [5] A.R.Patel and A.V.Rao; J.Cryst.Growth **43**, 351(1978).
- [6] K.V.Kurian and M.A.Ittyachen; J. Mater, Sci. **15**, 1724(1980).
- [7] K.Suryanarayana and S.M.Dharamaprakash; Mater.Chem.Phys.**42**, 92(2000).
- [8] S.K.Arora; Advanced in gel growth,A review progress in crystal growth and characterization of materials **4**, 345(1981).
- [9] S.K. Arora, Vipul Patel,Kothari and Brijesh Amin; Crystal growth and design **343-349**,4(2004).
- [10] S.A. Firdous, I. Quasim,M.M.Ahmad and P.N.Kotru;Bull.Mater.Sci.**377 – 382**,33 (2010).

[11] K. Nakamoto 1970 'Infrared Spectra of inorganic and co-ordination Compounds' (New York;John wiley and sons Inc) 2nd edn..

[12] S.J.Nandre, S.J.Shitole and R.R.Ahire, Archives of Physics Research, 2012, 3(1) PP70-77.

[13] S.J.Nandre, S.J.Shitole, S.S.Sonawane and R.R.Ahire, International Journal of Basic and Applied Research, special issue 2012, 125-128.

[14] Nisha Santha kumaria, P. Kalainathan, S. Cryst.Res. Technol.4 (2008)317.

[15] Kalaisevi. D., Mohan Kumar. R, and R Jayavel, Cryst.Res.Technol.8 (2008)851.



Physical and Morphological Study of Barium Oxalate Crystals Grown by Agar-Agar Gel Method

H. S. Pawar¹, S. J. Nandre², S. D. Chavhan³ and R. R. Ahire³

¹V.J.N.T. Late Dalpatbhau Rathod Junior College, Mordadtanda (Dhule) M.S

²Department of Physics, Uttamrao Patil Arts and Science College, Dahiwel, (Dhule) M.S

³Department of Physics S.G. Patil Art's, Commerce and Science College, Sakri (Dhule) M.S

ABSTRACT

Barium oxalate crystals were grown by agar-agar gel through the single diffusion technique. The tendency of barium oxalate crystals to cylindrical growth was demonstrated. The optimum growth conditions barium oxalate was achieved by controlling the parameters like, concentration of gel, concentration of reactants, aging period and reversing of reactants. The crystal structure of grown material was determined by TGA, DTA, DSC and EDAX.

Keywords: Crystal growth, Barium oxalate, TGA, DTA, DSC, and EDAX.

Introduction

The growth of crystal occurs not only in the crust of Earth or in laboratory but also in a living body. Many crystals, particularly, bio-materials and proteins, cause various ailments and health related problems. The urinary stones are usually composed of either pure or mixed crystals of calcium oxalate, brushite, struvite, and hydroxyapatite and carbonate apatite [1]. Arthropathies, i.e., bone and joint diseases, are caused by crystals such as hydroxyapatite, calcium pyrophosphate and monosodium urate monohydrate [2]. There are other crystals which play important role in various ailments, for instance, f.c.c. type ferritin crystals in development of cataract [3] and cholesterol crystals for cardiovascular diseases and gall stones [4]. This bio-crystallization occurring in human body causes suffering and it is not desirable to occur. This has been discussed in detail by the predecessors of the present author [5-7]. There are several micro-organisms which synthesize crystals, for example, magneto-tactic bacteria synthesizing magnetite [8], chrysophytes [9] diatoms and act in opoda synthesizing siliconous materials and S. layer bacteria synthesizing gypsum and calcium carbonate surface layers [10]. Calcite crystals are found in mollusk shells [11] and as a component in gall stones [12]. The earlier crystal growth study was divided into two parts :(1) The study of the equilibrium between the crystal and surrounding medium(2) The study of the kinetics of growth.

Experimental

Experimental procedure 5 gm of agar-agar powder was dissolved in to hot double distilled water mixed with 0.5 M to 1 M barium chloride solution was incorporated then again the mixture was stirred to make homogenous mixture. The crystallizing vessel were used essentially consist of standard glass tube having inner diameter 2.5 cm and the length 25 cm. Gelling mixture poured in glass test tubes. These tubes were hermitically sealed to prevent evaporation and contamination of the exposed surface by dust particles of atmosphere or atmospheric

impurities and were kept undisturbed. Usually in 3 to 4 days the gel was to be set which depends on the environmental temperature. It was observed that the mixture in a glass tube was initially transparent and slowly turned light white. The water slowly evaporated and gel was completely set. After ensuring firm gel setting, it was kept for aging for 3 to 4 days. After that 0.5 M to 1 M solution of oxalic acid was added as a supernatant over the set gel. Nucleation was observed after 5 to 6 days and crystals started to grow. White color, larger size, transparent and shining crystals were obtained in the gel, as shown in fig.1, Optimum condition tabulated in table 1, [13].

Table 1 Optimum conditions for barium oxalate crystal grown by agar-agar gel method

Concentration of agar-agar gel	5 %
Concentration of reactant, strontium chloride	1M
Concentration of supernatant, oxalic acid	1 M
Room temperature	27 ⁰ C
Gel aging period	4 days
Growth period	25 - 40 days
Quality of crystals	White colour, larger size (1mm × 1mm) transparent, shining crystals

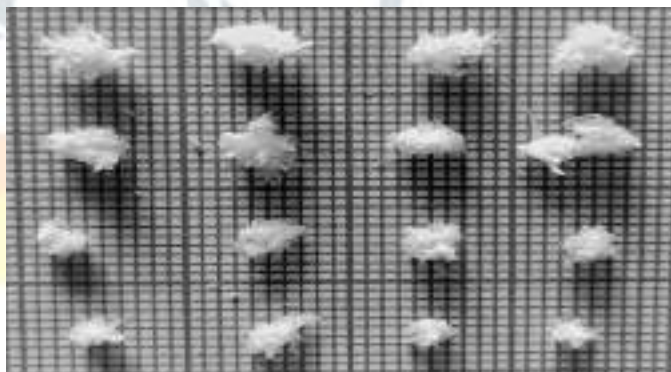


Fig.1 (a) Barium crystal inside the test tube (b) Opaque and shiny crystals

Result and Discussion-

Thermo-Gravimetric Analysis (TGA)

TGA was carried out at Department of Physics, Shivaji University Kolhapur, TGA curve for barium oxalate is shown in figure.2. From the thermo gram of barium oxalate one can observe that

- i) The compound is stable up to 50⁰C.
- ii) 5.165% weight loss in temperature range 50⁰C. To 172⁰C may be due to dehydration of water molecule and up to 172⁰C there is no further loss of weight.
- iii) 25.68% weight loss in temperature range 172⁰C to 277⁰C from the dehydrated compound corresponds to loss of CO.
- iv) 36.68% weight loss in temperature range 277⁰C to 435⁰C corresponds to loss of CO₂.
- v) 13.45% weight loss in temperature range 435⁰C to 478⁰C.
- v) The residue remains stable from 478⁰C and decompose the material. [14-16].

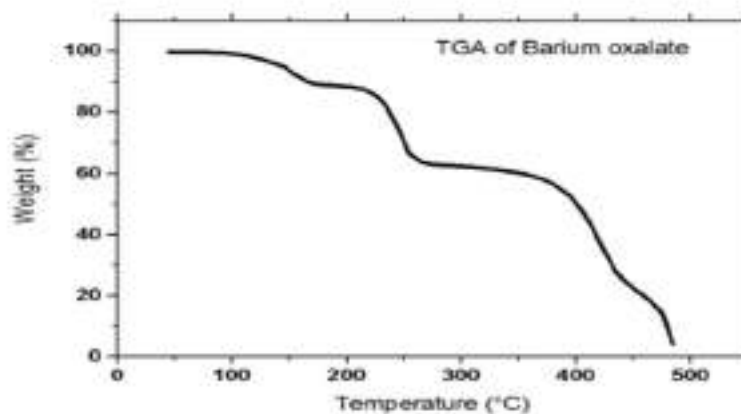


Figure 2 TGA of Barium oxalate crystal grown by agar-agar gel

TGA data indicates that the grown crystals contains water molecule,

Table 2 TGA Data of Barium oxalate

Stage	Temperature range	Observed % weight loss	Calculated % weight loss	Loss of molecule in stage
I	50 ⁰ C-172 ⁰ C	5.165%	5.045%	H ₂ O
II	172 ⁰ C-277 ⁰ C	25.68%	25.8%	It may be CO
III	277 ⁰ C-435 ⁰ C	36.68%	35.99%	CO ₂
IV	435 ⁰ C-478 ⁰ C	13.45%	13.56%	-

Differential Thermal Analysis (DTA)

DTA was carried out at Department of Physics, Shivaji University Kolhapur. DTA curve for barium oxalate is shown in figure3. From the thermo gram of barium oxalate one can observe that.

In DTA curve of barium oxalate by agar-agar gel at 37.51⁰C an endothermic peak is observed due to the loss of bulk of water of crystallization. The decomposition of oxalate is observed at the onset due to complete dehydration. In DTA curve the exothermic peaks at 153.⁰C to 154.54⁰C shows the decomposition of oxalate. Loss of weight at the temperature range 153.⁰C relates to the loss of water of crystallization which is endothermic in character.

Loss of weight at the temperature 250.07⁰C endothermic peak is observed that means the weight loss with respect to temperature of the grown crystals was further supported by

DTA results. DTA data is shown in table- 3

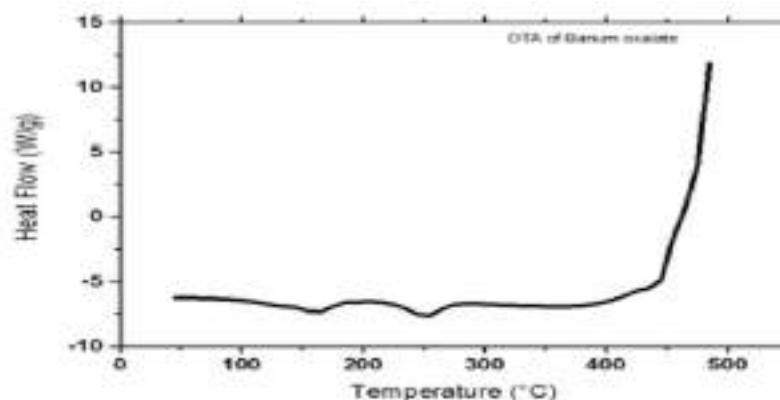


Figure 3 DTA of Barium oxalate

Table no.3 DTA data of barium oxalate

Peak recorded	Peak height	Nature	$\Delta H(J/gm)$
37.51 ⁰ C	-0.600	Endothermic	-0.6406
154.54 ⁰ c	-0.5	Exothermic	-0.5344
250.07 ⁰ c	-0.4	Endothermic	-0.4613

Differential Scanning Calorimeter (DSC)

DSC was carried out at Department of Physics, Shivaji University Kolhapur, The DSC thermogram was recorded in the temperature range from 25⁰C to 450⁰C. Microcrystalline (powdered) samples of barium oxalate crystals were taken for DSC studies and the weight of the sample 8.5230mg. The sample was hold for 10 min in air to evaporate water due to moisture and then heated from 25⁰C to 450⁰C. at the rate 10c/min in Air .After reaching the temperature of 450⁰C, the sample was hold for I minute at 450⁰C and then again cooled from 450⁰C to 25⁰C at the rate of 10C/min in Air.

The DSC curve for barium oxalate gel grown crystal shown in figure 4. And the DSC data collected from this curve is tabulated in the table 4.

Step-I

i) The initiation temperature is 225⁰C and equilibrium temperature 277⁰C. At 225⁰C (initiation temperature) initiation of phase change start & is completed at peak endo-down temperature of 250.07⁰C (transition temperature). The temperature at which the sample and the reference come to the thermal equilibrium by thermal diffusion appears to be at 277⁰C. The peak appeared in the DSC curve at 154.54⁰C indicates the phase transformation due to loss of water molecules and formation of stable anhydrous barium oxalate. This is the good agreement with the TGA curve,

ii) Area under the curve is 5707.384 mJ.

iii) Heat of transition ΔH i.e. enthalpy change of transition 517.56 J/g which 0.51756kJ/mole. Since molecular weight is 1g/mole, $\Delta H_{tr} = \Delta H_f$ i.e. heat of phase transformation is also 0.5756 kJ/mole, where ΔH_f is enthalpy change of new phase transformation or it is called heat of phase formation.

Step-II

- i) The initiation temperature is 430⁰C and equilibrium temperature is 450⁰C. At 430⁰C (initiation temperature) initiation of phase change starts and is completed at peak endo- down temperature of 438.76⁰C (transition temperature). The temperature at which the sample and the reference come to the thermal equilibrium diffusion appears to be 450⁰C. The further phase transition occurs at temperature 438.76⁰C due to the loss of carbon and H₂O and formation of stable barium oxalate. This is good agreement with TGA Curve.
- ii) Area under the curve is 232.43mJ.
- iii) Heat of transition ΔH i.e. enthalpy change of transition 21.99J/g which is 0.02199KJ/mole. Since molecular weight is 1 g/mole, Hence $\Delta H_{tr} = \Delta H_f$ i.e. heat of phase transformation is also 0.02199KJ/mole. Where ΔH_f enthalpy change of new phase transformation or it is called heat of phase formation. DSC data is shown in table- 4.

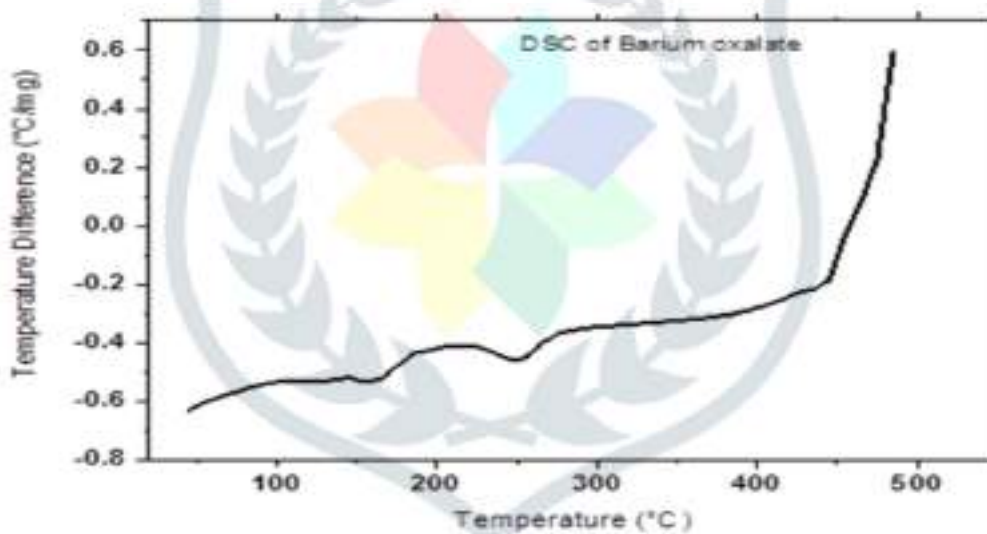


Figure 4 DSC curve for Barium oxalate

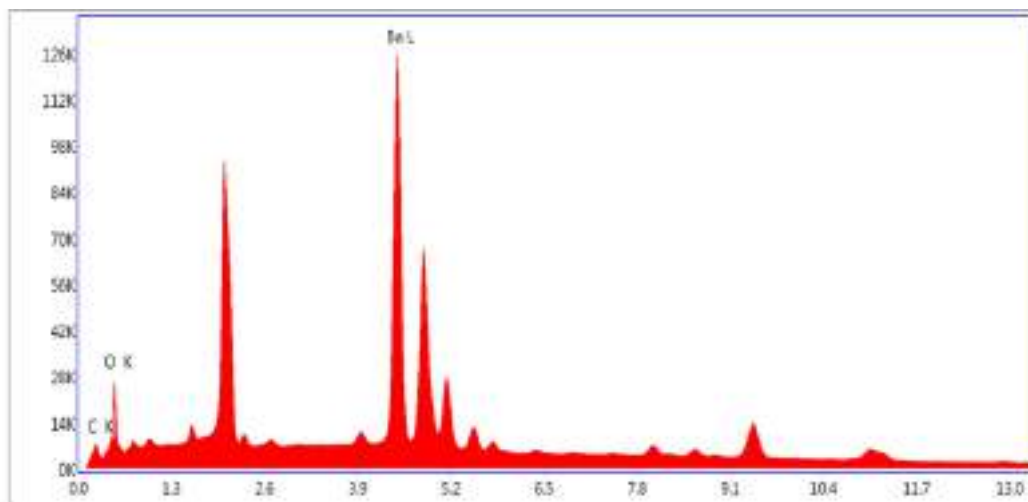
DSC data is shown in table- 4

Sample	Weight of the sample	Stage	Change in the enthalpy(ΔH)	Transition temperature (Tr)
Barium oxalate	0.8523gm	I	0.51756KJ/mole	250.07 ⁰ C
		II	0.02199KJ/mole	438.76 ⁰ C

Energy Dispersive Analysis by X-rays (EDAX) –

Energy Dispersive analysis by X-ray (EDAX) is used for the quantitative analysis of barium oxalate and is also called as elemental analysis. Fig 5& Table No 5 shows, in present work elemental analysis of gel grown barium oxalate crystals was Department of Physics, Shivaji University Kolhapur. It conclude that the (weight

& atomic %) of copper (Cu) in the grown crystal measured by EDAX are very close with the values calculated from the molecular formula.[17-20]



eZAF smaryt quant Results

Element	Weight%	Atomic%	Net.Int	Error	%	K ratio	Z	R	A	F
Ck	7.36	34.64	443.18	7.82	0.05	0.05	1.47	0.75	0.47	1.00
Ok	8.71	30.80	991.30	7.87	0.05	0.05	1.42	0.77	0.39	1.00
Barium	83.93	34.56	5594.20	2.05	0.80	0.80	0.91	1.07	1.03	1.03

Conclusions —

The present work reports the growth and characterization of barium oxalate single crystals. We have demonstrated the formation of barium oxalate single crystals in agar-agar gels. Barium oxalates exhibits micro-rod-like and spherulites growth (flower) shape are observed. Further to obtain good quality single crystals of barium oxalate, both reactants –barium chloride and oxalic acid were interchanged. With barium chloride incorporated gels result only fibers. These facts have been explained by taking in account the interaction of the reactants ions with the sodium and silica ions. The effect of temperature on growth of barium oxalate crystals showed that there is a decrease in nucleation density at higher temperature which is due to the increases of the aqueous solubility of barium oxalate.

References

- [1] M. Menon, B. G. Parulkar and G. W. Drach; Campbell's Urology, W. B. Saunders, New York, 9th Edition,3 (1998) 2662-2676.
- [2] S. J. Gupta; J. Indian Rheumatol Assoc., 10(2002) 5-13.
- [3] D. G. Brooks, K. Manova-Todorova, J. Farmer, L. Lobmayr, R. B. Wilson, R. C. Eagle, Jr., T. G. St. Pierre and D. Stambolian; Invest. Ophthalmol. Vis. Sci., 43(2002)1121.
- [4] S. P. Wrenn; "Engineering Approaches to Cholesterol-Linked Diseases", (2001).

- [5] V. S. Joshi; Ph. D. Thesis, Saurashtra University, Rajkot (2001).
- [6] K. C. Joseph; Ph.D. Thesis, Saurashtra University, Rajkot, (2005).
- [7] B. B. Parekh; Ph. D. Thesis, Saurashtra University, Rajkot (2006).
- [8] R. B. Frankel and R. P. Blakemore; "Eds in Iron Biominerals, Plenum", New York, (1991).
- [9] J. Kristiansen and R. A. Andersen; "Eds in Chrysophytes Aspects and Problems", Cambridge University Press, Cambridge (1986).
- [10] M. Sarikaya; Proc. Natl. Acad. Sci. USA, B96(1999) 14183.
- [11] C. E. Bowen and H. Tang; Comp. Biochem. Physiol., 115A(4)(1996)269.
- [12] D. S. June and E.S. Weley; Science, 159 (1968)1113.
- [13] P.V.Dalal and K.B.Saraf, : "Bull.Mater.Sci" Vol.29 N0.5,2006 421-425.
- [14] K.S.Raju, Johan Varughese and M.A.Ittyachen; " Bull. Mater.Sci." 21(1998)375.
- [15] D.K.Sawant, H.E.Patil, D.S.Bhavsar, K.D.Girase and J.H.Patil; "Journal of Thermal Analysis and Calorimetry," 107 (2012)3.
- [16] N. S. Patil, P. A. Savale, S. K. Bachhav and S. T. Pawar ; ' Archive of physics research', Vol2(1), (2011). 39-47,
- [17] D. K. Sawant., H. M. Patil and D. S. Bhavsar., 'Pelagia research Library, DCS' Vol2(3), (2011) 63,
- [18] D. K. Sawant., H. M. Patil and D. S. Bhavsar., 'Scholars Research Library Archives of Physics Research', Vol2(2), (2011). 67.
- [19] S.J.Nandre, S.J.Shitole and R.R.Ahire; "Journal of Nano and Electronic Physics" Vol.4,4,(2012)4013.
- [20] M.Selvapandiyan, S. Sudhakar and M.Prasath; "Int. Journal of Engineering Research and Application", Vol. 7,8,(3) (2017), 65-72.

Vidya Vikas Mandal's
Sitaram Govind Patil Arts,
Science and Commerce College,
Sakri Tal. Sakri Dist. Dhule 424 304



NAAC
ACCREDITED

विद्या विकास मंडळाचे,
सिताराम गोविंद पाटील कला,
विज्ञान आणि वाणिज्य महाविद्यालय,
साक्री ता. साक्री जि. धुळे ४२४ ३०४

Affiliated to Kavayitri Bahinabai Chaudhari North Maharashtra University, Jalgaon

Website : www.sgpcsakri.com

Email : vidyavikas2006@rediffmail.com

Ph : 02568-242323

3.3.2.1 Research Paper Published in Peer Reviewed and Referred Journals



Growth and Characterization of Cobalt Oxalate Crystal by Ager-Ager Gel Method

H.S.Pawar¹, S.J. Nandre², N.B.Sonawane³, **S. D. Chavhan⁴** and R.R.Ahire⁵

¹V.J.N.T. Late Dalpatbhau Rathod Junior College, Mordadtanda (Dhule)

²Department of Physics, Uttamrao Patil Arts and Science College, Dahiwel, (Dhule) M.S

³Department of Physics, Karm. A.M. Patil Arts, Commerce and Science College, Pimplaner (Dhule) M.S

^{4,5}Department of Physics S.G. Patil Art's, Commerce and Science College, Sakri (Dhule) M.S

Abstract

We have grown the cobalt oxalate crystals by adopting single diffusion technique via agar-agar gel. The tendency of cobalt oxalate crystals to form splices, twins, spherulites and dendrites was demonstrated. The growth dynamic of cobalt oxalate was studied by controlling the parameters like, concentration of gel, concentration of reactants, aging period and reversing of reactants. Physical properties of the grown crystals were analyzed by XRD, and FTIR techniques and the results are discussed.

KEYWORDS: Gel, Crystal, Gel Growth, Crystal Growth, XRD, and FTIR

Introduction

Crystals grown by the gel method has gained interest in the research community because it is cheap and easy to grow single crystals of alkaline-earth metal oxalates [1] and transition metal oxalates [2]. These materials have interesting properties like low solubility in water [3], decomposition before freezing point [4], interesting optoelectronic properties. Their role in analytical chemistry and subsequently in industries [5, 6] has created an opportunity for the researcher to investigate every scientific aspect of these materials. Therefore, efforts are being made to investigate and study the physical and chemical properties of these materials. Recently, there are reports on the growth of mixed-ligand complex formation using cadmium oxalate [7]. In the present study, we have presented the optimization of growth parameters to grow the cobalt oxalate single crystals using the agar gel method.

Materials and Methods

Materials used to grow the cobalt oxalate crystals are cobalt chloride, oxalic acid, and agar-agar gel. All the chemicals used for the experiment were used without any further purification. Sodium silicate glass test-tubes were used as crystallizing vessels. The test-tubes were filled with the first reactant (cobalt chloride) of desired volume and morality. The second reactant, oxalic acid having a concentration range of 0.5 to 1.0 M, was poured along the walls of the test-tube into the set-gel, and allowed to diffuse into the gel medium. The open end of the tube was closed with cotton plugs and kept undisturbed. The said procedure was carried out at room temperature. The ions of the supernatant solution reacted with ions of the first reactant via capillaries formed in gel medium. After six to seven days, nucleation kick-started at the gel-solution interface. The chemical reaction that occurred between the two reactants is given as follows:



The diamond-shaped opaque crystals were obtained in the test-tube. The crystals were harvested by washing them carefully with acetone and collected for further characterization. Table 1 shows the optimized crystal growth parameters for the cobalt oxalate crystals.

Sr.No	Condition Single Diffusion	Condition Single Diffusion
1	Percentage of gel	2.0 %
2	Concentration of cobalt chloride	1.0M
3	Concentration of oxalic acid	1.0M
4	Volume of cobalt chloride	5.0 ml
5	Volume of oxalic acid	15 ml
6	Gel setting period	34 Hours
7	Gel aging period	4 days

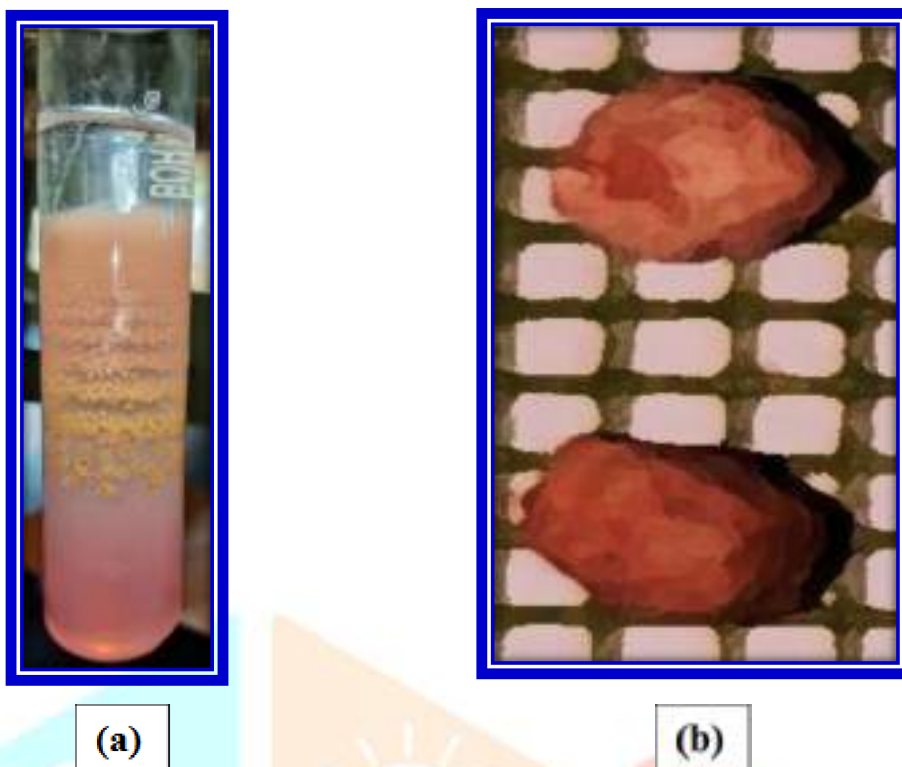


Figure 1:(a) in situ growth of Cobalt oxalate crystals in test-tube and (b) optical photograph of cobalt oxalate crystals

Result and discussion

The crystal structure analysis of the grown cobalt oxalate crystal was done via X-ray diffraction. X-ray pattern was recorded from the range of 10 to 80 degrees. The occurrence of highly resolved intense peaks at specific Bragg angles 2θ indicates the high crystallinity of the grown material and revealed monoclinic structure. The obtained crystal data has been compared with the JCPDS data and it closely matched with the reported JCPDS no. 037-0719. The unit cell parameters ($a = 5.39820 \text{ \AA}$, $b = 5.03100 \text{ \AA}$, and $c = 5.73590 \text{ \AA}$) are close to the reported cell parameters of $\text{CoC}_2\text{O}_4 \cdot 2\text{H}_2\text{O}$, indicating the monoclinic phase of cobalt oxalate crystal. Comparative data is tabulated in Table 2 for the gel-grown cobalt oxalate crystal.

Table 2. Comparison of unit cell parameters of cobalt oxalate.

Parameters	Calculated	JCPDS data
System	Monoclinic (P)	Monoclinic
a	9.67638 \AA	6.4534 \AA
b	6.7156 \AA	7.5009 \AA
c	8.6822 \AA	10.940 \AA

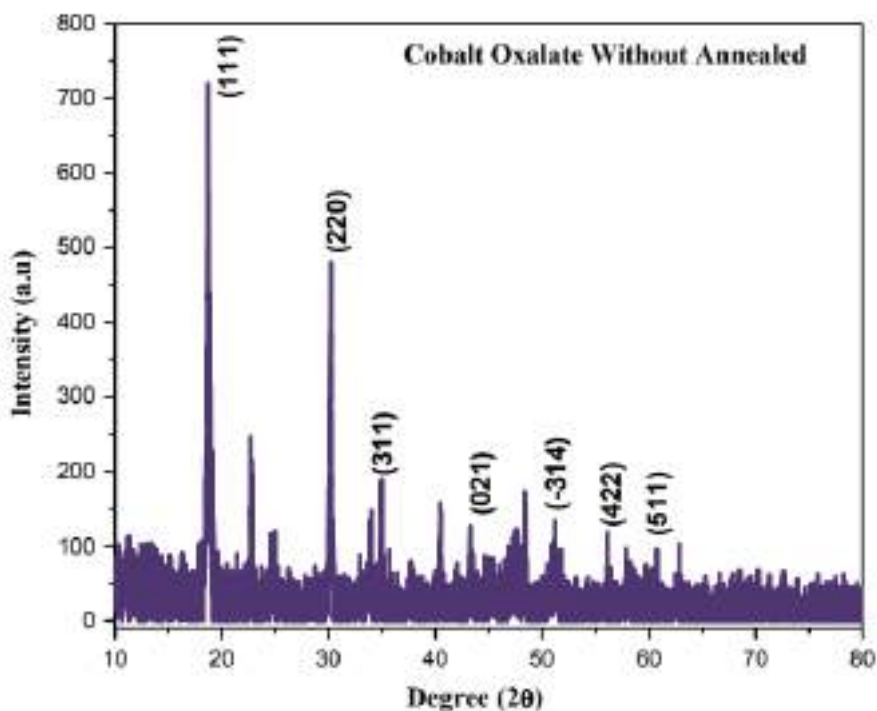


Figure 2: X-ray diffraction pattern of gel-grown cobalt oxalate crystal.

4.2 Fourier transform infrared (FTIR) Spectra

The Fourier transform infrared (FTIR) spectrum of cobalt oxalate was recorded at room temperature in the spectral range $500 - 4500\text{cm}^{-1}$ by KBr pellet method using SHIMADZU spectrophotometer at the department of Physics, Shivaji University Kolhapur. Figure 3 shows the FTIR spectrum of cobalt oxalate. The spectrum shows various frequencies of vibrational modes which confirm the presence of oxalate in the crystal.

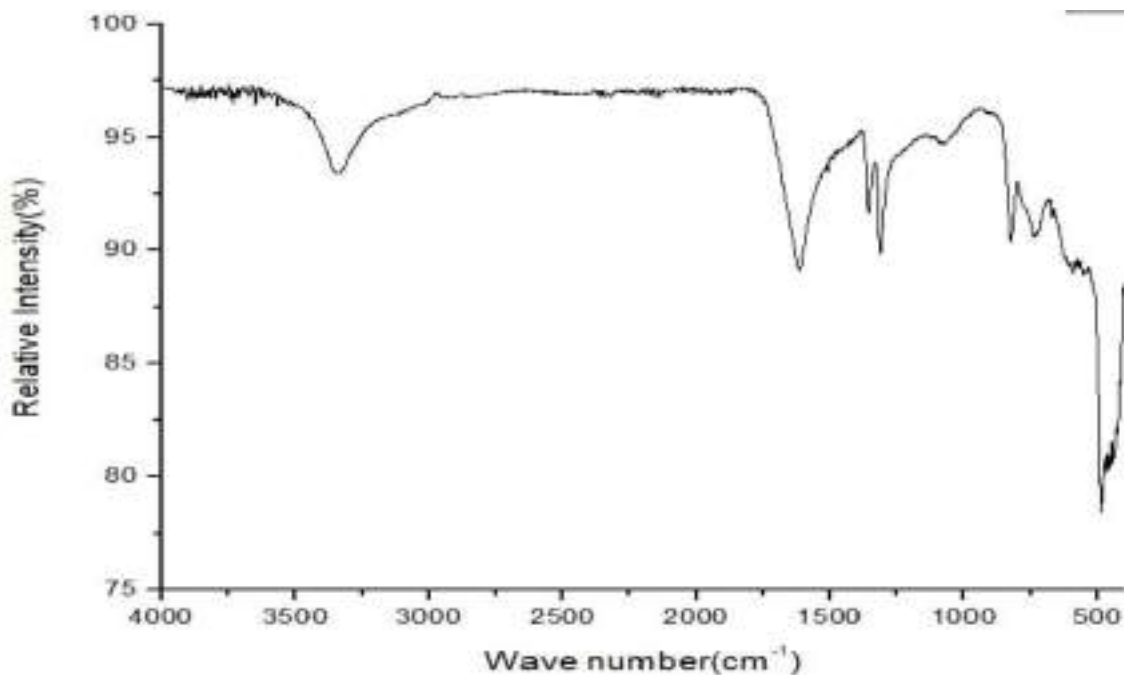


Figure 3: FTIR of Cobalt oxalate grown crystal

The sharp peak at 3300.18 cm^{-1} is attributed to the stretching of O–H group, indicating the presence of water of crystallization or water of hydration. However the peak at 1710.00 cm^{-1} to 1665.00 cm^{-1} correspond to α,β -unsaturated aldehydes, and ketones. The two identical sharp peaks around 1367.93 and 1327.43 cm^{-1} correspond to an asymmetric and symmetric stretch of C–H rock, respectively. Thus the FTIR spectroscopy confirmed the growth of cobalt oxalate crystals due to the presence of water of crystallization.

Conclusions

Cobalt oxalate crystals were grown by gel method using agar- agar gel in well size and shape. XRD powder diffraction patterns and analysis shows the crystalline nature of crystal with monoclinic phase. Different functional groups revealed by FTIR show the metal bond and different vibrations in the sample.

Acknowledgements

The authors are grateful to principal Dr. R. R. Ahire, V.V.M's, S. G. Patil college, Sakri, for providing laboratory facilities. Our special thanks are to Prof Mukesh Padvi, Department of Physics, Shivaji University Kolhapur, for providing facility for XRD and FTIR characterizations. One of the authors (SJN) is thankful to Dr. B. D. Borse, principal, Uttamrao Patil College Dahivel for his inspiring suggestions.

References

- [1] A. Pactor, *Kristall und Technik*, vol.12,no.7,pp.729–735, 1977.
- [2] S.K.Arora and T.Abraham, *Journal of Crystal Growth*,vol.52,no.2,pp.851–857,1981.
- [3] J. Dennis and H. K. Henisch, *Journal of The Electrochemical Society*,vol.114,no.3,pp.263–266, 1967.
- [4]N.V.Prasad,G.Prasad,T.Bhimasankaram,S.V.Surya-narayana, and G. S. Kumar, *Bulletin of Materials Science*,vol. 19, no. 4, pp. 639–643, 1996.
- [5] M. I. Diaz-Guemes, A. S. Bhatti, and D. Dollimore, *Thermochimica Acta*,vol.106,pp.125–132,1986.
- [6] Y. Okamoto and W. Brenner,*Organic Semiconductors*,ReinholdPublishing, Chapman & Hall, London, UK, 1964.
- [7] W. B. Schaap and D. L. McMasters, *Journal of the American Chemical Society*, vol.83, no.23, pp.4699–4706, 1961.
- [8] S.J.Nandre, S.S.Sonawane,R.R.Ahire and S.J.Shitole, *Der Pharma Chemica*, 2014, 6(3), PP.33-38.
- [9] S.J.Nandre, S.S.Sonawane, R.R.Ahire and S.J.Shitole, *Journal of Scientific Review*, 2014,1(1),1-6.
- [10] S.J.Nandre, S.S.Sonawane, R.R.Ahire and S.J.Shitole *Renewable Research Journal*, 2014, 3(1),PP. 47-52.
- [11] S.J.Nandre, S.J.Shitole, and R.R.Ahire, *International Journal of Chemical and Physical Sciences*, 2014, 1,PP.123-130.
- [10] AnilkumarKodge et al.,*Int.J.ofEng.Sci.and Tech.*,2011,3(8), 6381-6390. [11] Paul Bowen et al., *Nanoscale*, 2010, 2, 2470–2477.
- [12] Ren, L et al. *B. Q. Chem. Phys. Lett.* 2009, 476, 78–83.
- [13] R. L. Frost et al.*Chinese Science Bulletin*,2003, 48(17), 1844-1852.
- [14] Joanne Hayley Smith, Ph.D.Thesis, University of Natal.2001. [15] E Romero et al. *J.cond.-mat.mtrl –sci*, 2010,
- [15] S. J. Joshi, K. P. Tank, B. B. Parekh, M. J. Joshi, *Cryst. Res. Technol.* 45, No. 3, 303 – 310, 2010.
- [16] J. J. de Yoreo and P. Vekilov, *Crystal Growth*, vol. 35, pp. 24–30, 2008.
- [33] S. M. Arifuzzaman and S. Rohani, *Journal of Crystal Growth*, vol. 267, no.3-4, pp. 624–634, 2004.



Thermal and Morphological Study of Transition Metal Cobalt Oxalate Crystal Grown By Agar-Agar Gel Technique

H. S. Pawar¹, S. J. Nandre², S. D. Chavhan¹ and R. R. Ahire³

¹V.J.N.T. Late Dalpatbhau Rathod Junior College, Mordadtanda (Dhule) M.S

²Department of Physics, Uttamrao Patil Arts and Science College, Dahiwel, (Dhule) M.S

³Department of Physics S.G. Patil Art's, Commerce and Science College, Sakri (Dhule) M.S

ABSTRACT

In this article, we have reported fabrication of various morphological of cobalt oxalate. Cobalt oxalate crystals were grown by agar-agar gel through the single diffusion technique. The tendency of cobalt oxalate crystals to spherulites growth was demonstrated. Also Liesegang ring are observed. The cobalt oxalate preparation method was played crucial role on the crystal structure and its morphology. The optimum growth conditions cobalt oxalate was achieved by controlling the parameters like, concentration of gel, concentration of reactants, aging period and reversing of reactants. The crystal structure of grown material was determined by TGA, DTA and EDAX.

Keywords: Crystal growth, cobalt oxalate, TGA, DTA and EDAX.

Introduction:

Growth of crystal ranges from a small inexpensive technique to a complex sophisticated expensive process and crystallization time ranges from minutes, hours, days and to months. The starting points are the historical works of the inventors of several important crystal growth techniques and their original aim. Crystals are used in semiconductor physics, engineering, as electro-optic devices etc., so there is an increasing demand for crystal [1-5]. For years, Natural specimens were the only source of large, well-formed crystals. The growth of crystals generally occurs by means of following sequence of process. Diffusion of the molecules of the crystallizing substance through the surrounding environment. Diffusion of these molecules over the surface of the crystal to special sites on the surface. Today almost all naturally occurring crystals of interest have been synthesized successfully in the laboratory [6-9]. It is now possible only by crystal growth techniques.

Materials and Methods

Materials used to grow the cobalt oxalate crystals are cobalt chloride, oxalic acid, and agar-agar gel. All the chemicals used for the experiment were used without any further purification. Sodium silicate glass test-tubes were used as crystallizing vessels. The test-tubes were filled with the first reactant (cobalt chloride) of desired volume and morality. The second reactant, oxalic acid having a concentration range of 0.5 to 1.5 M, was poured along the walls of the test-tube into the set-gel, and allowed to diffuse into the gel medium. The open end of the tube was closed with cotton plugs and kept undisturbed. The said procedure was carried out at room temperature. The ions of the supernatant solution reacted with ions of the first reactant via capillaries formed in gel medium. After six to seven days, nucleation kick-started at the gel-solution interface. The chemical reaction that occurred between the two reactants is given as follows:



The diamond-shaped, spherulites, opaque crystals were obtained in the test-tube. The crystals were harvested by washing them carefully with acetone and collected for further characterization. Table 1 shows the optimized crystal growth parameters for the cobalt oxalate crystals.

Table 1 shows the Optimum condition of cobalt oxalate crystal

Sr.No	Condition Single Diffusion	Condition Single Diffusion
1	Percentage of gel	2.0 %
2	Concentration of cobalt chloride	1.0M
3	Concentration of oxalic acid	1.0M
4	Volume of cobalt chloride	5.0 ml
5	Volume of oxalic acid	15 ml
6	Gel setting period	34 Hours
7	Gel aging period	4 days

Liesegang rings - are a phenomenon seen in many, if not most, chemical systems undergoing a precipitation reaction under certain conditions of concentration and in the absence of convection. Rings are formed when weakly soluble salt are produced from reaction of two soluble substances, one of which is dissolved in a gel medium [10]. The phenomenon is most commonly seen as rings in a Petri dish or bands in a test tube; however, more complex patterns have been observed, such as dislocations of the ring structure in a Petri dish, helices', and Saturn rings in a test tube [11]. Despite continuous investigation since rediscovery of the rings in 1896, the mechanism for the formation of Liesegang rings is still unclear.

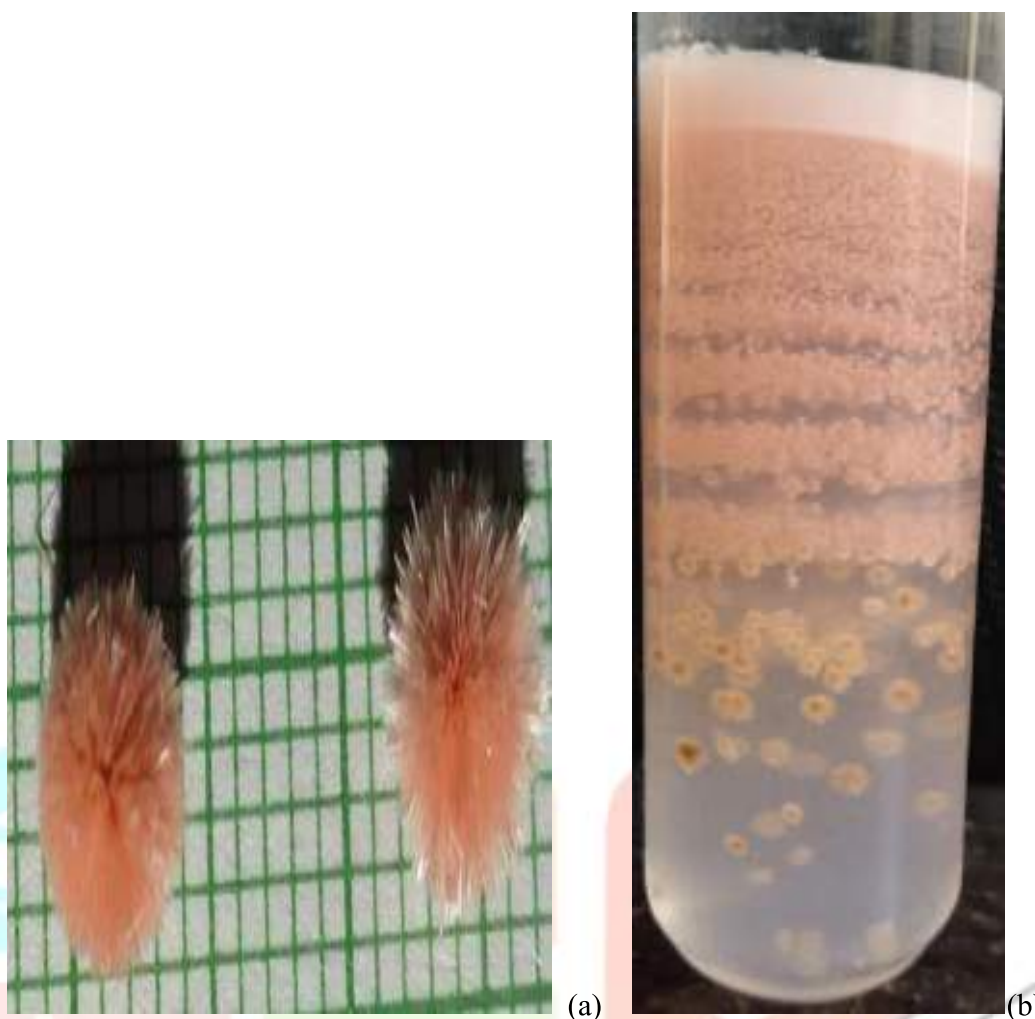


Fig. 1(a) Shows the spherulites cobalt oxalate crystals (b) Shows the formation of Liesegang rings

Result and Discussion-

Thermogravimetric Analysis (TGA) of Cobalt Oxalate- The thermogram of cobalt oxalate crystal were obtained with the help of SDT Q600 V20.9 Build 20. TGA/DTA/DSC thermal analyser available at Materials Characterization Laboratory Department of Materials Science and Engineering, Yonsei University, Room No. B307, Engineering Hall 2, 50 Yonsei-ro, Seodaemun-gu, Seoul 120-749, Republic of Korea. The TGA curve of cobalt oxalate agar-agar gel grown crystal is as shown in fig (2), the percentage of the weight loss in the different stages of decomposition of cobalt oxalate are presented in the table (2). There is good agreement between the observed and calculated weight. The four stages of decomposition are described as below: In the first stage decomposition occurs in the temperature range 30°C to 177°C in which weight loss of 17.46% agrees very well with the calculated weight loss 17.58%. Thus it is clear that the crystals are hydrate and the weight loss calculation clearly indicate that cobalt oxalate crystals have nine water molecule as water of crystallization. It is notice that the sample losses water of hydration and becomes anhydrous at 177°C .

In the second stage of decomposition in the temperature range 200°C to 247°C , the total weight loss 3.411% is seen which is due to the loss 3C and $3\text{H}_2\text{O}$ this is well agreement with calculated weight loss of 3.50%. Then an anhydrous cobalt decomposes into cobalt oxalate.

In the third stage of decomposition total weight loss 36.88% was observed in the temperature range 247°C to 260°C which corresponds to the loss of 2CO. This weight loss agrees very well with the calculated weight loss 37.00%. Thus cobalt oxalate further decomposes into cobalt carbonate.

Finally in the temperature range 892°C to 930°C, total weight loss of 2.538% was obtained. This loss is attributed to the loss of CO₂. This is in well agreement with the calculated weight loss of 2.8%. Thus the cobalt carbonate finally turns into cobalt oxide at 930°C. Which is confirmed by residual weight up to the end of analysis 2.538%. This is in good agreement with calculated residual weight of 2.80%.[12-14]

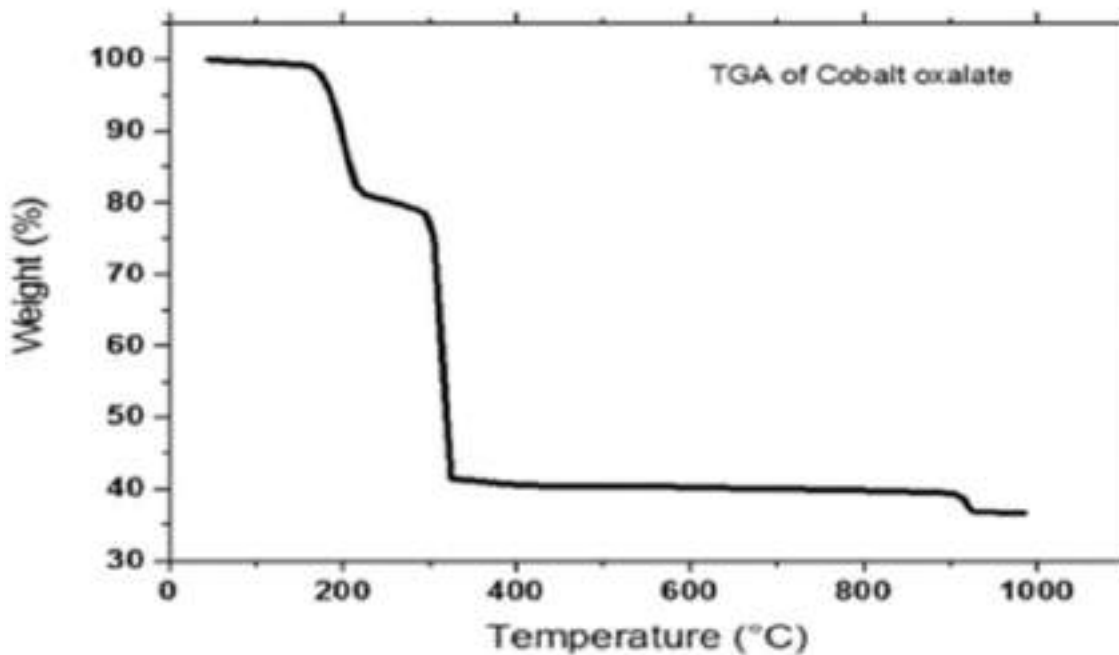


Fig.2 Shows the TGA Curve of Cobalt oxalate crystal grown by agar-agar gel technique

Table 2 Summarized data of TGA results of decomposition process of cobalt oxalate crystals

Stage	Temperature range °C	Observed Weight loss %	Calculated Weight loss %	Loss of Molecule in stage
I	30-177°C	17.46%	17.58%	9H ₂ O
II	200-247°C	3.41%	3.50%	3C and 3H ₂ O
III	247-260°C	36.88%	37.00%	2CO
IV	892-930°C	2.538%	2.80%	CO ₂

Differential Thermal Analysis (DTA) –

The DTA curve for cobalt oxalate agar- agar gel grown crystal is as shown in figure(3) and the DTA data collected from this curve is tabulated in the table(3). In DTA curve we observe two endothermic peak at 208.25°C and 919°C and one exothermic peak at 310°C are due to decomposition of hydrated cobalt oxalate into anhydrous cobalt oxalate. In the first stage of decomposition, peak at 208.25°C is attributed to loss of first

4H₂O molecules immediately followed by another endothermic peak at 919^oC which corresponds 2H₂O molecules. The endothermic peaks observed in the DTA curve corresponds to the total weight loss of Nine water molecule in TGA curve [15-17].

Table 3 DTA data of Cobalt oxalate

Peaks recorded	Nature
208.25 ^o C	Endothermic
919 ^o C	Endothermic
310 ^o C	Exothermic

The exothermic peak at 310^oC due to the decomposition of anhydrous cobalt oxalate into cobalt oxalate. The exothermic peak attributed to the loss of 4C molecule and endothermic at 208.25^oC is attributed to the loss of 3 water molecules. The endothermic peak at 919^oC is due to the decomposition of cobalt oxalate carbonate to cobalt oxide which is attributed to the loss of 2CO₂.

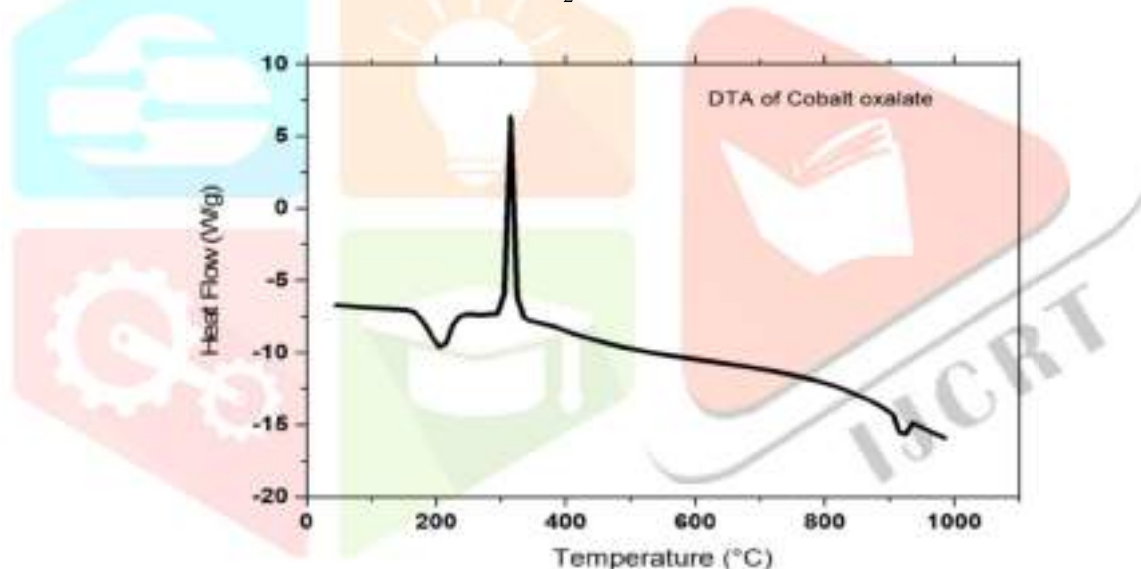


Figure 1 DTA curve for Cobalt oxalate

Energy Dispersive Analysis by X-rays (EDAX) –

The chemical composition of as grown crystals is analyzed by Energy Dispersive X-ray Analysis (EDX). Fig. 4 shows the EDX spectrum which confirms the presence of expected elements O,C and Cu. The stoichiometric composition was computed using experimental and theoretical results of EDX. Energy Dispersive analysis by X-ray (EDAX) is used for the quantitative analysis of cobalt oxalate and is also called as elemental analysis. It conclude that the (weight & atomic %) of copper (Cu) in the grown crystal measured by EDAX are very close with the values calculated from the molecular formula.[18-22].

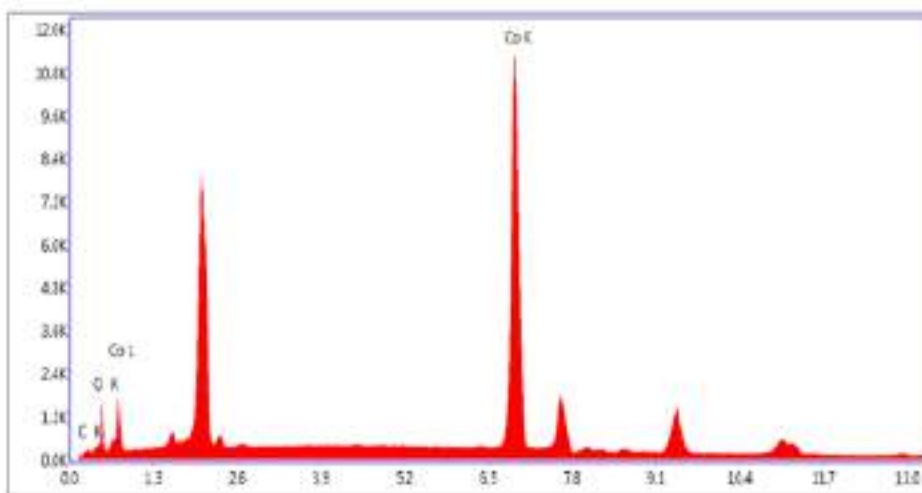


Figure 2EDAX of Cobalt oxalate

Table 4 EDAX of cobalt oxalate

Element	Weight%	Atomic%	Net.Int	Error	%	K ratio	Z	R	A	F
Ck	2.22	9.46	44.68	19.14	0.01	0.05	1.33	0.84	0.21	1.00
Ok	2.41	7.71	227.93	10.39	0.01	0.05	1.28	0.86	0.42	1.00
Cobalt	95.37	82.83	6779.47	1.88	0.97	0.80	0.98	1.01	1.0	1.03

Conclusions —

The present work reports the growth and characterization of cobalt oxalate single crystals. We have demonstrated the formation of cobalt oxalate single crystals in agar-agar gels. Cobalt oxalates exhibits star shaped, opaque and spherulites growth (flower) shape are observed. Further to obtain good quality single crystals of cobalt oxalate, both reactants –cobalt chloride and oxalic acid were interchanged. With cobalt chloride incorporated gels result only fibers. These facts have been explained by taking in account the interaction of the reactants ions with the sodium and silica ions. The effect of temperature on growth of cobalt oxalate crystals showed that there is a decrease in nucleation density at higher temperature which is due to the increases of the aqueous solubility of cobalt oxalate.

Conclusions-

Transition metal cobalt (II) oxalate crystal was grown by gel method using agar agar gel in well size and shape. Red –pink colour crystal were observed. In contrast bigger and better shape of red pink block crystal of cobalt oxalate observed, however, longer growth time was needed to grow the crystal.

Reference

1. R. N. Singh, Madhu, R. Awasthi, S. K. Tiwari, *Int. J. Hydrogen energy*. 34, 4693,(2009).
2. S. D. M. Jacques, O. Leynaud, D. Strusevich, A. M. Beale, G. Sankar, C. M. Martin, P. Barnes, *Angew. Chem. Int. Ed.* 45, 445 (2006).
3. W. X. Kuang, Y. N. Fan, Y. Chen, *Langmuir*, 16, 5205 (2000).
4. A. W. Sleight, B. L. Chamberland, *Inorg. Chem.* 7, 1672 (1968).
5. U. Kersen, L. Holappa, *Appl. Phys. A: Mater. Sci. Process.* 85, 431 (2006).
6. Ramamoorthy, R., Kanagasabai, V., Kausalya, R., Impact of celebrities' image on brand, *International Journal of Pure and Applied Mathematics*, V-116, I-18 Special Issue, PP-251-253, 2017.
7. Ramamoorthy, R., Kanagasabai, V., Vignesh, M., Quality assurance in operation theatre with reference to fortis malar hospital, *International Journal of Pure and Applied Mathematics*, V-116, I-14 Special Issue, PP-87-93, 2017
8. Ramya, N., Arthy, J., Honey comb graphs and its energy, *International Journal of Pure and Applied Mathematics*, V-116, I-18 Special Issue, PP-83-86, 2017
9. Ramya, N., Jagadeeswari, P., Proper coloring of regular graphs, *International Journal of Pure and Applied Mathematics*, V-116, I-16 Special Issue, PP-531-533, 2017.
10. Polezhaez, A.A.; Muller, S.C. (1994). "Complexity of precipitation patterns: Comparison of simulation with experiment". *Chaos: An Interdisciplinary Journal of Nonlinear Science*. 4 (4): 631–636. Bibcode:1994Chaos...4..631P. doi:10.1063/1.166040. PMID 12780140.
11. LLOYD, FRANCIS E.; MORAVEK, VLADIMIR (1930). "Further Studies in Periodic Precipitation". *J. Phys. Chem.* 35 (6): 1512. doi:10.1021/j150324a002.
12. P.N. Kotru, K.K. Raina and M.L. Koul, "J Mater Sci Lett." 6:711-14 1987.
13. P.N. Kotru, N.K. Gupta, K.K. Raina and I.B. Sharma, "I Mater Sci.;" 21:83-9, 1986.
14. T.V. Albu, S.L. Plostinaru, and E. Segal, "J Thermal Anal.," 50:425-30. 1997.
15. K.S. Raju, Johan Varughese and M.A. Ittyachen; "Bull. Mater. Sci." 21, 375. (1998).
16. D.K. Sawant, H.E. Patil, D.S. Bhavsar, K.D. Girase and J.H. Patil; "Journal of Thermal Analysis and Calorimetry," 107, 3. (2012).
17. N. S. Patil, P. A. Savale, S. K. Bachhav and S. T. Pawar ; 'Archive of physics research', Vol2(1), 39-47, (2011).
18. D. K. Sawant., H. M. Patil and D. S. Bhavsar., 'Pelagia research Library, DCS' Vol2(3), 63, (2011).
19. D. K. Sawant., H. M. Patil and D. S. Bhavsar., 'Scholars Research Library Archives of Physics Research', Vol2(2), 67. (2011).
20. S.J. Nandre, S.J. Shitole and R.R. Ahire; "Journal of Nano and Electronic Physics" Vol.4,4,4013. (2012)
21. M. Selvapandiyan, S. Sudhakar and M. Prasath; "Int. Journal of Engineering Research and Application", Vol. 7,8,(3), 65-72. (2017).
22. P S Rohith, N. Jagannatha and K V Pradeep Kumar. *AIP Conference Proceedings* 2220, 060003 (2020); <https://doi.org/10.1063/5.0001222>.

Liquid Exfoliation of Decagonal Quasicrystals and Its Light Out-Coupling Performance in Organic Light-Emitting Devices

Anbalagan Ramakrishnan, Kiran Kishore Kesavan, **Sudam Chavhan**,
Mangey Ram Nagar, Jwo-Huei Jou,* Sinn-Wen Chen,* Haw-Wen Hsiao, Jian-Min Zuo,
and Lin Yu Hung

Decagonal quasicrystals are receiving considerable attention because of their unique crystallographic structure, electrical, magnetic, and mechanical properties. Hence, anisotropic decagonal nano-quasicrystals (NQC) will have potential applications in multifunctional devices. Here, the decagonal NQCs are prepared from an anisotropic bulk sample by liquid exfoliation via the ultrasonic process at room temperature. The NQCs have high transmittance and are incorporated into green organic light-emitting diodes via solution and dry processes for light out-coupling. The overall device performance is markedly enhanced with NQC incorporation. A power efficacy of 31.4 lm W^{-1} is achieved at 1000 cd m^{-2} with a 37% increment for the solution-processed device. For the dry-processed device, 66.4 lm W^{-1} is obtained with an increment of 108%. These NQCs can be made free standing, providing OLED devices an extremely convenient and effective measure for maximizing out-coupling of the generated light, near 80% of which would otherwise be trapped and wasted within.

1. Introduction

Quasicrystals are unusual crystals with nonperiodicity, but they retain long-range ordering with lack of translational symmetry. Quasicrystals are classified according to their symmetry (8-, 10-, and 12-fold) and quasi-periodicity (one (1D), two (2D), and three (3D) dimension). They have unique structural, mechanical, physical, and chemical properties.^[1–3] Further, size reduction of quasicrystals leads to high strength.^[4]


Nowadays, 2D atomically thin-layered materials have potential applications in electronics and semiconductor technologies because of their unique physical, optical, and electrical properties.^[5,6] 2D layered materials are stacked by van der Waals interlayer (weak) bonding and able to exfoliate into few or atomic thin layers with a crystalline nature.^[7] Similarly, a large area of mono- and few-layers of 2D quasicrystals have been prepared from the 3D icosahedral Al–Pd–Mn quasicrystal by liquid exfoliation.^[8] The stability of the Al–Pd–Mn quasicrystal was retained after the exfoliation with icosahedral symmetry. Still, the exfoliation technique is not explored in other quasicrystals with different symmetry. Particularly, decagonal quasicrystal shows its unique nature with two-dimensional quasiperiodic planes, whereas Al–Co–Cu based alloys stand out as a stable decagonal quasicrystal with a wide composition range.^[9] The stability of the quasicrystal was found to increase with increasing Co concentration and a stable decagonal single crystal grown in the Al–Cu–Co alloys.^[10,11] The bulk Al–Co–Cu quasicrystal has high electrical conductivity in both the periodic and quasiperiodic direction, and behaves like a metallic conductor.^[12] Since the decagonal quasicrystals (Al–Co–Cu) show two-dimensional quasiperiodicity and one-dimensional periodicity in bulk, it is more convenient to exfoliate stable quasicrystal with a few layers of thickness. In general, one- to three-dimensional (1D, 2D, and 3D) quasicrystals have attracted significant interest in various applications. In particular, photonic quasicrystals have been used to improve the targeted spectrum efficiency.^[13–15] The photonic quasicrystal structure guides to couple out the trapped light in the waveguide because of the total internal reflection.^[16] In addition,

Dr. A. Ramakrishnan
Department of Chemical Engineering
National Tsing Hua University
Hsinchu 300, Taiwan

K. K. Kesavan, **Dr. S. Chavhan**, M. R. Nagar, Prof. J.-H. Jou, L. Y. Hung
Department of Materials Science and Engineering
National Tsing Hua University
Hsinchu 300, Taiwan
E-mail: jjou@mx.nthu.edu.tw

Prof. S.-W. Chen
Department of Chemical Engineering and High Entropy Materials Center
National Tsing Hua University
Hsinchu 300, Taiwan
E-mail: swchen@mx.nthu.edu.tw

H.-W. Hsiao, Prof. J.-M. Zuo
Department of Materials Science and Engineering
University of Illinois-Urbana Champaign
1304 W Green Street, Urbana, IL 61801, USA

 The ORCID identification number(s) for the author(s) of this article can be found under <https://doi.org/10.1002/adpr.202000042>.

© 2020 The Authors. Published by Wiley-VCH GmbH. This is an open access article under the terms of the Creative Commons Attribution License, which permits use, distribution and reproduction in any medium, provided the original work is properly cited.

DOI: 10.1002/adpr.202000042

quasicrystal-structured substrates have also been implemented to enhance the efficiency of OLED applications.^[17–19] However, until now, the direct use of quasicrystal materials in OLED applications has not been examined.

In addition, organic light-emitting diodes (OLEDs) continue to play a pivotal role in modern lighting and display technologies. The advantageous features specifically associated with OLEDs, such as low turn-on voltage, diffused light emission, high to low color temperature tunability, rapid response time, excellent color gamut, and flexibility have been integrated and reinforced in state-of-art electronic gadgets. However, high-efficiency OLED devices have yet to materialize. A major limiting factor is the failure to extract all emitted light. The internal loss of the light of up to 40–60% is mainly due to the large differences between the refractive indices of the indium tin oxide (ITO)/organic layer and glass substrate and air.^[20–21] To minimize these losses, the surface plasmonic method^[24] and various light extraction methods have been adopted, such as Bragg diffraction grating,^[25] low-index grids,^[26] and nanostructured surface substrates.^[27] However, most of the available methods are expensive as well as too complex, for large-scale production.^[26,28,29]

In the present study, a novel approach of the Al–Co–Cu based nano-quasicrystal is designed and developed for OLED application. Nano-size quasicrystals (Al–Co–Cu) are synthesized by liquid exfoliation via the ultrasonic-assisted process. Nano-quasicrystals are used for external light out-coupling and

significant improvements of OLED power efficiencies, EQE, and luminance are achieved.

2. Results and Discussion

2.1. Structure and Composition Analysis of Bulk and Exfoliated Quasicrystals

The x-ray diffraction (XRD) patterns of the Al–Co–Cu quasicrystal are shown in Figure 1a, with the sharp Bragg diffraction patterns indicating the stability of the decagonal quasicrystals. The diffraction patterns of the decagonal quasicrystals are identified with six independent indices according to Mukhopadhyay et al.^[30] report. Different diffractions with various compositions were reported, such as Co concentration containing Al–Co–Cu quasicrystals with icosahedral and decagonal quasicrystal patterns.^[9] Increasing Co concentration leads to a single decagonal quasicrystal phase. In the present study, Al–Co–Cu quasicrystal was prepared with high Co concentration and also annealed for a long time to obtain a stable quasicrystal phase. According to the crystal growth studies,^[10,11] the decagonal quasicrystal plane is stacked along the ten-fold axis and then they are grown along the periodic direction [000001] and perpendicular to the quasiperiodic directions. After the liquid exfoliations (Figure 1a), the obtained sample retained the decagonal quasicrystals' nature without secondary phases. The relative intensity of the

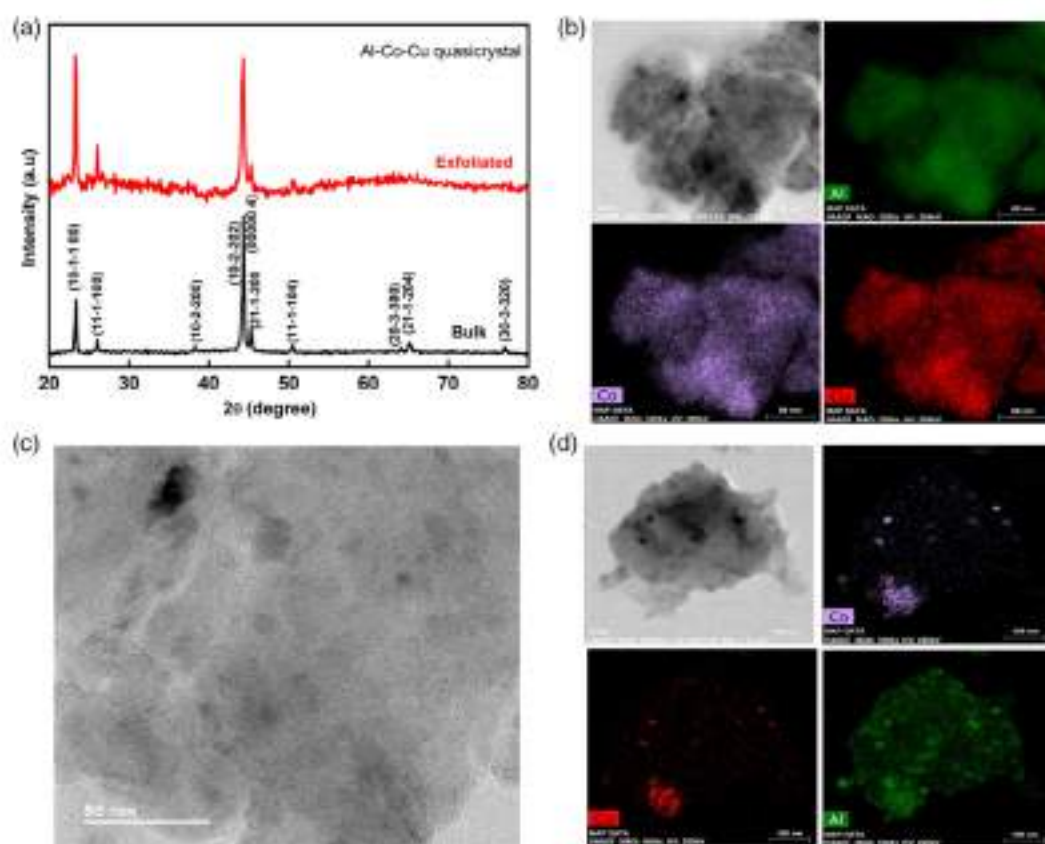


Figure 1. a) Powder XRD pattern of bulk and exfoliated quasicrystals, b,c) TEM mapping of exfoliated quasicrystals and d) High-magnification image of exfoliated quasicrystal and height profile (inserted).

(101100) plane increased as compared to the (000004) plane in exfoliated samples. Moreover, no significant change in peak position was found in the exfoliated quasicrystal as compared with the bulk quasicrystal. The XRD result indicates the quasicrystal nature increased after exfoliation as the thickness of the layer decreased. The obtained results differ from the 2D Al–Mn–Pd quasicrystals, which were exfoliated from 3D icosahedra quasicrystal.^[8] The exfoliated decagonal quasicrystals show similar behavior to that reported in the few layer 2D transmission metal chalcogenides.^[31,32]

The bright field transmission electron microscope (TEM) image of the exfoliated quasicrystal is shown in the Figure 1b. A sheet-like morphology with an ≈ 325 nm lateral size of quasicrystals was observed. The elemental mapping of the exfoliated quasicrystal confirmed the presence of the Al, Co, and Cu elements and their uniform distribution in the sample. The average elemental composition of the sample is determined to be 68.89 at% of Al-17.79 at% of Co-13.3 at% Cu had slightly higher Al content as compared with the prepared bulk quasicrystal. The high-magnification image of the thin layers of 2D quasicrystal images is shown in Figure 1c. Nonhomogeneity in the surface was found and the nano-quasiparticles were placed on the sheet morphology. The nano-quasicrystal is unstable under high-resolution beam conditions and lost its structural properties. However, it is not deformed into the crystalline nature and became amorphous.

For more information of the exfoliation quasicrystals, a thin layer was chosen for TEM analysis. Bright field image and elemental mapping of the exfoliated quasicrystal, as shown in Figure 1d, show the exfoliated decagonal quasicrystal consists of a few layers of nanosheets. In addition, small-sized nanoparticles are observed on the top of the nanosheets. The elements are distributed uniformly in the nanoparticles, although their composition shows excess Al.

In contrast, lower concentrations of Co and Cu with Al-rich conditions were observed in a few layers of the nanosheets, as reported in the 2D Al–Mn–Pd quasicrystals.^[8] In case of Al–Mn–Pd,^[8] the atomic positions of all the elements (Al, Mn, and Pd) were calculated using density functional theory (DFT) calculations, whereas the thin atomic layer Al sheet formed initially, Mn and Pd atoms later formed on top of the Al sheet to stabilize the structure. However, they did not clearly report the elemental distribution on the Al sheet in the experimental details. The present study observed Al sheet formation with Co and Cu distribution from the energy dispersive X-ray analysis (EDAX) Map. It is concluded that Co and Cu are formed on the top of the Al sheet to form a stable quasicrystal nature. In addition, small nano-quasicrystals found on the sample with higher Co and Cu concentration. From the XRD result, no significant shift in exfoliated nano-quasicrystal occurs by varying the Co and concentrations, indicating large size nano-quasicrystals are more dominant than small nano-quasicrystals in the diffraction pattern. The Co and Cu deficiency might lead to more defects in nanolayered quasicrystals. The concentration of Co and Cu increased with increasing thickness of the nanostructured quasicrystals up to the bulk limit.

The AFM image of exfoliated quasicrystals drop coated on the ITO/glass substrate is shown in Figure 2a. Exfoliated quasicrystals with various height distributions from 5 to 35 nm were observed with different surface morphology. The lateral size of the nanoparticles also varies from 100 to 600 nm and they

are placed on top of the quasi-nanosheets. The obtained nanodecagonal quasicrystal morphology and size differ from the 2D flakes of the Al–Mn–Pd.^[8] The decagonal QCs could grow up to a few nm in size in single crystal form.^[10] During the sonication, the large size particles were broken into nanoparticles and also removed during the centrifuge with high speed. The NQCs dispersion in 3D view is shown in Figure 2b. A large number of NQCs are distributed from 5 to 15 nm height with a maximum density of around 9 nm and distributed up to 35 nm, as shown in Figure 2c. The thickness of the NQCs is comparable with the TEM results.

Wavelength-dependent transmission and the absorption of ITO, as well as external out-coupling of NQC on the ITO/glass substrate are shown in Figure 2d. Almost more than 90% of the transmission was demonstrated at a wavelength of 500–580 nm in the emission region of the emitter (PO-01). The corresponding absorption was observed in all the samples, indicating the NQCs did not observe a significant wavelength in the green emission region. Hence, the effect of surface plasmonic polarization could be ruled out. This indicates scattering of light at a low wavelength by NQCs became more transparent at a high wavelength in the measured range, particularly, in the green light region. The NQC-like particles might scatter the light and the NQC sheets became transparent.

2.2. OLED Device Performance with Quasicrystal Incorporation in External Approach via Solution Process

Figure 3a,b represents the schematic illustration of the decagonal nano-quasicrystals utilized device structures. To clearly understand the nano-quasicrystals' role, both solution-processed (Figure 3a) and the dry-processed (Figure 3a) device were fabricated with NQC. The NQCs were deposited on the rear side of the substrate for external out-coupling.

A comparison of the electroluminescent characteristics of the solution and dry-processed OLED devices with and without quasicrystals in terms of power efficiency (η_p), current efficiency (η_c), and external quantum efficiency (EQE) at 100, 1000, and 10 000 values of each parameters is summarized in Table 1. D1 and D2 represent OLED devices without and with NQCs in solution process.

The performance of the device with nano-quasicrystal (D2) improved with a power efficiency of 31.4 lm W^{-1} (Figure 4a), current efficiency of 31.1 cd A^{-1} (Figure 4b), and EQE of 13.1% at 1000 cd m^{-2} . Overall power efficiency, current efficiency, and EQE increased to 37 and 31%, respectively, as compared to the device fabricated (D1) without quasicrystals. The plot of luminance versus the applied bias voltage shown in Figure 4c shows a decrease in the operating voltage of the device with nano-decagonal quasicrystal. The luminance increased with NQCs and reached a maximum at $18 800 \text{ cd m}^{-2}$, as compared to the device ($16 430 \text{ cd m}^{-2}$) without NQCs.

2.3. OLED Device Performance with Quasicrystal Incorporation in External Approach via Dry Process

Devices D3 and D4 represent without and with NQCs prepared from the dry process. The best performance was observed for the

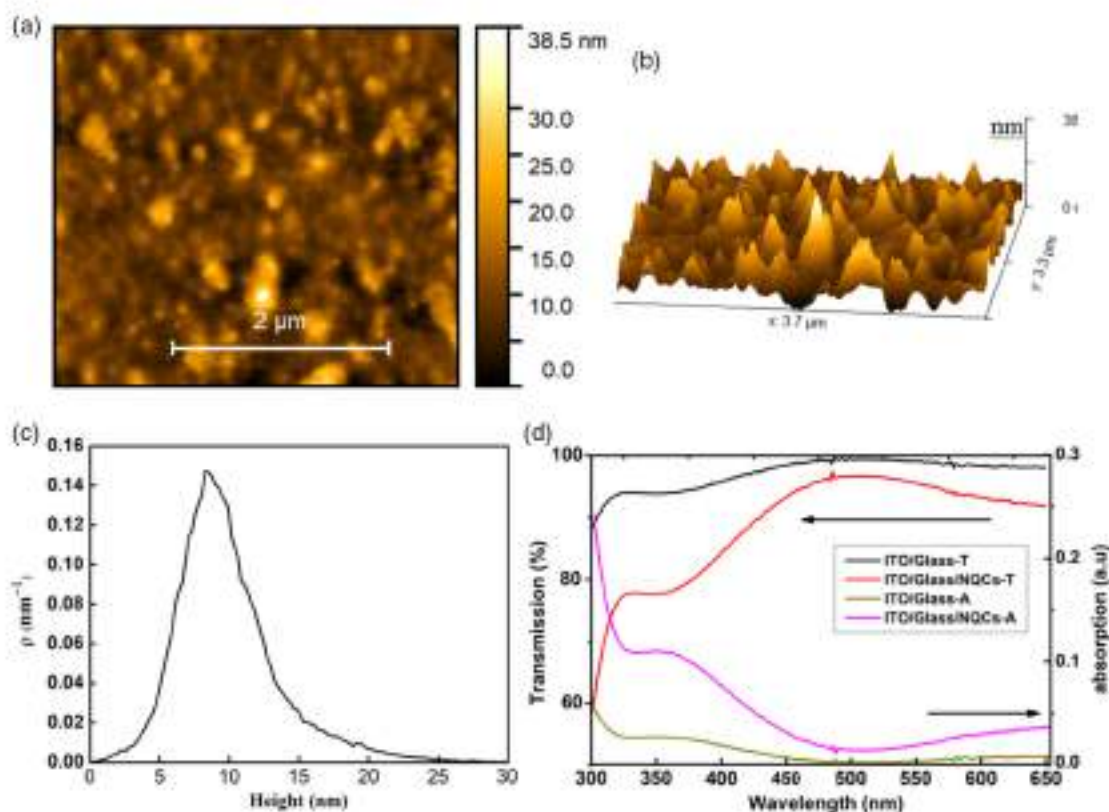


Figure 2. a) AFM image of exfoliated quasicrystal b) 3D view, c) statistical density of NQCs with high profile, and d) transmittance and absorption versus wavelength spectrum of NQC on/back side of the ITO/glass substrate.

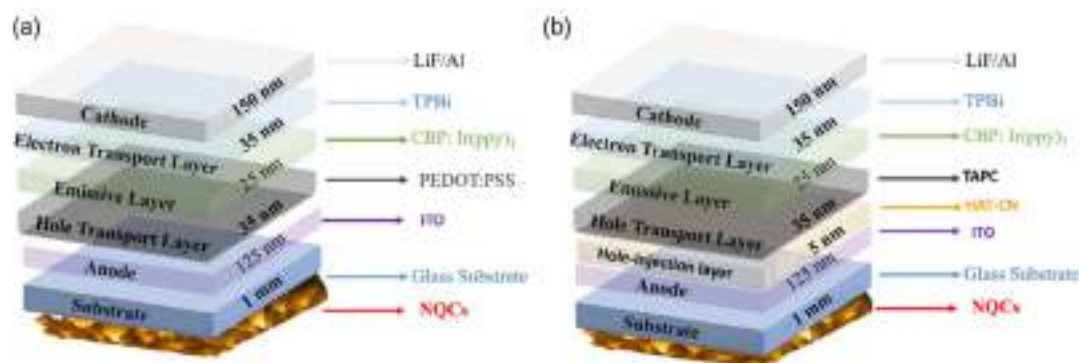


Figure 3. Modified decagonal nano-quasicrystals as external out-coupling in a) solution process and b) dry process.

Table 1. Effect of decagonal nano-quasicrystals on green devices performance from the perspectives of operation voltage (OV), power efficiency (PE), current efficiency (CE), external quantum efficiency (EQE), CIE coordinates, and maximum luminance.

Fabrication process	Device	OV [V]	Power efficiency [lm W^{-1}]	Current efficiency [cd A^{-1}]		EQE [%]	Max Lumi. [cd m^{-2}]
				@100/1000/10 000 [cd m^{-2}]			
Solution	D1 (W/O)	3	32.1/22.9/7.1	30.51/26.4/8.98	11/10/4.9	16 430	
Processed	D2 (W/NQC)	3.2	47.9/31.4/10.2	47.04/31.1/10.1	15.2/13.1/6.9	18 800	
Enhancement [%]	-	-	49/37/44	50.17/17.6/13	38/31/41	-	
Dry	D3 (W/O)	3	50.1/31.8/11.4	56.8/47.3/26.4	15.4/12/7.1	18 740	
Processed	D4 (W/NQC)	2.8	58.3/66.4/32.5	51.2/70.8/55	14.6/19.5/15.2	37 000	
Enhancement [%]	-	-	16/108/41	-/50/108	-/63/114	-	

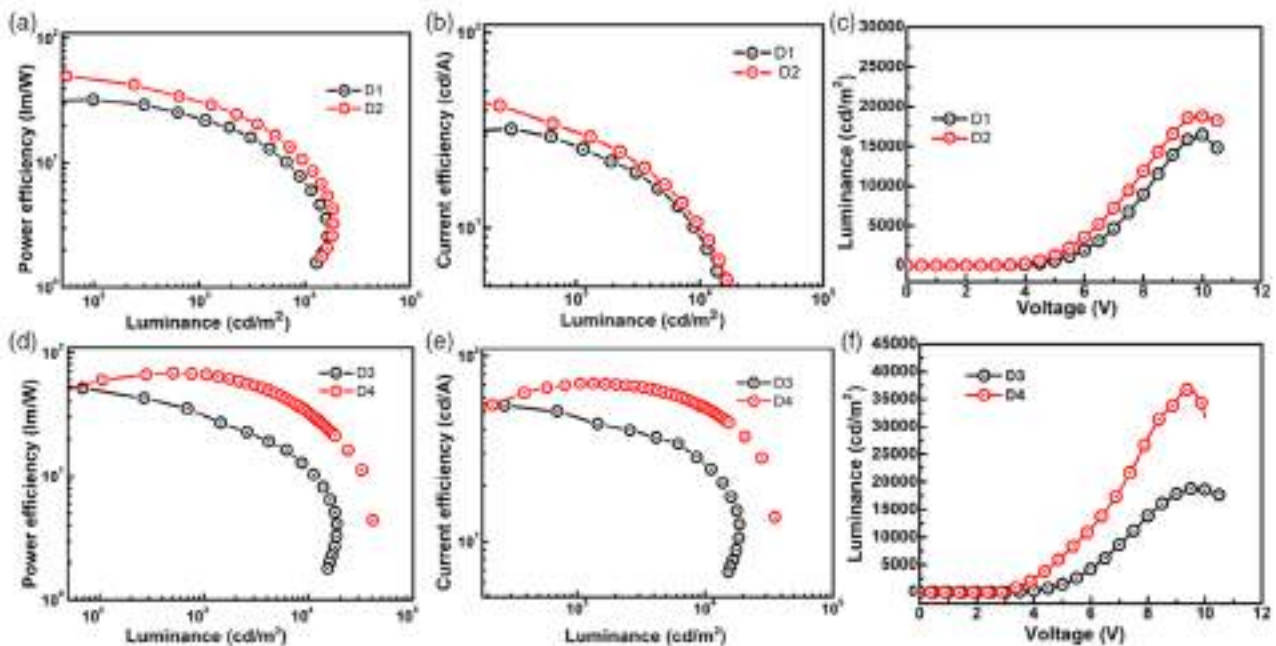


Figure 4. a,d) power efficiency, b,e) current efficiency, and c,f) luminance of OLED devices in solution and dry process, respectively.

external out-coupled NQCs fabricated device (D4), as measured by a power efficiency (Figure 4d) of 66.4 lm W^{-1} , current efficiency (Figure 4e) of 70.8 cd/A , and EQE of 19.5% at 1000 cd m^{-2} . The obtained power efficiency, current efficiency, and EQE increased in corresponding luminance values by 108%, 50%, and 63%, respectively, as compared to the OLED without a quasicrystal (D3). A significant enhancement of device performance at high luminance has been reported in various light-coupling methods.^{133–164} The performance of OLED device with NQCs is less at 100 cd m^{-2} and it enhanced at high luminance.

The luminance versus applied voltage graph (Figure 4f and Table 1) shows the operating voltage of the decagonal nano-quasicrystals with external coupling (D4) is lower than the normal device (D3), indicating the QC nanoparticles help to reduce the operating voltage of the fabricated OLED devices by out-coupling. The luminance enhanced with NQCs and reached a maximum at $37\,000 \text{ cd m}^{-2}$, as compared to the device ($18\,760 \text{ cd m}^{-2}$) without NQCs. Similarly, the luminance was enhanced by external out-coupling in lens-free OLED devices.^{133, 571} The superior out-coupling performance of the decagonal nano-quasicrystal device is attributed to scattering 1) by large size NQCs, 2) by defects in the few layer NQCs via light propagation.

Figure 5 shows the normalized electroluminescent spectra of all the devices with and without the quasicrystals. The peaks of the emission spectra for the green OLED devices reveal the emission from all devices in the green region. The nature of the EL spectra emission seems to be very similar to all green OLED devices.

3. Conclusion

For the first time, decagonal nano-quasicrystals are prepared by liquid exfoliations and their decagonal quasicrystal nature is

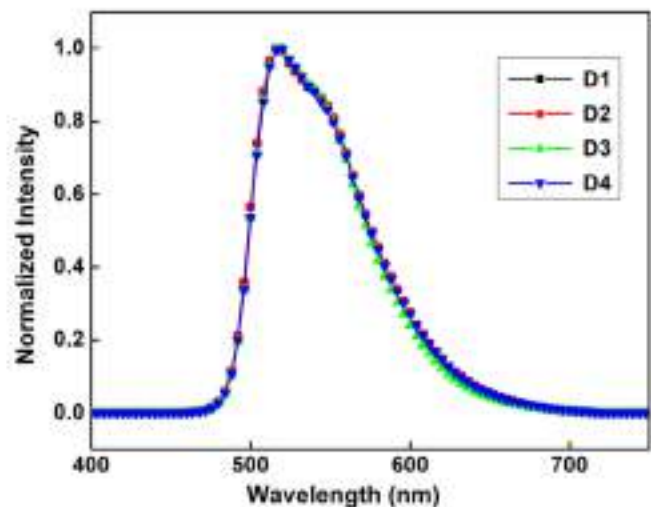


Figure 5. Normalized electroluminescence (EL) spectra as a function of wavelength of the studied OLED devices via solution and dry process.

confirmed. The NQCs are successfully incorporated into external out-coupling via solution and dry process for green light OLED devices. The incorporation of nano-quasicrystals improved the power efficiency (37% and 108%), current efficiency (17.6% and 50%), and EQE (31% and 60%), by improving light out-coupling performance at 1000 cd m^{-2} in solution and dry process, respectively.

The maximum luminance with NQCs is achieved at $37\,000 \text{ cd m}^{-2}$ as compared to the device ($18\,760 \text{ cd m}^{-2}$) without NQCs in dry process. This is a low cost and free standing nano-quasicrystal with scalable method for light out-coupling applications in OLED devices as compared with quasicrystal-patterned devices. In general, different quasicrystals have various

crystallographic dimensions with symmetry and a band gap, which can be explored in the future. The novel application of decagonal nano-quasicrystals in the OLED devices is the ideal platform for different quasicrystal materials in optoelectronic applications.

4. Experimental Section

For preparing bulk quasicrystal ($Al_{60}Co_{10}Cu_{14}$), high-purity elemental metals of Al (99.999%), Co (99.95%), and Cu (99.9%) were weighed according to the stoichiometry and arc-melted in an argon atmosphere. The arc-melted sample was then placed in a graphite crucible and sealed inside a quartz tube under a vacuum of 10^{-2} Pa. The sealed sample was then annealed at 900 °C for 15 days, which was followed by water quenching. A total of 10 mg of prepared quasicrystal in powder form was placed in DMF *N,N*-dimethylformamide solvent (50 mL) and sonicated for 60 h. Following sonication, the sample was centrifuged at 5000 rpm for 10 min to separate and remove the unexfoliated quasicrystals. The exfoliated sample with the DMF solution was then dispersed in ethanol and drop casted on a glass substrate for XRD, on a Si substrate for atomic force microscopy (AFM) analysis and a carbon-coated 200 mesh Ni grid for TEM analysis.

XRD was carried out on all samples for phase identification using D2 (Bruker, USA). The morphology and elemental analysis (EDS) of the quasicrystals were performed using a FEI Talos F200X (FEI, USA). The topological information was carried out by AFM (Bruker, Dimension ICON, USA) in the tapping mode at room temperature under ambient conditions. Transmission spectrum was obtained using a UV-vis spectrophotometer U-3010 (Hitachi, Japan).

For solution process, the quasicrystal containing DMF solution of 400 μ L was drop cast on the bottom of the glass substrate at 180 °C in a glove box under a nitrogen atmosphere. Later, PEDOT:PSS as a hole injection/transport layer, and EML solution CBP and Ir(ppy)₃(acac) were spin coated on the ITO/glass substrate for 20 s at 4000 and 2500 rpm, respectively, in a nitrogen-filled glove box. The depositions of TPBi as an electron transport layer, LiF as an electron injection layer, and Al as a cathode layer were carried out using a high-vacuum thermal evaporator.

For dry process, the quasicrystal containing DMF solution of 400 μ L was drop cast on the bottom of the glass substrate at 180 °C in a glove box under a nitrogen atmosphere. On ITO-coated glass substrate, 5 nm 1,4,5,8,9,11-hexaazatriphenylene-hexacarbonitrile (HAT-CN) as a hole injection layer (HIL), a 35 nm di-[4-(*N,N*-ditolylamino)-phenyl]cyclohexane (TAPC) as a hole transport layer (HTL), CBP, TPBi, LiF, and Al were fabricated via sequential thermal evaporation for both the organic and inorganic materials under high vacuum (10^{-6} Torr) conditions. A reference device was fabricated without quasicrystals.

Device Characterizations: The characterization of the final device was done in an ambient atmosphere without encapsulation. The current-voltage-luminance characterization was carried out using a computer-interfaced Keithley 2400 electrometer and Minolta CS-100A luminance-meter. Emission spectra were recorded by a PR-655 spectroradiometer. The emission area of the OLED device was 0.09 cm², calculated from the overlapping of the ITO and Al electrodes.

Acknowledgements

The authors acknowledge the Ministry of Science and Technology of Taiwan (MOST 106-2221-E-007-094-MY3 and MOST-109-2811-E-007-052) for its financial support.

Conflict of Interest

The authors declare no conflict of interest.

Keywords

light out-coupling, nano-quasicrystals, OLEDs

Received: August 19, 2020

Revised: September 21, 2020

Published online:

- [1] D. V. Louzguine-Luzgin, A. Inoue, *Annu. Rev. Mater. Res.* **2008**, *38*, 403.
- [2] J. Dubois, *Chem. Soc. Rev.* **2012**, 6760.
- [3] P. Taylor, S. J. Poon, *Adv. Phys.* **2006**, *41*, 303.
- [4] Y. Zou, P. Kuczera, A. Sologubenko, T. Sumigawa, T. Kitamura, W. Steurer, R. Spolenak, *Nat. Commun.* **2016**, *7*, 1.
- [5] S. Kang, D. Lee, J. Kim, A. Capasso, H. S. Kang, J. W. Park, C. H. Lee, G. H. Lee, *2D Mater.* **2020**, *7*, 022003.
- [6] K. Khan, A. K. Tareen, M. Aslam, R. Wang, Y. Zhang, A. Mahmood, Z. Ouyang, H. Zhang, Z. Guo, *J. Mater. Chem. C* **2020**, *8*, 387.
- [7] Y. Shi, H. Zhang, W. H. Chang, H. S. Shin, L. J. Li, *MRS Bull.* **2015**, *40*, 566.
- [8] T. P. Yadav, C. F. Woellner, S. K. Sinha, T. Sharifi, A. Apte, N. K. Mukhopadhyay, O. N. Srivastava, R. Vajtai, D. S. Galvaeo, C. S. Tiwary, P. M. Ajayan, *Adv. Funct. Mater.* **2018**, *28*, 1801181.
- [9] T. M. An-Pang Tsai, A. Inoue, *Mater. Trans.* **1989**, *30*, 463.
- [10] A. R. Kortan, F. A. Thiel, H. S. Chen, A. P. Tsai, A. Inoue, T. Masumoto, *Phys. Rev. B* **1989**, *40*, 9397.
- [11] R. A. Ribeiro, S. L. Bud'ko, F. C. Laabs, M. J. Kramer, P. C. Canfield, *Philos. Mag.* **2004**, *84*, 1291.
- [12] J. Dolinsek, S. Vrtnik, A. Smontara, M. Jagodic, Z. Jaglicic, B. Bauer, P. Gille, *Philos. Mag.* **2008**, *88*, 2145.
- [13] Z. V. Vardery, A. Nahata, A. Agrawal, *Nat. Photonics* **2013**, *7*, 177.
- [14] A. Ledermann, L. Cademartiri, M. Hermatschweiler, C. Toninelli, G. A. Ozin, D. S. Wiersma, M. Wegener, G. V. O. N. Freymann, *Nat. Mater.* **2006**, *5*, 942.
- [15] Z. Ovanesyan, P. R. Pudasaini, A. Gangadharan, *Opt. Mater. Express* **2013**, *3*, 1332.
- [16] M. Y. Chang, C. C. Lin, M. Y. Huang, in *Proc. AM-FPD 2016 – 23rd Int. Workshop on Active-Matrix Flatpanel Displays and Devices-TFT Technologies and FPD Materials (FTFMD)*, IEEE, Kyoto, Japan **2016**, pp. 78–80.
- [17] M. Rippa, R. Capasso, L. Petti, G. Nenna, A. De, G. Del Mauro, G. Maglione, C. Minarini, *J. Mater. Chem. C* **2015**, *3*, 147.
- [18] K. Chang, C. Li, J. Pan, K. Cheng, *Opt. Express* **2014**, *22*, A567.
- [19] C. H. H. Yu, M. H. K. Cheng, *Appl. Phys. A* **2015**, *121*, 499.
- [20] S. Nowy, B. C. Krummacker, J. Frischeisen, N. A. Reinke, W. Brütting, *J. Appl. Phys.* **2008**, *104*, 123109.
- [21] D. Mehta, K. Saxena, *Proc. AS/D-06* **2006**, *2*, 198.
- [22] D. Luo, Q. Chen, B. Liu, Y. Qiu, *Polymers* **2019**, *11*, 384.
- [23] S. Reineke, M. Thomschke, B. Lüsser, K. Leo, *Rev. Mod. Phys.* **2013**, *85*, 1245.
- [24] J. Santander, L. Fonseca, S. Udina, S. Marco, **2007**, <https://doi.org/10.1016/j.snb.2007.07.003>.
- [25] J. Hauss, T. Bockrocker, B. Riedel, U. Geyer, U. Lemmer, M. Gerken, *Appl. Phys. Lett.* **2011**, *99*, 103303.
- [26] Y. Sun, S. R. Forrest, *Nat. Photonics* **2008**, *2*, 483.
- [27] G. Gomard, J. B. Preinfalk, A. Egel, U. Lemmer, *J. Photonics Energy* **2016**, *6*, 030901.
- [28] Z. Li, X. Li, X. Lin, H. Wang, Y. Fu, B. Zhang, J. Wu, Z. Xie, *Org. Electron.* **2019**, *75*, 105438.
- [29] D. Nolan, W. Senaratne, D. Baker, L. Liu, *Int. J. Appl. Glas. Sci.* **2015**, *6*, 345.
- [30] N. K. Mukhopadhyay, E. A. Lord, *Acta Crystallogr. A Found. Crystallogr.* **2002**, *58*, 424.

- [31] C. Kim, T. P. Nguyen, Q. Van Le, J. M. Jeon, H. W. Jang, S. Y. Kim, *Adv. Funct. Mater.* **2015**, *25*, 4512.
- [32] M. Park, T. P. Nguyen, K. S. Choi, J. Park, A. Ozgur, S. Y. Kim, *Electron. Mater. Lett.* **2017**, *13*, 344.
- [33] S. Altazin, L. Penninck, B. Ruhstaller, *Handb. Org. Light Diodes* **2018**, *1*.
- [34] B. A. Al-Asbahi, M. H. Haji Jumali, C. C. Yap, M. Mat Salleh, *J. Nanomater.* **2013**, 561534.
- [35] J. H. Lin, W. L. Chang, H.-Y. Lin, T.-H. Chou, H.-C. Kan, C. C. Hsu, *Opt. Express* **2013**, *21*, 22090.
- [36] T. W. Koh, J. A. Spechler, K. M. Lee, C. B. Arnold, B. P. Rand, *ACS Photonics* **2015**, *2*, 1366.
- [37] J. Song, K. H. Kim, E. Kim, C. K. Moon, Y. H. Kim, J. J. Kim, S. Yoo, *Nat. Commun.* **2018**, *9*, 3207.



Synthesis and characterization of ZnO nanoparticles by sol-gel method.

A. Joy Singh, Th. Ranjana Devi, *Sudam Chavhan*¹ & Sanjeev Girase^{2*}

Department of Physics,

S. Kula Women's College, Nambol, Manipur

V. V. M's S. G. Patil ASC College, Sakri, (M.S.) 424304(India)

²K.V.P.S.'s, S. P. D. M. College, Shirpur,
Maharashtra- 425 405 (India)

Abstract

Zinc oxide nanoparticles were prepared by sol-gel technique via two different approaches having by employing zinc sulphate and sodium hydroxide. In the first approach, NaOH was added dropwise with regular interval (ZnO-A) whereas in the second approach NaOH was directly mixed with ZnSO₄ solution (ZnO-B). The physical properties of the synthesized nano-particles were studied by X-ray diffraction technique and scanning electron microscope to investigate the structure and morphology of the material, respectively. It was observed that the both the grown ZnO particles revealed the crystalline properties. From the Debye-Scherrer formula, the particle size of ZnO-A was found to be 10nm whereas for ZnO-B it was found to be 7.7 nm. The SEM morphology exhibited the grown particles have uniformity. The synthesized ZnO particles could be used for various opto-electronic devices.

Keywords: Debye-Scherrer Formula, sol-gel, FWHM, Whatman filter paper.

Introduction

Due to diverse technological applications, ZnO has been an active area of research for more than half a century. It has many interesting optoelectronics properties such as wide band gap (~3.37 eV), a large excitation binding energy of 60 meV and high dielectric constant. Therefore, it can be used in the fabrication of electronics and optical devices such as UV/blue laser (Jhonson *et al* 2001), light-emitting diodes (LEDs), Solar Cells, and Organic light-emitting diodes (OLEDs). The size dependent optical properties of this material are very interesting and it can also be tailored with annealing temperature.

Because of these properties, it can be used for the wide range of applications like fabrication of switching element, transistors (Arnold *et al* 2002) and detectors. It is transparent to the most of the solar spectrum, therefore widely used for window material in solar cells, optical waveguide, light modulators and optical sensors. Therefore the controlled synthesis of good quality ZnO nanostructures, nano crystals (Singh & Gopal 2008a), nano wires, nano belts and other nano architecture are very important. Several routes are employed to synthesis the ZnO nano materials particularly solvothermal (Dev *et al* 2006), thermal evaporation (Pan *et al* 2001, Kong *et al* 2004), solid state pyrolysis (Wang *et al* 2003), chemical vapour deposition (Fay *et al* 2005; Xiang *et al* 2007), molecular beam epitaxy (Agasheet *et al* 2004)

and laser ablation (Singh *et al* 2008) etc. These technologies are very expensive and difficult to use for large area fabrication. Therefore, to overcome these difficulties, we have adopted the low-cost sol-gel technique to grow the ZnO nanomaterials.

In this paper we report the characterization of ZnO nanomaterial synthesized by ZnO different method using hydroxide route. Structural and surface morphology properties have been studied by using X- Ray Diffraction and Scanning Electron Microscope techniques.

EXPERIMENTAL

ZnO is prepared by conventional precipitation method using sodium hydroxide and zinc sulphate solutions. Calcinations of zinc hydroxide gives zinc oxide in powder form. For the preparation of zinc hydroxide, sodium hydroxide solution is mixed with sodium sulphate solution in two ways, in the first approach (i.e. ZnO-A) sodium hydroxide is mixed drop wise with zinc sulphate solution and for second approach (ZnO-B) it has been mixed in one-shot with the same.

First of all homogeneous solution of NaOH is prepared by dissolving 1.6 g of NaOH (Merk Specialties Private Ltd, India) in 40 g of distilled water. The pH value of NaOH was found 11.57. The recorded humidity and temperature during experiment was found 29% and 34.5⁰C respectively.

Similarly, a homogeneous solution of ZnSO₄ (Chemical Corporation of India) in 120 ml of water. Then NaOH solution was mixed drop wise with regular interval of time with continuous stirring for 35 min. The mixture was allowed to stir for next 30 minute more and left it for another 48 hours. The obtained product was filtered using Whatman filter paper and washed properly with deionised water to remove all the sulphate ions etc. The white precipitate containing zinc hydroxide was spread on the glass substrate. The glass substrate was placed in an oven and alternate heating and cooling was applied. First of all it was heated at 150⁰C for one hour then allowed to cool for 30 minute. The process of heating for one hour and subsequent cooling for 30minute was repeated for five times. Hence after total heating for five hour, ZnO-A is collected in powder form.

Similarly in method (B) again similar solution of NaOH and ZnSO₄ as in method (A) having same pH value and at room temperature were prepared. In this method NaOH solution was allowed to mix in one-shot in ZnSO₄ solution. The mixture was allowed to stir continuously for 12 hour then left for 72 hour. After 72 hour the mixture was filtered out by Whatman filter paper and washed properly through with deionised water to remove all the sulphate ions etc. After washing properly the residue i.e. zinc hydroxide was spread on a glass substrate. After applying similar process of heating and cooling as in method (A) i.e. subsequent heating for 1 hour and cooling for 30 minute for five times, ZnO-B is collected in powder form.

RESULT AND DISCUSSION

Surface morphology study by SEM:

The morphology of synthesized powder was investigated with scanning electron microscope (SEM, Edex). Figure 1(a) and (b) show the morphology of the ZnO film prepared by sol-gel technique for both methods. Method (A) and method (B) give the ZnO nanomaterial in the form of cluster and nanosheets showed in figure 1(a) and 1(b) respectively. The image obtained by SEM shows that the particle prepared by method (A) exist in cluster form whereas that obtained in method (B) does not exist in cluster form. The particles prepared by this process are named as ZnO- A and ZnO –B.



Figure 1(a): SEM image of ZnO - A prepared by method - A



Figure 1(b): SEM image of ZnO - B prepared by method - B

Crystal Structure study by XRD:

The crystalline property of synthesized powder was investigated with XRD (Mini Flex, Rinku Corporation, Japan). The X-ray diffraction data were recorded with Cu K_{α} radiation have wavelength 1.5418 Å. The intensity data was collected over the range 10° to 70° . The most intense peak (Fig.2 a and b) were considered for the sample ZnO- A and ZnO -B. the peaks are very intense which shows that the the grown material is crystalline in nature. The peak of ZnO -B is more intense with respect to ZnO- A. it shows that ZnO -B is more crystalline than ZnO- A. by calculating the FWHM values of the above sample, the sizes of the crystals are calculated by Debye Scherer Formula (Vermeulen *et al* 2007). The size of ZnO- A and ZnO -B were found 10nm and 7.7 nm respectively. The size of the particle prepared by the method as for ZnO -B is more fine with respect to ZnO- A.

The size of the crystal in the direction perpendicular to the reflecting plane is given by Debye Scherer Formula

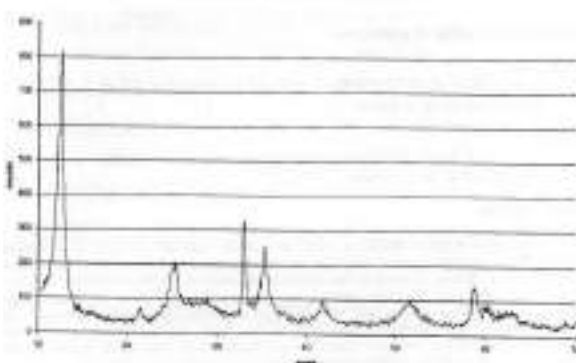


Figure 2(a) : XRD plot for ZnO-A

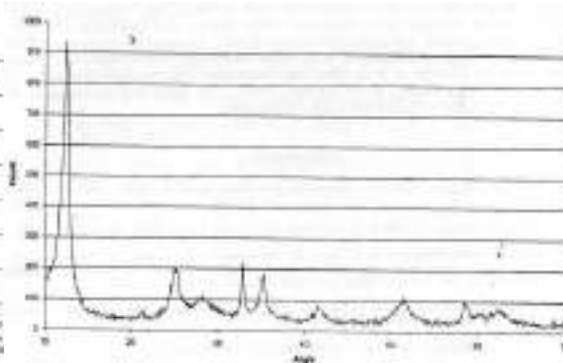


Figure 2(b): XRD plot for ZnO-B

$$D = \frac{k\lambda}{\beta \cos\theta}$$

Where k is constant its value lies from 0.89 to 1.39 depending on the specific geometry of the scattering object. For two dimensional lattices the value of k was found to be 0.89 while that of three dimensional lattices is 1.3. β is the FWHM of the peak in radians, θ is the diffraction peak position and λ is the wavelength of the x-rays used.

The experimental result was found to be

For ZnO- A: $2\theta = 12.56$, $\theta = 6.28$, β (FWHM)=0.01396(in radian), $K=0.89$.

Size of ZnO-A, D_1 - **10.0nm**

For ZnO -B: $2\theta = 12.40$, $\theta = 6.20$, β (FWHM)=0.01815(in radian), $K=0.89$.

Size of ZnO-B, D_1 - **7.7nm**

Conclusion

Synthesis method plays an important role in monitoring structural properties of materials as shown by the Scanning Electron Microscope and X-ray Diffraction study of ZnO nanomaterials. It was found that the particle of ZnO-B is highly crystalline and size of particle is also very fine with respect to the sample prepared by method -A. This morphological change due to difference in applied physical parameters i.e. due to different sedimentation time and stirring time. So, by changing synthesis method we can obtain different types of ZnO nanomaterials and change the crystallinity of ZnO nanomaterials.

Acknowledgement

The authors express sincere thanks to Dr. O.N. Srivastava, Department of Physics, Banaras Hindu University, Varanasi, for providing SEM facility and Dr. Amarendra Narayan, Department of Physics, Patna University for providing XRD facility, also thanks to Dr. N.A. Karimi, Department of Physics, B N College, Patna for stimulate discussions and thanks to UGC New Delhi for providing financial assistance for running the project under no. F.No. 35-17/2008(SR).

References

1. Agashe C, Kulth O, Hupke J, Zastrow U, Ruched and Wutting M (2004). *J. Appl. Phys.* **95**; 1911
2. Arnold M, AvourishPh, Pan Z W & Wang Z L (2002). *J. Phys. Chem.* **B107**; 659
3. Bahadur H, Shrivastava A K, Divi H, Cahndra H, Basu A, Samanta S B, Sood K N, Ramkishore, Sharma R K, Rashmi, Vivekananda Bhatt, Prem Pal & Sudhir Chandra (2007), *Indian J Pure & Appl Phys*, **45**; 395
4. Chen S Q, Zhang J & Feng X (2005). *Appl. Surf Sci.* **241**; 384
5. Dev A, Kar s, Chakrabarti S. and Chaushuri S (2006). *Nanotechnol.* **17**; 1533
6. Fay S, Kroll U & Bucher C (2005), *Sol. Energy Mater Sol. Cells.* **86**; 385
7. Haase M, Weller H, & Hangleina A (1998). *J. Phys. Chem.* **92**; 482
8. Jhonson J, C, Yan H, Schaller R D, Haver L H, Saykally R J & Yang P (2001). *J. Phys Chem.* **B 105**; 113875
9. Kong X Y, Ding Y & Wang Z L (2004). *J. Phys Chem.* **B 108**; 570
10. Pan Z W, Dai & Wang Z L (2001). *Science.* **291**; 1947
11. Singh S C & Gopal R. (2008a). *Phys Chem.* **E 112**; 724
12. Vermeulen H, van Hattem J M, Strom-Versloot M N & Ubbink D T (2007). "Tropical silver for treating infected wounds", *Cochrane Database of Systematic Review (1)*; **CD005486**. Doi: 10. B 1002/ 14651858, **CD005486 Pub2. PMID 17253557.**
13. Wang Z, Zhang H, Zhang L, Yuan J, Yan S & Wang C. (2003). *Nanotechnol.* **11**; 14.
14. Yadav B C, Srivastava, Richa & Alok Kumar. (2007). *Inter. J. of Nanotechnology and Application*, 1(**No-2**); 1-11.

STUDY OF CROP RANKING IN DINDORI TAHSIL, NASHIK DISTRICT, MAHARASHTRA
STATE, INDIA

Dr. Sachin Ranu Govardhane

V.V.Ms S.G. Patil Arts, Science & Commerce College Sakri (Dhule)

ABSTRACT

The cropping pattern is based on both time and space sequence of crops. The variety in cropping pattern is the result of physical economic and social factors. The crop pattern in any region cannot remain static due to the variations in the rainfall amount and nature of inputs and environmental instability. Moreover, introduction of new high yielding varieties of seeds, irrigation facilities and technical knowledge are responsible for temporal changes. The cropping pattern undergoes changes in response to the changing physical and cultural environment. For an appreciation of temporal variations in study area twenty years have been taken into account and study was made with considering a real strength. The present study is carried out basically with the help of secondary data in 2011 year. The secondary data has been collected from Department of Agriculture, DindoriTahsilNashik District. The results of the study indicate that Grapes &Fruits are first rank crops in the western part of the study area whereas fodder, Oilseeds, Jowar, Bajara and Other Cereals are the first ranking crop in the dry areas of DindoriTahsil.

KEYWORDS: Crop ranking, cropping pattern

INTRODUCTION:

Agriculture plays a vital role in the economy of a country and it is the backbone of our economic system. Agricultural regionalization is important step for agricultural development and through which we understand the regional imbalance and disparities. The study of agriculture region is of great importance in geographical studies. The regional dominance of various crops can be determined by comparing the relatively a real strength of various crops. This can be obtained by ranking them, for each paragon, according to the percentage of the total harvested cropland occupied by each crop (Porwal 1994). The simplest form of the agricultural regionalization of first order is based on either the dominating crop (first ranking crop) or a specific indicator used to define an area. On the basis of crop dominance and ranking device, regions like Corn Belt, Cotton Belt were defined for the United States by American geographers (Singh and Dhillon, 1994). The crop ranking has been done on the basis of dominance of area under specific crops.

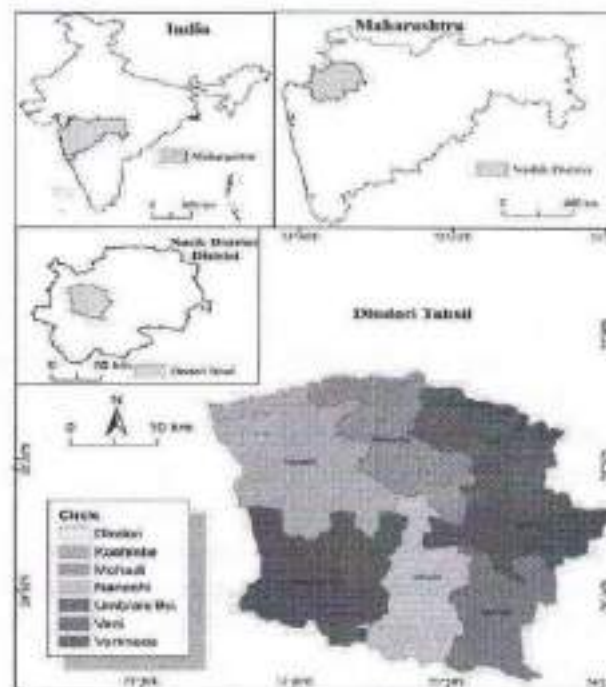
The cropping pattern is based on both time and space sequence of crops. The variety in cropping pattern is the result of physical economic and social factors. The physical environment provides a wide range of possibilities for growing crops, but the social and economic conditions determine as to which the crops to be grown are and how much of it is to be devoted to different crops. In fact, social and cultural values strongly influence the cropping pattern especially in the countries where agriculture is a way of life. The farming communities have developed their own techniques and tradition, which affect the growth of crops. These crops are not always being grown when they are best adapted to, nor when these can be grown most economically (Ningaraju and Arun Das 2017).

STUDY AREA:

The Dindori tehsil lies in west central part of the Nashik District of Maharashtra state. Out of four administrative divisions Dindori Tehsil lie under Nashik sub division. The absolute geographical location of the tehsil can be express as 20° 03' 25" North latitude to 20° 27' 06" North latitude and 73° 34' 06" East

longitude to $74^{\circ} 00' 06''$ East longitudes. The Kadva River flows west to east. Dindori tehsil is bounded by Peth tehsil towards the west, Surgana tehsil in north-west, Kalwan tehsil towards the north-east, Chandwad and Niphad tehsil towards the east and Nashik tehsil towards the south. Climatologically, it lies in the rain heavy rainfall zone of the Western Ghats and geomorphological, it is located in the Unanda in north and Kadava basin south, a part of upper Godavari basin. The total geographical area (TGA) of the tehsil is about 1342.19 square km. It is about 08.64 percent of TGA of Nashik District. According census the total population during year 2001 of tehsil was 264727 and it was increase up to 315709 during 2011. The population density of the tehsil is 239 persons per square km according to 2011 census. According to abstract of census handbook the tehsil comprises of 157 villages and one urban center i.e. Dindori. The villages are subdivided into various sub circles in 2001 there were four revenue circles in 2011 those circles were modified into six subgroups namely Dindori, Mohadi, Umbrale, Vani, Varkheda, Koshinbe and Nanashi (Map no 1.1)

MAP NO.1: Location Map



OBJECTIVES

The present paper is aimed at implementing the cropping pattern detection method for understanding the land use/land cover change in Dindori Tehsil taken place over the period of 2011 present century. The main objective of the present study is to assess cropping pattern and crop ranking in the Dindori Tehsil.

DATA SOURCES AND METHODOLOGY:

The present study is carried out basically with the help of secondary data in 2011 year. The secondary data has been collected from Department of Agriculture, Dindori Tehsil Nashik District.

RANKING OF CROPS:

The percentage area under each crop was determined simply by ranking them for study area in order to have percentage of the total net sown area working by each crop. Ranking of crops gives an understanding into the geographical reality of the cropping pattern. Also, ranking of crops helps in knowing the crops which contend with each other to improvement more hectare under cultivation. Afterwards measuring the relative gift of different crops in a geographical unit the process of planning can be introduced more sensibly for the best use of the available land for cultivation. A careful use of land with acceptable inputs in detail can help in rising the agricultural production even in the fewer fertile, soil. Thus, the study is useful in doppelganger regional disparities in the agricultural income and economy. Without the major crops of the Dindori Tahsil are studied in their ranking order and the areal strength of each crops is resolute, a suitable association of soil and soil inspirational crops for each situation cannot be determined.

RANKING METHOD

Ranking method can be studied by expressive and measurable methods to outline the ranking of separate crops according to their areas of position in each element unit. The crop with the larger percentage segment to the net sown area forms the first ranking crop and the crop with the next largest share becomes the second ranking crop. Also calculations have been made up to 01to 10th ranking crops have been plotted in figure table 1.1, 1.2 and 1.1 for the year 2011.

Table No 1.1: Crop Ranking village wise Frequency in 2011

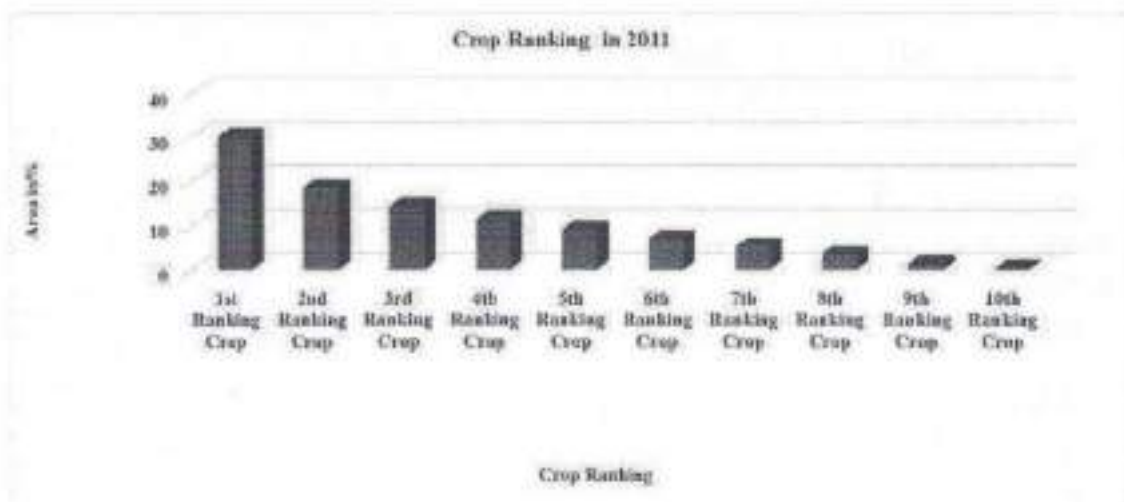
Ranking Crops	1 st and villages	2 nd villag es	3 rd villag es	4 th villag es	5 th villag es	6 th villag es	7 th villag es	8 th villag es	9 th villag es	10 th villag es
Oilseeds	11	37	29	30	31	10	5	3	1	0
Other Cereals	37	19	20	13	22	24	16	6	0	0
Vegetables	10	26	18	16	14	24	22	19	8	0
Grapes & Fruits	53	23	10	7	7	17	16	15	8	1
Wheat	10	18	33	37	33	9	13	4	0	0
Spices	0	0	0	3	5	3	11	31	60	44
Sugarcane	1	1	3	2	1	8	11	8	40	82
Pulses	0	9	12	17	23	42	32	20	2	0
Fodder	31	4	8	7	9	13	19	37	20	9
Rice	4	20	24	25	12	7	12	14	18	21
Total Villages	157	157	157	157	157	157	157	157	157	157

Table 1.2: Rank wise area in percent in year 2011

Crop Ranking	2011	
	Area in Hectors	Area in Percent
1 st Ranking Crop	4731.08	30.13
2 nd Ranking	2886.65	18.39

Crop		
3 rd Ranking Crop	2238.03	14.25
4 th Ranking Crop	1766.31	11.25
5 th Ranking Crop	1410.85	8.99
6 th Ranking Crop	1082.55	6.90
7 th Ranking Crop	814.73	5.19
8 th Ranking Crop	531.62	3.39
9 th Ranking Crop	198.80	1.27
10 th Ranking Crop	39.38	0.25

Graph no 1.1: Crop ranking area in % year of 2011



The first ranking crops in the Dindori tehsil. Eight crops have been identified as first ranking crops during the year 2011. These Eight crops are, namely, Oilseeds, Other Cereals, Vegetables, Grapes & Fruits, Wheat, Sugarcane, Fodder and Rice crop. Out of these all crops Other Cereals (37), Grapes & fruits (53), Fodder (33), Oilseeds (11) While in 2011 the Other Cereals (37), Grapes & fruits (53) and Fodder (31) having almost 81 percent of total area of the tehsil within first ranking crop. During 2011 the first ranking crops were occupied about 4731.08 hectares area which is about 30.13 percent of total area of the tehsil. While the 2011 the grapes in fruits occupied largest area in first ranking. After grapes and fruits the other cereal and fodder crops were first ranked spatially located at western and middle part of the villages within the tehsil. the crop ranking in which farmers are mainly focus to produce cash crops like grapes and fruits because suitable soil condition and major irrigation facility available nearby Kadava river basin and Kadava dam. Also several vineries industries were established in the south eastern part of the Dindori tehsil which is responsible to increase in area under Grapes and Fruits. In western part of the tehsil other cereal and fodder crop were produces by farmers because of most of population is tribal and the focus on traditional trend of cropping pattern.

Ten ranking crops area increased by 39.38 percent on 2011 determining on 0.25 percent area of the tehsil. Table 1.1 and 1.2 indicating the village wise area under tenth ranking crops. The major crop were sugarcane (103), rice (29) and spices (11) in 2001. These crop cultivating 13.66 (36.80 percent), 14.11 (38.01 percent)

and 4.89 (13.17 percent) hectore area respectively. In 2011 the same major crop were cultivated in the tehsil but the area under rice (16.63 percent) crop significantly decrease while area under spices (27.42 percent) were significantly increase. In which except south eastern part of rice cultivated area all other area under sugarcane crop. There were some patches of spices in central part of the tehsil. In 2011 patches of spices and area under sugarcane were significantly increase. While the area under rice cultivated villages were decreased.

CONCLUSION

The overall differences between wet and dry taluks can be as follows

- 1) Rich crop has been cultivated as first ranking crop in the western part and Grapes & Fruits is first rank crops in eastern part of the study area.
- 2) Fodder, Oilseeds, Jowar, Bajara and Other Cereals are the first ranking crop in the dry area in Dindori Tahsil whereas the wet crops like sugarcane and Grapes & Fruits is produced as the first.
- 3) There is a intermix of Oilseeds, Fodder, Jowar and Other Pulses as forth and fifth ranking crops in the study area in different periods.
- 4) Among the dry taluks, other pulses and Fodder are the second and third ranking crops.
- 5) There exist differences in the ranking of crops, between wet and dry taluks with in the same ranks up to fifth rank. The middle order ranks like sixth, seventh and eight ninth, tenth possess few wet crops in the dry taluks. This type of trend cannot be noticed in, eleventh and twelfth crops between wet and dry taluks.

REFERENCES:

- Gadekar Deepak Janardhan (2016) Regional disparities of agricultural development in Ahmednagar District, MS, India. International Journal of Research in Social Sciences, Volume-6, Issue-8, Pp 389-403.
- Husain, M. (2010) Systematic Agricultural Geography. New Delhi, India: Rawat Publication.
- Ningaraju, and Dr. S Arun Das. (2017). "CROPPING PATTERN AND CROP RANKING OF MYSORE DISTRICT." International Journal of Research - Granthaalayah, 5(4), Pp334-338.
- Porwal, M. C. (1997) Remote sensing analysis of environmental resources for planning and development. Delhi, India: APH Publishing Corporation, Pp302.
- Singh, J. and Dillon, S. S. (1994) Agriculture Geography. Tata McGraw-Hill publishing Company Limited New Delhi, India.
- Vipin Kumar (2017) Study of Cropping Pattern, Crop Ranking and Crop Combination in Somb River Basin at Lower Shiwalik Hills, International Journal of Advanced Remote Sensing and GIS, Volume 6, Issue 1, pp. 2297-2305.

SCHEDULED CASTE POPULATION GROWTH RATE IN NANDURBAR DISTRICT: A GEOGRAPHICAL PERSPECTIVE

***Dr. Vijay. R. Baviskar**
Head, Dept. of Geography
B. P. Arts, S. M. A. Sci. & K. K. C. Comm.
College, Dhule Road, Chalisgaon
E-mail:- drvijavkar5@gmail.com
E-mail:- vbaviskar15@gmail.com

****Dr. Sachin R. Govardhane**
Assistant Professor, Dept. of Geography
S. G. Patil A. S. C. College, Sakri, Dist-
Dhule
E-mail:- sachingovardhane@gmail.com

ABSTRACT

The Scheduled Caste population belts are specially demarcated the high inclination of growth rate. He present research work is showing the growth rate index of scheduled caste population. The Nawapur and Nandurbar talukas denote highest growth rate index in 1971-81 and 2001-11. The majority of the population is from the scheduled caste population of these tehsils while Akkalkuwa -07.18 (1971-81) & -04.51 (2001-2011) and Akrani (Dhadgaon) (2001-11) -04.51 Taluka observed as the lowest growth rate index.

KEYWORDS

Growth Rate, Growth Rate Index, Fertility, Mortality, Inaccessibility etc.

INTRODUCTION

Population growth rate is a major factor which indicates the past and future of a population. The population growth rate shows the change of population size as a factor of time. The population growth rate deals with the study of the average decadal rate of change of population size. The present research work attempt to study four decadal variation population growths in Nandurbar district. Looking at the population growth during the inter-censal period 1971 to 2011 the growth rate observed between 20 to 40 percent in the census of 1971 and 37.51 to 15.87 percent in the census of 2011.

OBJECTIVES

1. To study the scheduled caste decadal growth rate index of the study region.

THE STUDY AREA

Astronomically Nandurbar district extends between $21^{\circ} 50'$ to $22^{\circ} 17'$ North latitude and $73^{\circ} 31'$ to $74^{\circ} 50'$ East longitude. The region is bounded by Dhule district on east and south, While on the west by Surat district of Gujarat state and on the north by Badhwani and Jhabua

district of Madhya Pradesh state. The Nandurbar district with a geographical area of 5034.23 sq km. has an amorphous shape. According to the census, 2011 quantity of urban population is very low with 16.72 percent of total population in the district and 83.28 percent of the total is living in rural areas.

RESEARCH METHODOLOGY

This study is based on the trustworthy and truthful census data. It is not possible to conduct an individual enumeration of the required data from door to door in the study region. The required secondary data has been collected from the District census handbook (1971-81, 1981-91, 1991-2001 and 2001-2011).

The geographical study of over 40 years i.e., from 1971-2011 has been analyzed for scheduled caste population. For a detailed study of changes in the decadal growth rate index of scheduled caste population of specific talukas. The collected data has been processed and analyzed by using the different statistical technique. The tabulated data has been presented by the figures.

For the measurement of population growth rate index following formula has been employed;

$$GRI = \frac{TPa}{TPb}$$

Where,

GRI= Growth Rate Index

TPa= Total Population of Scheduled caste in 2001-11

TPb= Total Population of Scheduled caste in 1971-81

RESULTS AND DISCUSSION OF FINDINGS

Fig. no 1.0 shows the trend of decadal growth rate index of Scheduled caste population of Nandurbar district. There is a large variation hence the dominant tribal taluka.

Table No 1.0 Nandurbar District: Growth of Total Scheduled Caste Population 1971 To 2011

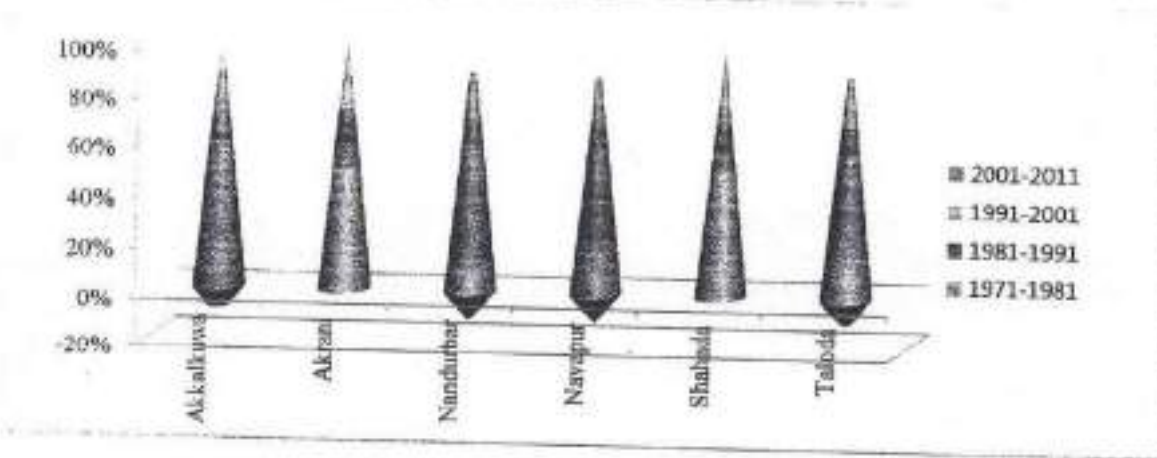
Sr. No.	Name of Talukas	Growth Rate Index 1971-81	Growth Rate Index 1981-91	Growth Rate Index 1991-01	Growth Rate Index 2001-11	Change In Growth Rate Index (1971-81 to 2001-11)
1	Akalkuwa	-07.18	127.63	07.80	-04.51	2.67
2	Akrani (Dhadgaon)	81.95	39.48	36.01	10.38	-71.57
3	Nandurbar	15.28	-21.96	06.22	141.53	126.25
4	Navapur	35.34	-37.36	30.92	192.49	157.15
5	Shahada	67.81	26.65	01.18	37.20	-30.61

6	Taloda	17.40	-12.44	12.67	73.04	55.64
	Study Region	35.01	07.03	53.62	75.02	39.92

Source: Computed by author.

Table No.1.0 shows the over 40 years i.e. from 1971-2011 has been total Scheduled Caste population in Nandurbar District. In last four decades the total Scheduled Caste population,

Fig. No. 1.0 Nandurbar District: Growth of Total Scheduled Caste population 1971-81 To 2001-2011



Have substantially increased. During 1971-2011 population in the Nandurbar District region has recorded an increase of +162.15 percent, whereas growth rate in a region during 1971-81, was +37.51 percent. Contrary to this during the year, a 1981-91 decrease in the population was 07.03 percent. 1991-2001 increase in the population was +53.62 percent and 2001-2011 this year total Scheduled Caste population is decreasing was +15.87 percent respectively.

During 1971-1981 this period the region's total Scheduled Caste population growth was +37.51 percent. Among the Tahsil of the region, the negative change was recorded in Akkalkuwa Tahsil with -07.18 percent. In the study region, there is a found high tribal concentration in a specific zone. In 1971-81 there are found large variations in the total Scheduled Caste population growth were noticed in Talukas. Among the Tahsil of the region, the highest total Scheduled Caste population growth was found in Akrani (Dhadgaon) Taluka with 81.95 percent followed by Shahada Taluka with 67.81 percent

respectively. Also, the lowest total Scheduled Caste population growth was found in Nandurbar Taluka with 15.28 percent followed by Taloda and Navapur Taluka with 17.40 and 35.34 percent. In the 1971-91 decades due to the epidemic diseases, natural calamities and of droughts the death rate was increased hence negative population growth has been recorded. Correspondingly, 1981-91 in the highest total Scheduled Caste population growth was recorded in Akkalkuwa Taluka with 127.63 percent followed by Akrani (Dhadgaon) and Shahada Taluka with 39.48 and 26.65 percent respectively. The highest negative change was recorded in Navapur Taluka with -37.36 percent followed by Nandurbar and Taloda Taluka with -21.96 and -12.44 percent respectively. In this decade due to the migration, the negative change has been recorded.

During 1991-2001 this period the highest total Scheduled Caste population growth was found in Navapur Taluka with 30.92 percent followed by Akrani (Dhadgaon) and Taloda Taluka with 36.01 and 12.67 percent respectively. In lowest population growth was recorded in Shahada Taluka with 01.18 percent followed by Nandurbar and Akkalkuwa Taluka with 06.22 and 07.85 percent correspondingly. During the period of 2001-2011, the highest total Scheduled Caste population growth was found in Navapur with 192.49 percent followed by Nandurbar Taluka with 141.53 percent in that order. In lowest total Scheduled Caste population growth was recorded in Akrani (Dhadgaon) Taluka with 10.30 percent followed by Shahada and Taloda Taluka with 37.20 and 70.22 percent respectively. In the negative total Scheduled Caste, population growth rate was recorded Akkalkuwa Taluka with -04.51 percent

According to relevant data and observations, there is found a wide variation of total Scheduled Caste population growth in the study area. Beside that the decadal growth also varies in the 1971-2011 up to 4 Taluka noticed or negative change. In 1971-91 due to the epidemic diseases, natural calamities occur and its effect on the growth of population. But in 1981-1991 due to the out-migration, the population growth was recorded as negative. Population growth rate is the unifying variable linking the various facets of population ecology thus analyses of population regulation, density dependence, resource and interference competition and the effects of environmental stress are all best undertaken with population growth rate as the response variable.

CONCLUSION:

1. The average growth rate index of study region is recorded 37.51 during 1971-81. 07.03

2. The average growth rate index of study region is recorded 07.03 during 1981-91.
3. The average growth rate index of study region is recorded 53.62 during 1991-2001.
4. The average growth rate index of study region is recorded 15.87 during 2001-11.
5. The average change in growth rate index of S. T. population is 39.92 in the study area.

REFERENCES:

- 1) Census Handbook Nandurbar, Dhule Districts 1991, 2001, 2011.
- 2) Mukherjee, Gargee And Sharma Sarla (2008): "A Study Of Fertility Pattern Of Raipur District, Chattisgarh State", The Deccan Geographer, Vol-50, Pp. 47.
- 3) Sabina Bano (2012): "Gender Disparity In Varanasi City", The Deccan Geographer, Vol. 50, June-2012.
- 4) Nagraj H. And Somana N. (2012) "Fertility And Mortality Pattern in Mysore District", The Deccan Geographer, Vol. 50, Dec 2012, Pp. 91.
- 5) Ghosh, B.N. (1985) "Fundamentals Of Population Of Geography", Sterlings Publication, New Delhi.
- 6) Caldwell, J.C. (1980): "Mass Education as A Determinant Of The Timing Of Fertility Decline, Population And Development Review 6 (2): Pp.225-255.
- 7) Eva Kiss, (2007): " An Assessment Of Health And Population In Hungary", The Deccan Geographer, International Geographical Journal of India, Vol. 45, No. 2

***Dr. Vijay. R. Baviskar**
 Head, Dept. of Geography
 B. P. Arts, S. M. A. Sci. & K. K. C. Comm.
 College, Dhule Road, Chalisgaon
 E-mail:- drvijaykar5@gmail.com
 E-mail:- vbaviskar15@gmail.com

****Dr. Sachin R. Govardhane**
 Assistant Professor, Dept. of Geography
 S. G. Patil A. S. C. College, Sakri, Dist-
 Dhule
 E-mail:- sachingovardhane@gmail.com

IMPACT OF COVID-19 PANDEMIC IN INDIAN ECONOMY*

BY

Dr. Govardhane Sachin Ranu*

Asst. Prof. Dept. of Geography V. V. Mandal's S. G. Patil Arts, Science & Comm. College, Sakri, Dhule, Maharashtra' sachingovardhane@gmail.com

Dr. Borase Sudhakar Jagannath*

Asst. Prof. Dept. of Geography, G. E. Society's RNC Arts, JDB Comm. & NSC Sci. College Nashik Road, Maharashtra. borasesudha@gmail.com

Abstract:

The epidemic of Covid – 19 has spread not only across the country but all over the world and its outbreak is an unprecedented blow to the Indian economy. The Government of India has announced a number of measures to address the situation, ranging from additional funding for food, security and healthcare to sector-related incentives and tax extensions. The long-term nationwide lockdown, the global economic downturn, and the relative disruption of supply and demand chains have left the economy facing a long period of recession and are likely to continue to do so. This study has shown the potential impact of the shock on various sectors such as the manufacturing sector. This research paper seeks to present a set of policy recommendations for financial services, banking, infrastructure, Indian agriculture, real estate, other services and specific sectors.

Keywords: Covid – 19, Indian Economy, Varies sectors.

Received 06 June 2021, Accepted 20 June 2021, Published 26 June 2021

*Correspondence Author: Dr. Govardhane Sachin Ranu

1. Introduction:

Outbreaks of the corona virus pose a serious threat to billions of people worldwide. In addition to being detrimental to human health, global trade is affecting the entire economic system and trade and commerce worldwide. The first outbreak of the disease occurred in December 2012 in Wuhan, China. The World Health Organization (WHO) is fully monitoring its global threat and thus it is declaring 30 January 2020 as a public health emergency of international concern. The virus began to spread at an unprecedented rate in various countries around the world on March 11, 2020, forcing the WHO to declare it an epidemic, now the whole world is facing this useless and harmful enemy. Many countries are under lockdown and everything has come to a standstill, including normal life, social and social conditions. The first case of corona virus was reported in Kerala on January 30, 2020. As many patients were found in different cities of India, on 24th March 2020, the Government of India declared

a lockdown in every corner of the country and took necessary action. The metropolises of Delhi, Mumbai, Ahmadabad Kolkata, Chennai are densely populated which has given rise to a spurt in cases of covid-19 and these cities are the engines for growth and development of Indian Economy

2. Objectives:

The entire business world is in the cycle of the corona virus. As the virus is having a severe and rapid effect, companies need to come up with appropriate strategies to deal with this difficult situation. Therefore, the objectives of this study are as follows.

1. To understand the impact of Covid – 19 on the Indian economy.
2. To find out the challenges for different sectors in Indian economy
3. To create awareness among the people about impact of Indian economy due to Covid – 19.

3. Sources of Research Papers:

The study is descriptive nature. Secondary Sources such as Books, Research Journals Magazines, Internet and Daily News papers.

4. Impact of COVID-19 in Various Indian Sectors:

Covid-19 has set foot in India and has taken the country into a major crisis. Corona virus disease has become a world-changing phenomenon and is not only a humanitarian crisis but also an economic and social crisis. This affects the business environment and it grows worldwide and many times over. Due to the rapid spread of the corona virus, a number of factors are bound to limit their business operations, which hinders the economic functioning of many industries that contribute to growth. The impact on different sectors of the economy is highlighted below.

4.1 Primary Sector:

Primary sector includes information and manufacturing and raw material related industries. The sector employs about 43.21% of India's population and contributes about 16.1% of Indian GDP. It supplies raw materials to the secondary sector and provides the basic necessities of human life.

4.1.1. Agricultural industry:

Travel restrictions for lockdowns in the agricultural sector have led to a shortage of agricultural workers, leading to a decline in production. Also, the lockdown period (epidemic) all over the country (or across the continent) is consistent with the harvest season of the "Rabi" crop, but due to the shortage of labor, the crop remained in the field without any problems. The markets for the raw materials used

for this have gone down and so have the complaints of the farmers. The revenue of tea-based industries has declined significantly as most of their production is now being exported.

4.1.2. Mining Industry:

Outbreaks appear to be exacerbated by the overall demand for metals and minerals all over the country (or continents), which has led to lower rates. Mining firms have also seen their share prices fall sharply.

4.2 Secondary sector:

The secondary sector employs about 24.89% of the population and accounts for 29.6% of Indian GDP. It embraces industries engaged in the production and distribution of manufactured goods or construction activism, which provides support to both the primary and service sectors.

4.2.1. Manufacturing Industries:

The manufacturing industries are picking up the brunt of the corona virus as they discontinue their production in a short time. The value of the goods in the production center or warehouse of these industries has come down and the machines have been idle for a long time. The biggest hurdles that industries faces are cash flow disruptions and supply chain disruptions.

4.2.2 Automobile Industry:

With almost all plants shut and imports being sealed up, there is a steep decline in production and sales of the automobile companies impelling them to declare pay cuts. The situation will be awful even during post lockdown period due to fall in income levels.

4.2.3 Textile and Apparel Industry:

This industry is workplace for over 45 million people in the country but temporary closure of production units has increased their hurdles leading to lay-offs. The terminations of exports and imports have adverse impact on the spinning mills in India as the exports of fabne, yarn and other materials have disrupted.

4.2.4. Pharmaceutical and Chemical Industries:

These industries are heavily dependent on imports of large quantities of drugs and raw materials from China. Import restrictions also affect these industries.

4.2.5. Electronic Industry:

The finished goods and raw materials used in this industry are mainly supplied to China. The spread of the corona virus has reduced the good production and sales of electronics and also disrupted the supply chain.

4.2.6. Solar Power Industry:

Solar power project builders depend on Chinese imports. About 80% of the solar modules and solar cells used in India are from Chinese manufacturers. Thus Indian solar project developers began to face a shortage of raw materials and their stocks were limited.

4.3 Service Sector:

About 31.9% of the population is employed in the service sector which accounts for 54.3% of Indian GDP.

4.3.1. Tourism and Hospitality Industries:

Tourism and hospitality is the biggest industry in the corona virus crisis and the most important industry to resume this initiative. The lockdown has hampered the flow of tourists, hitting the tourism and hospitality industries.

4.3.2. Transportation Segment:

Outbreaks appear to be exacerbated during this time of year. Airlines, cruise and road cargo operators have been hit hard by border closures and travel restrictions. Some airlines are not even in a position to refund their customers for flights canceled due to lockdown.

4.3.4. Healthcare Segment:

According to FICCI, the healthcare department is at the center of this global test. Demand for this specialty has grown significantly as a result of recent corporate scandals. Private hospitals are available to provide the government with all the help it needs.

4.3.5. IT Segment:

IT segment is reeling under corona virus crisis as there is immense dwindle in global deal activities as well as growth rate. They are downsizing their work force to tussle with the presence scenario.

4.3.6. BFSI Segment:

Covid-19 has impacted the BFISI department with its annual report on the waste of their business and the increase in their non-performing loans. In this emergency situation, employees as well as operating and technical difficulties were shown by the banks and the lack of agility in the banking and financial system.

4.3.7. Media and Entertainment Industry:

The corona virus has forced the release of many films to be postponed, shooting has calmed down, and cinemas cannot harm the industry.

4.3.8. Retail Segment:

The closure of shops and malls that do not sell essential commodities has led to an increase in revenue and a lot of loss of jobs. Retail stores selling essential commodities have increased demand for export-oriented retail shelves.

Conclusion:

In India, this has not yet begun in a systematic manner and needs to be prioritized along with the steps to address the health crisis. By rationalizing the tax rate or providing a tax rate, the impact of Covid-19 on the Indian economy will be curtailed, perhaps after the implementation of the measures. As for the measures needed to combat the economic impact of the rapidly spreading corona virus, government policymakers need to implement substantial targeted financial, comprehensive economic stimulus and policy rate cuts to help normalize economic policy as the Covid-19 crisis continues. . Probably a challenge for producers I will have to face numerous fronts. Producers will also need to look beyond their own financial consciousness if they need to coordinate closely with the public sector to create the necessary plans for the safety of the people and the turmoil of their work while keeping the lights on in public works. Some will be brown, but austerity measures must be taken to safeguard long-term goals.

SOURCES AND REFERENCES:

- Dr. Kishore Kumar Das and Shalini Patnaik (2020) The Impact of Covid – 19 in Indian Economy – An Empirical Study, International Journal o Engineering and Technology Vol.11, Issue 3, pp-194-202
- Nilofar Izhar (2011) "Geography and Health A Study in Medical Geography. A.P.H. Publishing Corporation New Delhi.
- Sudashan, R. M. (2011). India's National Rural Employment Guarantee Act: Women's Participation and Impacts in Himachal Pradesh, Kerala and Rajasthan.
- S.K. Shelar (2012) "Introduction to Medical Geography". Chandralok Prakashan. Kanpur-208021(India)

- S.J. Borase and S. K. Shelar (2017) Environmental Impact on Human Health-A study in Medical Geography Research paper
- S.J. Borase and S.K. Shelar (2019) Comparative study of infected patients with malaria and dengue in Nashik District Research paper. Electronic Interdisciplinary International Research Journal (EIJRJ) Volume – VII, Special Issue – XIV pp.11 -21
- S.J. Borase (2020) Impact of Covid -19 on the Rural Life Research Paper AJANTA Prakashan. Volume – IX, Issue III, July- sep, pp 36-40
- V.J Kamble & S.J. Borase (2020) State wise Depiction of Covid – 19 in India Research Paper AJANTA Prakashan Volume – IX, Issue III, July- sep, pp 59-64
- Daily News paper- Times of India, Lokmat Times, Divya Marathi

Impact of 1/4th sub lethal concentration of Cypermethrin and Fenvalerate on Acid and Alkaline phosphatase enzymes of fresh water fish *Channa marulius* (Ham Buch).

^aBhoi, S. S. and ^bPatole, S. S.

^aDepartment of Zoology, Uttamrao Patil Arts and Science College Dahiwel. (M. S.) 424304.

^bDepartment of Zoology, V.V.M's S.G. Patil Arts, Science and Commerce College Sakri (M. S.).

Corresponding Author: bhoiss16@gmail.com

ABSTRACT

The present study is aimed to investigate acid and alkaline phosphatase enzymes in liver, muscle and gill tissues of *Channa marulius* exposed to 1/4th sub lethal concentration of Cypermethrin and Fenvalerate. In present study the activity of acid and alkaline phosphatase enzymes in liver and gill were decreased, whereas in muscle it was increased in exposure period as compared to control groups.

Key Words: Acid phosphatase, Alkaline phosphatase, Cypermethrin, Fenvalerate.

INTRODUCTION

Fishes are very sensitive to a wide variety of toxicants in water, various species of fish show uptake and accumulation of many contaminants or toxicants such as pesticides (Srinivasan et al., 2011). Due to accumulation of pesticides in tissues produces many physiological and biochemical changes in the fishes and freshwater fauna by influencing the activities of several enzymes and metabolites (Rajini et al., 2014). Cells naturally contain enzymes for their functions such that damages to cellular membrane lead to their escape into the blood where their presence or activities can easily be measured as an index of cell integrity (Abalaka et al., 2011). Certain serum chemistry could be used to identify tissue damage (Susan et al., 2010). Phosphatase is mainly localized at cell membrane. Any damage in the cells may result in alteration in phosphatase activity (Shabnam and Badre Alam, 2012). Phosphatases are good indicators of stress condition in the biological system (Yi et al., 2009). Phosphatases are of two types, namely, Acid phosphatase and alkaline phosphatase. Acid phosphatase, the liposomal enzyme plays a vital role in autolysis degradation of tissues

capable of catalytic transphosphorylation where as Alkaline phosphatase is an enzyme found throughout the body, but it is mostly found in the liver, bones, kidney and digestive system. The lysosomes system has been shown to be very sensitive to change in the intra and extra cellular environment and subsequently to be involved directly or indirectly in controlling many physiological and pathological processes (Nafisa and Pirazada, 2016).

The present investigation was assessing the phosphatase activity in gill, liver and muscle of *Channa marulius* exposed to 1/4th sub lethal concentrations of Cypermethrin and Fenvalerate.

MATERIAL AND METHODS

The fresh water fish *Channa marulius* weighing (15±5 g) and length (10±3 cm) were collected from Kan and Panzara river of Sakri Tahsil (Dhule). Live fishes were brought to the laboratory and thoroughly washed under tap water and acclimatized in laboratory conditions for 15 days. They were fed with standard fish diet (Tokyu grow certified company). Water in the tank was changes after 2 days of interval. Technical grade Cypermethrin (25%) and Fenvalerate (ISAGRO ASIA), 20% (EC) were purchased from Sushil Agricultural pesticide and fertilizer Agency, Sakri for present study.

The fishes were divided into a 4 group, each group of ten healthy fishes were transferred to plastic tough having capacity of 10 litres and they exposed to 1/4th sub lethal concentrations of Cypermethrin (0.06 ppm) and Fenvalerate (0.085 ppm). One group was kept as control. At the end of exposure period, fish were randomly selected for biochemical study. Tissues like muscle, gill and liver were excised rapidly and processed for the biochemical estimation. Acid and alkaline phosphatase was estimated by Kinetic method by using kits which are manufactured by Autospan, Span Diagnostics, Ltd. Surat, Gujarat State India (Aspen Laboratories Pvt. Ltd. Delhi).

RESULTS AND DISCUSSION

A comparative data of liver, muscle and gill ACP and ALP levels in control and fish exposed to 1/4th sub lethal concentrations of Cypermethrin and Fenvalerate have been presented in Table1 and 2(Fig 1 and 2).

Cypermethrin

In the present investigation the liver acid phosphatase enzyme was decreased in the treated with 1/4th sub lethal concentration of Cypermethrin. The liver acid phosphate was 3.12, 2.91, 2.55, 2.45 and 2.40µ/l in control, 24 h, 48 h, 72 h and 96 h of exposure

respectively. The acid phosphatase content in muscle tissues of control fish was 4.18 and fish exposed to 1/4th sub lethal concentration of Cypermethrin contained 4.60, 4.72, 4.99 and 4.71 μ /l for 24 h, 48 h, 72 h and 96 h respectively acid phosphatase were increased significantly over control. In present study the ACP of gill observed in control fish was 2.03 and exposed fish contained 1.63, 1.64, 1.42 μ /l and 1.30 μ /l for 24 h, 48 h, 72h and 96 h respectively. The acid phosphatase level was decreased after 1/4th sub lethal concentration of Cypermethrin intoxication when compared with control. The fish exposed to 1/4th sub lethal concentration of Cypermethrin the liver alkaline phosphatase levels was decreased by 4.36, 3.98, 4.09, 3.56 and 3.04 μ /l in control, 24 h, 48 h, 72 h and 96 h respectively (Table 14). At the end of 96 h exposure ALP were decreased over control. The alkaline phosphatase in muscle tissue of control fish was 4.66 \pm 0.49 μ /l and fish exposed to 1/4th Cypermethrin was 4.67l, 5.18, 6.15 and 8.05 μ /l for 24 h, 48 h, 72 h and 96 h respectively. ALP showed an increased in all concentrations applied, on the 24 h to 96 h of observation. In the present investigation the fish *Channa marulius* treated with 1/4th sub lethal concentrations of Cypermethrin a perceptible decrease of alkaline phosphatase was observed in the gill for 24 h, 48 h, 72 h, 96 h and control respectively. The alkaline phosphatase of exposed fish was, 2.12, 2.08, 1.81 and 1.56 μ /l respectively control was 2.36 μ /l. The alkaline phosphatase activity in fish was decreased.

Fenvalerate

Liver acid phosphatase enzyme level indicated 3.12, 3.12, 3.10, 3.04 and 3.02 μ /l gain after control, 24 h, 48 h, 72 h and 96 h duration at 1/4th sub lethal concentration of Fenvalerate. Liver acid phosphatase was decreased when compared to control. The level of acid phosphatase exhibited remarkable changes from a mean control to exposure period, when the fish exposed to 1/4th sub lethal concentration of Fenvalerate. The acid phosphatase in muscle tissue was 7.54, 6.58, 6.02, 5.75 and 4.18 on exposure to 24 h, 48 h, 72 h, 96 h and control respectively. Acid phosphatase found to be increased for 96 h over control. The fish exposed to 1/4th sub lethal concentration of a Fenvalerate the acid phosphatase enzyme activities of gill for 24 h, 48 h, 72 h and 96 h showed 2.07, 2.05, 2.04, 2.01 μ /l respectively and control was 2.03 μ /l. The acid phosphatase was decreased in exposure periods over the control. At 1/4th sub lethal concentration of Fenvalerate exposed fish liver alkaline phosphatase level was decreased. The level of alkaline phosphatase was 4.36, 4.35, 4.33, 4.32 μ /l and 4.24 μ /l in control, 24 h, 48 h, 72 h and 96 h respectively. Alkaline phosphatase decreased as compared to control. The level of alkaline phosphatase in muscle showed changes from a mean control level to exposure, when the fishes were exposed to 1/4th sub

lethal concentration of Fenvalerate. The alkaline phosphatase in muscle tissue was 8.71, 9.26, 10.15, 11.73 and 4.66 μ /l on exposure to 24 h, 48 h, 72 h, 96 h and control respectively found to be increased for 96 h. In the present investigation the fish exposed to 1/4th sub lethal concentrations of Fenvalerate a perceptible decrease in the gills alkaline phosphatase has been observed in 24 h, 48 h, 72 h, 96 h exposure as 2.45, 2.38, 2.36, 2.27 μ /l respectively and mean control was 2.36 μ /l. The alkaline phosphatase activity was decreased in gills as compared to control.

At the end of the exposure period decrease in acid and alkaline phosphatase of liver and gills of fish exposed to pesticide Cypermethrin Fenvalerate. While in muscles acid and alkaline phosphatase activities were increased in fish exposed to pesticide. Findings in the present study are corroborated with findings of Shamshun et al (2010) reported decreased serum alkaline phosphatase value in the air breathing catfish, *Clarias batrachus* as a result of stress induced by low doses of Lead. Kumar et al (2012) reported a reduction in gill, liver and kidney alkaline phosphatase activity of *Carscious auratus* exposed to Azadiractin. The freshwater fish, *Clarias gariepinus* when exposed to sub lethal concentrations of Cypermethrin then its impact on the activity of alkaline phosphatase in the liver was studied. It was reported that the alkaline phosphatase activity was significantly inhibited (Gabriel et al., 2012). Palanisamy et al (2012) reported a notable Reduction in alkaline phosphatase activity in the whole body homogenate of *Mystus cavasius* when exposed to industrial effluent of Chromium. Reduced in the tissue alkaline phosphatase of the fish *Labeo bata* has been observed by Sarower et al (2012). Decrease in alkaline phosphatase level in blood was reported in *Claria gariepinus* exposed to sub lethal concentration of a synthetic Pyrethroids pesticide Cypermethrin (Ojutiku et al., 2013). Sudhish, 2013 reported that the freshwater fish, *Clarias batrachus* exposed to sub lethal concentrations of Rogar, the acid phosphatase and alkaline phosphatase activity was significantly reduced. Alkaline phosphatase is a widely observed enzyme in vertebrate species. It is mainly found in several tissues like liver, bone, kidney, intestine, epidermis etc. of the animals (Sripriya et al., 2015). Decreased activity of acid phosphatase was also reported in the blood of pesticide Dimethiote treated freshwater fish, *Catla catla*. (Mohammad et al, 2015). In fresh water teleost, *Labeo rohita* the Monocrotophos insecticide caused no significant difference in alkaline phosphatase activity in comparison with the control fishes (Devi et al., 2016). Kalaimani and There was an increase in the activity of acid phosphatase in Phosphamidon treated freshwater fish, *Labeo rohita* (Christobher et al 2016). Similar observations were made by Deshmukh (2016) in the *Channa striatus* exposed to endosufan. Kandeepan (2017) study on *Labeo rohita*, the alkaline

phosphatase activity has been decreased significantly in intestine and liver tissues with increasing sub lethal concentrations of Phosalone at different exposure period from 24 - 96 hours and this decrease may be due to the inhibition of enzyme activity by the pesticide Phosalone.

Table-1: Effects of sub lethal concentration 1/4th (0.06 ppm) of Cypermethrin on ACP and ALP in the liver, muscle and gill of *Channa marulius*.

Parameters	Tissues	Control	1/4 th dose concentration of Cypermethrin			
			24 h	48 h	72 h	96 h
Acid Phosphatase (μ /l)	Liver	3.12 \pm 0.046	2.91 \pm 0.022 (-7.21)*	2.55 \pm 0.06 (-22.35)**	2.45 \pm 0.04 (27.34)**	2.40 \pm 0.03 (-30.0)***
	Muscle	4.18 \pm 0.18	4.60 \pm 0.97 (9.13)*	4.72 \pm 0.86 (11.44)*	4.99 \pm 0.87 (16.23)*	4.71 \pm 0.06 (11.25)*
	Gill	2.03 \pm 0.03	1.63 \pm 0.05 (-20.83)**	1.64 \pm 0.042 (-23.78)**	1.42 \pm 0.04 (21.42)**	1.30 \pm 0.03 (56.15)***
Alkaline Phosphatase (μ /l)	Liver	4.36 \pm 0.056	3.98 \pm 0.08 (-9.54)*	4.09 \pm 0.063 (-6.60)*	3.56 \pm 0.05 (-22.47)**	3.04 \pm 0.086 (-7.92)*
	Muscle	4.66 \pm 0.49	4.67 \pm 0.55 (0.21)NS	5.18 \pm 1.22 (10.03)*	6.15 \pm 0.20 (24.22)**	8.05 \pm 0.83 (42.11)**
	Gill	2.36 \pm 0.020	2.12 \pm 0.04 (-11.32*)	2.08 \pm 0.03 (-13.46)**	1.81 \pm 0.01 (30.38)**	1.56 \pm 0.04 (51.28)***

Table-2: Effects of sub lethal concentration 1/4th (0.085 ppm) of Fenvalerate on ACP and ALP in the liver, muscle and gill of *Channa marulius*.

Parameters	Tissues	Control	1/4 th dose concentration of Fenvalerate			
			24 h	48 h	72 h	96 h
Acid Phosphatase (μ /l)	Liver	3.12 \pm 0.046	3.12 \pm 0.037 (0.32)NS	3.10 \pm 0.03 (0.96)NS	3.04 \pm 0.05 (-2.96)NS	3.02 \pm 0.07 (-3.64)NS
	Muscle	4.18 \pm 0.18	7.54 \pm 0.48 (33.02)**	6.58 \pm 0.06 (23.25)**	6.02 \pm 0.38 (16.11)*	5.75 \pm 0.05 (12.17)*
	Gill	2.03 \pm 0.03	2.07 \pm 0.03 (-0.96)NS	2.05 \pm 0.05 (-1.95)NS	2.04 \pm 0.04 (-2.45)*	2.01 \pm 0.9 (-3.98)*
Alkaline Phosphatase (μ /l)	Liver	4.36 \pm 0.056	4.35 \pm 0.05 (-0.22)NS	4.33 \pm 0.096 (-0.69)NS	4.32 \pm 0.07 (-0.92)NS	4.24 \pm 0.06 (-2.83)*
	Muscle	4.66 \pm 0.49	8.71 \pm 0.16 (33.65)**	9.26 \pm 0.16 (35.63)**	10.15 \pm 0.59 (41.28)**	11.73 \pm 0.72 (49.19)**
	Gill	2.36 \pm 0.020	2.45 \pm 0.045 (-0.81)NS	2.38 \pm 0.05 (-3.78)NS	2.36 \pm 0.04 (-4.66)NS	2.27 \pm 0.06 (-8.81)**

Mean \pm S.D. values differ significantly ($p < 0.05$) within same column. *Significant value: $p < 0.05$, ** $p < 0.01$, *** $p < 0.001$. NS = Non-Significant ($p > 0.05$). Values in the parenthesis are percentage change over control treated as 100 per cent.

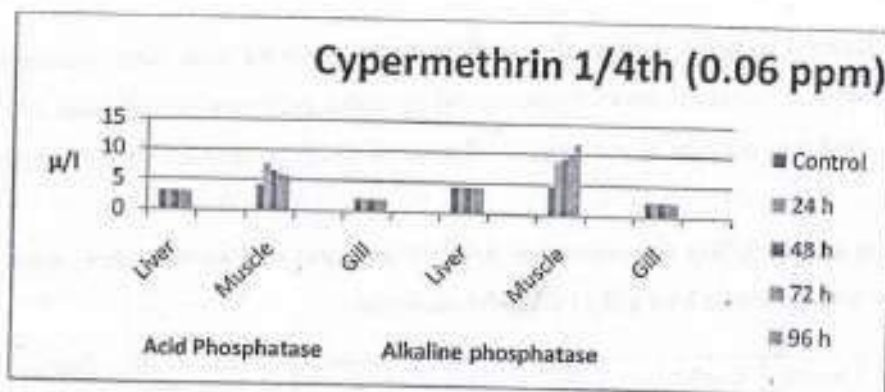


Fig 1 Effects of sub lethal concentration $1/4^{\text{th}}$ (0.06 ppm) of Cypermethrin on ACP and ALP in the liver, muscle and gill of *Channa marulius*.

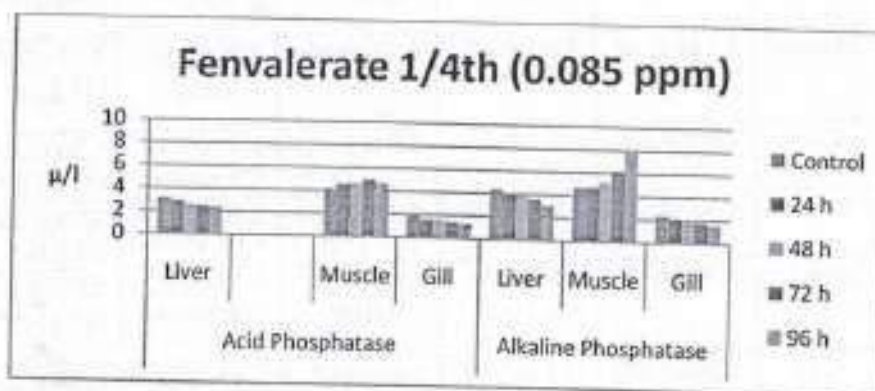


Fig 2 Effects of sub lethal concentration $1/4^{\text{th}}$ (0.085 ppm) of Fenvalerate on ACP and ALP in the liver, muscle and gill of *Channa marulius*.

CONCLUSION

We conclude that the acid phosphatase and alkaline phosphatase enzyme levels in the fish organs like liver, gill and muscle are altered by the effect of Cypermethrin and Fenvalerate in *Channa marulius*. Therefore, these chemicals should be handle with care and prevent its entrance in to aquatic environment.

ACKNOLWEDGEMENT

The authors are grateful to the principal, V. V. M^S S.G. Patil Arts, Science and Commerce College, Sakri Dist. Dhule (M.S.) for providing necessary laboratory facilities. Also thankful to Zoological Survey of India, Western Regional Station, Akurdi, Pune (M.S.) for the identification of fish.

REFERENCES

1. Abalaka, S. E., Esievo, K. A. N. and Shoyinka, S. V. O. (2011). Evaluation of biochemical changes in *Clarias gariepinus* adults exposed to aqueous and ethanolic extracts of *Parkia biglobosa* pods. *Afri. J. Biotechnol.* 10: 234-240.
2. Christobher, S., Perisamy, M., Sughanti, P. and Saravapan, T. S. (2016). Effect of Phosphamidon on haematological and biochemical parameters of fresh water fish, *Labeo rohita*. *Int. J. Fauna and Biol. Stud.* 3(1): 114-116.
3. Deshmukh, D. R. (2016). Haematological responses in fresh water fish *Channa striatus* exposed to endosufan. *Biosci. Discov.* 7(1): 67-69.
4. Devi, A. K., Binukumari, S. and Vasanthi, J. (2016). Effect of enzymes in the fresh water fish, *Labeo rohita* during acute and chronic sub lethal exposure to the pesticide Monocrotophos. *Int. J. Appl. Res.* 2(5): 1067-1072.
5. Gabriel, U. U., Akinrotimi, O. A., Ariwerikuma, V. S. (2012). Changes in metabolic enzymes activities in selected organs a tissue of *Clarias gariepinus* exposed to Cypermethrin. *J. Environ. Eng. Technol.* 1(2):12-18.
6. Kalaimani, S. and Kandeepan, C. (2017). Effect of organophosphate pesticide on the freshwater fish *Labeo rohita* (Hamilton). *Ind. J. Nat. Sci.* 8 (44):12700- 12706.
7. Kumar, A., Sharma, B. and Pandey, R. S. (2012) Alterations in nitrogen metabolism in freshwater fishes, *Channa punctatus* and *Clarias batrachus*, exposed to a commercial-grade K-Cyhalothrin, REEVA-5. *Int. J. Expt. Path.* 93(1):34-45.
8. Mohhammad, I. H., Baidyanath, K. and Mumtaj, A. (215). Acute toxicity behaviour response and biochemical composition of blood of common carp, *Catla catla*, (Hamilton) on organophosphate insecticide, Dimethiote. *Int. J. Curr. Microbiol. App. Sci.* 4(5): 1189-1199.
9. Nafisa, S. and Pirazada, J. A. S. (2016). Impact of Organophosphate pesticide, Methyl Parathion and Chlorpyrifos on some tissue enzymes in fish (*Ahanius dispar*). *Indian J. Mar. Sci.* 45(7): 869-874.
10. Ojutiku, R. O., Asuwaju, F. P., Ayanda, I. O., Obande, R. A. and Agbelege, O. O. (2013). Effect of acute toxicity of Cypermethrin on some biochemical parameters of juveniles of *Claria gariepinus* (Burchell, 1822), *Int. J. Engi. Sci. Inven.* 2(3): 1-7.

11. Rajini, A., Gopi, R. A., Bhuvana, V., Goparaju, A. and Anbumani, S. (2014). Alachlor 50% EC induced biochemical alterations in *Clarias batrachus* during and after cessation of exposure. *Int. J. Fish. Aqua. Stud.* 2(2): 59-63.
12. Palanisamy, P., Sasikal, G., Mallikaraj, D., Bhuvaneshwar, N. and Natarajan, G. M. (2012). Activity levels of phosphatase of air breathing catfish, *Mystus cavasius* exposed to electroplating industrial effluent Chromium. *Biol. Med.* 4(2):60-64.
13. Sarower, E., Mahfuj, M., Belal, H. M. and Minar, M. H. (2012). Biochemical composition of an endangered fish, *Labeo bata* (Hamilton, 1822) from Bangladesh waters. *American J. Food Technol.* 7(10):633-641.
14. Shabnam, A. and Badre, A. A. (2012). Alphamethrin toxicity effect on the reproductive ability and the activities of phosphatase in the tissues of zebra fish, *Danio rerio* *Int. J. Life Sci. and Pharma. Res.* 2(1): 89-100.
15. Shamsun, N., Chandan, K., Kavitha, M. and Mamta, K. (2010). Lead induced alteration in blood profile of air breathing catfish, *Clarias batrachus* Linn. *The Bioscan an Int. Quar. J. Life Sci.* 2: 335-341.
16. Sreenivasan, R. S., Krishna, M. P. and Deecaraman, M. (2011). Effect of Phosphatase activity in the hepatopancreas and muscle of the fresh water female field crab, *Spiralothelphusa hydrodroma* (Herbst) treated with Cypermethrin, *Int. J. Pharma. Sci. Drug Res.* 3 (2): 123-126.
17. Sripriya, R., Kumar, K. and Rajendran, K. (2015). Seasonal variation of serum enzymes of Indian freshwater eel, *Anguilla bicolor* (McClelland), *Int. J. Fish. Aqua. Stud.* 3(2): 50-54.
18. Sudhish, C. (2013). Impact of pesticide Rogar toxicity on serum phosphomonoesters levels of freshwater catfish *Clarias batrachus*. *J. Appl. Nat. Sci.* 5 (1): 20-23.
19. Susan, T. A., Sobha, K., Veeraiah, K. and Tilak, K. S. (2010). Studies on biochemical changes in the tissues of *Labeo rohita* and *Cirrhinus mrigala* exposed to Fenvalerate technical grade. *J. Toxicol. Environ. Heal. Sci.* 2(5):53-62.
20. Yi, X., Ding, H., Lu, Y., Liu, H., Zhang, M., Jiang, W. (2009). Effects of long-term exposure on hepatic antioxidant defense and detoxifying enzyme activities in crucian carp (*Carassius auratus*). *Chemosphere*, 68:1576-158.

EFFECT OF BIODEGRADABLE PLASTIC PAPER ON GROWTH AND REPRODUCTION OF EARTHWORM, *EUDRILUS EUGENIAE*.

B. C. More, Y. M. Nandre, H. M. Shaikh¹, and S. S. Patole^{}**

Department of Zoology, Karm, A. M. Patil Arts, Commerce & Kal, Annasaheb N. K. Patil Science College, Pimpalner, Dist. Dhule, Maharashtra, India.

¹Department of Zoology, ASC College, Kusumba, Dist. Dhule (M. S.).

^{**} Professor and HOD, Department of Zoology, S. G. Patil College, Sakri (Dhule).

ABSTRACT

Present study deals with the effect of biodegradable plastic paper on growth and reproduction of earthworm (*Eudrilus eugeniae*). A mixture of Soil + Cow-dung + Earthworms was treated as control, whereas this mixture along with biodegradable plastic paper (1%) served as experimental material. The mixtures were incubated for 60 days, and thereafter, growth and reproductive performance of earthworm was observed. Maximum growth, number juveniles and cocoons were recorded in control, while those were significantly decreased in the experimental material. Thus, severe effect of biodegradable plastic on growth and reproduction of earthworm was observed.

Keywords: Biodegradable plastic, soil, cow-dung, earthworm, juveniles, Cocoons

Introduction

Earthworm have been proved as the best decomposers of organic waste (More and Patole, 2013). Present investigation was undertaken to find out the effect of biodegradable plastic paper fragments (which is often used by the farmers for mulching, covering and other farm operations) on reproductive behaviour of earthworm (*Eudrilus eugeniae*).

Material and methods

The earthworms were procured from horticulture nursery, Department of Agriculture, Sakri, Dist. Dhule. Those were maintained in the mixture of cow dung and soil for 15 days. One month old cow dung (CD) and black cotton soil was collected from cow shed and agricultural field respectively. Biodegradable plastic paper was purchased from local market.

The experiment was performed in the plastic bags having capacity of around 5 kg. Two groups of vermi-beds were prepared. The control vermi-bed contained 50 % soil + 50 % CD + earthworms (50), while experimental vermi-bed was comprised of 49 % soil + 50 % CD + 1 % biodegradable plastic + earthworms (50). Sufficient water was added to the mixtures so as to keep them moist.

Biodegradable plastic paper was cut into pieces (1 cm x 1 cm) and mixed with experimental beds. Worms with equal size were selected, their weights recorded and then added in both control and experimental beds next day. The bags were kept in the laboratory undisturbed for 60 days with intermittent water spray.

The experiment was terminated on the 60th day. The contents were removed and dried for two days. All large worms, small juveniles and Cocoons were carefully removed, washed, counted, dried and their dry weights were recorded.

Results and discussion

Table 1 : Effect of plastic on earthworm.

Sr. No.	Group	Weight of worms (g)		% increase	count	
		Initial	Final		cocoons	juveniles
1	Control	24	33	37.5	30	62
2	Experimental	23	28	21.7	22	56

The results obtained have been summarised in Table 1. Both vermi-beds showed increase in the weight of worms, however, the weight of the worms from control group was higher than that noticed in the experimental group. It seems that

biodegradable plastic papers might have eaten by earthworms.

References

More B.C. and Patole S. S. (2013) *Uttar Pradesh J. Zoo.*33(1): 51.

EFFECT OF YOGA THERAPY ON TSH AND BMI

Y. M. Nandre, B. C. More and S. S. Patole*

Dept. of Zoology, Karm. A. M. Patil Arts, Commerce & Kai, Annasaheb N. K. Patil Science, College, Pimpalner, Dist. Dhule, Maharashtra, India.

Dept. of Zoology, S. G. Patil - ASC Senior College, Sakri, Dhule, Maharashtra, India.

ABSTRACT

Twenty men and women subjects were divided in two groups, the experimental or yoga and control groups. Yoga and pranayama therapy was practiced on experimental group. The level of TSH, weight and height of all the subjects were measured and body mass index (BMI) was calculated, before starting yoga and after 6 weeks of yogic training. The influence of yogic practices showed statistically significant decrease s in the levels of TSH and BMI.

Key words: yoga, pranayama, ujai, kapalbhati, hypothyroidism, BMI, TSH.

Introduction

In order to evaluate efficacy of selective yoga therapy in the management of hypothyroidism, and its effect on body mass index (BMI) and Thyroid Stimulating Hormone (TSH) present investigation was undertaken.

Material and Methods

The present research work was carried out in the Department of Zoology, Karm. A. M. Patil Arts, commerce & Kai, Annasaheb N. K. Patil Science Senior College, Pimpalner, District Dhule. The subjects included in this investigation were mild to moderate cases of Hypothyroidism, with Serum TSH level in between 5.0 - 46.6 m IU/ml. Those were within the age group of 18-60 years. The subjects with cardiac diseases, pregnant women, suffering with auto immune diseases, Patients suffering from any kind of diagnosed / clinically seems to be neurological and orthopedic disorders and those having Body weight more than 90 kg were excluded. The subjects were selected from Pimpalner town. The study was under taken at Sant Thekarsingh Dnyanpeeth Highschool, Pimpalner.

Twenty subjects were thus included in the experimental trial, after screening by inclusion and exclusion criteria, and randomly segregated into two groups, each group had 10 patients. Group- 1 was Experimental or Yoga group. The subjects from this group were executed to life style modification, including specific Yoga techniques and diet restriction of 1600 Kcal/day.

Group-2 was Control group. The subjects from this group were also executed for life style modification with diet restriction of 1600 Kcal/day.

The study protocol was ethically approved by the Institutional Ethical Committee. An informed consent of the volunteers was undertaken in an approved format. Control group was not exposed to any yogic practices. Yoga therapy was, however, introduced to the experimental group, which contained Asanas, Pranayamas, Meditation and Relaxation techniques in a proper sequence. Asanas were taught for a period of 30 minutes, Pranayama for 20 minutes, Meditation for 5 minutes and Relaxation for 15 minutes. All the practices were taught gradually.

Yoga schedule included 7 Pranayamas (Bhastrika : 2 - 3 min.,

Kapalbhati : 5-10 min., Bahya with tribandh : 2 times, Anulom-Vilom : 10-20 min., Brahmari and Udgeet : 25min. and Ujjayi : 25times), 12 Asanas (Vajrasana, Suptavajrasana, Simhasana, Tadasana, Trikonasana, Paschimottanasana, Pawanamuktasana, Bhujangasana, Shalabhasana, Dhanurasana, Makarasana and Ustrasana) and Micro-exercises for relaxation of hand and legs, as per the 'theory of Swami Ramdev' (Acharya Balkrishna, 2007).

The Yoga program was undertaken from February 1, to March 17, 2017 during 5.30 to 6.45 AM. It was scheduled for 6 days/ week and continued for 6 weeks. The basal level of TSH, weight and height were measured before starting and completion of yogic training. The Body mass index was calculated as $BMI = \text{Weight (Kg)} / \text{height}^2(\text{m})$ as described by Malcolm Kendrick. (2015). Statistical methods used were one way analysis of variance (ANOVA) and student 't' test for descriptive statistics and 'p' value.

Results and Discussion

Table 1 gives an account on pre and post-yoga changes in experimental and control groups. As compared to the non-yoga group, yoga group revealed significant improvement in BMI and TSH levels. Singh and Barnwal (2014) also found significant effect of yogic practices on TSH. Specific yogic poses (Sarvangasana, Halasana, Ustrasana, Matsyasana, Bhujangasana) can stimulate throat area by squeezing and stretching, massaging thyroid gland (Chatterjee and Mondal, 2010).

The results obtained during present study are similar to those obtained by Krishna Sharma (2016). Similarly Syeda Islam and Dhiren Deka (2016) also reported that yoga increases TSH level to a normal range. The results, however, are contradictory to the results recorded by Gordon et. al. (2008) who reported no significant change in TSH, T3 & T4 levels after practice of yoga.

Acknowledgements

The authors are grateful to all respondents. They are thankful to the Head master, Sant Thakursingh Draynpeeth High school, Pimpalner, Principal of Karm.A.M. Patil Arts, Commerce and Kai N. K. Patil Science Sr. College Pimpalner, Tal.Sakri Dist. Dhule (MS), India. For providing facilities to perform the work.

References

- Acharya Balkrishna. (2007). "Yog in Synergy with Medical Science" First Edition Divya Prakashan, Patanjali Yogpeeth, Haridwar. pp 234-236.
- Chatterjee S. and Mondal S. (2010)., *Yoga Mimamsa*, **42(1)**: 40-47.
- Gordon L, Morrison E.Y, Mc Growder D, Penas Y.E., Zamoraz, E.M, Lindo, R'A, (2008). *Am J. Biotechnol*, **4(1)**: 35.
- Krishna Sharma. (2016). *Global Journal for Research Analysis*, **5(8)**: 3739.
- Malcolm Kendrick. (2015).. <https://www.independent.co.uk>.
- Singh, S. and Barnwal, S. (2014).. *AMASS Multilateral Research Journal*, **6(1)**:40-48.
- Syeda Semin Islam and Dhiren Deka, (2016).. *IJMDRR*, **1(16)**:1.

Table1: Effect of yoga on weight, BMI and TSH.

Experimental Criteria	scores		% Relief (significance level)
	Pre -Test	Post-Test	
Weight (in kg.)	74.5	71.2	4.61%*
B. M. I. (kg/m ²)	27.23	25.87	4.99%**
TSH mIU/ml.	14.45	1.95	86.50%***
Control Criteria	scores		% Relief (significance level)
	Pre -Test	Post -Test	
Weight (in kg.)	72.4	72.1	0.41% NS
B. M. I. (kg/m ²)	27.67	27.57	0.36% NS
TSH mIU/ml.	12.6	11.8	5.34% NS

All values are expressed as mean score- Weight, BMI-Body Mass Index, TSH- Thyroid Stimulating Hormone, Test-Pre-Before yoga intervention, Test-Post- After yoga intervention, NS-Non Significant (P>0.05), Significant values: *P<0.05, **P<0.01, ***P<0.001.

Antibacterial activity of plant extracts against *Xanthomonas axonopodis* P.v. *Punicae* causing Bacterial blight of Pomegranate (*Punica granatum* L.)

Arangale K. B.^{1*}, Bagwan R.A.², Whagmare D.N.³, Giri S. P.⁴

^{*1,4,4} Padmashri Vikhe Patil Arts, Commerce and Science College

Pravaranagar, Loni, Tal- Rahata, Dist. - Ahmednagar (M.S.),

²Government Institute of Science, Aurangabad.

³Sitaram Govind Patil Arts, Science & Commerce College, Sakri, Dist. Dhule (M.S.)

Abstract- Pomegranate (*Punica granatum* L.) is an ancient fruit, belonging to the smallest botanical family puniceae. It is the important fruit crop cultivated throughout the world. The crop is affected by 'Bacterial blight' caused by *Xanthomonas axonopodis* pv. *punicae*, which is responsible for the failure of crop. It results in the dropping of leaves as well as fruits. It is very hard to manage the disease with chemicals as well as antibiotics and farmers suffer from heavy economic losses. In the present study, aqueous, and Methanol extracts of Five medicinally useful plants were used against *Xanthomonas axonopodis* pv. *punicae* in vitro. The plant extracts showed antibacterial activity and caused inhibition of growth of *Xanthomonas axonopodis* pv. *Punicae*. Among them, Karanj (*Pongamia pinnata* L.) and Tulsi (*Ocimum sanctum* L.) caused maximum inhibition of the test bacterium. In the plant extracts showed antibacterial activity and caused inhibition of growth of *Xanthomonas axonopodis* pv. *Punicae*.

Key Words- Bacterial blight, Antibacterial, Pomegranate, *Xanthomonas axonopodis* pv. *Punicae*.

INTRODUCTION

Pomegranate (*Punica granatum* L.) is belonging to the smallest botanical family puniceae. The Pomegranate (*Punica granatum* L.) is an ancient fruit crop of India. Pomegranate has been associated with high nutritional value, many health benefits and its entire plant has great economic and therapeutic value. Pomegranate is also well known for various medicinal properties and nutritive values. (Julie Jurenka, 2008). It is native to Iran. It is the important fruit crop cultivated throughout the world. India is largest pomegranate producer in the world sharing about 36 per cent of the world's production and above 30 per cent of the international Trade. (Gargade and Kadam, 2015). The average of total production is 8 lakh tons per annum in India (Pawar et al., 2014). The crop is affected by 'Bacterial blight' caused by *Xanthomonas axonopodis* pv. *punicae*, which is responsible for the failure of crop.

Studies were conducted in different parts of the world identified *Xanthomonas axonopodis* P.v. *Punicae* as the causal organism of bacterial blight, which is a gram negative short rod bacterium. The pathogen infects all the cultivated varieties nevertheless of age of the plants. The infection appears as yellowish water soaked circular spots on the plant part and later converted to irregular injuries. In advanced stages of infection, tissue necrosis occurs on the leaves and twigs. In the case of fruits the disease develops into cracks and later the fruit became completely back and dries off. This is one of the most damaging diseases of pomegranate. Due to bacterial blight of pomegranate, the yield loss was noted up to 90 per cent (Chowdappa et al., 2018). It results in the falling of leaves as well as fruits. It is very hard to manage the infection with chemicals as well as antibiotics and farmers suffer from heavy economic losses.

The pathogen can infect in any stage of growth of the plant. The damage is observed on fruits which develop black oily spots later become completely black cracking and dries off. In advanced stage of infection tissue necrosis occurs on leaves and twigs. Use of chemicals in agriculture causes several opposing and environmental dangers(Shanthi,2011).The primary disease management includes spraying bleaching powder, farmyard manure, urea, Bordeaux mixture to control bacterial blight of pomegranate (Yenjerappa *et al.*,2014).Regular use of chemicals in agriculture land causes killing of flora and fauna of the soil, increase in development of resistance in plant pathogen against chemicals and residual toxicity remains in plant and animals. To overcome this problem, there is growing interest worldwide in the utilization of sustainable material for pathogen control (Madhiazhagan *et. al.*, 2002).

In the present study, aqueous, and Methanol extracts of Five medicinally useful plants were used against *Xanthomonas axonopodis* pv. *punicae* in vitro. The plant extracts showed antibacterial activity and caused inhibition of growth of *Xanthomonas axonopodis* pv. *Punicae*.

Aims and Objectives-

To isolate pathogenic bacteria from affected fruit samples and to screen the ability of different plant extracts to inhibit the pathogens and control pathogenic bacteria causing bacterial blight to pomegranate.

Materials and Method-

Collection of diseased plant parts of Pomegranate plant

Disease infected Pomegranate fruits were collected from field located at village Rajuri Tal- Rahata, district Ahmednagar, Maharashtra, India.

Isolation and Identification of pathogen from lesions on diseased fruit

The disease infected portion of fruits were surface sterilized with 0.1% mercuric chloride (HgCl₂) solution for one minute and washed three times with sterile distilled water and mixed gently with sterile scalpel in sterile saline. The presence bacteria in fruit lesion was confirmed by performing ooze test. The suspension was serially diluted and plated on sterile Petri plate with Nutrient Glucose Agar medium with composition Beef extract-0.3%,peptone-0.5%,glucose-0.25%, agar-2%, pH 6.8 (Mondaler *et.*, 2009).The inoculated plates were incubated at 30°C for 72 hours. After the incubation typical mucoid yellow color colonies were selected and screened for morphological and bio-chemical characteristics according to Bergy's manual of determinative Bacteriology and identified as *Xanthomonas*.

Preparation of aqueous plant extracts

Leaves of the medicinal plants such as Pongamia (*Pongamia pinnata* L.), Periwinkle (*Catharanthus roseus* (L.) G. Don.), Tulsi (*Ocimum santum*L.), Shatavari (*Asparagus racemosus* Willd.), Adulsa (*Adhatoda vasica* Nees.) were collected from different sites of sonai, Tal- Newasa, Ahmednagar (M.S.) The plant material was wash tap water remove soil and dust particles and then dry in shady place temperature (25 ± 2°C). Plants leaves was crush in mixture and to make fine powder. Fifty grams of leaves powder was crush in 50ml of sterile distilled water using mortal and pestle. The extracts was filter double layered cheese cloth, and then through Whatman filter paper No.1. The Filter extracts centrifuged at 5000 rpm for 20 minutes supernatant was stored in sterilized bottle and labeled properly. Finally the filtrate was passed through syringe filter of 0.2 µm pore size for sterilization. This filtrate served as 100 per cent standard solution. Filtrate was diluted to 5 per cent and 10 per cent concentration using sterile distilled water. The standard solution was stored at 4°C for further use (Kulshrestha *et. al.*, 2015).

Preparation of methanol plant extract

Leaves of the plants were thoroughly washed and dried under shade at the room temperature (20 ± 2°C). The dried leaves were then ground to a fine powder in an electric grinder. Stock solutions of the extract were prepared by adding ground leaf powder

to 200 ml of each solvent (w/v, 1 g/ 10 ml). Methanol solvents were used for extraction. Prepared extracts were then shaken for 6 hours for homogenous mixing of ground leaf powder in the solvent. After that each extract was passed through Whatman filter paper no.1. Final filtrate was then concentrated to 10 per cent crude extract on a mini rotary evaporator under vacuum at 20°C and was utilized for the experiments (Digvijay et al., 2014).

In vitro Antimicrobial activities of the extract against *Xanthomonas axonopodis* pv. *punicae*

Forty-eight hours old bacterial culture of *Xanthomonas axonopodis* pv. *Punicae* was seeded into the nutrient agar medium at lukewarm temperature (40°C), mixed well and poured into sterile Petri plates. Wells of 4 mm diameter was prepared using a cork borer and plant extracts (0.02 ml) were filled in wells. Three replicates were maintained for each extract at 5 per cent and 10 per cent separately. Plates containing nutrient agar with bacterial suspension without any leaf extract were maintained as control. All these Petri plates were incubated at room temperature (28 + 2°C) for 48 hrs. (Bonyadi et al., 2009).

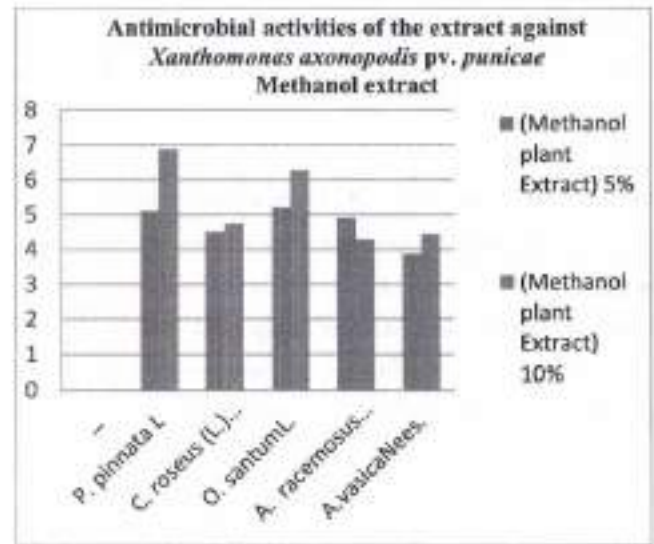
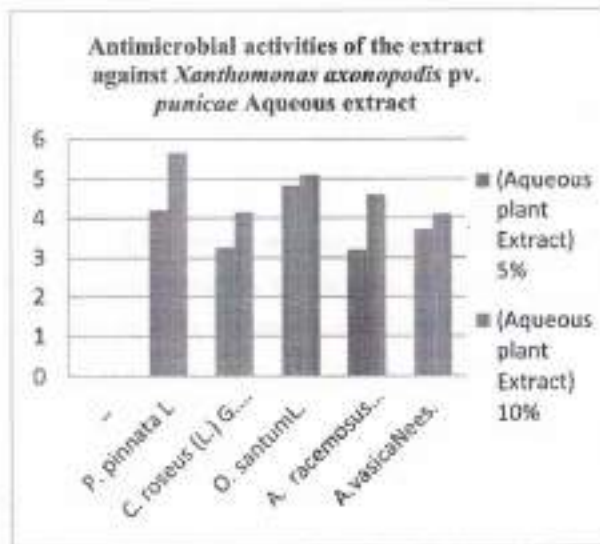
RESULTS AND DISCUSSION

The results of the present study shows that all the plant extract inhibited the pathogen. Higher concentration of aqueous and methanol plant extract show high inhibited compared lower concentration in all three replication. Among the plant extract in case of 5% concentration maximum inhibition zone 4.83 cm in aqueous and 5.20 cm in methanol extract of *O. santum* L. In case of 10% concentration *P. pinnata* L exhibited maximum inhibition 5.66 cm in aqueous and 6.90 cm in methanol extract. *C. roseus* (L.) G. Don. and *A. vasica* Nees both plants Shows lesser inhibition zone formed. (Table No. 01).

Table No. 01: *In vitro* Antimicrobial activities of the extract against *Xanthomonas axonopodis* pv. *punicae*

Sr. No.	Common Name	Botanical Name	Inhibition Zone (cm)* (Aqueous plant Extract)		Inhibition Zone (cm)* (Methanol plant Extract)	
			5%	10%	5%	10%
1	Control (Sterile Distilled Water)	-	0.00	0.00	0.00	0.00
2	Pongamia	<i>Pongamia pinnata</i> L.	4.20	5.66	5.12	6.90
3	Periwinkle	<i>Catharanthus roseus</i> (L.) G. Don.	3.25	4.15	4.50	4.75
4	Tulsi	<i>Ocimum santum</i> L.	4.83	5.10	5.20	6.27
5	Shatavari	<i>Asparagus racemosus</i> Willd.	3.20	4.59	4.90	4.28
6	Adulasa	<i>Adhatoda vasica</i> Nees.	3.70	4.10	3.88	4.45

*. Mean of three replications.



CONCLUSION

Bacterial blight of Pomegranate is a major disease of the Pomegranate crop that affects around 50% of the production. The present study to find the ecofriendly method of controlling bacterial blight of pomegranate. Pongamia and Tulsii are show that the maximum inhibition of the *Xanthomonas axonopodis* pv. *Punicae* bacteria so these both plant are useful for the controlling of the infection.

REFERENCES

- o Bonyodi R. B., Awad V. and Nirichan K. B., (2009) Antimicrobial activity of the ethanolic extract of *Bryopsis lactuosa* leaf, stem, fruit and seed, *Afr. J. Biol.* 15(2): 3565-3567.
- o Chowdappa, A., Kamalakannan, A., Kousalya, S., Gopalakrishnan, C. and Venkatesan, K., (2018) Eco-Friendly Management of *Xanthomonas axonopodis* pv. *Punicae* Causing Bacterial blight on Pomegranate, *Int. J. Pure App. Biosci.* 6(5): 290-296.
- o Digvijay, Bhardwaj, S. and Kumar, P., (2014) Antibacterial activity of *Juniperus communis* and *vitex negundo* gainst *Xanthomonas axonopodis* pv. *punicae* in vitro, *World Journal of Pharmaceutical Research* 3(10):1489-1500.
- o Gargade V. A. and Kadam D.G. (2015) In vitro evaluation of antibacterial potential of *Pongamia pinnata* L. against *Xanthomonas axonopodis* pv. *punicae*, phytopathovar of Bacterial blight of Pomegranate (*Punica granatum*), *Int. J. Curr. Microbiol. App. Sci.* 4(5): 824-833.
- o Julie Jarenska MT (2008) Therapeutic applications of pomegranate (*Punica granatum* L.): A review. *Alternative Medicine Review.* 13: 123-144.
- o Kulshrestha, S., Chaturvedi, S., Jangir, R. and Agrawal, K., (2015) In vitro Evaluation of Antibacterial Activity of Some Plant Leaf Extracts against *Xanthomonas axonopodis* pv. *Phaseoli* isolated from Seeds of Lentil (*Lens culinaris* Medik.). *International Research Journal of Biological Sciences* 4(7):59-64.
- o Madhuchagan K, Ramadoss N, Anaradha R. (2002) Antibacterial effect of planton common pathogen: *Journal of Mycology plant pathology.* 32(1):68-69.
- o Pekar Mahesh, Kadam Manoj and Bipinraj Kunchinzeas Nirichan. (2014) In vitro control of bacterial blight causing organism (*Xanthomonas axonopodis* pv. *punicae*) of pomegranate. *Journal of Environmental Research and Development* 8 (3a), 568-573.
- o Shanthy S, Elamathy S, Pinnaselvam, A, Radha N. (2011) Anti-xanthomonas activity of *Pongamia pinnata* linn leaves cow urine extract- a natural cost effective eco friendly remedy to bacterial leaf blight of paddy (BLB). *Journal of Pharmacy Research.* 4(3): 650-652.
- o Venjerappa S.T., Nargund V.B., Ravikumar M.R. and Byadagi A.S. (2014) Efficacy of bactericides and antibacterial chemicals against bacterial blight of pomegranate, *International Journal of plant Protection.* 7(1):201-208.

8. Renewable Energy Sources: Remedies of Energy Crisis in India

Dr. Jyoti Sahasrao Wakode

Assistant Professor, Department of Economics, V. M. Mandal's Sitaram Govind Patil Arts, Science and Commerce College, Sakri, Dist. - Dhule.

Abstract

Energy crisis is the vital problem that the world faces in the present decade it is due to the continuous growth of population and energy consumption. It is very common in country like India where most of the population (over 40 %) has no access to modern energy product services on an average energy demand is expected to rise 7.4 % annually in the for next 25 % years. The present paper highlights the proper solution over the energy crisis in India which has proven as an ideal solution for the energy crisis. Researcher tries to attempt how renewable energy sources are stated its relevance during the time of energy crisis in India.

Keywords: Energy crisis, Renewable and non-renewable energy, Solar, Wind energy.

Introduction

According to **International energy agency (IEA)** more than 28% share of the world total energy will be consumed in India and China by the year 2030 therefore a significant amount of energy must come from renewable energy sources. National action plan on climate change (NAPCC) was formed in 2008 for climate change controlled has also considered role of renewable energy in total energy production of India. NAPCC has also set a target to increase the renewable energy share in total energy production up to 15% till year 2020 which clearly shows India's commitment towards a sustainable development. The basic challenge is to fulfill the energy requirement is a sustainable way and one of the best available action is current scenario is renewable energy sources.

Remedies of Non renewable energy in India

India is ranked fifth electricity generation capacity in the world. About 70% of India's electricity capacity from fossil fuel India is largely dependence on fossil fuel imports to meet its energy demand by 2030. India's dependency on energy imports is expected to exceed 53% of the country's total energy consumption. Fossil fuels based energy sources are not good to any country

its emit a high amount of toxic gases such as NO_x , CO_x and SO_x gases which is injurious to health and environment. These fossil fuels sources like Coal, Natural gas and oil etc.

Coal: Currently, coal is the main source of energy in India. 54% of total electricity generation is coal-based and more than 70% of the energy generated is from coal-based power plants. Although, India has the third highest reserve of coal in the world. There is still a great amount being imported every year. In 2013, 10 million tons of coal were imported from Indonesia. According to expert, an increase in consumption of coal is ineluctable. According to **BP "Energy Outlook 2035"** reports India is expected to replace the united states as the second largest coal consumer in 2024 (after china). By then, China and India must account for 63% and 29% respectively of global coal demand growth up to 2030. Coal is also hazardous and toxic to human beings and other living things (86). Coal ash contains the radioactive elements uranium and thorium. According to the **Clean Air Task Force** will estimated that "air pollution from coal-fired power plants account for more than 13,000 premature deaths, 20,000 heart attacks, and 1.6 million lost workdays in the U.S. each year."

Liquefied Natural Gas (LNG) LNG plays an important part when we talk about the energy crisis in India. In march 2012, natural gas reserves in India were an estimated at 1330.26 billion cubic meters. Since then, there has been a steady increase in the availability of natural gas, mostly due to indigenous discoveries of more reserves. India is currently the sixth largest liquefied Natural Gas (LNG) importer in the world and is expected to move up third place by 2020. Using the indigenous reserve will not only help supply power to India, but its export would also help balance expenses of equivalent imports.

Crude oil: Along with coal LNG, crude oil is a major source in India. Oil is imported to supply all the needs that the others reserves are unable to respond. The combination of rising oil consumption and fairly unwavering production levels leaves India highly dependent on imports to meet its consumption needs. However, volatility of petroleum products is one of the greatest problems in India's energy markets since they fluctuate every fortnight. According to **planning commission, 2016-17** "India will manage an approximate 6.7 million tones of oil and by 2021-22, this number will rise to 850 million tones. Even so, this amount will meet only 70 % of the expected demand. Remaining 30 % will still be dependent on imports. So the renewable energy sources are the best solution of energy crisis in India.

Current Situation of Renewable energy sources in India

India's renewable energy sector is amongst the world's most active players in renewable energy utilization, especially solar and wind electricity generation (86). As of June 2016, India had grid connected installed capacity of about 42.85 GW non-conventional renewable technologies-based electricity capacity, about 14.15% of its total, exceeding the capacity of major hydroelectric power for the first time in history. Since 2015 onwards the MNRE began laying down actionable plans for the renewable energy sector under its ambit to make a quantum jump, building in the country. (Annual report 2015-16) MNRE renewable energy targets have been upscale to grow from just under 43GW in April 2016 to 175 GW from solar power, 60GW from wind power, 10GW from Bio power and 5GW from Small hydro. The ambitious target would see India quickly becoming one of the leading green energy producers in the world and surpassing numerous developed countries. The government intends to achieve 40% cumulative electric power capacity from non fossil fuel sources by 2030. Table 1 shows that grid interactive renewable electricity in India.

Installed grid interactive renewable power capacity in India as of December 31, 2016 (RES MNRE)

Source	Total Installed capacity (MW)	2022 Target (MW)
Wind	28700.44	60,000.00
Solar	9012.66	100,000.00
Biomass	7856.94	10,000.00
West-to-power	114.08	
Small Hydro Power	4333.85	5,000.00
Total	50017.97	175,000.00

Source: MNRE

The above figures refer to newer and fast developing renewable energy sources and are managed by the Ministry for New and Renewable Energy (MNRE). In addition as of Dec 31, 2016 India had 50,017.97 MW of installed large hydro capacity, which comes under the ambit of Ministry of Power.

In terms of meeting its ambitious 2022 targets, as of April 30, 2016, wind power was almost half way towards its goal, whilst solar power was below 7% of its highly ambitious target, although expansion is expected to be dramatic in the near future. Bio energy was also at just under half way towards its target whilst small hydro.

Wind power

Wind power accounts nearly 8.6% of India's total installed power generation capacity and generated 28,604 million (MU) in the fiscal year 2015-16 which is nearly 2.5% of total electricity generation. The capacity utilization factor is nearly 14% in the fiscal year 2015-16 (15% in 2014-15). 70% of wind generation is during the five months duration from May to September coinciding with Southwest monsoon duration.

As of 2015, Denmark generates 40% of its electric power from wind, and at least 83 other countries around the world are using wind power to supply their electric power grids. In 2014 global wind power capacity expanded 16% to 369,553 MW. Yearly wind energy production is also growing rapidly and has reached around 4% of worldwide electric power usage 11.4% in the EU. A 2008 study released by the U.S. Department of Energy noted that the capacity factor of new wind installations was increasing as the technology improves, and projected further improvements for future capacity factors. In 2010, the department estimated the capacity factor of new wind turbines in 2010 to be 45%. The annual average capacity factor for wind generation in the US has varied between 29.8% and 34.0% during the period 2010-2015.

Solar Power

Solar power in India is a fast-growing industry and as of 31 December 2016, the country's solar grid had a cumulative capacity of 9,012.66 megawatts (MW) or 9.01 gig watts (GW). In January 2015, the Indian government expanded its solar plans, targeting US\$100 billion of investment and 100 GW of solar capacity, including 40 GW directly from rooftop solar, by 2022. The rapid growth in deployment of solar power is recorded and updated monthly on the Indian Government's Ministry of New and Renewable Energy website. Large scale solar power deployment began only as recently as 2010, yet the ambitious targets would see India installing more than double that achieved by world leaders China or Germany in all of the period up to 2015 year end.

In January 2016, the Prime Minister of India, Narendra Modi, and the President of France, Mr. François Hollande laid the foundation stone for the headquarters of the International Solar Alliance (ISA) in Gwalpahari, Gurgaon. The ISA will focus on promoting and developing solar energy and solar products for countries lying wholly or partially between the Tropic of Cancer and the Tropic of Capricorn. The alliance of over 120 countries was announced at the Paris COP21 climate summit. One of the hopes of the ISA is that wider deployment will reduce


CONTENTS OF ENGLISH PART - I


S.No.	Title & Author	Page No.
1	Indian Writing in English and Globalization Ass. Pro. Bhagyashree Sambhaji More	1-5
2	The Impact of Globalization on Post - Colonial Literature Mr. Deepak A. Mali	6-9
3	Reflections on Online Teaching & Learning in Teacher Education Institutions Dr. Dipali Gaudhi	10-14
4	Comparative Study of Covid - 19 Pandemic on Ecotourism of Jhalawar District (Rajasthan), India Divyendu Sen Dr. Shuchita Jain	15-20
5	Covid-19 Pandemic: Impact on Indian Tourism Sector CMA. Ganesh Namdev Zingade Miss. Rima Balkrushna Hibare	21-25
6	COVID - 19 and Market Dead Prof. Gopal Eknath Ghumatkar Prof. Pratiksha Narayan Tikar	26-28
7	Covid - 19 Lockdown : A Boom for E-Learning Dr. Jaideep Hire	29-38
8	Renewable Energy Sources: Remedies of Energy Crisis in India Dr. Jyoti Sahadeo Wakode	39-43
9	Globalization and Feminist Literature Kavita Suresh Khare	44-48
10	Entrepreneurship and Role of Exim Bank of India Dr. Krishan Kumar Khatri	49-53
11	Moving Ahead with Times : Gamification In Science Education Manisha Singh	54-63
12	Impact of COVID- 19 on Climatic & Environmental Conditions-A Hypothetical Study Manju R. Mishra	64-68

The information and views expressed and the research content published in this journal, the sole responsibility lies entirely with the author(s) and does not reflect the official opinion of the Editorial Board, Advisory Committee and the Editor in Chief of the Journal "AJANTA".
Owner, printer & publisher Vinay S. Hatole has printed this journal at Ajanta Computer and Printers, Jaisingpura, University Gate, Aurangabad, also Published the same at Aurangabad.

Printed by

Ajanta Computer, Near University Gate, Jaisingpura, Aurangabad. (M.S.)

Printed by

Ajanta Computer, Near University Gate, Jaisingpura, Aurangabad. (M.S.)

Cell No. : 9579260877, 9822620877, 7030308239 Ph. No. : (0240) 2400877

E-mail : ajanta5050@gmail.com, www.ajantaprakashan.com

AJANTA - ISSN 2277 - 5730 - Impact Factor - 6.399 (www.sjifactor.com)